

**Activation and Subcellular Localisation of Caspases in Wild-type
p53-induced Apoptosis *in vitro* and Fas-induced Apoptosis *in vivo***

Thesis submitted for the degree of
Doctor of Philosophy
at the University of Leicester

by

Julia M. Chandler, BSc.(Hons)
Biochemical Toxicology Section
MRC Toxicology Unit

1998

UMI Number: U116162

All rights reserved

INFORMATION TO ALL USERS

The quality of this reproduction is dependent upon the quality of the copy submitted.

In the unlikely event that the author did not send a complete manuscript and there are missing pages, these will be noted. Also, if material had to be removed, a note will indicate the deletion.



UMI U116162

Published by ProQuest LLC 2013. Copyright in the Dissertation held by the Author.
Microform Edition © ProQuest LLC.

All rights reserved. This work is protected against
unauthorized copying under Title 17, United States Code.



ProQuest LLC
789 East Eisenhower Parkway
P.O. Box 1346
Ann Arbor, MI 48106-1346

Activation and Subcellular Localisation of Caspases in Wild-type p53-induced Apoptosis *in vitro* and Fas-induced Apoptosis *in vivo*

Julia M. Chandler

ABSTRACT

Caspases play a pivotal role in the execution phase of apoptosis induced by a wide variety of stimuli. Despite previous studies demonstrating caspase-3 processing following treatment with DNA-damaging agents, there has been no direct evidence of p53^{WT}-induced caspase activation. In this thesis an *in vitro* temperature-sensitive cell system was employed to study the effects of p53^{WT}. Consistent with previous studies, p53^{WT} induced morphological and biochemical changes characteristic of apoptosis.

p53^{WT}-induced activation of caspase-3 and caspase-7, supported by the cleavage of PARP and the fluorogenic substrate z-DEVD.afc, together with activation of caspase-8, supported by cleavage of the fluorogenic substrate z-IETD.amc, were directly demonstrated for the first time. In addition, indirect evidence for p53^{WT}-induced activation of caspase-6 was gained through the cleavage of lamin B₁ and supported by the cleavage of the fluorogenic substrate Ac-VEID.amc. Abrogation of p53^{WT}-induced apoptotic morphology, caspase activation, PARP and lamin B₁ proteolysis and cleavage of the fluorogenic substrates was achieved with the caspase inhibitor z-VAD.fmk. Evidence was also obtained to support the translocation of caspase-3 and caspase-7 from the cytosol to another subcellular compartment.

The issue of the different subcellular localisation of the substrates and the caspases which cleave them was addressed in the *in vivo* model of Fas-induced apoptosis in mouse liver. An agonistic Fas antibody induced apoptosis in mouse hepatocytes, which was associated with z-DEVD.afc cleavage activity. Both apoptotic morphology and z-DEVD.afc cleavage were blocked by z-VAD.fmk. Subcellular fractionation of the mouse livers demonstrated that whereas active caspase-3 remained in the cytosol, active caspase-7 was translocated to the mitochondrial and microsomal fractions. The observed cleavage of the endoplasmic reticular-specific substrate SREBP-1 following Fas-induced apoptosis is consistent with SREBP-1 being a substrate for the colocalised caspase-7, *in vivo*. Thus, differential distribution of the caspases may partly explain the existence of caspase homologues with similar substrate specificities.

For Mum, Dad and Rayne

ACKNOWLEDGEMENTS

I would like to thank all those who have advised, assisted and supported me during my time at Leicester.

In particular I would like to extend my thanks and show my appreciation to my two supervisors, Dr. Marion MacFarlane and Prof. Gerald M. Cohen, for their help, support, ideas and continuous enthusiasm for the subject.

For their invaluable technical assistance I would like to thank Mr. Roger Snowden, Dr. Kelvin Cain Mr. Dave Brown and Dr. Barbara Nolan.

For their friendship and for just being there; Siobhán and Mick Harkin, Carole Coquet, James Wolfe, Salmaan Hussain, Katharine Ayres, Xiaoming Sun, Huijun Zhu, Wendy Merrison, Richard Cooper, Darren Roberts and Jianguo Zhuang.

Finally I would like to thank the Medical Research Council for funding my studies at Leicester University.

ABBREVIATIONS

APC	adenomatous polyposis coli protein
Asp	aspartate residue
CAGE	conventional agarose gel electrophoresis
CHAPS	3-[(3-Cholamidopropyl)dimethylammonio]-1-propane sulfonate
DMEM	Dulbecco's modified eagles medium
DMSO	dimethylsulfoxide
DNA-PKcs	catalytic subunit of DNA-protein kinase
DTT	dithiothreitol
EDTA	ethylenediaminetetraacetic acid
FACS	fluorescence activated cell sorter
FIGE	field inversion gel electrophoresis
FITC	fluorescein isothiocyanate
h	hour(s)
HEPES	N-[2-hydroxyethyl]piperazine-N'-[2-ethanesulfonic acid]
(k)bp	(kilo)base pair(s)
kDa	kilodalton(s)
min	minute(s)
MOPS	3-[N-Morpholino]propanesulfonic acid
OD_{xnm}	optical density at a wavelength of x nm
PARP	poly(ADP-ribose) polymerase
PBS	phosphate buffered saline
PI	propidium iodide
PIPES	piperazine-N,N'bis[2-ethanesulfonic acid]
Pu/Py	purine/pyrimidine
R	region
PCNA	proliferating cell nuclear antigen
PMSF	phenylmethylsulfonyl fluoride
Rb	retinoblastoma
SDS-PAGE	sodium dodecyl sulphate-polyacrylamide gel electrophoresis
SREBP	sterol regulatory element binding protein
TEMED	N,N,N',N'-tetramethylethylenediamine
TLCK	N _α -p-tosyl-L-lysine chloromethylketone
TNF(R)	tumour necrosis factor (receptor)
Tween 20	polyoxyethylenesorbitan monolaurate
U1-70 kDa	70 kDa subunit of the U1 small nuclear riboprotein
v	volt(s)

CONTENTS

CHAPTER 1 – INTRODUCTION	1
1.1. Apoptosis	2
<i>1.1.1. Morphological and biochemical distinctions between apoptosis and necrosis</i>	<i>2</i>
<i>1.1.2. Physiological and pathological importance of apoptosis</i>	<i>3</i>
1.2. Inducers of Apoptosis	4
<i>1.2.1. Apoptosis induced by staurosporine</i>	<i>5</i>
<i>1.2.2. Apoptosis induced by receptor crosslinkage</i>	<i>5</i>
<i>1.2.3. Apoptosis induced by DNA-damaging agents</i>	<i>6</i>
1.3. p53	6
<i>1.3.1. Identification and characterisation of p53</i>	<i>6</i>
<i>1.3.2. Protein structure</i>	<i>7</i>
<i>1.3.3. Function in normal cells</i>	<i>8</i>
<i>1.3.4. Function following DNA damage</i>	<i>9</i>
<i>1.3.5. Induction of apoptosis</i>	<i>9</i>
<i>1.3.6. The role of p53^{WT} as a transcription factor</i>	<i>10</i>
<i>1.3.7. p53-dependent and independent apoptosis following DNA damage</i>	<i>12</i>
1.4. Genetic control of Apoptosis	13
<i>1.4.1. The apoptotic pathway in the nematode worm Caenorhabditis elegans</i>	<i>13</i>
<i>1.4.2. Mammalian homologues of Ced3 – the caspases</i>	<i>14</i>
1.4.2.1. General properties of the caspases	15
1.4.2.2. ICE/Caspase-1	16
1.4.2.3. CPP32/Yama/Apopain/Caspase-3	16
1.4.2.4. Mch3/ICE-LAP3/Caspase-7	17
1.4.2.5. Mch2/Caspase-6	18
1.4.2.6. MACH/FLICE/Mch5/Caspase-8	18
<i>1.4.3. Other members of the TNFR1 family</i>	<i>19</i>
<i>1.4.4. Mammalian homologues of Ced9 – the Bcl2 family</i>	<i>21</i>
<i>1.4.5. Ced4 – the elusive link</i>	<i>22</i>
1.5. Proteolytic cleavage of substrates	22
<i>1.5.1. Poly(ADP ribose) polymerase (PARP)</i>	<i>23</i>

<i>1.5.2. Nuclear lamins</i>	24
<i>1.5.3. Sterol regulatory element binding proteins</i>	24
<i>1.5.4. DFF – a connection between the caspases and DNA fragmentation</i>	25
<i>1.5.5. Subcellular localisation of caspases and their substrates</i>	25
1.6. Peptide inhibitors of Apoptosis	25
1.7. Project outline	26
CHAPTER 2 – MATERIALS AND METHODS	27
2.1. Materials	28
2.1a. Antibodies	28
2.1b. Animals	28
2.2. Methods	29
2.2.1. Cell culture	29
<i>2.2.1a. Murine Erythroleukaemic Cell lines (MEL cells)</i>	29
<i>2.2.1b. Murine Myeloid Leukaemic Cell lines (M1, LTRphe132 and LTR6)</i>	29
2.2.2. Assessment of apoptosis	29
<i>2.2.2.1. Flow cytometry and fluorescence microscopy</i>	29
<i>2.2.2.1a. Flow cytometry</i>	30
<i>2.2.2.1b. Fluorescence microscopy</i>	30
<i>2.2.2.2. DNA content analysis</i>	30
2.2.3. Electrophoretic methods	31
<i>2.2.3.1. Conventional agarose gel electrophoresis</i>	31
<i>2.2.3.2. Field inversion gel electrophoresis</i>	32
<i>2.2.3.3. SDS-polyacrylamide gel electrophoresis</i>	33
2.2.4. Western blotting	35
2.2.5. Lysate preparation and fluorimetric assays	36
<i>2.2.5a. Cell lysate preparation</i>	36
<i>2.2.5b. Fluorimetric assay</i>	37
2.2.6. Anion-exchange chromatography	38
2.2.7. In vivo administration of anti-Fas receptor antibody JO2 and z-VAD.fmk	39
2.2.8. Tissue preparation and histopathological examination	39
2.2.9. Mouse liver fractionation	40

2.2.10. Cell counting	41
2.2.11. Bradford procedure for protein determination	41
2.2.12. FACS scan analysis of change in p53 conformation	42
2.2.13. Nuclei isolation	42
2.2.14. Densitometry	42
2.2.15. Preparation of recombinant caspases	42
2.2.16. Electron microscopy	44
CHAPTER 3 – CELL CYCLE EFFECTS IN MEL CELLS	45
3.1. Introduction	46
3.2. Results	48
<i>3.2.1. Staurosporine-induced cell cycle arrest and apoptosis in MEL C88 cells</i>	<i>48</i>
<i>3.2.2. Effect of protein synthesis and topoisomerase II inhibitors on MEL C88 cells</i>	<i>52</i>
<i>3.2.3. Staurosporine induces apoptosis more rapidly in DP16-1 than in C88 cells</i>	<i>56</i>
3.3. Discussion	59
3.4. Summary	61
CHAPTER 4 – CHARACTERISATION OF LTR6 CELLS	62
4.1. Introduction	62
4.2. Results	64
<i>4.2.1. p53^{WT}-induced apoptosis in murine LTR6 cells</i>	<i>64</i>
<i>4.2.2. Incubation of LTRphe132 and M1 cells at 32.5°C does not induce apoptosis</i>	<i>68</i>
<i>4.2.3. p53^{WT} induces apoptosis in LTR6 cells after 14–16 h at 32.5°C</i>	<i>70</i>
<i>4.2.4. A shift in temperature induces a change in the p53 status of LTR6 cells</i>	<i>70</i>
<i>4.2.5. Temperature-shift does not induce changes in the level of the p53 protein</i>	<i>73</i>
<i>4.2.6. Temperature-shift induces a sub-G1 peak but no cell cycle arrest</i>	<i>73</i>
<i>4.2.7. Detection of large fragments of DNA following p53^{WT}-induced apoptosis</i>	<i>77</i>
4.3. Discussion	80
4.4. Summary	83
CHAPTER 5 – CASPASES IN P53^{WT}-INDUCED APOPTOSIS	84
5.1. Introduction	85

5.2. Results	86
5.2.1. <i>z-VAD.fmk inhibits p53^{WT}-induced internucleosomal cleavage</i>	86
5.2.2. <i>z-VAD.fmk only partially inhibits apoptosis assessed by flow cytometry</i>	87
5.2.3. <i>Processing of caspases in p53^{WT}-induced apoptosis</i>	90
5.2.4. <i>Proteolytic cleavage of PARP and lamin B₁ in p53^{WT}-induced apoptosis</i>	93
5.2.5. <i>Activation of caspases as assessed by cleavage of fluorogenic substrates</i>	95
5.2.6. <i>Activation of caspases-3 and -7 is not induced in LTRphe132 cells at 32.5°C</i>	97
5.2.7. <i>Effects of z-VAD.fmk on p53^{WT}-induced processing of caspase-3, -7 and -8</i>	99
5.2.8. <i>Effect of z-VAD.fmk on DEVDase, IETDase and VEIDase activities</i>	102
5.2.9. <i>Characterisation of LTR6 cell lysates with caspase substrates and inhibitors</i>	105
5.2.10. <i>Separation of caspase activities using anion-exchange chromatography</i>	106
5.3. Discussion	110
5.4. Summary	116

CHAPTER 6 – SUBCELLULAR LOCALISATION OF CASPASES

IN LTR6 CELLS **117**

6.1. Introduction	118
6.2. Results	119
6.2.1. <i>Following p53^{WT}-induced apoptosis, caspase activity is not solely cytosolic</i>	119
6.2.2. <i>Active caspases-3 and -7 translocate from the cytosol</i>	121
6.2.3. <i>Subcellular localisations of active caspases-3 and -7</i>	125
6.3. Discussion	129
6.4. Summary	132

CHAPTER 7 – SUBCELLULAR LOCALISATION OF CASPASES IN

FAS-INDUCED APOPTOSIS IN VIVO **133**

7.1. Introduction	134
7.2. Results	135
7.2.1. <i>Fas-induced apoptosis, liver damage and caspase-3/7-like proteolytic activity are blocked by z-VAD.fmk</i>	135
7.2.2. <i>Procaspase-3 and active caspase-3 are in the cytosol</i>	138
7.2.3. <i>Active caspase-7 is located in the microsomal and mitochondrial fractions</i>	140

<i>7.2.4. Assessment of fraction purity</i>	142
<i>7.2.5. Processing and activation of caspase-8 in Fas-induced apoptosis in vivo</i>	142
<i>7.2.6. Fate of microsomal SREBP-1 in Fas-induced apoptosis in mouse liver</i>	146
<i>7.2.7. Cleavage of SREBP-1 by recombinant caspases</i>	148
<i>7.2.8. Fas-induced apoptosis in other organs</i>	149
7.3. Discussion	151
7.4. Summary	157
CHAPTER 8 – GENERAL DISCUSSION	159
CHAPTER 9 – REFERENCES	170
Appendices	196

LIST OF FIGURES

Chapter 1

1.1. Functional domains of the human p53 tumour suppressor protein	8
1.2. Functions of p53 ^{WT} following damage to DNA	11
1.3. Genetic components of the apoptotic pathway in <i>Caenorhabditis elegans</i>	14
1.4. Assembly of the Death Receptor complex and activation of caspases	20

Chapter 2

2.1. Set-up of transfer 'sandwich'	35
2.2. Gradient employed for elution of RESOURCE Q anion-exchange column	39
2.3. Liver fractionation scheme	41

Chapter 3

3.1. Fluorescence microscopy of MEL C88 cells	49
3.2. STS-induced internucleosomal cleavage of DNA in MEL C88 cells	50
3.3. STS-induced cell cycle arrest at G ₂ M in MEL C88 cells	51
3.4. Cell cycle distribution of C88 cells following treatment with STS	52
3.5. Internucleosomal cleavage in C88 cells induced by CHX, VP16 and ActD	54
3.6. Effect of CHX, VP16 and ActD on cell cycle in MEL C88 cells	55
3.7. STS-induced internucleosomal cleavage in MEL DP16-1 cells	56
3.8. STS-induced sub-G1 population in MEL DP16-1 cells	57
3.9. STS-induced sub- G1 population in MEL DP16-1 cells	58

Chapter 4

4.1. p53 ^{WT} -induced apoptosis assessed by morphology and CAGE	65
4.2. p53 ^{WT} -induced apoptosis assessed quantitatively by flow cytometry	67
4.3. A 22 h temperature-shift does not induce apoptosis in LTRphe132 or M1 cells	69
4.4. Time-dependent increase in p53 ^{WT} -induced apoptosis	71
4.5. A conformational change in p53 is induced after incubation at 32.5°C	72
4.6. Expression of p53 in M1, LTRphe132 and LTR6 cells	75

4.7. p53 ^{WT} induces apoptosis without an arrest in the cell cycle	76
4.8A. FIGE of LTR6 cells following temperature-shift to the permissive temperature	78
4.8B. FIGE of LTR6 cells following temperature-shift to the permissive temperature in the presence or absence of TLCK	79

Chapter 5

5.1. z-VAD.fmk inhibits p53 ^{WT} -induced internucleosomal cleavage of DNA	87
5.2A. z-VAD.fmk only partially inhibits apoptosis induced by p53 ^{WT}	88
5.2B. Low concentrations of z-VAD.fmk inhibit nuclear condensation	89
5.3. Processing of caspases-3 and -7 accompanies p53 ^{WT} -induced apoptosis	91
5.4. Processing of caspase-8 accompanies p53 ^{WT} -induced apoptosis	92
5.5. Cleavage of PARP and lamin B ₁ accompanies p53 ^{WT} -induced apoptosis	94
5.6. p53 ^{WT} -induced z-DEVD.afc cleavage activity in LTR6 cell lysates	96
5.7. Temperature-shift alone does not induce processing of caspases-3 and -7 or cleavage of PARP and lamin B ₁	98
5.8A. Effect of z-VAD.fmk on processing of caspases-3 and -7	100
5.8B. Effect of z-VAD.fmk on processing of caspase-8	101
5.9. Effect of z-VAD.fmk on proteolysis of PARP and lamin B ₁	103
5.10. Effect of z-VAD.fmk on LTR6 cell lysate cleavage activities	104
5.11. Activities of combined LTR6 cells lysates	104
5.12. Inhibition of z-DEVDafc, z-IETD.amc and Ac-VEID.amc cleavage activities	106
5.13. Caspase-3 and caspase-7 in column fractions	109

Chapter 6

6.1. Preparation of cytosol and P20 pellets	119
6.2. DEVDase activity in fractions from LTR6 cells	121
6.3. Translocation of caspases-3 and -7 from the cytosol	122
6.4. Cleavage of PARP in the absence of processing of caspases-3 and -7	124
6.5. Processing of PARP in isolated nuclei	127
6.6. Processing of caspase-3 and caspase-7 in isolated nuclei	128

Chapter 7

7.1. Fas-induced hepatocyte apoptosis <i>in vivo</i> is inhibited by z-VAD.fmk	136
7.2. Fas-induced mouse liver DEVDase activity is inhibited by z-VAD.fmk	137
7.3. DEVDase activity in subcellular liver fractions	138
7.4. Active caspase-3 is localised in liver cytosol following Fas-induced apoptosis	139
7.5. Active caspase-7 is localised primarily in liver mitochondrial and microsomal fractions following Fas-induced apoptosis	141
7.6. Subcellular distribution of GST π and cytochrome c oxidase subunit IV	143
7.7. Processing of caspase-8 following Fas-induced apoptosis	145
7.8. Cleavage of the endoplasmic reticular-specific substrate SREBP-1	147
7.9. Cleavage activities of caspases-3, -6 and -7	148
7.10. Cleavage of SREBP-1 by recombinant caspases	150

LIST OF TABLES**Chapter 1**

1.1. Morphological and biochemical characteristics of apoptosis and necrosis	3
1.2. Nomenclature and active sites of the caspases	15
1.3. Pro- and anti-apoptotic functions of homologues of bcl2	21
1.4. Caspase substrates and the caspases responsible for their cleavage	23

Chapter 3

3.1. STS does not induce a cell cycle arrest in cycling MEL DP16-1 cells	58
--	----

Chapter 4

4.1. p53 ^{WT} does not induce an arrest in any phase of the cell cycle	74
---	----

Chapter 5

5.1. z-DEVD.afc cleavage activity in confined to temperature-shifted LTR6 cells	99
5.2. Separation of caspase activities following anion-exchange chromatography	107

CHAPTER 1 – INTRODUCTION

1. INTRODUCTION

1.1. Apoptosis

1.1.1. Morphological and biochemical distinctions between apoptosis and necrosis

Apoptosis, a greek word describing the falling of leaves from trees, is a morphological description of an ordered, and tightly controlled mechanism of programmed cell death important in the development of multicellular organisms, maintenance of tissue homeostasis, maturation of the immune response and protection against some of the most incurable human diseases. Unlike necrosis which results from a massive toxic or physical insult in large areas of a tissue or organ, and is characterised by the induction of an inflammatory response and a loss of cellular structure (Kerr, *et al.* 1972), apoptosis occurs in single cells as a result of specific stimuli and is characterised by the ordered altruistic destruction of the condemned cell, generally in the absence of an immune response. Cells undergoing apoptosis characteristically display a contracted morphology with condensed nuclear material and dilatation of the endoplasmic reticulum. The subsequent formation of membrane blebs containing cytoplasmic and nuclear material allows the careful packaging of material from the dead cell and avoids a potentially catastrophic immune response (Kerr, *et al.* 1972; Wyllie, *et al.* 1980; Arends and Wyllie, 1990). Biochemically, apoptosis is associated with changes in membrane permeability, the ordered fragmentation of DNA, initially to large fragments of ≥ 50 kbp (Brown, *et al.* 1993), and then subsequently into fragments of 180–200 bp following the internucleosomal cleavage of DNA (Wyllie, 1980; Arends, *et al.* 1991).

The cleavage of DNA between the nucleosomes has become a hallmark of apoptosis and can be visualised as a ‘laddering’ pattern on agarose gels following electrophoresis, providing a qualitative indication of apoptosis. The identity of the enzyme responsible for the characteristic cleavage of DNA during apoptosis has been much debated, with possible candidates being a $\text{Ca}^{2+}/\text{Mg}^{2+}$ -dependent endonuclease and DNase I (reviewed in Walker, *et al.* 1994). However, given its activation after the irreversible commitment to death, it has also been postulated that an enzyme may be activated which is not specific to the apoptotic process. Most recently, in a murine system, a further candidate has been proposed, caspase activated DNase (CAD; Enari, *et al.* 1998), which cleaves an inhibitory molecule (ICAD) to allow the release of CAD and facilitate the subsequent cleavage of DNA. Importantly, blockade of CAD activity fails to prevent apoptosis, with phosphatidyl serine exposure, caspase-3 activation and

eventual loss of mitochondrial function still occurring. *In vivo*, after the apoptotic processes of proteolysis, condensation of nuclear material and DNA cleavage have occurred, the remains of the dead cell are engulfed by neighbouring macrophages and digested (Duvall, *et al.* 1985; Savill, *et al.* 1990).

Table 1.1. Morphological and biochemical characteristics of apoptosis and necrosis (reviewed in Raffray and Cohen, 1997)

Apoptosis	Necrosis
Endoplasmic reticulum dilatation	
Ordered fragmentation of DNA	Unordered degradation of DNA
Organelles remain largely intact	Cells and organelles swell
Cells shrink	Cells swell
No inflammatory response	Inflammatory response
Single cell phenomenon	Occurs in large areas of tissues/organs
Physiological role	Pathological process

1.1.2. Physiological and pathological importance of apoptosis

The importance of apoptosis both in physiological and pathological circumstances has become apparent. A role for apoptosis in normal physiological processes was recognised as long ago as the middle of the 19th century (reviewed in Clarke and Clarke, 1996). Many organisms in which apoptosis is deficient in some way show signs of aberrant development. For example, the nematode worm develops with more cells than usual (Ellis, *et al.* 1991) and *Drosophila* die prematurely (White, *et al.* 1994). Similarly, in mammals, an intact, functioning apoptotic mechanism is crucial for sculpting digits in the fetus (Milligan, *et al.* 1995; Jacobson, *et al.* 1996), in the creation of lumina (Coucovanis and Martin, 1995) and in the deletion of cells in organs which overproduce them, for example excessive neurones in the brain (Barde, 1989; Oppenheim, 1991). However, perhaps one of the most striking examples of the importance of apoptosis is its role in the development of the immune system. A defective immune system has potentially catastrophic consequences and is avoided by the apoptotic deletion of unproductive or autoreactive B and T cells (Liu, *et al.* 1989). Despite the myriad physiological mechanisms apparently controlled by apoptosis, the reason for such an

interest is perhaps due to the association of inappropriate apoptosis (ie. too much or too little) with many of the most intractable and debilitating of human diseases. Cancer, a disease that claims the lives of a third of the people who develop it, has long since been considered a disease of uncontrolled cell proliferation, whereby cells ‘ignore’ the normal constraints on their growth and proliferate uncontrollably. What is now clear is that while deregulated growth certainly plays a role in tumourigenesis, and is ultimately responsible for neoplasia, the loss of the apoptotic mechanism within damaged cells substantially contributes to the formation of a tumour. In other words, cancer is the result of the combination of insufficient apoptosis and deregulated cell proliferation.

At the other end of the spectrum, excessive apoptosis has been implicated in the pathology of Huntingdon’s disease, Acquired Immune Deficiency Syndrome (AIDS; reviewed in Ameisen, *et al.* 1995) and several neurological disorders including Parkinson’s disease (Hara, *et al.* 1997; Johnson, *et al.* 1996). Thus, a better understanding of the biochemical mechanisms underlying this mode of programmed cell death could go a long way to identifying cellular targets offering therapeutic possibilities. Although we are some way from manipulating the apoptotic pathway to cure the described diseases, apoptosis does have its place in the clinical setting. Chemotherapy remains the mainstay of anti-neoplastic therapy. The reasons behind why tumour cells should be more susceptible to anti-cancer drugs than normal cells remains controversial. The scenario that rapidly dividing cells are more sensitive to the employed DNA-damaging agents is difficult to rationalise as many normal, regenerating tissues proliferate as rapidly as tumours (Waldman, *et al.* 1997). However, regardless of the precise mechanism, many cells which die do so via apoptosis, illustrating another reason for understanding the mechanisms behind the apoptotic pathway.

1.2. Inducers of apoptosis

The potential therapeutic value of an understanding of the mechanisms behind apoptosis is clear, and several classes of agent have been employed in a variety of cell lines in the pursuit of such an understanding. Examples include dexamethasone-induced apoptosis in primary thymocytes (Wyllie, 1980), growth factor withdrawal (Duke and Cohen, 1986; Ishizaki, *et al.* 1995), staurosporine-induced apoptosis in many cell lines (Bertrand, *et al.* 1994; Jacobson, *et al.* 1996; Weil, *et al.* 1996; Jarvis, *et al.* 1994), ceramide (Martin, *et al.* 1995; Mizushima, *et al.* 1996; reviewed in Skowronski, *et al.*

1996), calcium ionophores (Shi, *et al.* 1989), thapsigargin (Jiang, *et al.* 1994), crosslinkage of certain cell surface receptors (Ogasawara, *et al.* 1993; Itoh, *et al.* 1991) and DNA-damaging agents such as etoposide (Walker, *et al.* 1991; Fearnhead, *et al.* 1995a) and γ -irradiation (Lowe, *et al.* 1993b; Clarke, *et al.* 1993).

1.2.1. Apoptosis induced by staurosporine

Staurosporine, a naturally occurring microbial alkaloid first isolated from *Streptomyces staurosporeus* (Omura, *et al.* 1977), was initially described as an inhibitor of protein kinase C (PKC; Tamaoki, *et al.* 1986), through its strong association with the catalytic subunit. However, it has subsequently been identified as a non-specific inhibitor of many protein kinases at physiologically relevant concentrations (Kiyoto, *et al.* 1987; Nakano, *et al.* 1987), and is regarded as a universal inducer of apoptosis (Jarvis, *et al.* 1994; Jacobson, *et al.* 1996). Staurosporine induces apoptosis in a variety of nucleated cells without the requirement of protein synthesis (Jacobson, *et al.* 1996), as evidenced by the induction of the apoptotic phenotype in the presence of the protein translation inhibitor cycloheximide. This suggested that the apoptotic machinery preexists within cells, an hypothesis which has been supported by others (Fearnhead, *et al.* 1995b). However, in other systems this is apparently not the case as the use of inhibitors of protein synthesis prevents the induction of apoptosis (Duke and Cohen, 1986; Martin, *et al.* 1988; Oppenheim, *et al.* 1990). In addition, cycloheximide and the transcription inhibitor actinomycin D, which intercalates between 2 G/C base pairs and binds to the narrow groove of DNA, have both been shown to induce apoptosis in some systems (Onishi, *et al.* 1993; Bicknell, *et al.* 1994). Thus apoptosis in different systems may or may not depend on *de novo* synthesis of proteins.

1.2.2. Apoptosis induced by receptor cross-linkage

Apoptosis can be induced both *in vivo* and *in vitro* by a variety of different stimuli. One of the best characterised *in vivo* models is Fas-induced hepatocyte apoptosis in mice (Ogasawara, *et al.* 1993). Crosslinking of the Fas/APO-1/CD95 receptor with the Fas ligand (FasL) or an agonistic antibody leads to trimerisation of the Fas receptor and initiation of the intracellular events that culminate in the apoptotic phenotype (Trauth, *et al.* 1989; Yonehara, *et al.* 1989; Itoh, *et al.* 1991). Thus, mice injected with an anti-Fas antibody show rapid induction of liver destruction, with hepatocytes displaying

morphology consistent with apoptosis, and animals are typically dead within a few hours of exposure. The Fas receptor is a type I membrane receptor belonging to the TNF receptor (TNFR) family (Itoh *et al.* 1991; Oehm *et al.* 1992; Nagata and Golstein, 1995), and possesses three cysteine-rich domains in its extracellular region, a hydrophobic region which spans the plasma membrane and an intracellular domain containing a stretch of 80 amino acids with considerable homology to the corresponding sequence in TNFR-1, which is responsible for transduction of the death signal (section 1.4.2.6).

1.2.3. Apoptosis induced by DNA-damaging agents

To reduce the chances of neoplasia, it is essential for cells that have sustained damage to their DNA to either have it repaired or be prevented from dividing and perpetuating the mutation. One way this can be achieved is by eliminating the cells via apoptosis. Many classes of DNA-damaging agent induce apoptosis. The chemotherapeutic agent etoposide (VP16), which prevents the uncoiling of supercoiled DNA by inhibition of topoisomerase II, induces apoptosis in immature thymocytes (Walker, *et al.* 1991), in human leukaemic U937 cells (Bicknell, *et al.* 1994) and in human monocytic THP.1 cells (Zhu, *et al.* 1995). Ionising radiation causes DNA strand breaks and results in apoptosis in immature thymocytes (Clarke, *et al.* 1993; Lowe, *et al.* 1993b). Of particular interest is the observation that DNA-damaging agents usually require the presence of a specific protein to induce apoptosis. This protein is the nuclear phosphoprotein, p53 (Clarke, *et al.* 1993; Lowe, *et al.* 1993b).

1.3. p53

1.3.1. Identification and characterisation of p53

p53 was originally isolated as a 53 kDa protein bound to the large tumour antigen (T-ag) in simian virus 40 (SV40) transformed cells (Lane and Crawford, 1979). Subsequently it was designated a tumour suppressor gene based on observations that it is mutated in over half of all human tumours (Hollstein, *et al.* 1991) and that mice which do not contain a functional p53 protein, after initially developing normally, go on to develop an excessive number of neoplastic lesions (Donehower, *et al.* 1992). Hence, wild-type p53 (p53^{WT}) may be considered as a tumour suppressor protein, whereas the p53 null genotype, or the possession of a mutant protein, may be considered oncogenic. However, the situation is, in reality, more complicated. The conferred phenotype depends in many

cases on the precise nature of the p53 mutation, and ranges from loss of growth suppressing properties to a discernible induction of oncogenic characteristics (Zambetti and Levine, 1993). Thus, there is considerable variation between cells that contain no mutant p53 protein and cells where p53 is present, but contains a point mutation.

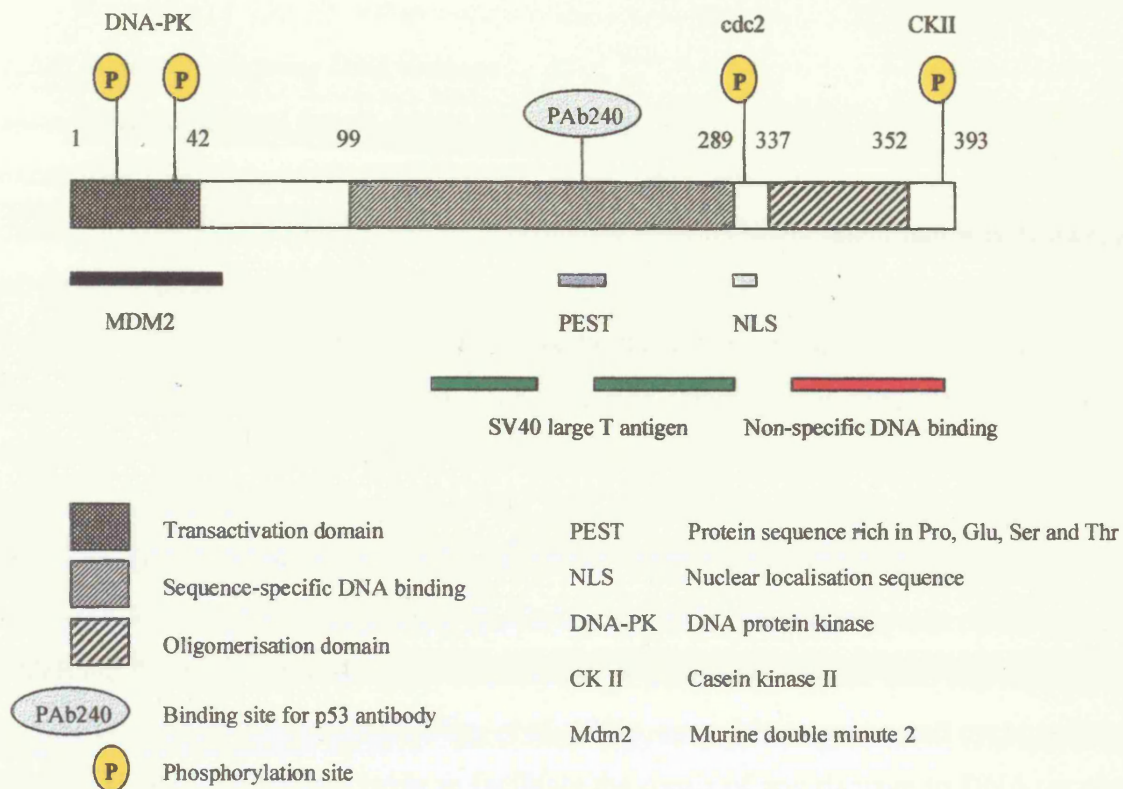
Whereas mutated, non-functional tumour suppressor genes such as p53 and the retinoblastoma (Rb) protein are a feature of many cancerous lesions, the deregulated, increased expression of other proteins such as c-Myc and bcl2 contributed substantially to the neoplastic phenotype. The elevated expression of these so-called 'dominant protooncogenes' is apparent in virtually all tumours (Spencer and Groudine, 1991). Thus, while p53 mutation is the most common single event in tumour development, many factors ultimately act in concert to cause neoplasia.

1.3.2. Protein structure of p53

The human and murine p53 proteins contain 393 and 390 amino acids, respectively, and in each case are encoded by a gene consisting of 11 exons (the first of which is non-coding (reviewed in Soussi, *et al.* 1990). An important functional feature of p53 is its phosphorylation by various kinases at different sites along the length of the p53 molecule, although the functional significance of p53 phosphorylation is poorly understood. The overall phosphorylation state of the p53 protein is lower in the G0/G1 phase of the cell cycle, compared with S phase (Bischoff, *et al.* 1990).

The p53 protein contains several relatively well-defined functional domains, the most important of these being a transactivation domain (amino acids 1–42; Unger, *et al.* 1992), a sequence-specific DNA binding domain (amino acids 99–289; Pavletich, *et al.* 1994), a nuclear localisation sequence (NLS; amino acids 310–319; Addison, *et al.* 1990; Shaulsky, *et al.* 1990) and an oligomerisation domain (amino acids 337–352; Stürzbecher, *et al.* 1992). The functional domains of human p53, together with some of the more important phosphorylation sites within the molecule are shown schematically in Fig. 1.1.

Fig. 1.1. Functional domains of the human p53 tumour suppressor protein



1.3.3. Function in normal cells

In normal cells the half-life of the p53 protein is 20–40 minutes. Levels of p53 change at different stages of the cell cycle, rising as the cell cycle progresses and peaking at late G1, just as the cell is entering into S phase. The rapid degradation of p53 following completion of S phase of the cell cycle, is thought to correlate with the non-exposure of PEST sequences (sequences rich in proline, glutamate, serine and threonine). Conversely p53 displaying PEST sequences is not rapidly degraded (Crook and Vousden, 1992). PEST sequences are thought to target normally short-lived proteins for degradation by the ubiquitin-proteasome pathway, and removal of this sequence results in an abnormal build-up of p53 protein (Unger, *et al.* 1993).

A prolonged p53-induced arrest at the G0/G1 interface caused by the build up of p53 in late G1, allows time for damage to DNA to be repaired and restricts the passage of damaged genes to daughter cells. In addition, this mechanism may have a role to play in preventing the birth of defective offspring, since mice irradiated while pregnant produce

fewer offspring, but the offspring which are produced show very little increased incidence of birth defects (Norimura, *et al.* 1996).

1.3.4. Function following DNA damage

DNA-damaging agents were described in section 1.2.5. Although there are exceptions (Strasser, *et al.* 1994; Bracey, *et al.* 1995; MacFarlane, *et al.* 1996), DNA-damaging compounds induce apoptosis primarily via a p53-dependent pathway (Lowe, *et al.* 1993b; Clarke, *et al.* 1993).

The p53 protein has been described as the ‘Guardian of the Genome’ (Lane, 1992). Following DNA damage caused by agents such as ionizing radiation, UV light and the topoisomerase II inhibitor etoposide (VP16), transiently increased levels of p53^{WT} can be detected. It has been proposed that the p53 response is initiated via recognition of damaged DNA by the C-terminal domain of the protein, which then results in an increased level of intracellular p53 (Reed, *et al.* 1995). Increased levels of the protein which are due to post-translational stabilisation of the protein, rather than any increase in its transcription or translation (Kastan, *et al.* 1991), may either cause a cell cycle arrest at the G0/G1 phase of the cell cycle to facilitate the repair of any damage to DNA, or may lead to the demise of the cell by apoptosis (Yonish-Rouach, *et al.* 1991). In addition to well documented evidence for the role in p53 in the induction a cell cycle arrest at G0/G1 there is some data to support the participation of p53 at the G₂M phase of the cell cycle. Using REF52 cells transfected with temperature-sensitive p53val¹³⁵ a shift in temperature (inducing a conformation change in p53 from mutant to wild-type) caused a cell cycle arrest at both G0/G1 and G₂M, although the arrest at G0/G1 was more marked (Stewart, *et al.* 1995).

1.3.5. Induction of apoptosis

A useful tool in the study of the different cellular functions of p53 has been the use of the temperature-sensitive mutant p53 protein. The temperature-sensitive p53 gene contains a mutation which results in an amino acid substitution from alanine to valine at position 135 of the encoded protein, which shows mutant characteristics at the restrictive temperature of 37.5–39°C, but is indistinguishable from the wild-type protein at 32.5°C (Milner and Medcalf, 1990). p53 null M1 cells transfected with the gene encoding the

above temperature-sensitive p53 protein have been shown to undergo apoptosis when incubated at the permissive temperature for several hours (Yonish-Rouach, *et al.* 1991).

Interestingly, p53^{WT}-induced apoptosis in this system occurs independently of a cell cycle arrest at G0/G1 (Yonish-Rouach, *et al.* 1993), suggesting a certain degree of dissociation between the cell cycle checkpoint and the onset of apoptosis. In support of this, others have shown that in murine erythroleukaemic (MEL) cells, the cytokines erythropoietin and IL-3, while effectively inhibiting p53^{WT}-induced apoptosis, have no effect on the imposed cell cycle arrest at G0/G1 (Lin and Benchimol, 1995). However, the lack of a cell cycle arrest in p53^{WT}-induced apoptosis in M1 cells may equally be the result of the over-expression of the p53^{WT} overwhelming the cell with a negative growth signal, and causing it to undergo apoptosis.

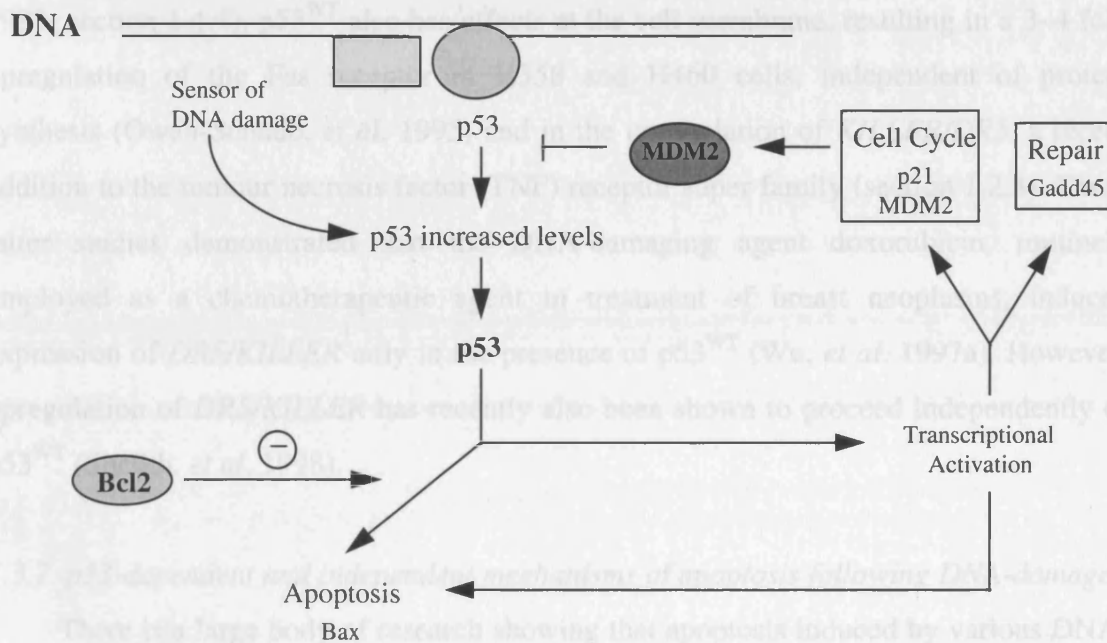
1.3.6. The role of p53^{WT} as a transcription factor

Inherent in the role of p53^{WT} in both the control of cell cycle progression and the induction of apoptosis is its function as a transcription factor. The promoter regions of several genes, involved both in the progression of the cell cycle and apoptosis, possess a consensus binding sequence for the p53^{WT} protein. The consensus binding sequence consists of two stretches of the nucleotide sequence 5'-PuPuPu C (A/T) (A/T) G PyPyPy-3', separated by up to 13 bp (El-Deiry, *et al.* 1992) and sequence-specific binding of p53^{WT} at the promoter region of the target gene results in either transcriptional activation or repression. Since mutations in the p53 protein usually occur in the region of the protein involved in the sequence-specific binding of DNA (amino acids 99–289; Harris, 1993), a feature of mutant p53 proteins is the inability to transcriptionally activate or repress target genes. The N-terminal transactivating domain and the central sequence-specific DNA binding domains (Fig. 1.1) function together to *transactivate* and *transrepress* several genes involved in controlling cell cycle progression and inducing apoptosis (Fig. 1.2).

p53^{WT} *transactivates* *GADD45* (growth arrest and DNA damage 45) resulting in a growth arrest at G0/G1 phase of the cell cycle, as well as the promoter of *mdm2* (murine double minute 2). The 90 kDa oncogenic product of the *mdm2* gene forms a complex with p53 via a specific sequence at its N-terminus (Böttger, *et al.* 1997; Kussie, *et al.* 1996) and is thought to be a key negative regulator of p53 function (Wu, *et al.* 1993). Indeed, recently the association of Mdm2 with p53 has been shown to target p53 for

degradation by the ubiquitin-dependent proteasome pathway and thus lead to the termination of the anti-proliferative and apoptosis-inducing effects of p53 (Haupt, *et al.* 1997; Kubbutat, *et al.* 1997). The observation that p53 accumulates in cells with a defective ubiquitin pathway (Chowdary, *et al.* 1994) further supports regulation of the protein levels in this manner.

Fig. 1.2. Functions of p53^{WT} following damage to DNA



In independent studies the gene *Waf1/Cip1* was also identified as a target for transcriptional activation by p53 (El-Deiry, *et al.* 1993; Xiong, *et al.* 1993). The p21 protein product of this gene has been shown to inhibit members of the cyclin/cdk family and to suppress the growth of various human tumour cells *in vitro* (Xiong, *et al.* 1993), although there is some evidence that this gene is not required for p53-mediated apoptosis (Caelles, *et al.* 1994). The p53^{WT}-induced accumulation of the proteins described above may have different roles to play depending on the phase of the cell cycle during which the DNA damage occurs. DNA damage prior to S phase would inhibit cdk activity via p21 upregulation to block cell cycle progression. However, following DNA damage after the initiation of S phase, p21 blocks DNA replication by binding to proliferating cell nuclear antigen (PCNA; Luo, *et al.* 1995), thereby preventing PCNA-mediated activation

of the δ -subunit of DNA polymerase. Prevention of these checkpoint mechanisms through the inability of faulty p53 to initiate cell cycle checks would allow replication to proceed unmonitored and facilitate cell division in the presence of damaged DNA. In turn this could lead to the accumulation of mutations and chromosomal aberrations and an increased tumourigenic potential.

Sequence-specific binding of DNA by p53 increases transcription from the *bax* promoter and decreases transcription from the *bcl2* promoter (Miyashita, *et al.* 1994), ultimately increasing the Bax:Bcl2 protein ratio in favour of apoptosis (Oltvai, *et al.* 1993; section 1.4.4). p53^{WT} also has effects at the cell membrane, resulting in a 3–4 fold upregulation of the Fas receptor in H358 and H460 cells, independent of protein synthesis (Owen-Schaub, *et al.* 1995) and in the upregulation of *KILLER/DR5*, a recent addition to the tumour necrosis factor (TNF) receptor super family (section 1.2.3). These latter studies demonstrated that the DNA-damaging agent doxorubicin, routinely employed as a chemotherapeutic agent in treatment of breast neoplasms, induced expression of *DR5/KILLER* only in the presence of p53^{WT} (Wu, *et al.* 1997a). However, upregulation of *DR5/KILLER* has recently also been shown to proceed independently of p53^{WT} (Sheikh, *et al.* 1998).

1.3.7. p53-dependent and independent mechanisms of apoptosis following DNA-damage

There is a large body of research showing that apoptosis induced by various DNA-damaging agents is mediated by p53 (Lowe, *et al.* 1993b; Clarke, *et al.* 1993). However, there are equally some examples of apoptosis induced by DNA-damaging agents which apparently do not depend on a functional p53 protein (reviewed in Liebermann, *et al.* 1995).

One study showed that although lymphocytes from p53^{-/-} mice were radioresistant as one would expect, cycling lymphoma cells and activated T lymphocytes from the same animals remained apoptosis-proficient when irradiated or treated with genotoxic drugs (Strasser, *et al.* 1994), supporting the existence of at least one other mediator of DNA-damaging agent-induced apoptosis. Another study showed that while DNA-damaging agents induced apoptosis via a p53-dependent pathway in immature thymocytes and mature peripheral T-cells, the same agents were also capable of inducing p53-independent apoptosis in a specific subpopulation of immature thymocytes (MacFarlane, *et al.* 1996). Further studies demonstrated that while γ -irradiation failed to

arrest p53 null colorectal tumour cell lines in G1, the cells remained apoptosis-proficient despite their p53-null status (Bracey, *et al.* 1995).

There is also evidence that p53-dependent and independent mechanisms of apoptosis may cooperate in some cellular systems. One study showed that p53 null M1/2 cells can undergo p53-independent apoptosis following growth factor deprivation and p53-mediated apoptosis following reconstitution of p53^{WT} (Peled, *et al.* 1996). The p53-dependent pathway to apoptosis proceeded more rapidly than the p53-independent one, although induction of the pathways together further accelerated apoptosis, suggesting that at least some aspects of the two pathways are mutually exclusive.

1.4. Genetic control of apoptosis

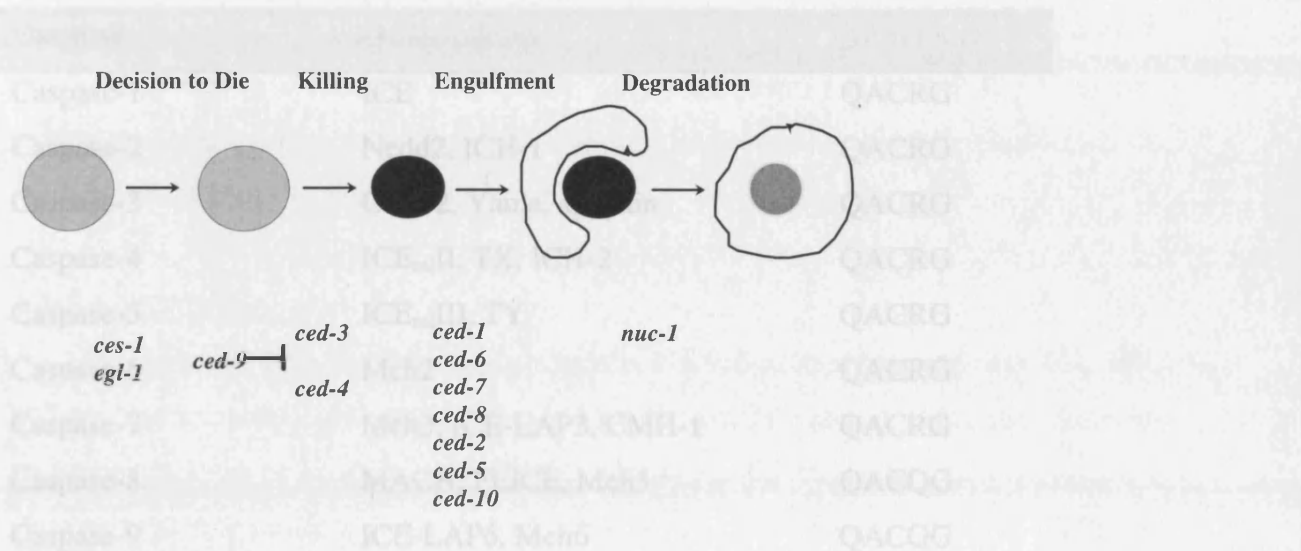
Despite the diversity of the apoptotic stimuli described in the sections above, they all precipitate the same dramatic apoptotic morphology. Consistent with this, the emerging tenet from all these studies is that the manifestation of the apoptotic phenotype is achieved through the activation of a central, common, evolutionarily conserved, genetically controlled executionary pathway.

1.4.1. The apoptotic pathway in the nematode worm *Caenorhabditis elegans*

The biochemical and morphological events which occur during apoptosis have been genetically studied in the nematode worm *Caenorhabditis elegans*. During the development of *C. elegans*, a precisely defined pattern of apoptosis occurs. Of the 1090 cells which comprise the immature organism, the same 131 are destined to die in each animal (Ellis, *et al.* 1991). To date several genes have been identified within this organism which have been assigned specific roles in the apoptotic process. For the majority of these genes mammalian homologues have yet to be identified. *Ced-1*, -2, -5, -6, -7, -8 and -10 (for cell death abnormal genes 1, 2, 5, 6, 7, 8 and 10, respectively) are involved in the engulfment and digestion of apoptotic neighbours (Ellis, *et al.* 1991; Fig. 1.3). Other genes are involved in the specification of apoptosis (*ces-1*, *egl-1*) and thus presumably encode the gene products which form the most apical components of the apoptotic pathway in the nematode worm. The most extensively studied genes have been those identified as having mammalian homologues, namely *ced3*, *ced4* and *ced9*. *Ced3* and *ced4* are absolutely required for cell death in the 131 designated cells, and their mutation results in fewer cells dying (Ellis and Horvitz, 1986). Conversely *ced9* is

required for the survival of the remaining 959 cells and any loss in function results in excessive cell death in cells otherwise destined to survive. An outline of the apoptotic pathway of the nematode worm is shown in Fig. 1.3.

Fig. 1.3. Genetic components of the apoptotic pathway in *Caenorhabditis elegans*



1.4.2. Mammalian homologues of *Ced3* – the caspases

The identification of *ced3*, a gene absolutely required for the apoptotic pathway to proceed in designated cells of the nematode worm, induced researchers to search for mammalian homologues. A high degree of homology was observed between the *ced3* protein and the mammalian interleukin-1 β -converting enzyme (ICE; 29% sequence identity), an enzyme responsible for the processing of inactive prointerleukin-1 β (proIL-1 β) to the mature proinflammatory cytokine IL-1 β (Black, *et al.* 1989; Kostura, *et al.* 1989). From these studies it became apparent that unlike the nematode worm, where *ced3* is the only 'aspartase' identified to date, mammals contain several *ced3* homologues, of which at least nine, in addition to ICE, have now been identified; CPP32/Apopain (Fernandes-Alnemri, *et al.* 1994; Nicholson, *et al.* 1995), Mch2 (Fernandes-Alnemri, *et al.* 1995a), NEDD2/Ich1 (Kumar, *et al.* 1994; Wang, *et al.* 1994a), Ich2/TX (Kamens, *et al.* 1995; Faucheu, *et al.* 1995), Mch3/ICE-LAP3 (Fernandes-Alnemri, *et al.* 1995b; Duan, *et al.* 1996a), Mch6/ICE-LAP6 (Duan, *et al.* 1996b; Srinivasula, *et al.* 1996), MACH/FLICE/Mch5 (Boldin, *et al.* 1996; Muzio, *et al.* 1996; Fernandes-Alnemri, *et al.* 1996) and Mch4 (Fernandes-Alnemri, *et al.* 1996). The simultaneous identification of the same homologues independently by different groups, led to confusion in their

nomenclature and resulted in the adoption of the trivial name ‘caspase’ (for cysteine aspartate protease; Alnemri, *et al.* 1996; Table 1.2).

Table 1.2. Table of nomenclature and active sites of the caspases (modified from Cohen, 1997)

Caspase	Other names	Active site
Caspase-1	ICE	QACRG
Caspase-2	Nedd2, ICH-1	QACRG
Caspase-3	CPP32, Yama, apopain	QACRG
Caspase-4	ICE _{rel} II, TX, ICH-2	QACRG
Caspase-5	ICE _{rel} III, TY	QACRG
Caspase-6	Mch2	QACRG
Caspase-7	Mch3, ICE-LAP3, CMH-1	QACRG
Caspase-8	MACH, FLICE, Mch5	QACQG
Caspase-9	ICE-LAP6, Mch6	QACGG
Caspase-10	Mch4	QACQG

1.4.2.1. General properties of caspases

As their name would suggest, caspases are a family of aspartate-specific cysteine proteases, which pre-exist in the cytoplasm as single chain inactive zymogens (reviewed in Cohen, 1997; Nicholson and Thornberry, 1997). The inactive caspase precursors are proteolytically processed to produce a small (~10 kDa) and a large (~20 kDa) subunit, two each of which combine to form the active tetrameric enzyme. Caspases may be divided into ‘initiator’ caspases with long prodomains (caspases-8, -9 and -10), which activate ‘effector’ caspases with short prodomains (caspases-3, -6 and -7), which in turn cleave intracellular substrates resulting in the dramatic morphological and biochemical changes of apoptosis (reviewed in Cohen, 1997; Nicholson and Thornberry, 1997; Fraser and Evan, 1996).

The active site cysteine residue is contained within the consensus sequence QACXG, where X is R, Q or G (Table 1.2), on the larger of the two subunits, although additional amino acids located on both the large and small subunits, contribute to the

active site of the enzyme (Wilson, *et al.* 1994). The caspases themselves cleave at the C-terminal side of aspartate residues, consistent with only one other mammalian enzyme, granzyme B, and providing the possibility of autoprocessing and/or the processing and activation of one caspase by another.

The caspases can be phylogenetically divided into three subfamilies; those most similar to ICE (caspases-1, -4 and -5), those most similar to ced3 and CPP32 (caspases-3, -6, -7, -8, -9 and -10) and the NEDD2 sub-family (Caspase-2). Although it is clear that several homologues have been identified to date in mammalian cells, only caspases-1, -3, -6, -7 and -8 will be discussed in more detail here.

1.4.2.2. ICE/Caspase-1

Procaspase-1 is a 45 kDa protein which is cleaved at aspartate residues 103, 119, 297 and 316 to produce a large (20 kDa) and small (10 kDa) subunit which combine with two other subunits to produce the (p20/10)² tetrameric active enzyme. Active caspase-1 requires aspartate residues in the P₁ position of its substrates together with an additional three amino acids in positions P₂–P₄. Diverse amino acids can be tolerated in positions P₂ and P₃, however, caspase-1 has a strong preference for tyrosine in the P₄ position, consistent with the cleavage site in its physiological substrate proIL1-β. Despite early studies demonstrating induction of apoptosis in Rat-1 fibroblasts by caspase-1 over-expression (Miura, *et al.* 1993), the involvement of caspase-1 in apoptosis is unclear. Mice which do not have caspase-1 develop normally, are healthy and fertile and show no dysfunction in any physiological apoptotic processes. Only Fas-induced apoptosis seems to be less responsive in caspase-1^{-/-} mice than in their normal counterparts (Kuida, *et al.* 1995; Li, *et al.* 1995).

1.4.2.3. CPP32/Yama/Apopain/Caspase-3

Caspase-3, one of the main effector caspases in the apoptotic pathway, was identified after searching expressed sequence tag (EST) databases with DNA sequences spanning the active site of caspase-1 and ced3 (Fernandes-Alnemri, *et al.* 1994). Caspase-3 is present in normal cells as an inactive 32 kDa zymogen, which requires initial processing at Asp¹⁷⁵, followed by processing at Asp⁹ or Asp²⁸ to yield a large subunit (19 or 17 kDa, respectively) and a smaller 12 kDa subunit (Nicholson, *et al.* 1995; Fernandes-Alnemri, *et al.* 1994). The active enzyme shares the same general

structure as caspase-1, with two 17 kDa and two 12 kDa subunits associating to form the holoenzyme, termed apopain (Nicholson, *et al.* 1995). Although only the quaternary structures of caspase-1 and caspase-3 have been determined, it is anticipated that the same structure is shared by all the caspases.

While caspase-1 and caspase-3 have similar structures, they have different substrate specificities. Caspase-3, like caspase-1 has an absolute requirement for an aspartate residue in the P₁ position, but its preferred tetrapeptide cleavage sequence is DXXD, consistent with its substrate poly (ADP-ribose) polymerase (PARP; section 1.5.1). In contrast to caspase-1^{-/-} mice, caspase-3^{-/-} mice fail to develop normally and die prematurely. In particular, mice deficient in caspase-3 show severely impaired brain development (Kuida, *et al.* 1996).

Murine homologues of caspase-3 have also been identified (Juan, *et al.* 1996). The sequences show > 80% identity with the human homologue, with the consensus sequence containing the active site cysteine being entirely conserved, together with the tetrapeptide cleavage site at the p17/p12 junction. Notably, however, the tetrapeptide at the prodomain/p17 junction, which is ESMD in the human homologue, is KSVD and KSMD in the mouse and rat homologues, respectively (Juan, *et al.* 1996).

1.4.2.4. Mch3/ICE-LAP3/Caspase-7

Using the same methodology employed for the isolation of caspase-3, researchers independently identified a further homologue, caspase-7 (Fernandes-Alnemri, *et al.* 1995b; Duan, *et al.* 1996). Like the other caspases, caspase-7 exists in normal cells as an inactive 35 kDa precursor which is activated first via cleavage at Asp¹⁹⁸ and then at Asp²³, to produce large and small subunits of 19 kDa and 12 kDa, respectively. Caspase-7 shows a high homology with caspase-3 (52% identity), and interestingly, active heteromeric enzymes can be engineered by combining the small subunit of caspase-3 and the large subunit of caspase-7, and vice versa (Fernandes-Alnemri, *et al.* 1995b). Consistent with this is the preference of caspase-7 to cleave the tetrapeptide sequence DXXD and the substrate PARP with an activity which is virtually indistinguishable from that of caspase-3 (Fernandes-Alnemri, *et al.* 1995b).

1.4.2.5. Mch2/Caspase-6

Caspase-6 is found in normal cells as a proform of approximately 34 kDa (Fernandes-Alnemri, *et al.* 1995a), which is processed by recombinant caspase-3, initially at Asp¹⁷⁹ and subsequently at Asp¹⁹³ and Asp²³ to yield subunits of 18 kDa and 11 kDa (Srinivasula, *et al.* 1996). Active, tetrameric caspase-6 effectively cleaves the sequence VEID↓N, consistent with its ability to proteolytically cleave nuclear lamins (Takahashi, *et al.* 1996; Orth, *et al.* 1996; section 1.5.2). In addition to the *in vitro* cleavage of caspase-6 by caspase-3, procaspase-6 has also been shown to be cleaved and activated by the cytotoxic enzyme granzyme B (Orth, *et al.* 1996).

1.4.2.6. MACH/FLICE/Mch5/Caspase-8

Apoptosis induced by cross-linkage of the Fas and TNFR1 receptors proceeds in the absence of *de novo* protein synthesis, suggesting the preexistence of all the necessary components (Yonehara, *et al.* 1989; Itoh, *et al.* 1991). Fas-induced apoptosis *in vivo* (Rodriguez, *et al.* 1996; Rouquet, *et al.* 1996; Küntzle, *et al.* 1997) and *in vitro* (Enari, *et al.* 1995; Chow, *et al.* 1995; Schlegel, *et al.* 1995; Armstrong, *et al.* 1996; Schlegel, *et al.* 1996; Kamada, *et al.* 1997) has been shown to involve the activation of caspases. The independent isolation of caspase-8 by two groups (Muzio, *et al.* 1996; Boldin, *et al.* 1996) provided the first physical link between the receptors at the cell membrane and the effector caspases which comprise the intracellular executionary apparatus of apoptosis. Using the yeast two hybrid system, the intracellular death domain of Fas (Itoh and Nagata, 1993; Tartaglia *et al.*, 1993) was found to associate with FADD (Fas-associating protein with death domain)/MORT1 via interaction with a homologous death domain at its C-terminus (Boldin *et al.* 1995; Chinnaiyan *et al.* 1995; Kischkel, *et al.* 1995). The N-terminal domain of FADD is able to induce apoptosis and has subsequently been termed the death effector domain (DED). It is through homologous association with this domain that caspase-8, is recruited to the death-inducing signalling complex (DISC; Boldin, *et al.* 1996; Muzio, *et al.* 1996).

The intracellular domain of TNFR1 similarly associates with an adaptor molecule, TRADD (TNFR1-associating protein with death domain; Hsu, *et al.* 1995), however, this does not directly interact with caspase-8 but requires a further association with FADD. Thus, both Fas and TNFR1 associate with FADD, either directly or indirectly, to facilitate the recruitment and activation of caspase-8. The cytoplasmic domain of TNFR1

also associates with RIP (Stanger, *et al.* 1995) via TRADD (Hsu, *et al.* 1996). RIP has been shown to induce apoptosis when overexpressed, and despite being isolated as a FADD-binding protein has a strong preference for TRADD. Indeed, RIP has been shown to be required for the mediation of TNF- but not Fas-induced apoptosis (Ting, *et al.* 1996). RIP in turn binds, via homologous domains, to CRADD (caspase and RIP adaptor with death domain)/RAIDD (RIP-associating Ich1/Ced3-homologous protein with death domain) which recruits caspase-2 to the complex via caspase-homologous regions towards its N-terminus (Ahmad, *et al.* 1997; Duan and Dixit, *et al.* 1997). Thus, caspase-2 and caspase-8 are recruited to the receptor-associated signalling complexes.

Caspase-8 itself exists in control cells as two isoforms (caspase-8a and -8b) of approximately 55 kDa (Scaffidi, *et al.* 1997) and contains two DED domains towards its N-terminus and possesses significant homology to ced-3 and members of the CPP32 subfamily of caspases at its C-terminus. Caspase-8 is activated following cleavage at Asp²¹⁰, Asp²¹⁶, Asp³⁷⁴ and Asp³⁸⁴ to yield large and small subunits of 18 kDa and 12 kDa, respectively (Muzio, *et al.* 1996; Boldin, *et al.* 1996). The observation that recombinant caspase-8 cleaves caspase-3 (Boldin, *et al.* 1996) provides a link between caspase-8 and the effector caspases at the heart of the executionary pathway. However, recombinant caspase-8 has been shown to cleave all other caspases identified to date, which places it at the apex of the caspase cascade (Fig. 1.4; Fernandes-Alnemri, *et al.* 1996; Srinivasula, *et al.* 1996).

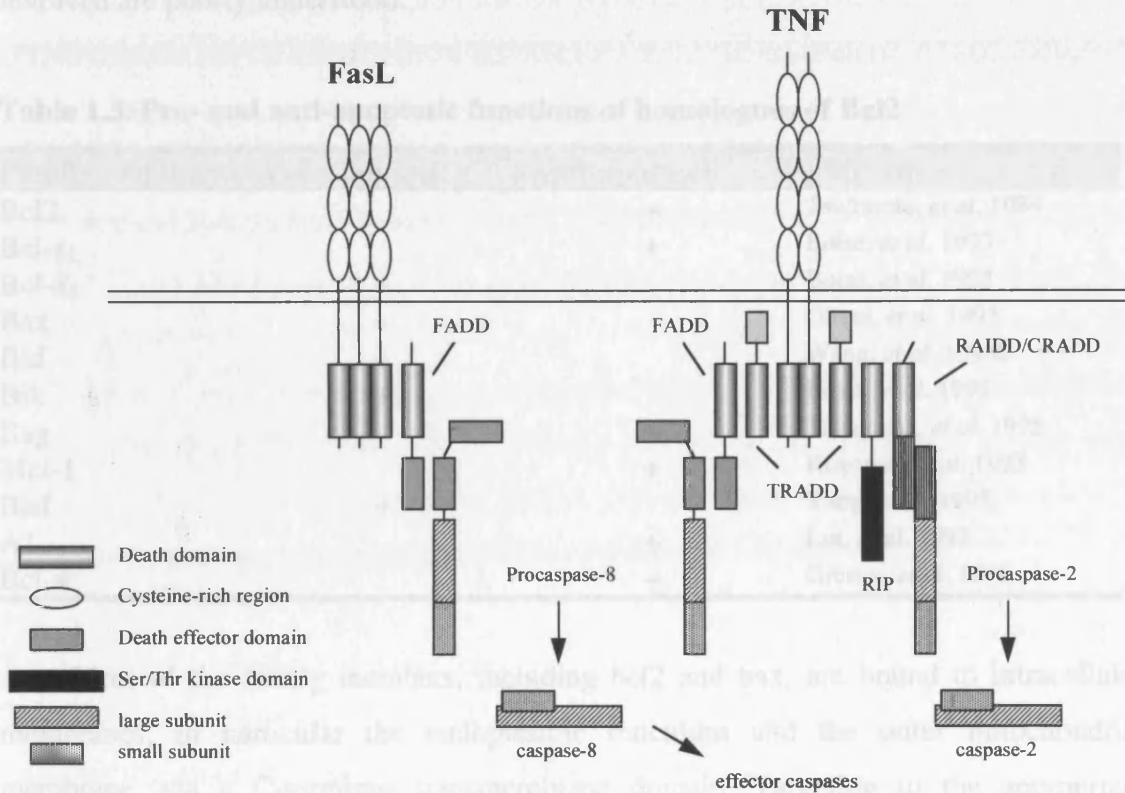
1.4.3. Other members of the TNFR1 family

In addition to FasL and TNF α , the role of other members of this family of ligands and their corresponding receptors in apoptosis has been studied. TRAIL/APO-2L induces apoptosis in a number of tumour cell lines (Wiley, *et al.* 1995; Pitti, *et al.* 1996; Marsters, *et al.* 1996), independently of FADD (Marsters, *et al.* 1996). TRAIL cross-links with several receptors belonging to the TNFR1 family. Interestingly, several groups have independently identified two receptors for this cytotoxic ligand. Of most note was the observation that while the first receptor, designated DR5/KILLER/TRICK2 (Pan, *et al.* 1997a; Sheridan, *et al.* 1997; MacFarlane, *et al.* 1997b; Wu, *et al.* 1997a; Screaton, *et al.* 1997), possessed the conserved 80 amino acid intracellular domain present in both the Fas and TNFR1 receptors, and similarly transduced the death signal, the second, TRID/DcR1/TRAIL-R3, lacked this domain and correspondingly failed to transduce the

death signal (Pan, *et al.* 1997b; Sheridan, *et al.* 1997; MacFarlane, *et al.* 1997b). These findings offer therapeutic possibilities as tumour cells express higher levels of the death domain-containing receptor than normal cells and are consequently more susceptible to TRAIL (reviewed in Guru, 1997).

In addition, the death-transducing proficient *DR5/KILLER/TRICK2* receptor is upregulated by DNA-damaging agents in a p53^{WT}-dependent manner (Wu, *et al.* 1997a). Thus, ligation of the Fas, TNFR1 and DR5 receptors at the cell surface can transduce the death signal into the cell which is then perpetuated through the interaction of homologous domains in key proteins, and results in the morphological and biochemical features of apoptosis.

Fig.1.4. Assembly of the Death Receptor complex and activation of caspases



1.4.4. Mammalian homologues of *Ced9* – the *Bcl2* family

As described in section 1.4.1, disruption of the *ced9* gene results in excessive cell death in *C. elegans*, consistent with a role for this gene in preventing apoptosis. The mammalian homologue of *ced9*, *bcl2*, was first identified at the chromosomal breakpoint of t(14:18)-bearing B cell lymphomas (Tsujimoto, *et al.* 1984), and the 26 kDa protein product has since been shown to prevent apoptosis in mammalian cells induced by a number of different stimuli, acting upstream of the activation of the caspases (Chinnaiyan, *et al.* 1996). Since the identification of *bcl2*, several homologues have been isolated, some of which, such as *bcl_{xL}* have similar anti-apoptotic effects, and some, such as *bax*, which are proapoptotic (Table 1.3). Although the family members are thought to function via their ability to form homo- and heterodimers, with the relative levels of pro- and anti-apoptotic homologues influencing the fate of the cell, the precise mechanisms involved are poorly understood.

Table 1.3. Pro- and anti-apoptotic functions of homologues of *Bcl2*

Family member	Pro-apoptotic	Anti-apoptotic	References
Bcl2		+	Tsujimoto, <i>et al.</i> 1984
Bcl-x _L		+	Boise, <i>et al.</i> 1993
Bcl-x _S	+		Boise, <i>et al.</i> 1993
Bax	+		Oltvai, <i>et al.</i> 1993
Bid	+		Wang, <i>et al.</i> 1996b
Bik	+		Boyd, <i>et al.</i> 1995
Bag		+	Takayama, <i>et al.</i> 1995
Mcl-1		+	Kozopas, <i>et al.</i> 1993
Bad	+		Yang, <i>et al.</i> 1995
A1		+	Lin, <i>et al.</i> 1993
Bcl-w		+	Gibson, <i>et al.</i> 1996

Most of the family members, including *bcl2* and *bax*, are bound to intracellular membranes, in particular the endoplasmic reticulum and the outer mitochondrial membrane, via a C-terminus transmembrane domain. Targeting to the appropriate intracellular membrane is crucial for maximum biological effect (Zha, *et al.* 1996), thus determining the subcellular localisation of relevant proteins with which members of the *bcl2* family interact (section 1.4.5). *Bcl2* contains four regions (BH 1–4) which are conserved to different degrees in different homologues, and through which association with other family members occurs. The localisation of *bcl2* to the mitochondrial

membrane is consistent with its ability to block apoptosis induced both by reactive oxygen species (Buttke and Sandstrom, 1994) and collapse of the mitochondrial transmembrane potential (Zanzami, *et al.* 1996).

1.4.5. *Ced4 – the elusive link*

While mutational analyses of the *ced4* gene in *C. elegans* demonstrated its requirement in apoptosis, a mammalian homologue remained elusive. Recently, however, a human homologue Apaf-1 (apoptosis activating factor 1; Zou, *et al.* 1997) has been identified, which sheds light on how caspases and their intracellular regulators, the bcl2 family, interact; a previously reported interaction of ced9 with ced3 via ced4 (Wu, *et al.* 1997b) was shown to be mirrored in mammalian systems.

Apaf-1 is a 130 kDa protein with three functional domains; an N-terminus domain with ced3 homology, a central ced4 homologous region and a C-terminus containing 12 WD40 repeats shown previously to be involved in the interaction of several regulatory proteins (Neer, *et al.* 1994). Apaf-1 binds cytochrome c (a known mediator of apoptosis whose release from mitochondria is prevented by bcl2; Kluck, *et al.* 1997; Yang, *et al.* 1997) and the N-terminus of caspase-9 (Li, *et al.* 1997), which in the presence of dATP, can activate caspase-3 *in vitro*. Bcl_{xL}, an anti-apoptotic member of the bcl2 family, has recently been shown to interact with Apaf-1 (Pan, *et al.* 1998; Hu, *et al.* 1998) and attenuate its ability to activate caspase-9 and caspase-3. Thus, it would seem that in normal cells bcl_{xL} bound to Apaf-1 prevents the activation of caspase-9 (and other caspases; Hu, *et al.* 1998), but upon receipt of an apoptotic stimulus disassociates to facilitate the activation of caspase-9 and thus the effector caspase, caspase-3.

1.5. Proteolytic cleavage of substrates

Studies on apoptosis have linked extracellular events at the cell membrane to apical ‘initiator’ caspases and subsequently to ‘effector’ caspases. These effector caspases such as caspase-3, caspase-6 and caspase-7 can proteolytically cleave several cellular substrates, some of which are thought to contribute to the apoptotic morphology.

Caspases cleave many proteins during apoptosis (reviewed in Martin and Green, 1995; Table 1.4), resulting in four general outcomes (reviewed in Villa, *et al.* 1997). Proteolysis may lead to activation of the substrate (eg. PKC δ , sterol regulatory element binding proteins [SREBP] and DNA fragmentation factor [DFF]), deactivation of the

substrate (eg. DNA-PKcs and the retinoblastoma protein [Rb]), loss of cellular structure (eg. nuclear lamins and Gas2) or may have no known function (eg. poly (ADP ribose) polymerase, fodrin and the 70 kDa protein component of the U1 small nuclear riboprotein [U1-70 kDa]). In addition, many of the caspases have overlapping substrate specificities *in vitro*, making the identification of the precise caspases responsible for the cleavage of specific substrates *in vivo* difficult.

Table 1.4. Caspase substrates and the caspases responsible for their cleavage

Substrate	Caspase(s)	Sequence around cleavage site					References
		P ₄	P ₃	P ₂	P ₁	↓P ₁ '	
PARP	Caspase-3	D	E	V	D ²¹³	G	Lazebnik, <i>et al.</i> 1994 Kaufmann, <i>et al.</i> 1993
	Caspase-7						
Lamin A/C	Caspase-6	V	E	I	D ²³⁰	N	Rao, <i>et al.</i> 1996
Lamin B	Caspase-6	V	E	V	D ²³⁰	S	
SREBP-1	Caspase-3	S	E	P	D ⁴⁶⁰	S	Wang, <i>et al.</i> 1995 Pai, <i>et al.</i> 1996
	Caspase-7						
SREBP-2	Caspase-3	D	E	P	D ⁴⁶⁸	S	Wang, <i>et al.</i> 1995 Pai, <i>et al.</i> 1996
	Caspase-7						
DNA-PKcs	Caspase-3	D	E	V	D ²⁷¹²	N	Han, <i>et al.</i> 1996
PKCδ	Caspase-3	D	M	Q	D ³³⁰	N	Emoto, <i>et al.</i> 1995
Rb	Caspase-3	D	E	A	D ⁸⁸⁶	G	Janicke, <i>et al.</i> 1996
APC							Browne, <i>et al.</i> 1994 Browne, <i>et al.</i> 1998
DFF	Caspase-3						Liu, <i>et al.</i> 1997
U1-70 kDa	Caspase-3	D	G	P	D	G	Song, <i>et al.</i> 1996

1.5.1. Poly (ADP ribose) polymerase

Poly (ADP ribose) polymerase is an enzyme involved in the maintenance of genome integrity and is the best characterised protein cleaved during apoptosis. Intact PARP is a 116 kDa protein which contains two zinc fingers at the N-terminal DNA-binding domain and a C-terminal catalytic domain (Kaufmann, *et al.* 1993). During apoptosis in a variety of cell lines, PARP is cleaved at DEVD²¹³↓G, separating the DNA-binding domain from the catalytic domain, to produce signature apoptotic fragments of 89 kDa and 25 kDa. PARP is cleaved *in vitro* by a protease activity resembling ICE (prICE; Lazebnik, *et al.* 1994) and by caspase-3 and caspase-7, although their relative contributions to PARP cleavage *in vivo* is not known. Likewise it is not clear why PARP should be a target protein during apoptosis. One possibility is that as a sensor of fragmented DNA, it would be highly active during apoptosis, which would necessitate

extensive catabolism of NAD⁺ and polymerisation of ADP-ribose, resulting in the exhaustion of vital energy supplies (Zhang, *et al.* 1994; Kaufmann, *et al.* 1993; Earnshaw, 1995).

1.5.2. Nuclear Lamins

The cleavage of nuclear lamins during apoptosis may precipitate some of the nuclear morphological changes (Lazebnik, *et al.* 1995; Neamati, *et al.* 1995). Studies have shown that the caspase responsible for lamin cleavage is distinct from that involved in the cleavage of PARP (Lazebnik, *et al.* 1995). Caspase-6 is identified as the only caspase to date which is capable of efficiently cleaving nuclear lamins *in vitro* (Orth, *et al.* 1996; Takahashi, *et al.* 1996), and may be the major caspase responsible *in vivo*. However, it is also possible that cleavage of lamins may be mediated by a Ca²⁺-regulated serine protease associated with the nuclear scaffold (Clawson, *et al.* 1992). The cleavage of nuclear lamins may not just have a passive role in the collapse of nuclear structure, but rather may facilitate the later events involved in nuclear breakdown (Rao, *et al.* 1996).

1.5.3. Sterol regulatory element binding proteins 1 and 2

Sterol regulatory element binding proteins (SREBPs) belong to the basic-helix-loop-helix-leucine zipper (bHLH-ZIP) family of transcription factors (Wang, *et al.* 1993; Yokoyama, *et al.* 1993) and regulate sterol metabolism within cells. Under normal, relatively sterol-rich conditions, the 125 kDa proteins remain bound to the endoplasmic reticulum via two C-terminal transmembrane regions. Following sterol depletion the protein is cleaved and the resulting 68 kDa N-terminal portion migrates to the nucleus where it binds the SRE-1 (Briggs, *et al.* 1993) to activate transcription from the low density lipid (LDL) receptor and 3-hydroxy-3-methyl-glutaryl CoA synthase (HMG CoA synthase) promoters to increase sterol metabolism (Wang, *et al.* 1994b). The 68 kDa fragment is rapidly degraded by a calpain-like protease, preventing the accumulation of sterol by a classic negative feedback mechanism. Both SREBP-1 and SREBP-2 are cleaved during apoptosis by a caspase(s) at the distinct, but near-by sites, DSEPD⁴⁶⁰↓S and DEPD⁴⁶⁸↓S, respectively (Wang, *et al.* 1995), similarly resulting in the translocation of the transcriptionally active N-terminal portions to the nucleus, although the consequence of this during apoptosis is unknown.

1.5.4. DFF – a connection between the caspases and DNA fragmentation

As described above, one substrate cleaved during apoptosis is the DNA fragmentation factor (DFF). This protein is a heterodimer comprising two subunits of approximately 40 and 45 kDa (Liu, *et al.* 1997). Caspase-3 cleaves the larger of the two subunits (DFF45) at two sites *in vitro* to produce an active protein, which is sufficient to promote DNA cleavage. A similar cleavage pattern is observed in cells undergoing apoptosis (Liu, *et al.* 1997), and DFF activation has also recently been documented in HL60 cells following treatment with chemotherapeutic drugs (Granville, *et al.* 1998). Thus, DFF provides a link between caspase activation and DNA fragmentation, a well documented feature of apoptosis.

Notably, DFF45 exhibits ~76% sequence identity with murine ICAD (Caspase-activated DNase inhibitor; Enari, *et al.* 1998; section 1.1.1), suggesting that ICAD could represent a murine homologue of DFF45. In an extension to these studies a human nuclease has recently been identified which is regulated by the caspase-sensitive DFF protein. This caspase-activated nuclease (CPAN; Halenbeck, *et al.* 1998) degrades naked DNA and displays a high degree of homology with CAD.

1.5.5. Subcellular localisation of caspases and their substrates

The caspase substrates identified to date have been localised to several subcellular compartments. PARP, lamins A, B and C and Rb, are confined to the nucleus, whereas others, such as SREBP-1 and -2, and APC are located in the endoplasmic reticulum and cytosol, respectively. In contrast, the caspases responsible for the cleavage of these substrates have generally been assigned a cytoplasmic location (Ayala, *et al.* 1994; Nicholson, *et al.* 1995), and no caspase homologues have been specifically located in any other cellular compartment, including the nuclei or endoplasmic reticulum. Consequently, obvious questions exist as to how cytosolic caspases cleave substrates which are located in distinct subcellular compartments.

1.6. Peptide inhibitors of apoptosis

In order to dissect the apoptotic pathway, and to determine the sequence of caspase activation, reversible and irreversible peptide inhibitors displaying different degrees of selectivity have been developed (Nicholson, 1996). The peptides were developed to mimic the preferred cleavage sites for the different caspases. Inhibitors based around the amino acid sequence YVAD, which mimics the cleavage site in pro-IL1 β , selectively inhibit caspase-1, those based around DEVD, the cleavage site in PARP, selectively inhibit caspases-3 and -7, those based around VEID, the cleavage site in lamins A and C, selectively inhibit caspase-6, and those based around IETD, the processing site at the p17/p12 junction in caspase-3, selectively inhibit caspase-8. Previous studies have suggested that whereas the aspartate residue in the P₁ position of the substrate is required for cleavage by a caspase, it is the residue in the P₄ position which has a role to play in governing the specificity of the caspase-substrate interaction. A much used tripeptide inhibitor, z-VAD.fmk, inhibits apoptosis in many systems (Fearnhead, *et al.* 1995c; Zhu, *et al.* 1996; Greidinger, *et al.* 1996), and shows less selectivity due to the absence of an amino acid in the P₄ position, but is nevertheless a powerful tool in elucidating the apoptotic pathway.

1.7. Project Outline

The work presented in this thesis is aimed at advancing our understanding of the apoptotic process;

- 1) Initial aims were to characterise the apoptotic response in murine erythroleukaemic (MEL) cells and to assess the effects that the differential expression of genes known to have a regulatory role in apoptosis (eg. p53), had on the apoptotic outcome (chapter 3).
- 2) Previous studies have demonstrated caspase activation following treatment with DNA-damaging agents (Datta, *et al.* 1996). However, there has been no direct evidence linking p53 with activation of the caspases. Here a temperature-sensitive system was employed to identify caspases activated by p53 and to determine the sequence of their activation during apoptosis (chapters 4 and 5).
- 3) The problems posed by the different subcellular localisation of protein substrates and the caspases which cleave them during apoptosis was addressed both in the temperature-sensitive *in vitro* system (chapter 6) and in the well characterised *in vivo* model of Fas-induced apoptosis in mice (chapter 7).

CHAPTER 2 – MATERIALS AND METHODS

2.1. MATERIALS

Media and serum were purchased from GIBCO BRL (Paisley, Scotland,). Benzyloxycarbonyl-Asp-Glu-Val-Asp-7-amino-4-trifluoromethylcoumarin (z-DEVD.afc), benzyloxycarbonyl-Ile-Glu-Thr-Asp-7-amino-4-methylcoumarin (z-IETD.amc), acetyl-Val-Glu-Ile-Asp-7-amino-4-methylcoumarin (Ac-VEID.amc), benzyloxycarbonyl-Glu-Ser-Met-Asp-7-amino-4-methylcoumarin (z-ESMD.amc) and benzyloxycarbonyl-Val-Ala-Asp-fluoromethyl ketone (z-VAD.fmk) were from Enzyme Systems Inc. (Dublin, CA, USA). Acetyl-Tyr-Val-Ala-Asp-7-amino-4-methylcoumarin and all other chemicals, unless stated otherwise, were from Sigma Chemical Co. (Poole, Dorset, UK).

2.1a. ANTIBODIES

Primary (dilution)	*Secondary (dilution)	Origin of primary
p53 (Westerns; 1:1000)	Goat anti-mouse hrp (1:1000)	Pharmingen, CA, USA.
p53 (FACS; 1:500)	Goat anti-mouse FITC (1:100)	Pharmingen, CA, USA.
Bax (P-19; 1:1000)	Goat anti-rabbit hrp (1:2000)	Santa Cruz, CA, USA.
Bcl2 (N-19; 1:1000)	Goat anti-rabbit hrp (1:2000)	Santa Cruz, CA, USA.
caspase-1 (1:1000)	Goat anti-rabbit hrp (1:1000)	Santa Cruz, CA, USA.
caspase-3 (1:10 000)	Goat anti-rabbit hrp (1:2000)	Merck Frosst, Quebec, Canada.
caspase-7 (1:2000)	Goat anti-rabbit hrp (1:2000)	Xiao-Ming Sun, Leicester.
caspase-8 (1:2000)	Goat anti-mouse hrp (1:2000)	Xiao-Ming Sun, Leicester.
PARP (C210; 1:10 000)	Goat anti-mouse hrp (1:2000)	GG Poirier, Quebec, Canada.
lamin B ₁ (1:50)	Goat anti-mouse hrp (1:2000)	Serotec, Oxford, UK.
cytochrome <i>c</i> subunit IV (1:1000)	Goat anti-mouse hrp (1:2000)	Molecular Probes, Eugene, OR.
SREBP-1 (K-10; 1:1000)	Goat anti-rabbit hrp (1:1000)	Santa Cruz, CA, USA.
glutathione- <i>S</i> -transferase π (1:2000)	Goat anti-rabbit hrp (1:1000)	M. Manson, MRC, Leicester.

*The origins of the secondary antibodies were; goat anti-rabbit hrp and goat anti-mouse FITC, DAKO, Denmark; Goat anti-mouse hrp, Sigma, Poole, Dorset, UK.

2.1b. ANIMALS

Male Balb/c mice were bred in the Clinical Sciences Department of the University of Leicester.

2.2. METHODS

2.2.1. Cell Culture

2.2.1a. Murine Erythroleukaemic Cell lines (MEL cells)

The murine erythroleukaemic cell lines C88 and DP16-1 were cultured in Dulbecco's MEM, supplemented with 10% heat-inactivated fetal calf serum in CO₂/air (1:19) at 37°C.

2.2.1b. Murine Myeloid Leukaemic Cell lines (M1, LTR6 and LTRphe132)

The murine myeloid leukaemic cell lines M1 (parental; p53 null), LTRphe132 (non-temperature-sensitive mutant p53) and LTR6 (temperature-sensitive mutant p53) were generously given by Prof. M. Oren (Weizmann Institute, Rehovot, Israel). All three cell lines were cultured in RPMI 1640 medium with L-glutamine, supplemented with 10% heat-inactivated fetal calf serum in CO₂/air (1:19) at 37.5°C. The LTR6 and LTRphe132 cells were periodically subcultured in the above medium containing 400 µg/ml geneticin/G418 (GIBCO BRL; Paisley, Scotland, UK). For the temperature shift, cells were transferred to a second incubator maintained at 32.5°C in an atmosphere of CO₂/air (1:19). Experiments with LTR6, LTRphe132 and M1 cells were carried out at an initial density of 0.8×10^6 cells/ml in the standard culturing medium, minus G418.

2.2.2. Assessment of Apoptosis

2.2.2.1. Flow Cytometry and Fluorescence Microscopy

After the appropriate incubation period LTR6, M1 and LTRphe132 cells were warmed in 1 ml volumes at 37°C for 5 min. Samples were then incubated in the presence of 1.8 µM Hoechst 33342 for a further 10 min at 37°C. The samples were then removed and placed on ice for 3 min. After centrifugation at 200 g for 5 min at 4°C in a Sigma benchtop centrifuge the pelleted cells were resuspended in 900 µl of ice-cold phosphate buffered saline (PBS). 100 µl of a 5 µg/ml solution of propidium iodide (PI) was then added and the cells analysed on the flow cytometer or examined under the fluorescence microscope as described below.

2.2.2.1a. Flow Cytometry

Flow cytometry was carried out essentially as described before (Sun, *et al.* 1992). Cells were stained as above and analysis carried out using a Becton Dickinson Vantage flow cytometer with Lysis II software (Becton Dickinson, San Jose, CA). Analysis was carried out by examining cells at a flow rate of approx. 400–500 cells/sec. Viable and apoptotic cells were separated from normal cells based upon both a decrease in cell size and an enhancement of their Hoechst 33342 fluorescence. The Hoechst 33342 and the PI were excited using the 352 nm ultraviolet line of a krypton laser and the resultant blue (400–500 nm; Hoechst 33342) versus red (> 630 nm; PI) fluorescence recorded using linear amplification. The increase in the degree of Hoechst 33342 fluorescence correlates with a change in membrane permeability (Ormerod, *et al.* 1993).

2.2.2.1b. Fluorescence Microscopy

Cells were treated as above and examined using a fluorescence microscope (352 nm).

2.2.2.2. DNA Content Analysis

It has been established that a feature of apoptosis in many cell types is the ordered fragmentation of cellular DNA. The method detailed here is based on the ability of cells permeabilised with detergent to lose some of this fragmented DNA which causes their DNA content to fall below that of a 2N nucleus and correlates with the appearance of a sub-G1 peak.

After the appropriate incubation period, cells were pelleted and resuspended in 100 µl ice-cold PBS and fixed with 1 ml ice-cold 70% ethanol for 1 h. The cells were then pelleted and resuspended in 900 µl PBS containing 0.1% Triton-X-100 and left at 4°C overnight. 100 µl of a 5 µg/ml solution of PI was then added and the cells left at 4°C for 2–3 days before being analysed by flow cytometry. A FACScan flow cytometer (Becton Dickinson, San Jose, CA) was used to measure the red (PI) fluorescence of the cells. Data were collected from 5000 cells and LYSIS II software was used to determine the percentage of cells in each phase of the cell cycle.

2.2.3. Electrophoretic Methods

2.2.3.1. Conventional Agarose Gel Electrophoresis

After the appropriate incubation period 1×10^6 cells per sample were pelleted for conventional agarose gel electrophoresis (CAGE) to assess the incidence of internucleosomal cleavage of DNA (Sorenson, *et al.* 1990).

For the agarose gel, 1.8 g of agarose (Gibco BRL, Paisley, Scotland) was dissolved in 90 ml ultra pure water and 10 ml of $10 \times$ TBE (0.89 M Tris; 0.89 M Boric acid; 25 mM EDTA). After the agarose had completely dissolved, it was allowed to cool to 60°C before being poured into the casting tray. The comb was inserted immediately, while the gel was hot, any air bubbles were removed, and the agarose was left to set for at least 30 min.

The digesting gel was prepared by dissolving 0.16 g of agarose in a universal with 2 ml TBE, 13 ml of ultra pure water and 5 ml of a 10% solution of sodium dodecylsulphate (SDS). After the agarose had completely dissolved 350 μl of a 25 mg/ml solution of Proteinase K/7 ml of agarose was added. Before addition of this enzyme the prepared digesting gel was allowed to cool to 55°C , due to the lability of this enzyme. The digesting gel was pipetted into a trench cut out behind the formed wells and allowed to set for at least 30 min. While the digesting gel was setting, the samples were prepared for loading.

The cell pellets were resuspended in 11 μl of ultrapure water to lyse the cells and release the DNA. The RNA was digested by incubating the pellets with 6 μl of a 50 $\mu\text{g}/\text{ml}$ solution of RNase A for 20 min. The markers used on the conventional gels were either the 123bp ladder or the Hind III digest of phage λ DNA (Gibco BRL, Paisley, Scotland). 5 μl of loading buffer was added to each sample and the samples loaded immediately onto the gel.

The gel was run in $0.5 \times$ TBE, initially at 20 v for 1 h or until the samples had completely left the wells, and then for a further 3 h at 100 v. At the end of the run, the gel was removed from the tank, rinsed briefly in distilled water and incubated overnight at room temperature in distilled water containing 20 $\mu\text{g}/\text{ml}$ RNase A. The gel was then rinsed again with distilled water and stained in distilled water containing 1 $\mu\text{g}/\text{ml}$ ethidium bromide. The gel was then destained in several washes of distilled water, visualised under ultraviolet light and photographed.

2.2.3.2. Field Inversion Gel Electrophoresis

This method was used for the resolution of DNA fragments of > 50 kbp in length, and involves a gentler method of sample preparation than that used for CAGE to avoid shearing the DNA (Anand and Southern, 1990).

Preparation of Samples

After the appropriate incubation period 1.5×10^6 cells/sample were prepared for field inversion gel electrophoresis (FIGE). Cells were pelleted at 200 g for 5 min at 4°C in a Sigma benchtop centrifuge. The cell pellet was resuspended in 100 µl phosphate buffered saline-agarose (PBS-A) prewarmed to 43°C, and incubated for 10 min at 50°C. A further 100 µl of 1% prewarmed agarose in PBS-A was added to each sample and the sample mixed well. 100 µl of each sample was then pipetted into a prepared insert mould and left at 4°C for at least 30 min. After the plugs had set, they were incubated in NDS (1% lauryl sarcosine; 0.5 M EDTA; 10 mM Tris; pH 9.5) at room temperature for 30 min, before being supplemented with 1 mg/ml pronase and being incubated at 50°C in a gently shaking rotary oven for 48 h. The plugs were then rinsed twice NDS alone for 2 h to remove the pronase, and stored in NDS at 4°C until needed.

Electrophoresis

FIGE was carried out as previously described (Brown, *et al.* 1993). Following a 15 min continuous pulse, a 1 h cycle was set up to read 2.4 sec forward and 0.8 sec reverse pulse. An applied 1.5 ramp factor increased the respective pulse time 10-fold by the end of the 7 hour gel run. Under these conditions, large fragments of DNA were separated. *Saccharomyces cerevisiae* chromosomes (243–2200 kbp; Clontech, Cambridge, UK) and pulse markers (0.1–200 kbp; Sigma Chemical Co., Poole, Dorset, UK) were used as standards.

After the end of the run the gel was stained with ethidium bromide and destained as detailed in section 2.2.3.1.

2.2.3.3. SDS-Polyacrylamide Gel Electrophoresis (SDS-PAGE)

Solutions

Lower Gel Buffer 1.5 M Tris-HCl, pH 8.8
0.4% SDS

Upper Gel Buffer 0.5 M Tris-HCl, pH 6.8
0.4% SDS

Both the lower and upper gel buffers were filtered through a 0.45 µm filter.

Electrode Buffer 25 mM Tris
192 mM Glycine
1% SDS

Sample Buffer 62.5 mM Tris, pH 6.8
15% Glycerol
2% SDS
5% 2-mercaptoethanol
0.025 g Bromophenol Blue/50 ml

Gel preparation

The gel plates were cleaned with distilled water followed by ethanol and acetone, and were set in the casting tray according to the manufacturer's instructions. The appropriate percentage lower gels were mixed according to the table below, and degassed for 10 min before use.

	7%	10%	13%	15%
30% Acrylamide* (ml)	5.8	8.3	10.8	12.5
lower buffer (ml)	6.25	6.25	6.25	6.25
dist. H ₂ O (ml)	12.8	10.3	7.8	6.1

*Acrylamide was obtained from National Diagnostics.

After degassing 150 µl of a 0.1 g/ml solution of ammonium persulphate (APS) and 20 µl of TEMED was added to the gel and 21 ml of the gel mixture was poured between the plates. To ensure a flat surface to the top of the gel, the gel was gently overlaid with 2 ml of distilled water and allowed to set for 15 min.

While the lower gel was setting, the upper gel was prepared. For the upper gel, 2.7 ml of 30% acrylamide, 5 ml of lower gel buffer and 12.2 ml distilled water were mixed and degassed as described for the upper gel. After degassing was complete, 100 µl of APS and 20 µl of TEMED were added to the gel mixture and the upper gel was pipetted on top of the lower gel, the layer of distilled water having first been removed. The appropriate comb was placed immediately between the glass plates and the gel allowed to set for 45 min.

Sample preparation

After the appropriate incubation period 0.5×10^6 cells/sample were washed once in ice-cold PBS, snap frozen in liquid N₂ and stored at -80°C until required. The cell pellets were then resuspended in 80 µl of sample buffer, boiled for 3–5 min and loaded while still hot into the wells of the gel.

Electrophoresis

To run the gel 3 L of electrophoresis buffer was prepared. 2.5 L of the buffer was poured into the tank and chilled to 14°C, and the remaining 0.5 L was poured into the upper reservoir, previously secured to the glass plates. The samples were loaded into the wells in the upper gel. The gel was run at maximum voltage, with a constant current of 30 mA per gel until the bromophenol blue dye front reached the upper and lower gel interface. The lower gel was then run at 40 mA per gel until the dye front reached the bottom of the gel.

2.2.4. Western Blotting

Solutions

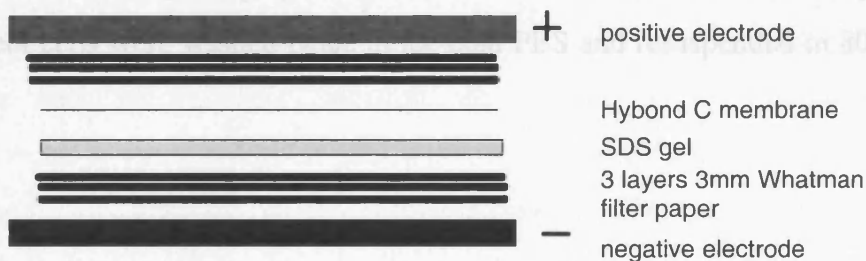
Transfer Buffer 25 mM Tris
 192 mM Glycine
 20% Methanol, pH 8.3

Tris-Buffered Saline 200 mM Tris
 (*TBS; 10 × solution*) 1.37 M NaCl, pH 7.6

Blocking Buffer 5% Non-Fat Dried Milk (Marvel™)
 0.1% Tween 20
 1 × TBS

An SDS-polyacrylamide gel was run as described in section 2.2.3.3. The gel, with the upper gel removed were then pre-shrunk in transfer buffer. At the same time a piece of Hybond-C extra supported nitrocellulose transfer membrane (Amersham, Little Chalfont, Bucks) was cut, wetted in distilled water and then left to equilibrate in transfer buffer for 15 min. The transfer sandwich was then set up as shown in Fig. 2.1, with care taken to eliminate any air bubbles, and inserted into the Biorad transfer tank, making sure that both positive terminals and both negative terminals were together.

Fig. 2.1. Set up of transfer ‘sandwich’



Transfer was carried out overnight at 30 v. After transfer the membrane was stained with Ponceau S to confirm even protein loading. Non-specific antibody-

protein interactions were prevented by a 1–2 h incubation of the membrane in Blocking buffer. The membrane was then incubated with the appropriate dilution of the desired primary antibody for 1 h at room temperature and then washed as follows;

2 × 5 min in Blocking buffer

1 × 10 min in Blocking buffer

2 × 5 min in 1 × TBS containing 0.1% Tween 20

1 × 10 min in 1 × TBS containing 0.1% Tween 20

The membrane was then incubated for 1 h the appropriate horseradish peroxidase (hrp)-conjugated antibody against immunoglobulins of the animal in which the primary antibody was raised. The above washes were then repeated, with an additional wash in 1 × TBS alone, before chemiluminescent detection using an ECL kit (Amersham, Little Chalfont, Bucks).

Chemiluminescence relies on the emission of light resulting from the dissipation of energy from a chemical in an excited state. Immediately following its oxidation, luminol is in an excited state which then decays to ground state via a light emitting pathway. In the ECL system oxidation of the luminol is achieved through the action of the antibody-conjugated horseradish peroxidase and is enhanced by the presence of phenols (Western blotting protocols, Amersham).

2.2.5. Lysate Preparations and Fluorimetric Assays

2.2.5a. Cell Lysate Preparation

In a standard lysate preparation 50×10^6 cells were used. After the appropriate treatment cells were washed twice in ice-cold PBS and resuspended in 80 μ l lysate buffer.

Lysate Buffer 50 mM PIPES/KOH, pH 6.5
2 mM EDTA
0.1% (w/v) CHAPS
5 mM Dithiothreitol (DTT)
20 µg/ml Leupeptin
10 µg/ml Pepstatin A
10 µl/ml Aprotinin
2 mM PMSF

The cells were frozen in liquid N₂ and thawed at 37°C three times and centrifuged at 20 000 g for 30 min at 4°C in a Sigma benchtop centrifuge and the supernatant retained. The recovered supernatant was transferred to tubes appropriate for the TLA120,2 rotor and centrifuged at 100 000 g for 45 min at 4°C in a Beckman Optima centrifuge. The supernatant (cell lysate) was retained and the protein content measured using the Bradford assay (Biorad; section 2.2.11).

2.2.5b. Fluorimetric Assay

The proteolytic activity in prepared cell lysates and isolated liver fractions was measured using a continuous fluorimetric assay modified from the method of Thornberry (1994). Cleavage of z-DEVD.afc, which mimics the caspase-3/-7 cleavage site within PARP releases the fluorescent moiety 7-amino-4-trifluoromethylcoumarin (afc). Cleavage of z-IETD.amc, which mimics the p17/p12 junction in caspase-3, Ac-VEID.amc, which mimics the caspase-6 cleavage site within lamin A/C, and Ac-YVAD.amc, which mimics the ICE cleavage site within pro-IL-1β, release the fluorescent moiety 7-amino-4-methylcoumarin (amc).

Liberation of afc and amc was measured using excitation wavelengths of 400 nm and 380 nm, and emission wavelengths of 505 nm and 460 nm, respectively. Lysates in 1.25 ml HEPES buffer (100 mM HEPES; 10% (w/v) sucrose; 0.1% (w/v) CHAPS; 10 mM DTT, pH 7.5) were assayed at 37°C in a modified cuvette holder fitted with a thermostat (Perkin Elmer LS50B luminescence fluorimeter). Routinely, assays contained 15–100 µg protein and 20 µM of the appropriate fluorogenic substrate.

Calculation of specific cleavage activities

Standard curves for the concentration (μM) of each fluorogenic substrate versus their relative fluorescence established x coefficients of 626.6 and 864.4 for afc and amc fluorescence, respectively. Hence to calculate the appropriate catalytic activity the following equation was used:

$$\text{Activity (nmol/ml)} = \frac{\text{slope (fluorescence units/time [sec])}}{\text{appropriate x coefficient (626.6 or 864.4)}}$$

The value was then corrected for protein content, for volume of assay ($\times 1.25$), for activity per min ($\times 60$) and converted to pmol/min ($\times 1000$), where appropriate.

For inhibitor studies, the appropriate concentration of the inhibitor was added to the cuvette and incubated for 15 min at 37°C , prior to the addition of the fluorogenic substrate. Analysis of the cleavage activity was then carried out as described above.

2.2.6. Anion-exchange Chromatography

Caspase activities were separated using a RESOURCE Q anion exchange column (1 ml, 6.4 mm diameter \times 30 mm bed height) from Pharmacia Biotech, Uppsala, Sweden. The column was equilibrated for 45 min in equilibration buffer;

Equilibration Buffer 20 mM Tris/HCl, pH 7.0 at 4°C

1.6 mM CHAPS

146 mM Sucrose

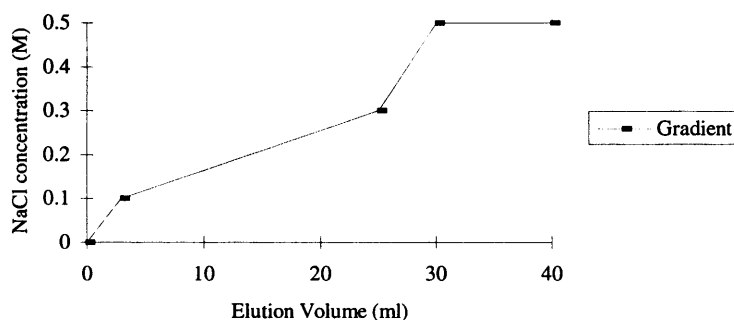
2 mM DTT

filter at $0.45 \mu\text{m}$.

Lysate prepared as described in section 2.2.5a was diluted to 4 ml in equilibration buffer and filtered at $0.45 \mu\text{m}$. Fractions (1 ml) were collected at a rate of one fraction/min. The NaCl gradient, shown in Fig. 2.2. was started and the sample loaded. After elution, the column was re-equilibrated. Each of the fractions

collected was assayed for the appropriate caspase cleavage activity, as described in section 2.2.5b.

Fig. 2.2. NaCl gradient employed for elution from RESOURCE Q anion-exchange column



2.2.7. *In vivo* administration of anti-Fas receptor Antibody JO2 and z-VAD.fmk

All injections were administered intravenously (tail vein). Male Balb/c mice aged between 6 and 8 weeks were injected either with 10 μ g of purified hamster mAb to mouse Fas (JO2) (Pharmingen, Los Angeles, CA) in 160 μ l of 0.9% (w/v) saline/12.5% (v/v) DMSO or 160 μ l of 0.9% (w/v) saline/12.5% (v/v) DMSO (controls). Where indicated, mice were injected with JO2 antibody (10 μ g) in 80 μ l of 0.9% (w/v) saline followed 5 min later by z-VAD.fmk (50 μ moles/kg) (Enzyme Systems Ltd, Dublin, CA) in 80 μ l of 0.9% (w/v) saline/25% (v/v) DMSO. Animals were sacrificed at the indicated times by cervical dislocation.

2.2.8. Tissue preparation and histopathological examination

Livers were removed and fixed in 10% formaldehyde in buffered saline. Representative sections of the left lateral, median and posterior lobes were stained with haematoxylin and eosin and examined for apoptosis.

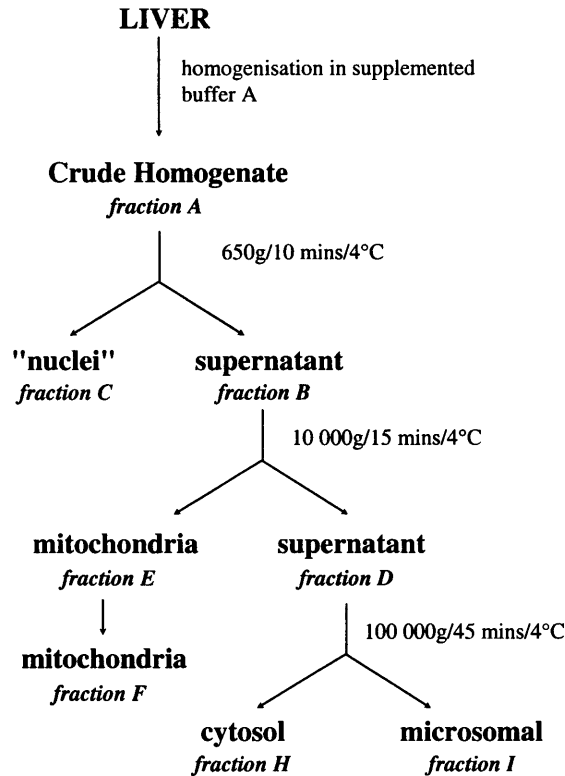
2.2.9. Mouse Liver Fractionation

Following the appropriate treatment the mice were culled by cervical dislocation and the livers removed and weighed. Livers were washed in Buffer A to remove excess hair and blood, before being chopped up and homogenised in a Dounce homogeniser in 5 mls of supplemented Buffer A.

Buffer A 0.3 M Mannitol
 5 mM MOPS
 4 mM KH₂PO₄
 1 mM EGTA, pH 7.4.

Supplements 5 mM DTT
 20 µg/ml Leupeptin
 10 µg/ml Pepstatin A
 10 µl/ml Aprotinin
 2 mM PMSF

Following homogenisation, the mouse livers were fractionated as described below and samples retained at each stage. The crude homogenate (*fraction A*) was centrifuged at 650 g/10 min/4°C in a Beckman centrifuge (GH 3.7 rotor). The resultant pellet was designated ‘nuclei’ (*fraction C*). The supernatant (*fraction B*) was further centrifuged in a Sigma benchtop centrifuge at 10 000 g/15 min/4°C to pellet the mitochondria (*fraction E*). The mitochondria were washed and repelleted twice in supplemented buffer A (*fraction F*). The supernatant from the 10 000g spin (*fraction D*) was then centrifuged at 100 000 g/45 min/4°C to separate the cytosolic supernatant (*fraction H*) and the microsomal pellet (*fraction I*). The protein content of the different fractions was determined using the Bradford procedure (Biorad; section 2.2.12.) and the samples retained at –80°C until required for further analysis. A summary scheme for the fraction of mouse liver is shown in Fig. 2.3.

Fig. 2.3. Liver fractionation scheme

2.2.10. Cell Counting

Cells were counted using a Casy 1 (Schärfe System, Reutlingen, Germany) cell counting and sizing system according to the manufacturer's instructions, using a 150 μm aperture for routine analysis.

2.2.11. Bradford Procedure for Protein Determination

Protein concentrations in cell lysates and liver fractions were determined using the Bradford procedure (Coomassie Brilliant Blue G-250, Bio-Rad, Hemel Hempstead, Herts). Routinely, 5 μl of a 1:10 dilution of the cell lysate or liver fraction was mixed in 1 ml of diluted (20% (v/v) in distilled H_2O) and the OD_{595} measured. A standard curve of OD_{595} was set up with several dilutions of a protein standard (bovine serum albumin, Bio-Rad), and the protein concentrations of the unknowns assessed.

2.2.12. FACS Scan Analysis of Change in p53 Conformation

Cells were treated as appropriate and 5×10^6 were used per sample. Cells were pelleted in a Sigma benchtop centrifuge at 200 g for 5 min at 4°C and resuspended in 100 µl PBS. The cells were then fixed with ice-cold 70% ethanol for 15 min, before being repelleted at 800 g for 5 min at 4°C before being washed twice in PBS. The cells were then incubated for 30 min at 37°C in the presence of the primary antibody (p53, Pharmingen; 1:500) in PBS/20% goat serum. After washing twice with PBS, the cells were incubated for 30 min at 37°C in the dark in the presence of the secondary anti-mouse FITC-conjugated antibody (DAKO) in PBS/20% goat serum, washed once in PBS, resuspended in 90 µl PBS and 10 µl PI and analysed on the FACS scan. Red fluorescence > 600 nm and green fluorescence 515–545 nm, were recorded.

2.2.13. Nuclei Isolation

The isolation of nuclei from cell suspensions was modified from a method described previously by Otto, (1990). 1×10^6 cells were centrifuged at 90 g/5 min/4°C in a Sigma benchtop centrifuge. The medium was removed and the cells resuspended in 750 µl ice-cold 1% (w/v) citric acid (free acid, pH 2.8), and left in 12-well plates for 20 min at 4°C. An equal volume of 1% (w/v) citric acid/0.2% (w/v) Tween 20 was added, and the cells left for 25 min at 4°C. The nuclei were pelleted at 1000 g/5 min/4°C, resuspended in 50 µl PBS (containing 10 µl of 5 µg/ml PI), and counted on the Schärfe system.

2.2.14. Densitometry

After chemiluminescent detection of protein bands, densitometry was performed on autorads to quantitate the signal. A Molecular Dynamics densitometer was used to measure the signal volume of each band of interest and the relative intensities calculated.

2.2.15. Preparation of recombinant caspases

The cDNAs of caspases-3, -6 and -7 were ligated into the multiple cloning site of a pET21b vector (Novagen, Abingdon, Oxford), containing a T7 promoter, a lac

operator and a His-Tag[®] leader sequence. 100 µl of competent BL21DE3 *E. coli* cells were transferred to precooled eppendorfs and incubated for 5 min at 4°C in the presence of 1 µl of the vector containing the appropriate caspase. The bacteria were streaked on L-Agar (LA) plates containing 100 µg/ml ampicillin (amp) and left overnight at 37°C. A single colony was picked and incubated for 6 h at 37°C in 5 ml Luria Broth (LB) containing 100 µg/ml amp. Cells were pelleted at 3200 rpm for 15 min (Beckman centrifuge) and resuspended in 5 ml fresh LB and used to inoculate 400 ml LB containing 100 µg/ml amp. The cells were incubated at 37°C in a shaking incubator until the OD₅₅₀ was ~0.7 and incubated for a further 30 min at 27°C.

Production of host T7 RNA polymerase was induced by incubation for 3 h at 27°C in the presence of 1 mM isopropyl β-D-thiogalactopyranoside (IPTG). The cells were pelleted at 5000 rpm for 10 min in a JA-14 rotor, washed once in cold PBS, transferred to 50 ml Falcon tubes (Falcon, Franklin Lakes, NJ) and stored overnight at –80°C. The pellets were resuspended in 5 ml Hepes buffer (20 mM Hepes; 0.1% CHAPS; pH 8.0) and lysed by 10 sonication cycles (15 sec on/ 45 sec off) at the maximum intensity. The cells were transferred to the appropriate tubes for the JA-17 rotor and centrifuged at 12 000 rpm for 20 min. The supernatant was removed and transferred to tubes for the Ti 70.1 rotor and centrifuged at 40 000 rpm for 30 min.

The supernatant (lysate) was then run on a nickel column. 500 µl of His-binding resin (Novagen) was pelleted at 2000 rpm for 5 min in a Sigma benchtop centrifuge. The pellet was washed three times in 1 ml Hepes buffer (above). After the final wash an equal volume of Hepes buffer was added to the pellet of His-binding resin to make a 50% slurry. The lysate was transferred to 15 ml Falcon tubes and to it was added 50 µl of the 50% slurry. The lysate was rotated on a daisy wheel at 4°C for 1 h and poured onto a chromaspin column (Clontech, Basingstoke, Hants), followed by an equal volume of Hepes buffer. The column was eluted 4–5 times with 500 µl of Hepes buffer containing 200 mM imidazole, and each 500 µl fraction assessed for caspase cleavage activity.

Active fractions were pooled and concentrated in VIVASPIN concentrators (Vivascience, Binbrook, Lincoln) with a 30 000 membrane (retains proteins with a

molecular weight of > 30 kDa), by centrifugation at 5000 g for 15 min in a Sigma benchtop centrifuge. The protein content was measured using the Bradford procedure (section 2.2.11), and the caspases stored at -20°C in the presence of 20% (v/v) glycerol.

2.2.16. Electron microscopy

Cell suspensions were fixed in 2% glutaraldehyde in 0.1 M sodium cacodylate buffer (pH 7.2), pelleted and post-fixed for 90 min in 1% osmium tetroxide and 1.7% potassium ferrocyanide. They were then stained *en bloc* for 1 h with 2% aqueous uranyl acetate, dehydrated and embedded in Araldite. Sections were stained with lead citrate.

**CHAPTER 3 – CELL CYCLE EFFECTS OF DIFFERENT CLASSES
OF APOPTOSIS-INDUCING AGENTS IN TWO MURINE
ERYTHROLEUKAEMIC (MEL) SUB-CELL LINES**

3.1. INTRODUCTION

Friend murine erythroleukaemic (MEL) cells are derived from spleen cells of a mouse infected with the polycythemic strain of the Friend virus (Friend, *et al.* 1971). Following infection the cells are halted and subsequently transformed at the pro-erythroid stage of development. Thus, terminal differentiation of the progenitor population into functional erythrocytes is prevented, and instead of having the limited three month life span of mature erythrocytes, the cells continue to proliferate indefinitely. There is some evidence that the infecting viral complex achieves cellular transformation, at least in part, by causing mutations in the p53 gene (Munroe, *et al.* 1990), thus an abnormal p53 status is a common characteristic of many, if not all, MEL cell lines. In addition, MEL cells grow independently of erythropoietin, probably due to expression of the viral protein gp55 which binds to, and activates, the erythropoietin receptor.

In this chapter, two MEL cell sublines, C88 and DP16-1, are characterised with respect to their responses to different classes of apoptosis-inducing compound. The C88 cells contain a mutant, non-active form of the tumour suppressor protein p53, whereas the DP16-1 cells are p53 null, containing no p53 message or protein (Ryan, *et al.* 1993). The initial characterisation experiments were performed with a view to using the DP16-1 subline as an appropriate recipient of foreign DNA encoding proteins relevant to the apoptotic pathway, particularly p53. The aim was to assess the modifying effects of these proteins towards apoptosis induced by a battery of different classes of agent, and to compare the effects against a p53 mutant or null background, which is one identified difference between the two MEL cell lines under investigation.

The apoptosis-inducing agents used here can be broadly divided into three groups; the broad spectrum protein kinase inhibitor staurosporine, inhibitors of protein synthesis, cycloheximide and actinomycin D (ActD), and the DNA-damaging agent VP16. Staurosporine is a broad spectrum protein kinase inhibitor at physiologically relevant concentrations (Tamaoki, *et al.* 1986; Kiyoto, *et al.* 1987; Nakano, *et al.* 1987) and is regarded as a universal inducer of apoptosis (Jarvis, *et al.* 1994; Jacobson, *et al.* 1996). Cycloheximide and actinomycin D, are both inhibitors of protein synthesis, but act at different stages of the process. Cycloheximide inhibits the peptidyl transferase activity of the 60S ribosomal subunit, and thus impairs translation, whereas actinomycin D intercalates between 2 G–C nucleotide base pairs of DNA to prevent

transcription. The DNA damaging agent VP16 inhibits topoisomerase II, preventing the relaxation of supercoiled DNA.

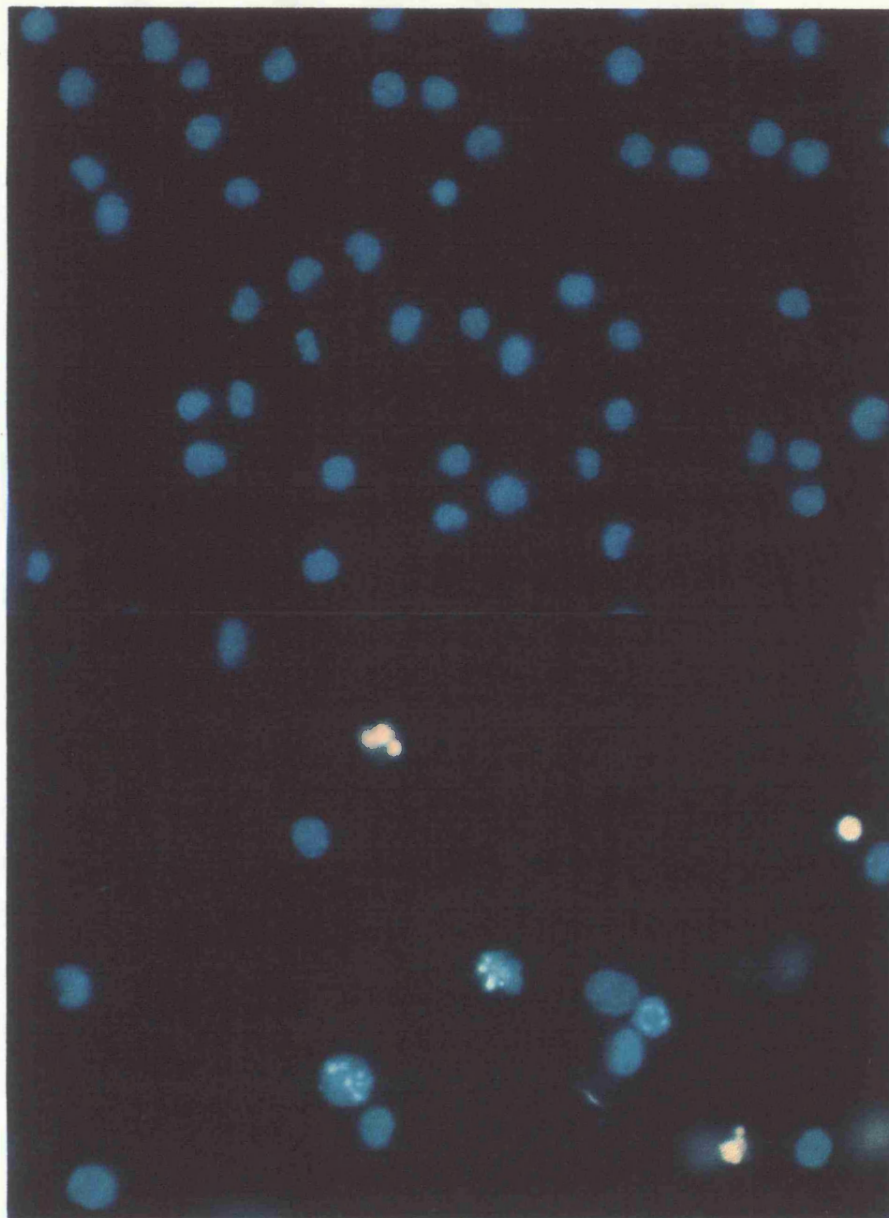
Various methods were used to qualitatively and quantitatively assess the incidence of apoptosis in these cells. Conventional agarose gel electrophoresis (CAGE; described in section 2.2.3.1) is a qualitative measure of apoptosis and is a method for visualising internucleosomal cleavage, a hallmark of apoptosis. Cells were also assessed morphologically by examination under the fluorescence microscope (2.2.2.1b) for incidence of chromatin condensation associated with the apoptotic phenotype. Apoptosis was quantitatively assessed by DNA content analysis (2.2.2.2), a method which relies on the ability of detergent-permeabilised cells to lose some of their DNA resulting in a DNA content of less than that of a diploid nucleus. Such cells are detectable as a sub-G1 population.

3.2. RESULTS

3.2.1. Staurosporine-induced cell cycle arrest and apoptosis in murine erythroleukaemic (MEL) C88 cells

To assess the effect of staurosporine (STS) on MEL C88 cells, cells were resuspended at 1×10^6 cells/ml supplemented DMEM (2.2.1a) and treated for varying lengths of time in the absence or presence of 0.2 μ M STS. Cells were harvested at the appropriate times and the degree of apoptosis assessed by the qualitative methods of fluorescence microscopy (2.2.2.1b) and CAGE (2.2.3.1) and the quantitative method of flow cytometric DNA content analysis (2.2.2.2). At this concentration, STS clearly induced morphological changes characteristic of apoptosis (Fig. 3.1B), as well as a time-dependent increase in the incidence of internucleosomal DNA fragmentation, visualised as increasing intensity of the DNA laddering pattern on agarose gels (Fig. 3.2). Internucleosomal fragmentation of DNA was clearly detectable 4–10 h after treatment with STS (lanes 4 and 6, respectively).

A MEL C88 Cells – 24 h Control



B MEL C88 Cells – 24 h with 0.2 μ M STS

Fig. 3.1. Fluorescence Microscopy of MEL C88 cells

MEL C88 cells were incubated for 24 h in the absence (A) or presence (B) of 0.2 μ M STS. Cells were stained with Hoechst 33342 and PI and prepared for fluorescence microscopy (2.2.1b). A) Normal, non-apoptotic cells, B) apoptotic cells showing characteristic condensation of nuclear chromatin.

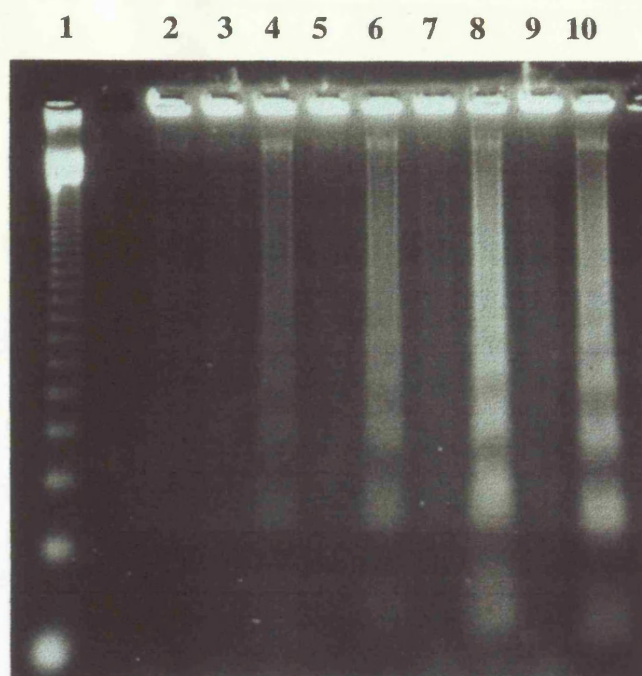


Fig. 3.2. STS-induced internucleosomal cleavage of DNA in MEL C88 cells

MEL C88 cells were incubated alone or in the presence of 0.2 μM STS for varying lengths of time. Lanes 2, 3, 5, 7 and 9 are C88 cells incubated alone for 0, 4, 10, 18 and 24 h, respectively. Lanes 4, 6, 8 and 10 are C88 cells incubated in the presence of 0.2 μM STS for 4, 10, 18 and 24 h respectively. Lane 1 is the 123 bp marker.

Staurosporine-induced apoptosis was accompanied by a profound alteration in the distribution of C88 cells in different phases of the cell cycle. A single addition of 0.2 μM STS induced a dramatic cell cycle arrest at G_2M , reflecting the inability of the population to proceed into mitosis. This cell cycle arrest was apparent as early as 4 h after treatment, and increased with time (Fig. 3.3 and Fig. 3.4), correlating with the increasing incidence of internucleosomal cleavage of DNA visualised on the agarose gel (Fig. 3.2). Interestingly, however, apoptosis was not associated with the appearance of a sub-G1 population. The sub-G1 population represents cells with a lower content of DNA than a normal diploid nucleus (2N), and is a measure of the ability of the permeabilised cell to lose some of its DNA fragmented during apoptosis. Thus, in this system the incidence of apoptosis was not associated with an increase in the percentage of cells in the sub-G1 population of the cell cycle, probably because cells are not dying from the G_0/G_1 phase of the cell cycle, in contrast to previous studies in other cells (Darzynkiewicz, *et al.* 1992).

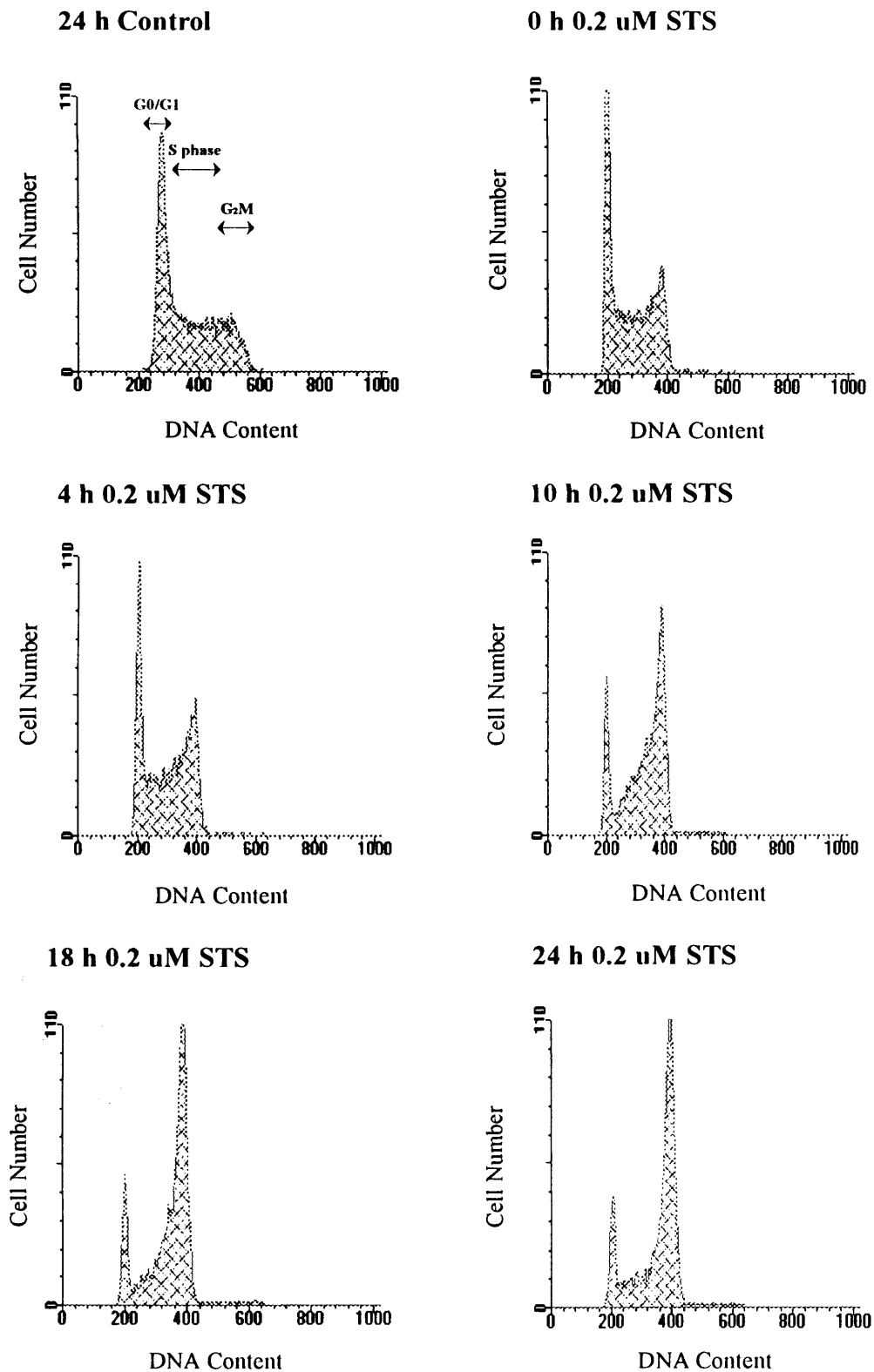


Fig. 3.3. STS-induced cell cycle arrest at G2M in MEL C88 cells

MEL C88 cells were incubated either alone or in the presence of 0.2 μ M STS over a time course of 24 h and fixed in 70% ethanol, stained with PI and analysed on the FACS Scan (2.2.2.2). DNA contents of 200 and 400 correspond to 2N and 4N nuclei, respectively. The phases of the cell cycle are indicated in the control panel.

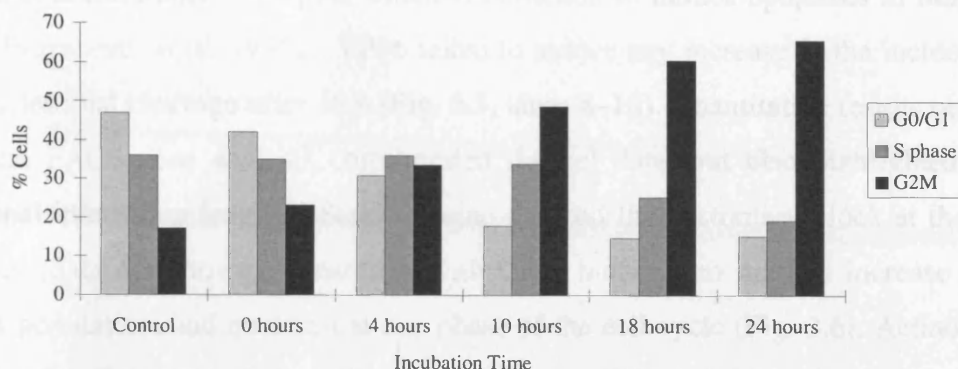


Fig. 3.4. Distribution of C88 cells in different phases of the cell cycle following treatment with 0.2 μ M STS

MEL C88 cells were incubated either alone (Control) or in the presence of 0.2 μ M STS over a timecourse of 24 h, fixed in 70% ethanol, stained with PI and analysed on the FACS scan (2.2.2.2). The percentage of cells in each phase of the cell cycle at each time point was then calculated. Results shown are from the data in Fig. 3.3.

To assess the requirement for an arrest at the G₂M interface of the cell cycle for apoptosis to occur in the MEL C88 cells, other agents were examined for their ability to induce both a cell cycle arrest at G₂M and apoptosis.

3.2.2. The effect of protein synthesis inhibitors and the topoisomerase II inhibitor etoposide (VP16) on MEL C88 cells

The translation inhibitor cycloheximide (CHX), the transcription inhibitor actinomycin D (ActD) and the topoisomerase II inhibitor VP16 have all been shown to induce apoptosis in several other cell systems (Onishi, *et al.* 1993, Fearnhead, *et al.* 1995a; Bicknell, *et al.* 1994). To study the effects of these compounds on MEL C88 cells, cells were resuspended at the standard density of 1×10^6 /ml and treated for 16 h with varying concentrations of CHX, ActD or VP16. Staurosporine at a concentration of 0.2 μ M was used as a positive control. CAGE showed that 50–100 μ M CHX induced a marked increase in the extent of internucleosomal cleavage after 16 h, indicative of apoptosis (Fig. 3.5, lanes 6 and 7), and was confirmed by the presence of a condensed morphology seen under the fluorescence microscope (data not shown). Incubation with 1 μ M ActD for 16 h induced a very high level of internucleosomal cleavage, which was similarly supported by fluorescence microscopy (Fig. 3.5, lane 12 and data not shown), but at 5 μ M the compound was toxic as shown by the ‘smearing’ of the DNA on the

gel, a characteristic of necrosis rather than apoptosis (Fig. 3.5, lane 13). Interestingly, even at concentrations of 20 μM , which is sufficient to induce apoptosis in other cell types (Fearnhead, *et al.* 1995a), VP16 failed to induce any increase in the incidence of internucleosomal cleavage after 16 h (Fig. 3.5, lanes 8–10). Quantitative results obtained from the FACS scan analysis corroborated the gel data, but also highlighted some additional interesting features. Staurosporine induced the customary block at the G₂M interface (data not shown). Treatment with CHX induced no marked increase in the sub-G1 population, and no arrest at any phase of the cell cycle (Fig. 3.6). Actinomycin D induced a distortion of the cell cycle in all experiments, although no pattern was readily noticeable. Of most interest was the observation that despite the inability of VP16 to induce apoptosis in the C88 cells it still caused a build up of cells in G₂M. This observation suggests a two tier effect, with VP16 at this concentration able to cause a cell cycle arrest at G₂M, but unable to induce apoptosis as assessed by laddering or fluorescence microscopy. However, at later timepoints VP16 may result in apoptosis, as cells will not survive indefinitely in G₂M.

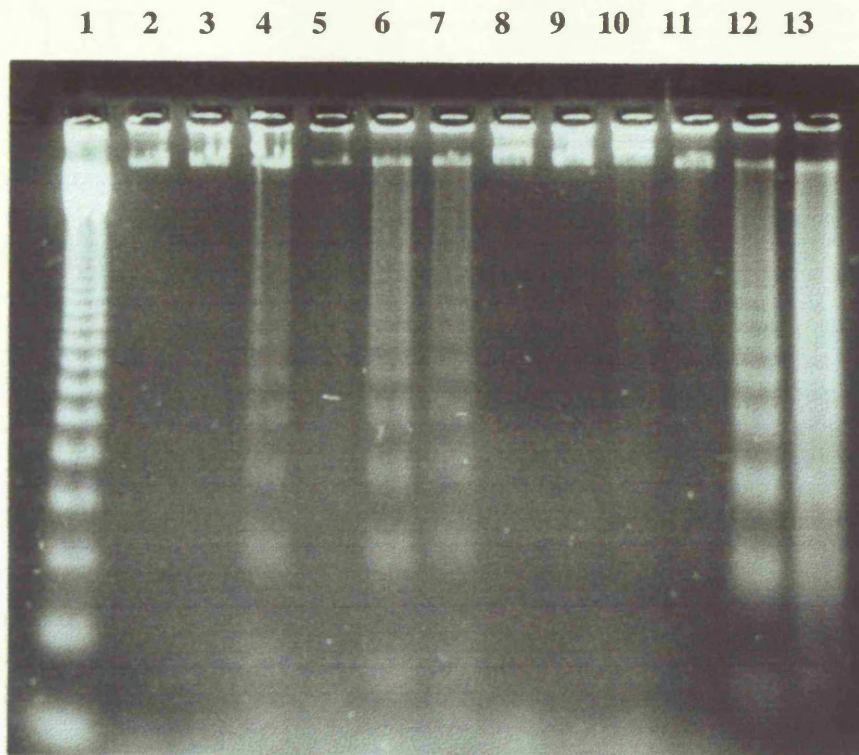
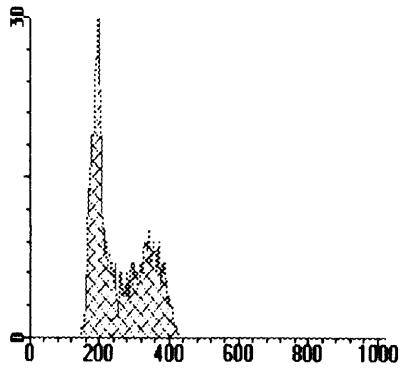
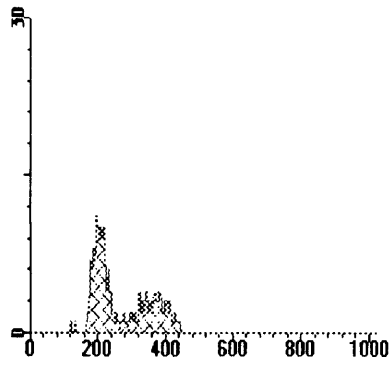


Fig. 3.5. Internucleosomal cleavage in C88 cells induced by CHX, VP16 and ActD. MEL C88 cells were incubated for 16 h either alone or in the presence of different concentrations of CHX (5, 50 or 100 μ M, lanes 5, 6 and 7, respectively), VP16 (5, 10 or 20 μ M, lanes 8, 9 and 10, respectively) or Act D (0.1, 1 or 5 μ M, lanes 11, 12 and 13, respectively), and prepared for CAGE (2.2.3.1). Lane 1 is the 123bp marker, lanes 2 and 3 are controls (16 h) and lane 4 is 0.2 μ M STS for 16 h as a positive control.

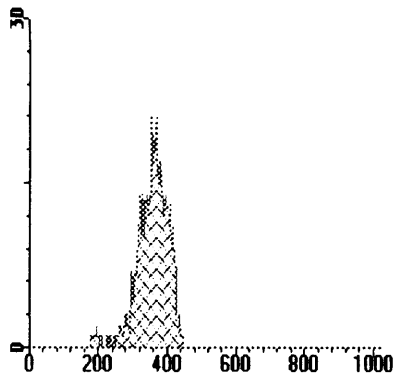
5 μ M Cycloheximide



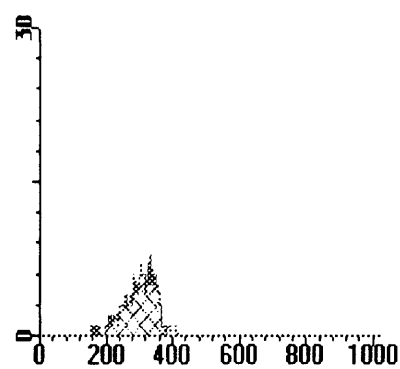
100 μ M Cycloheximide



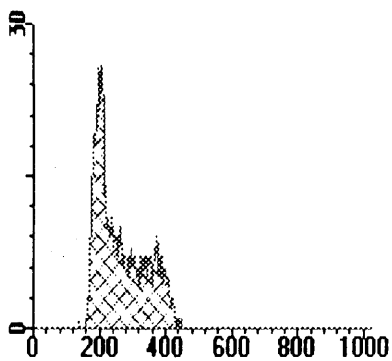
5 μ M VP16



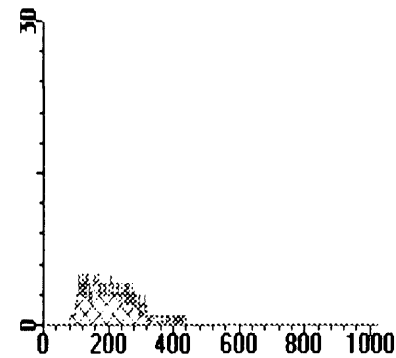
20 μ M VP16



0.1 μ M Actinomycin D



5 μ M Actinomycin D



Control

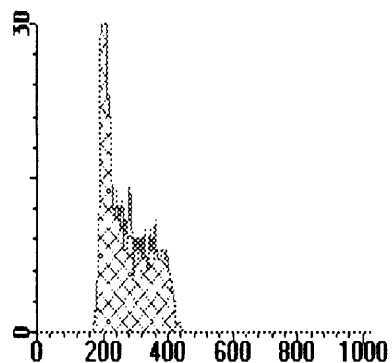


Fig. 3.6. Effect of CHX, VP16 and ActD on cell cycle in MEL C88 cells

MEL C88 cells were incubated either alone (Control) or in the presence of CHX, VP16 or Act D for 16 hours and analysed on the FACS Scan (2.2.2.2). Cell number is on the the y axis and DNA content is on the x axis. DNA contents of 200 and 400 represent 2N and 4N nuclei, respectively. The apparent loss of cells with higher concentrations of each agent is likely due to some of the 5000 events being below the analysis threshold. It is possible that the agents caused some cells to fragment and that these fragments were counted as events but were not large enough to analyse.

3.2.3. Staurosporine induces apoptosis in MEL DP16-1 cells more rapidly than in MEL C88 cells

To assess the apoptotic response of the DP16-1 cells to STS, cells were resuspended at 1×10^6 cells/ml in supplemented DMEM and incubated in the presence or absence of $0.2 \mu\text{M}$ STS for up to 8 h. Samples were taken at appropriate intervals and apoptosis assessed by CAGE (2.2.3.1) and DNA content analysis (2.2.2.2). In stark contrast to the results obtained using the C88 subline, CAGE showed that extensive internucleosomal cleavage was apparent within 4 h of treatment with $0.2 \mu\text{M}$ STS, with the maximum level already observed by this time (Fig. 3.7, lanes 5 and 6). Clearly the apoptotic responses of the C88 and DP16-1 cells are kinetically very different following treatment with STS.

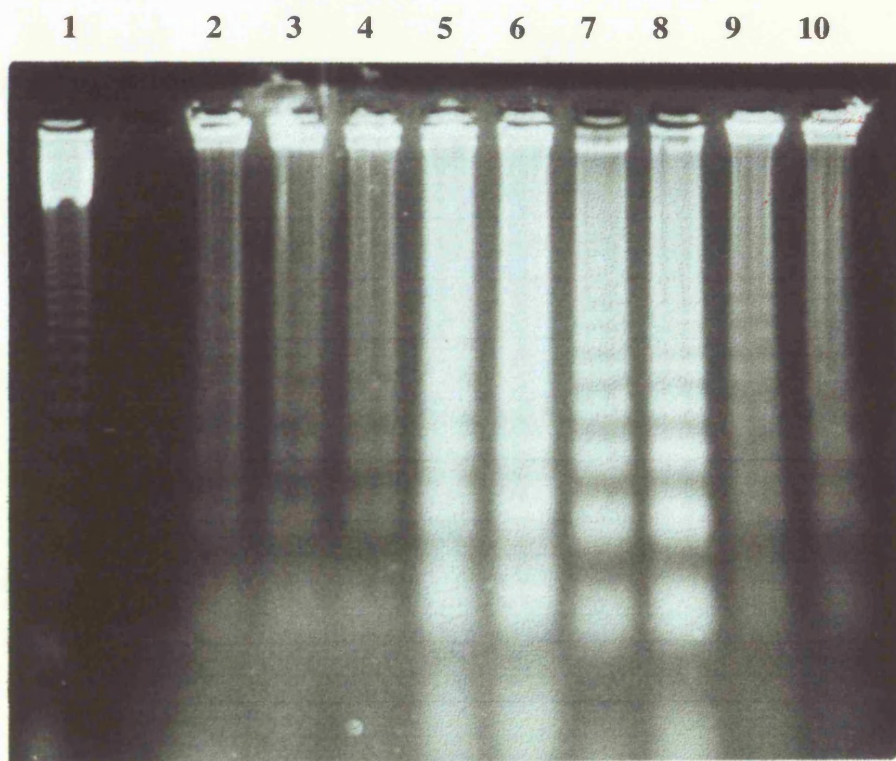
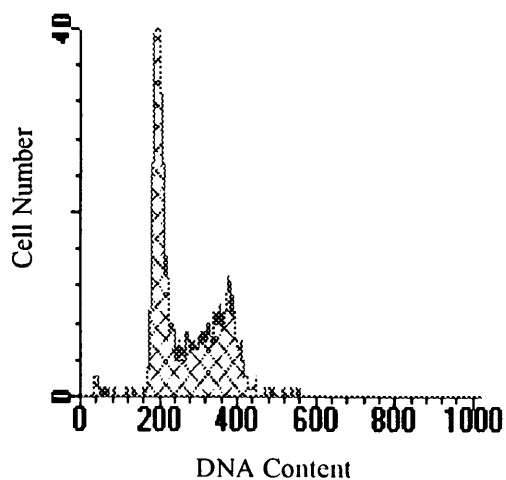


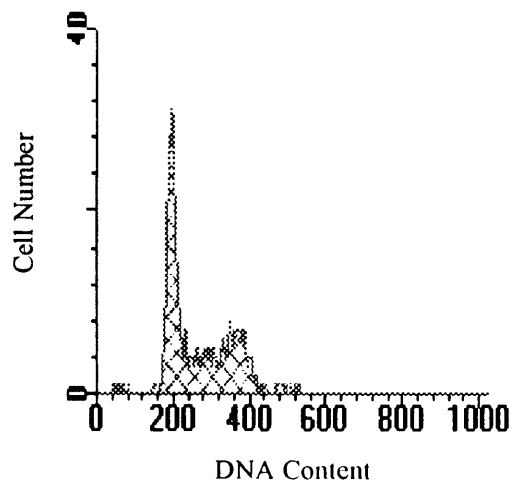
Fig. 3.7. STS-induced internucleosomal cleavage in MEL DP16-1 cells

MEL DP16-1 cells were incubated for varying lengths of time either alone or in the presence of $0.2 \mu\text{M}$ STS. Lanes 2 and 9–10 are DP16-1 cells treated alone for 2 and 8 h, respectively. Lanes 3–4, 5–6 and 7–8 are DP16-1 cells treated with $0.2 \mu\text{M}$ STS for 2, 4 and 8 h, respectively. Lane 1 is the 123bp marker.

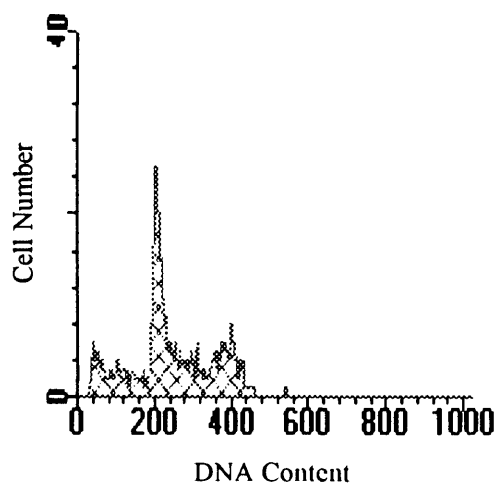
Control



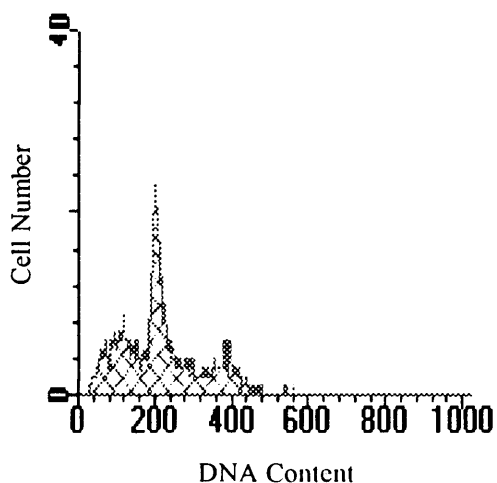
2 h 0.2 μ M STS



4 h 0.2 μ M STS



6 h 0.2 μ M STS



8 h 0.2 μ M STS

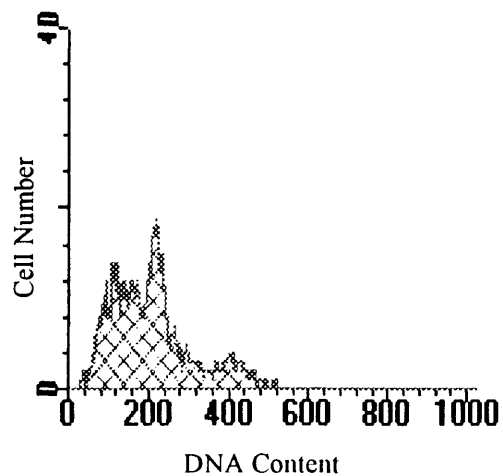


Fig. 3.8. STS-induced sub-G1 population in MEL DP16-1 cells

MEL DP16-1 cells were incubated either alone (Control) or in the presence of 0.2 μ M STS over a time course of 8 h and fixed in 70% ethanol, stained with PI and analysed on the FACS Scan (2.2.2.2). DNA contents of 200 and 400 correspond to 2N and 4N nuclei, respectively.

Further differences in the apoptotic response to STS were highlighted by analysis of DNA ploidy. Whereas STS induced apoptosis in C88 cells which was not manifested as a sub-G1 population (Fig. 3.3), in the DP16-1 cells STS induced a clear increase in the percentage of cells in the sub-G1 population (Fig. 3.8 and Fig. 3.9).

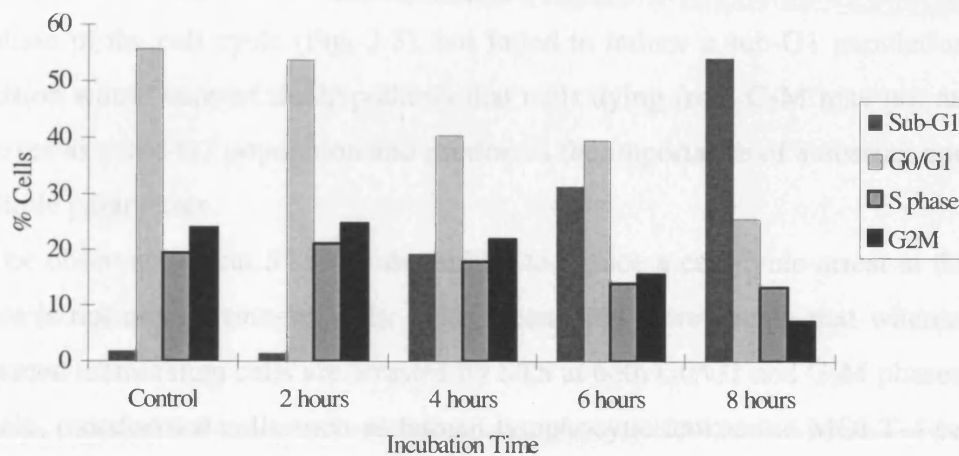


Fig. 3.9. STS-induced sub-G1 cell population in MEL DP16-1 cells

MEL DP16-1 cells were incubated either alone (Control) or in the presence of 0.2 μ M STS over a timecourse of 8 h, fixed in 70% ethanol, stained with PI and analysed on the FACS scan (2.2.2.2). The percentage of cells in each phase of the cell cycle at each time point was then calculated. The experiment shown is typical of several, and derived from data in Fig. 3.8.

Also in contrast to the effects on the C88 cells, in which STS induced a clear build up of cells at G₂M (Fig. 3.3), in the cells which remained cycling (ie. those cells not in the sub-G1 population), no cell cycle arrest was induced in the DP16-1 cells at any phase of the cell cycle (Table 3.1 and Fig. 3.8). The figures shown in Table 3.1 are derived only from the cycling cells in Fig. 3.9; ie. those cells that are not detectable as a sub-G1 population.

Table 3.1. STS does not induce a cell cycle arrest in cycling MEL DP16-1 cells

	G0/G1 (%)	S phase (%)	G ₂ M (%)
Control	56.2	19.7	24.1
2 h	53.9	21.1	24.9
4 h	50.0	22.3	27.4
6 h	56.8	20.2	22.7
8 h	55.3	28.9	15.8

3.3. DISCUSSION

Apoptosis was induced in MEL C88 cells by a variety of agents known to act in diverse ways. The indiscriminate protein kinase inhibitor, staurosporine (STS), induced characteristics of apoptosis after 4–10 h at a concentration of 0.2 μM . As well as inducing chromatin condensation and internucleosomal degradation of DNA, which was maximal after approximately 18 h (Figs. 3.1 and 3.2), STS induced a block at the G₂M phase of the cell cycle (Fig. 3.3), but failed to induce a sub-G1 population. This observation would support the hypothesis that cells dying from G₂M may not manifest themselves as a sub-G1 population and reinforces the importance of assessing apoptosis by multiple parameters.

The observation that STS has the ability to induce a cell cycle arrest at the G₂M interface is not new in tumour cells. It has been shown previously that whereas non-transformed mammalian cells are arrested by STS at both G₀/G₁ and G₂M phases of the cell cycle, transformed cells such as human lymphocytic leukaemic MOLT-4 cells are only able to be arrested at G₂M (Bruno, *et al.* 1992). This observation suggests that tumour cells can develop the ability to pass through the first cell cycle check point at G₀/G₁ without being phosphorylated by a protein kinase. However, in other cell types, STS has the ability to override a cell cycle arrest to uncouple premature mitosis from DNA damage-induced G₂M arrest, an effect which is dependent on *de novo* protein synthesis (Tam and Schlegel, 1992). In contrast, to that observed in the C88 cells, the maximum level of apoptosis in DP16-1 cells was induced with 0.2 μM STS within 4 h of treatment, as assessed by increased internucleosomal cleavage of DNA (Fig. 3.7) and the appearance of a sub-G1 peak (Fig. 3.8), with no block at either G₀/G₁ or G₂M being induced (Table 3.1). Following the reasoning above, this could suggest that the DP16-1 cells have progressed one stage further, and have lost the need for kinase mediation to allow them to pass through both G₀/G₁ and G₂M. Others have shown that following p53^{WT} induction in DP16-1 cells, apoptosis occurs predominantly from G1 in active cycling cells which would presumably manifest itself as a sub-G1 peak (Ryan, *et al.* 1993), in support of the data presented here (Figs. 3.8 and 3.9). Thus, the precise p53 status of the cell may influence the phase of the cell cycle from which cells predominantly die, and partially explain the differences observed between the C88 and DP16-1 cell lines. However, although p53 status is one difference between these two cell lines they are likely to differ in other respects as well.

An arrest in the cell cycle is not a prerequisite for the induction of apoptosis in MEL C88 cells. MEL C88 cells treated with various apoptosis-inducing agents were subjected to CAGE and cell cycle analysis. The results showed that the protein synthesis inhibitors cycloheximide and actinomycin D induced apoptosis in the C88 cells, as assessed by CAGE (Fig. 3.5), without having any discernible effect on the progression of cells through the cell cycle (Fig. 3.6). The involvement of protein synthesis in apoptosis is a complicated issue. In some systems, inhibitors of protein synthesis, such as cycloheximide, inhibit apoptosis (Martin, *et al.* 1988; McConkey, *et al.* 1989), in some their co-incubation with other known apoptosis-inducing agents has no effect, suggesting the pre-existence of at least some of the apoptotic machinery (Jacobson, *et al.* 1996; Fearnhead, *et al.* 1995b), and here and elsewhere apoptosis is induced by macromolecular inhibitors such as cycloheximide and actinomycin D (Cotter, *et al.* 1992; Waring, 1990).

Interestingly, the topoisomerase II inhibitor VP16 failed to induce apoptosis in C88 cells as assessed by CAGE (Fig. 3.5), although an arrest at the G₂M phase of the cell cycle was induced (Fig. 3.6). VP16 is a DNA-damaging agent through its inhibition of topoisomerase II, and it has been reported previously that such agents induce apoptosis primarily via a p53-dependent pathway (Clarke, *et al.* 1993; Lowe, *et al.* 1993b). Therefore, given the mutant p53 status of the C88 cells, it is perhaps not surprising that VP16 failed to induce apoptosis. The results, however, do suggest that the checkpoint mechanism at the G₂M interface was largely intact in C88 cells despite their deficiency in wild-type functional, p53. However, because the effect of VP16 was only assessed after 16 h, VP16 may have induced apoptosis at later timepoints by a p53-independent mechanism. Other studies in other systems have shown that cells induced to undergo apoptosis do not necessarily require a preceding cell cycle arrest at G₀/G₁ (Yonish-Rouach, *et al.* 1993; Lin, *et al.* 1995), suggesting that the apoptosis-inducing and cell cycle checkpoint functions of p53 are dissociable from each another, or that a protein other than p53 is responsible for the cell cycle checkpoint at G₂M.

As described in section 1.3.1, the exact nature of the p53 mutation can profoundly influence the cellular outcome (Zambetti and Levine, 1993). Thus, the difference between the mutant p53 and p53 null genotype could be responsible for the more rapid induction of apoptosis in the DP16-1 cells compared with the C88 cells, the failure of staurosporine to induce the same G₂M block in the DP16-1 cells as in the C88 cells or

the phase of the cell cycle from which cells predominantly die. In turn, this may influence the appearance of a sub-G1 peak in the DP16-1 cells and its absence in the C88 cells.

It is important to point out that, routinely, the background of laddering in DP16-1 cells was markedly higher than that seen in C88 cells (compare lane 2 in Figs. 3.2. and 3.7). It is a worrying possibility that this could be due to DNA cleavage during early differentiation in MEL DP16-1 cells (McMahon, *et al.* 1984). Proerythrocytes, by definition, must lose their nuclei during maturation to fully functional red blood cells. By the same token they must presumably degrade their DNA, posing an obvious problem in the study of apoptosis using this model system. Because of this potential problem it was felt that these cells were unsuitable for transient or stable transfection of genes such as p53. Because of our interest in determining the role of p53 in apoptosis, the project was continued in an M1 (murine myeloid leukaemic) cell line which also had the advantage of already being transfected with a temperature-sensitive mutant p53.

3.4. SUMMARY

MEL C88 and DP16-1 cells differ in their p53 status and also differ markedly in their response to the indiscriminate kinase inhibitor staurosporine. Staurosporine induces apoptosis in C88 cells over a time course of about 4–10 h in the presence of a cell cycle arrest at the G₂M phase of the cell cycle. In marked contrast, DP16-1 cells undergo apoptosis much more rapidly and in the absence of any discernible arrest in the cell cycle. Thus, an arrest at G₂M is not required for MEL cells to undergo apoptosis. The protein synthesis inhibitors cycloheximide and actinomycin D induced apoptosis in MEL C88 cells, although the topoisomerase II inhibitor VP16 failed to do so, consistent with the requirement of functional p53 for DNA-damaging agents to induce apoptosis. Although the two MEL sub-cell lines may have other phenotypical differences their different kinetics to apoptosis, and the differences observed in the effects of STS on progression of the cell cycle may equally be contributed to by their different p53 statuses.

**CHAPTER 4 – CHARACTERISATION OF THE MURINE
MYELOID LEUKAEMIC CELL LINE LTR6**

4.1. INTRODUCTION

Although there are exceptions (Strasser, *et al.* 1994; Bracey, *et al.* 1995; MacFarlane, *et al.* 1996), apoptosis induced by DNA-damaging agents such as ionising radiation and the topoisomerase II inhibitor etoposide (VP16) is mediated primarily via the nuclear phosphoprotein p53 (Clarke, *et al.* 1993; Lowe, *et al.* 1993b).

Following DNA damage the p53 protein will either induce a block at the G0/G1 phase of the cell cycle to facilitate the necessary repair mechanisms (Ryan, *et al.* 1993), or if the damage is too severe, may induce the cell to undergo apoptosis (Yonish-Rouach, *et al.* 1991). One of the best model systems for studying apoptosis is the use of cell lines containing a temperature-sensitive p53 protein (Michalovitz, *et al.* 1990; Yonish-Rouach, *et al.* 1991). LTR6 cells are a subclone of the murine myeloid leukaemic M1 cell line which have been stably transfected with a gene encoding a temperature-sensitive p53 protein. The transfected gene contains a mutation which results in an amino acid substitution from alanine to valine at position 135 in the encoded protein (Michalovitz, *et al.* 1990). The protein behaves as the mutant protein at 37.5°C (restrictive temperature) and is indistinguishable from the wild-type protein at 32.5°C (permissive temperature) (Michalovitz, *et al.* 1990; Milner and Medcalf, 1990). LTR6 cells shifted from 37.5°C to 32.5°C show no evidence of a cell cycle arrest (Yonish-Rouach, *et al.* 1993), but instead rapidly lose viability and undergo apoptosis (Yonish-Rouach, *et al.* 1991).

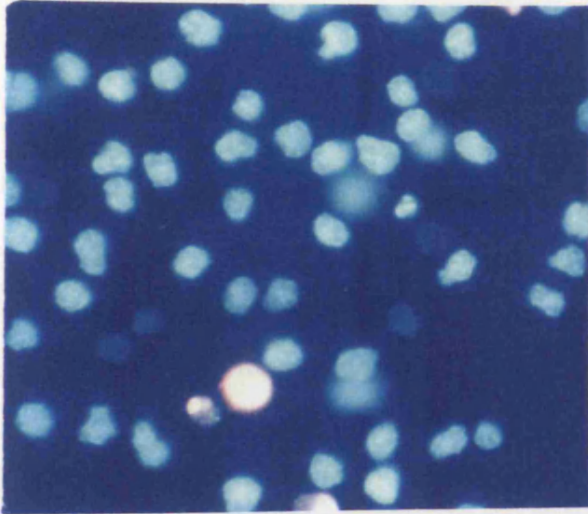
These initial studies were based largely on morphological analysis and the uptake of the cellular viability dye trypan blue, which is also taken up by cells with gross membrane damage, ie. necrotic cells, and does not specifically detect apoptotic cells. The aims of the experiments described in this chapter were to further characterise apoptosis induced by p53^{WT} in LTR6 cells, and to develop a more quantitative method of assessing the incidence of apoptosis based on a previously described quantitative flow cytometric method (Sun, *et al.* 1992). For the described experiments, three related cell lines were used; the LTR6 cells containing the temperature-sensitive mutant p53 protein, the control cell line LTRphe132, containing a non-temperature-sensitive mutant p53 protein and the M1, p53 null parental cell line, from which the other two lines are derived (Yonish-Rouach, *et al.* 1991).

4.2. RESULTS

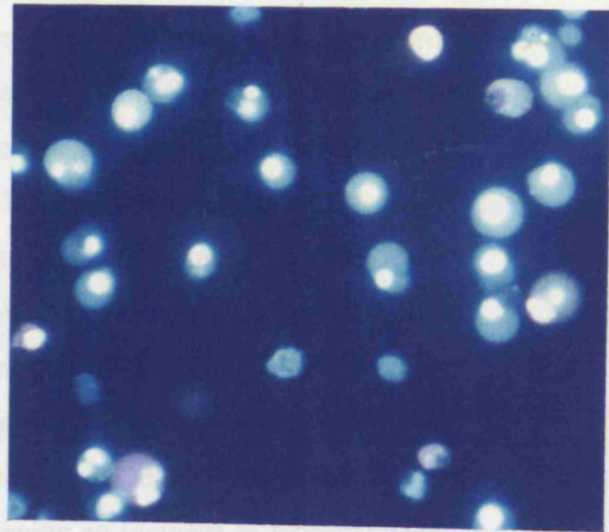
4.2.1. p53^{WT}-induced apoptosis in murine LTR6 cells

LTR6 cells were shifted to 32.5°C or retained at 37.5°C for 22 h. The incidence of apoptosis was assessed by morphological analysis, conventional agarose gel electrophoresis (CAGE) and a quantitative flow cytometric method based on the differential uptake of the two DNA-binding dyes Hoechst 33342 and propidium iodide (PI). Hoechst 33342 intercalates DNA at A–T base pairs and is taken up by all cells. However, the membrane changes that occur during the earlier stages of apoptosis facilitate its increased uptake and result in a corresponding increase in blue fluorescence. Propidium iodide is only taken up by non-viable cells due to gross membrane damage, thus normal, apoptotic and necrotic cells can be distinguished and apoptosis quantified. After 22 h at the permissive temperature, the LTR6 cells showed a characteristic apoptotic morphology with condensed nuclear chromatin (Fig. 4.1A) and an increased incidence of internucleosomal cleavage of DNA, visualised as an intense laddering pattern on conventional agarose gels (Fig. 4.1B).

A 37.5°C



32.5°C



B 1 2

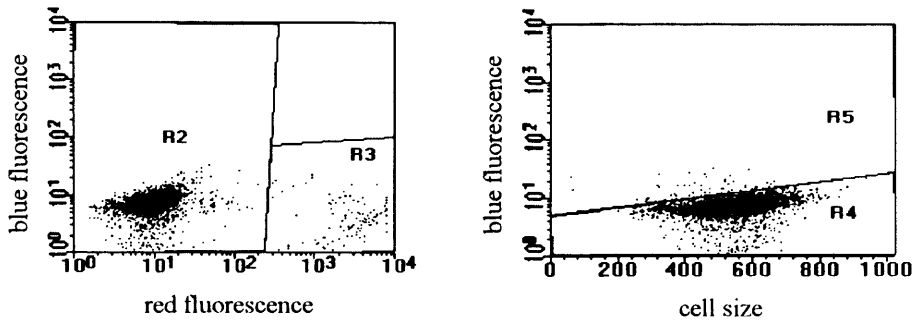


Fig. 4.1. p53^{WT}-induced apoptosis assessed by morphology and CAGE

LTR6 cells were either shifted to 32.5°C or retained at 37.5°C for 22 h. A) LTR6 cells were stained with Hoechst 33342 and PI as described in section 2.2.2.1 and examined under the fluorescence microscope. Left and right panels are LTR6 cells incubated for 22 h at 37.5°C and 32.5°C, respectively. B) LTR6 cells were prepared for CAGE as described in section 2.2.3.1. Cells were loaded at 0.5×10^6 /lane. Lanes 1 and 2 are LTR6 cells incubated for 22 h at 37.5°C and 32.5°C, respectively.

Analysis of the LTR6 cells by flow cytometry revealed that a 22 h shift to the permissive temperature also induced a marked increase in the percentage of cells showing increased Hoechst 33342 fluorescence (Fig. 4.2) from 1.4% in controls (Fig. 4.2A, R5) to 33.5% following a 22 h temperature-shift (Fig. 4.2B, R5). A 22 h shift to the permissive temperature also induced an increase in the percentage of cells in the PI-including population (R3), from 2.6% in controls (Fig. 4.2A, R3) to 14.4% (Fig. 4.2B, R3), which would suggest that p53^{WT} induced a degree of necrosis as well as apoptosis. However, the flow cytometric method is not able to discriminate between necrosis and secondary necrosis (ie. cells that show apoptotic morphology, but have sustained further damage to the cell membrane and have subsequently taken up PI), and comparison of regions R2 and R3 suggested that the PI-including cells are derived from the cells showing an increase in Hoechst 33342 fluorescence (Fig. 4.2B, left panel). Corroborating this, examination under the fluorescence microscope showed that < 5% of the PI-including cells were devoid of the chromatin condensation characteristic of apoptosis. Hence, total apoptosis in this system assessed by flow cytometry was expressed as % cells in R3 + % cells in R5. Taken together, the results clearly demonstrated that a temperature shift from 37.5°C to 32.5°C induced apoptosis in LTR6 cells after 22 h, as assessed by fluorescence microscopy, CAGE and Hoechst 33342/PI flow cytometry.

A 22 hours at 37.5°C



B 22 hours at 32.5°C

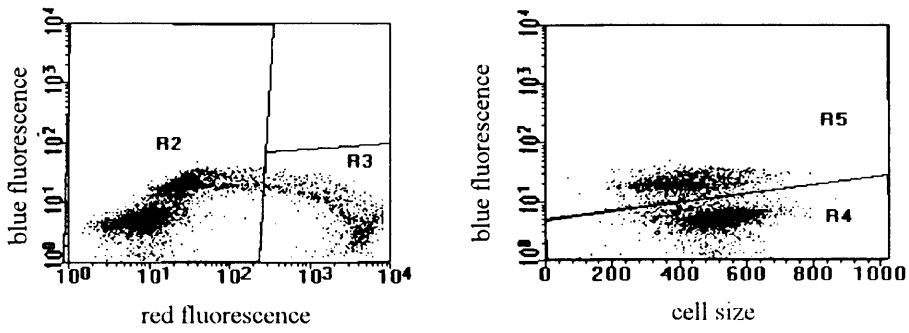
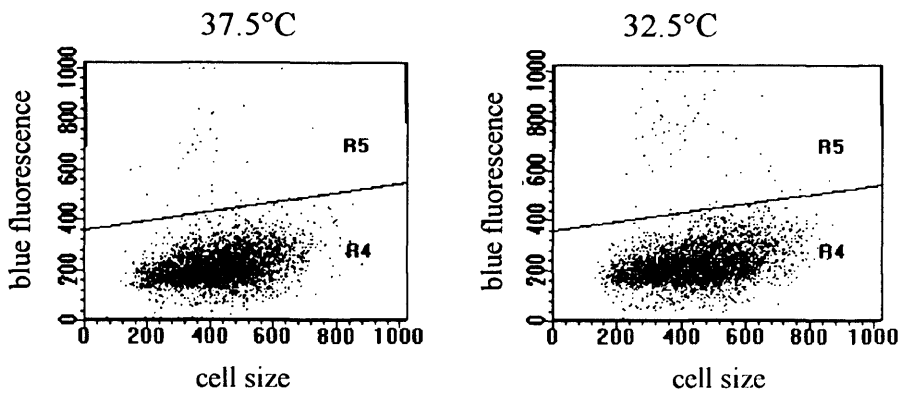


Fig. 4.2. p53^{WT}-induced apoptosis assessed by Hoechst 33342/PI flow cytometry
 LTR6 cells were retained at 37.5°C (A) or shifted to 32.5°C (B) for 22 h, and stained for flow cytometry as described in section 2.2.2.1a. A) The percentage of cells in regions (R) 2, 3, 4, and 5 is 93.5, 2.6, 91.5 and 1.4, respectively. B) The percentage of cells in R2, 3, 4, and 5 is 80.5, 14.4, 60.5 and 33.5, respectively. The blue and red fluorescence is derived from Hoechst 33342 and PI, respectively. The experiment shown is typical of several.

4.2.2. Incubation of LTRphe132 and M1 cells at the permissive temperature does not induce apoptosis

To confirm that the alteration in p53 status was responsible for the induction of apoptosis in LTR6 cells, the two control cell lines were also shifted to 32.5°C for 22 h. In marked contrast to the LTR6 cells, transferral of the LTRphe132 or M1 cells to the permissive temperature for 22 h did not induce an apoptotic population of cells (Fig. 4.3). The cells retained normal morphology and showed no increased incidence of internucleosomal cleavage of DNA (data not shown). In addition, no increase in the intensity of Hoechst 33342 fluorescence was observed; in M1 cells the temperature-shift induced 2.7% apoptosis compared with the 4.2% present in controls (Fig. 4.3A), and similarly in LTRphe132 cells, the temperature-shift induced 2.3% apoptosis compared with 3.4% in control cells (Fig. 4.3B). Thus the induction of apoptosis in the LTR6 cells following temperature shift was induced by a conformational change in p53 from mutant to wild-type, and was not a consequence of the change in temperature *per se*.

A M1 Cells



B LTRphe132 Cells

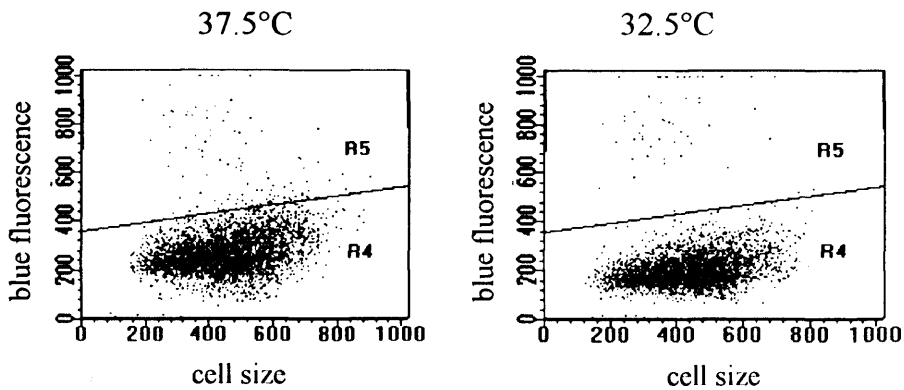


Fig. 4.3. A 22 h temperature-shift to 32.5°C does not induce apoptosis in LTRphe132 or M1 cells

M1 and LTRphe132 cells were shifted to 32.5°C or retained at 37.5°C for 22 h and the incidence of apoptosis assessed by flow cytometry as described in section 2.2.2.1. A) Control and temperature-shifted M1 cells; apoptosis is 4.2 % and 2.7%, respectively. B) Control and temperature-shifted LTRphe132 cells; apoptosis is 3.4% and 2.3%, respectively. The experiment shown is typical of several.

4.2.3. p53^{WT} induces apoptosis in LTR6 cells after 14–16 h at the permissive temperature

Studies of the properties of the temperature-sensitive p53 protein have shown that the conformational change from mutant to wild-type occurs within 2 h of a temperature-shift to 32.5°C (Michalovitz, *et al.* 1990). Indeed other studies have shown that cellular effects of wild-type p53 such as *transactivation* and *transrepression* of the *bax* and *bcl-2* promoters, respectively, are detectable as early as 4 h after shifting to the permissive temperature (Ginsberg, *et al.* 1991; Miyashita, *et al.* 1994; Miyashita and Reed, 1995). Therefore, to further dissect the pathway of p53^{WT}-induced apoptosis in LTR6 cells, the incidence of apoptosis was assessed at different times post-temperature-shift using the quantitative flow cytometric assay (Sun, *et al.* 1992). LTR6 cells were retained at 37.5°C for 22 h (control) or shifted to 32.5°C for up to 22 h. LTR6 cells transferred to 32.5°C and assessed by quantitative flow cytometry showed a time-dependent increase in apoptosis, which was marked after 14–16 h at the permissive temperature (Fig. 4.4). Cells retained at 37.5°C for 22 h showed a basal level of apoptosis of approximately 9% when assessed by this method (Fig. 4.4).

4.2.4. A shift in temperature from 37.5°C to 32.5°C induces a change in the p53 status of LTR6 cells

It is interesting to note from the section above that an incubation of at least 14 h at the permissive temperature is required to induce any significant increase in the incidence of apoptosis in LTR6 cells, as assessed by flow cytometry. As described above, studies from others have demonstrated that the conformational change from mutant to wild-type p53 occurs within 2 h of the shift in temperature (Michalovitz, *et al.* 1990), and that by 4 h other cellular events are already apparent (Miyashita, *et al.* 1994). Therefore the change in p53 conformation from mutant to wild-type was confirmed using a flow cytometric technique under native conditions, and an antibody specific to the mutant form of p53 (section 2.2.12; Fig. 4.5). The PAb240 antibody used is specific for an epitope on the p53 protein which is concealed in p53^{WT} and exposed in mutant p53 (Stephen and Lane, 1992). Therefore, under native conditions, the antibody will detect only the mutant form of the protein. The

use of a secondary FITC-conjugated antibody which when excited emits a green fluorescence which can be measured at a wavelength of 515–545 nm, allows any conformational change in p53 from mutant to wild-type to be detected and quantified. Thus, a reduction in green fluorescence corresponds to a conformational change from mutant to wild-type p53. The results clearly demonstrated that, after 22 h at the permissive temperature, a conformational change was readily detectable. A slight decrease in green fluorescence was also seen after 2 h at the permissive temperature (data not shown), indicating that as early as 2 h post-temperature-shift a conformational change had occurred in the p53 protein.

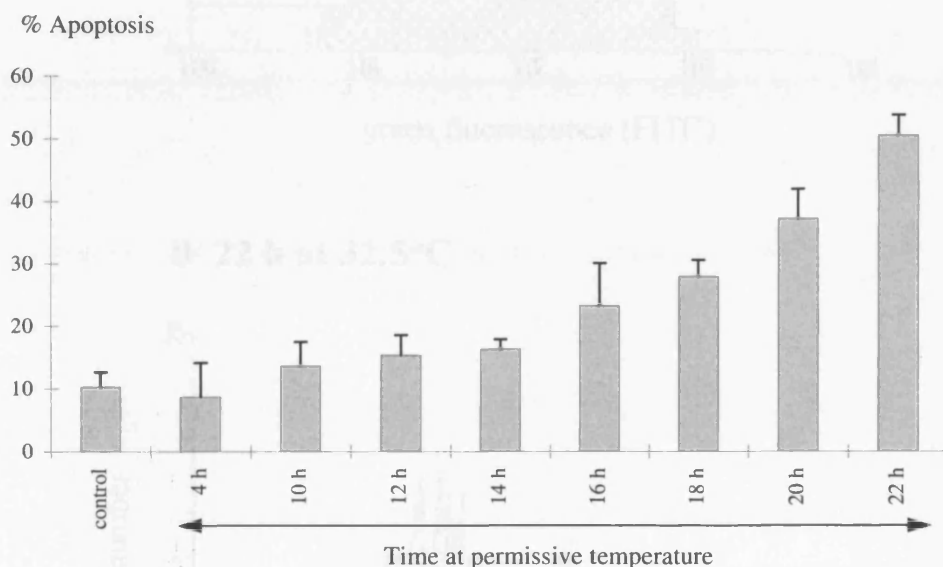
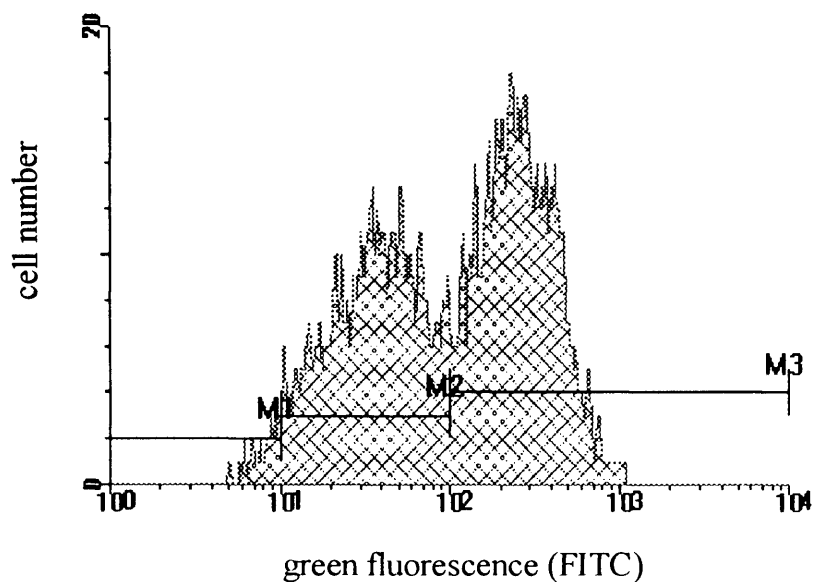


Fig. 4.4. Time-dependent increase in p53^{WT}-induced apoptosis

LTR6 cells were shifted for up to 22 h to 32.5°C, or left for 22 h at 37.5°C (control). Cells were double stained with Hoechst 33342 and PI and analysed by quantitative flow cytometry (section 2.2.2.1). The results are expressed as the mean ± SEM from 3 separate experiments.

A 22 h at 37.5°C



B 22 h at 32.5°C

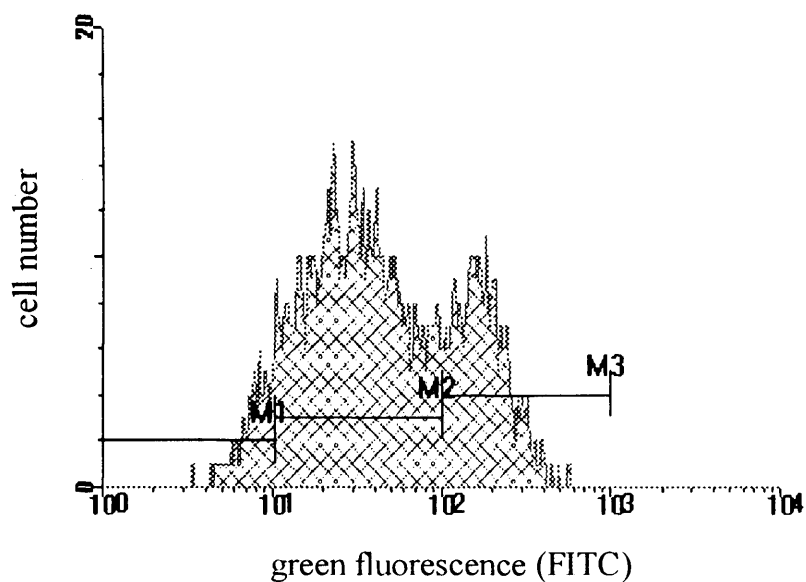


Fig. 4.5. A conformational change in p53 is induced after incubation at the permissive temperature

LTR6 cells were retained at 37.5°C (A) or shifted to 32.5°C (B) for 22 h, and prepared for FACS Scan analysis as described in section 2.2.13. A) Percentages of total cell population in regions M1, 2 and 3 are 2, 45, and 53, respectively. B) Percentages of total cell population in regions M1, 2 and 3 are 7, 66, and 27, respectively.

4.2.5. Temperature-shift does not induce changes in the level of the p53 protein

In addition, to confirm that the temperature-shift did not induce an increase in the levels of p53 protein within the cells and thus account for the induction of apoptosis, LTR6, LTRphe132 and parental M1 cells were either retained at 37.5°C or shifted to 32.5°C for 22 h. After the appropriate incubation time the proteins were separated by SDS/10% (w/v) polyacrylamide gel electrophoresis (PAGE) and Western blotting carried out. The levels of the p53 protein in the three cell lines before and after a 22 h shift to the permissive temperature were assessed using an antibody to p53. Under the denaturing conditions of SDS-PAGE, the PAb240 antibody detected both the mutant and wild-type forms of the protein, and therefore assessed the total amount of p53 within the cells. As expected the parental M1 cell line showed no detectable p53 protein either prior to or after the temperature-shift (Fig. 4.6, lanes 1 and 2, respectively). Both the control and temperature-shifted LTRphe132 cells (Fig. 4.6, lanes 3 and 4, respectively) and control and temperature-shifted LTR6 cells (Fig. 4.6, lanes 5 and 6, respectively), expressed comparably high levels of the protein at both the restrictive and permissive temperatures.

4.2.6. Temperature-shift induces a sub-G1 peak without inducing an arrest in the cell cycle

To further quantify the incidence of p53^{WT}-induced apoptosis, LTR6 cells were either retained for 24 h at 37.5°C (control) or shifted to 32.5°C for different lengths of time. After the appropriate incubation time cells were prepared for cell cycle analysis on the FACS scan. As has been previously described (Yonish-Rouach, *et al.* 1993), the temperature shift did not induce an arrest in the G0/G1 phase of the cell cycle but instead induced a sub-G1 peak characteristic of cells undergoing apoptosis (Darzynkiewicz, *et al.* 1992; Fig. 4.7). DNA fragmented during apoptosis is easily lost from cells permeabilised with detergent. If the resulting loss means that the DNA content is less than that of a normal diploid nucleus (2N) these cells will be apparent as a sub-G1, or hypo-diploid population. The degree of apoptosis assessed in this manner was comparable to that assessed by the Hoechst 33342/PI method. Analysis of the percentage of cells remaining in the cell cycle (ie. excluding those detectable as a sub-G1 peak) confirmed that a

temperature-shift did not cause cells to accumulate in any particular phase of the cell cycle (Table 4.1).

Sample	G0/G1 (%)	S phase (%)	G ₂ M (%)
Control	60	27	13
12 h	60	23	17
16 h	59	22	19
20 h	56	24	20
24 h	60	24	16

Table 4.1. p53^{WT} does not induce an arrest in any phase of the cell cycle

LTR6 cells were shifted for 12, 16, 20 or 24 h to 32.5°C or retained at 37.5°C for 22 h (control) and prepared and analysed on the FACS scan as described in section 2.2.2.2. The figures are expressed as the percentage of cycling cells in each phase of the cell cycle at each time point and correspond to the samples described in figure 4.7. Values are calculated from Fig. 4.7, and are representative of several experiments.

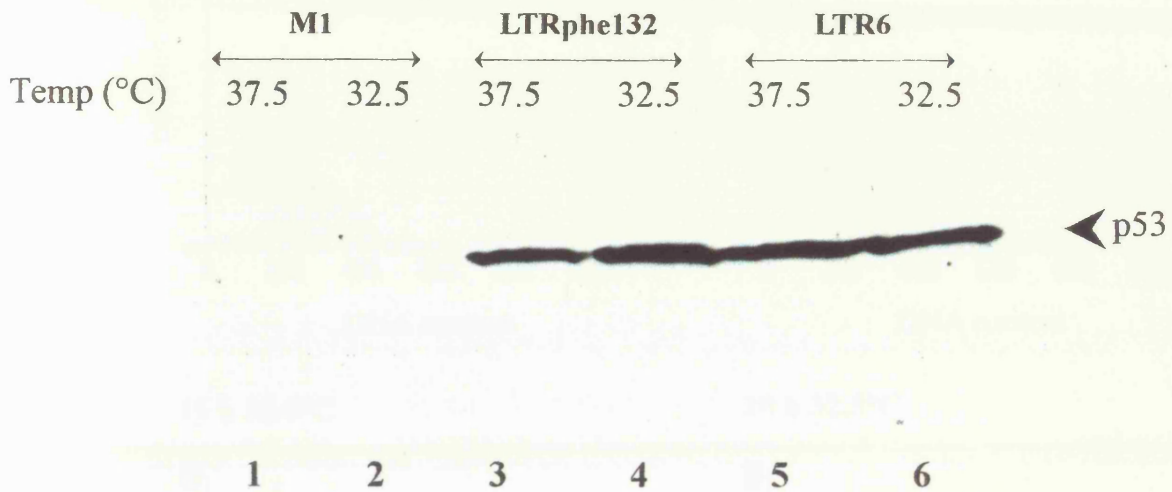


Fig. 4.6. Expression of p53 in M1, LTRphe132 and LTR6 cells

M1, LTRphe132 and LTR6 cells were shifted to 32.5°C or retained at 37.5°C for 22 h and examined by SDS/10% (w/v) PAGE and Western blotting using the PAb240 p53 antibody. The blot was probed and examined using enhanced chemiluminescence as described in section 2.2.4. The p53 protein is indicated.

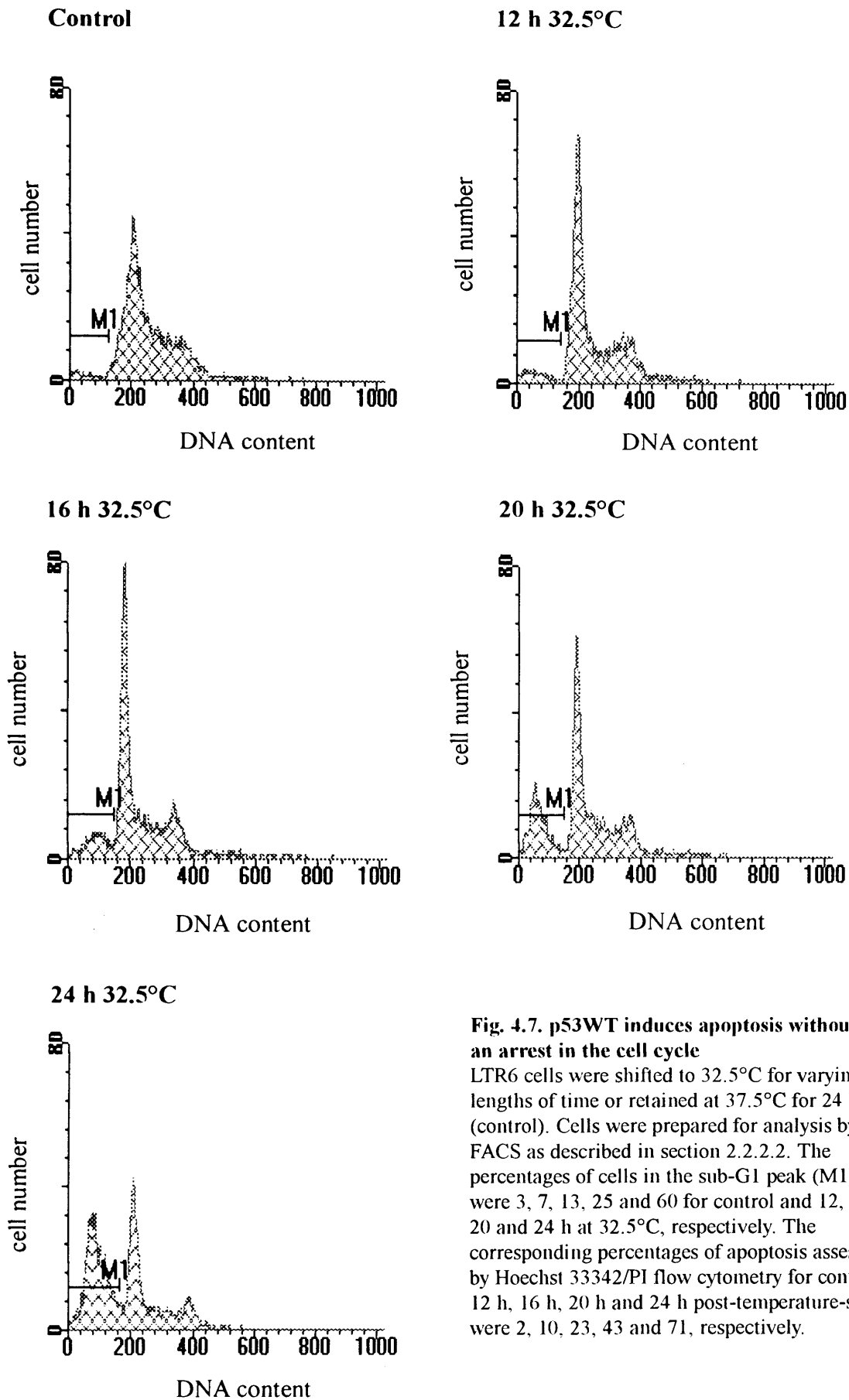


Fig. 4.7. p53WT induces apoptosis without an arrest in the cell cycle
 LTR6 cells were shifted to 32.5°C for varying lengths of time or retained at 37.5°C for 24 h (control). Cells were prepared for analysis by FACS as described in section 2.2.2.2. The percentages of cells in the sub-G1 peak (M1) were 3, 7, 13, 25 and 60 for control and 12, 16, 20 and 24 h at 32.5°C, respectively. The corresponding percentages of apoptosis assessed by Hoechst 33342/PI flow cytometry for control, 12 h, 16 h, 20 h and 24 h post-temperature-shift were 2, 10, 23, 43 and 71, respectively.

4.2.7. Detection of large fragments of DNA following p53^{WT}-induced apoptosis

From the results described so far it is apparent that the time course to apoptosis following the induction of p53^{WT} is relatively long, especially given that some conformation change from mutant to wild-type is detectable as early as 2 h after the shift to the permissive temperature. In the experiments described so far apoptotic characteristics such as increased Hoechst 33342 fluorescence and the induction of a sub-G1 peak of apoptotic cells have first been detectable in cells that have been shifted to the permissive temperature for between 14 and 16 hours (Figs. 4.4. and 4.7). No features characteristic of apoptosis have been detected prior to this.

A feature that has been described as occurring relatively early in the apoptotic process in several cell systems is the formation of DNA fragments of at least 50 kbp in size (Brown, *et al.* 1993). These large fragments of DNA precede the formation of the 180–200 bp fragments which arise from the internucleosomal cleavage of DNA (Brown, *et al.* 1993). Therefore, the incidence of large fragment formation was assessed using field inversion gel electrophoresis (FIGE) in LTR6 cells. LTR6 cells were shifted to 32.5°C for varying lengths of time and prepared for FIGE as described in section 2.2.3.2. Considerable difficulties were experienced in the detection of large fragments of DNA following temperature-shift to the permissive temperature of 32.5°C. The monocytic human tumour cell line THP.1 treated for 4 h with 25 µM VP16 was used as a positive control and showed a high incidence of large fragments as previously described (Zhu, *et al.* 1995; Fig. 4.8A, lane 10). However, LTR6 cells incubated at 32.5°C showed no increase in the formation of large fragments compared with controls (Fig. 4.8A, lanes 3–9). This observation suggested that either no large fragments were formed in these cells following p53^{WT} induction, or that their formation was too transient to allow their detection by electrophoresis.

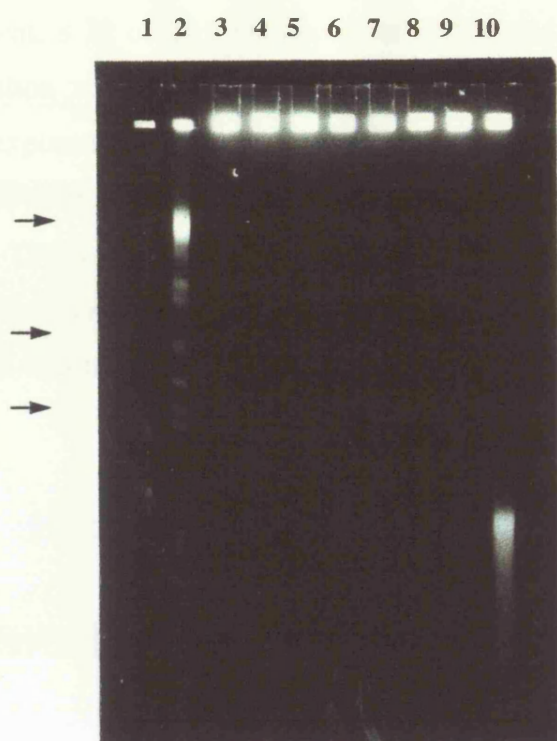


Fig. 4.8A. FIGE of LTR6 cells following temperature-shift to the permissive temperature

LTR6 cells were either retained at 37.5°C (Control; lane 3) or shifted for varying lengths of time to 32.5°C and prepared for FIGE as described in section 2.2.3.2. LTR6 cells shifted for 12, 14, 16, 18, 20 and 24 h are in lanes 4–9, respectively. Lane 10 is the positive control of THP.1 cells treated for 4 h in the presence of 25 μ M VP16. The markers in lanes 1 and 2 are 0.1–200 kbp markers and *S. Cerevisiae* chromosomes, respectively. The top, middle and bottom arrows represent DNA of 700, 460 and 50 kbp in length, respectively.

The serine protease inhibitor TPCK is capable of inhibiting the formation of internucleosomal cleavage of DNA, but not its cleavage into large fragments (Weaver, *et al.* 1993). Therefore, the use of TPCK in LTR6 cells could prevent internucleosomal cleavage of DNA, allowing the build up of large fragments and facilitating their detection by FIGE. Preincubation of LTR6 cells for 1 h in the presence of 10 or 25 μ M TPCK prior to a temperature-shift to 32.5°C allowed the detection of large fragments (Fig. 4.8B, lanes 9 and 10). However, in the LTR6 cells TPCK did not inhibit internucleosomal cleavage (data not shown). Furthermore, TPCK alone, in the absence a shift to the permissive temperature, induced a comparable level of large fragments (data not shown). These results demonstrate that large fragments are inducible in LTR6 cells, suggesting that following p53^{WT}

induction in the absence of TPCK, the fragments are simply too transient to detect. In this experiment, a 22 or 24 h incubation at 32.5°C did cause a degree of large fragment formation above that observed in the corresponding control samples, favouring the explanation that transient formation of large fragments occurs in LTR6 cells following p53^{WT}-induced apoptosis. However, the formation of large fragments with TPCK alone could be a phenomenon specifically associated with this compound in this system. Due to the difficulties experienced in detecting large fragments, FIGE was not used routinely as a method for assessing apoptosis in this system.

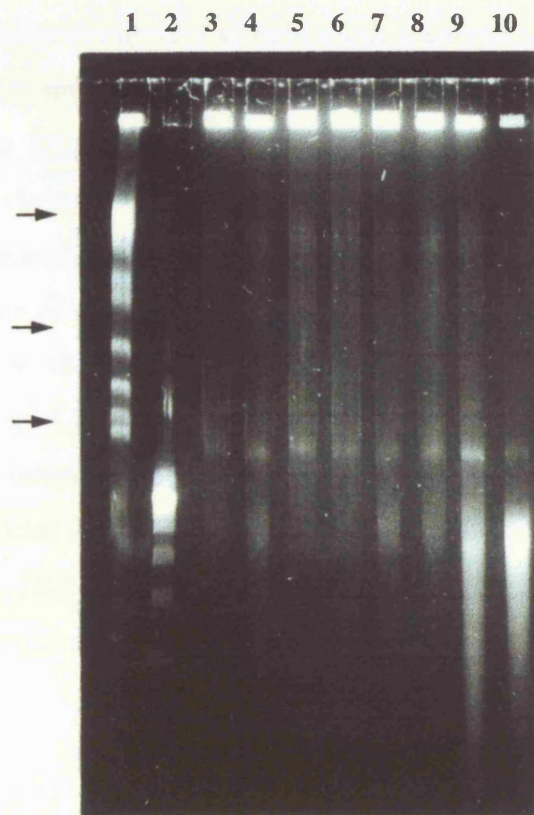


Fig. 4.8B. FIGE of LTR6 cells following temperature-shift to the permissive temperature in the presence or absence of TPCK

LTR6 cells were either retained at 37.5°C (control) for 22 h (lane 3) or 24 h (lanes 5 and 6) or shifted to 32.5°C for 22 h (lane 4) or 24 h (lanes 7 and 8) or incubated in the presence of 10 or 25 μ M TPCK prior to a 22 h shift to the permissive temperature (lanes 9 and 10, respectively) and prepared for FIGE as described in section 2.2.3.2. The markers in lanes 1 and 2 are *S. cerevisiae* chromosomes and 0.1–200 kbp markers, respectively. The top, middle and bottom arrows represent DNA fragments of 700, 460 and 50 kbp in length, respectively.

4.3. DISCUSSION

To study the mechanisms involved in p53^{WT}-induced apoptosis, a temperature-sensitive cell system was employed. LTR6 cells contain a transfected p53 gene encoding a temperature-sensitive protein which behaves as the mutant form at 37.5°C promoting cell growth and proliferation, and as the wild-type apoptosis-promoting protein at 32.5°C (Yonish-Rouach, *et al.* 1991). In these initial studies, apoptosis induced by a temperature-shift was assessed primarily by morphology and by exclusion studies using the cell viability dye, trypan blue (Yonish-Rouach, *et al.* 1991). The results in this chapter have confirmed the apoptosis-inducing effects of p53^{WT} and have described additional quantitative techniques for the more detailed examination of p53^{WT}-induced apoptosis in LTR6 cells.

A 22 h incubation at 32.5°C induced characteristic features of apoptosis in murine LTR6 cells, manifested morphologically by the profound condensation of nuclear chromatin (Fig. 4.1A) and biochemically by the increased incidence of internucleosomal cleavage of DNA (Fig. 4.1B). Field inversion gel electrophoresis also supported the transient formation of large fragments of DNA (Fig. 4.8B). The increased incidence of apoptosis was quantitated using a modified flow cytometric technique based on the differential uptake of two DNA-binding dyes, Hoechst 33342 and PI (Fig. 4.2; Sun, *et al.* 1992). Transferral of the control cell lines, LTRphe132 (non-temperature-sensitive mutant p53) and M1 (parental; p53 null), induced none of these characteristics of apoptosis, confirming that an alteration in the p53 status of LTR6 cells was responsible for the induction of apoptosis, and not the change in temperature *per se* (Fig. 4.3).

A more in depth study of the timecourse to apoptosis following a shift in temperature and a change in conformation of p53 was carried out in the LTR6 cells. Using the quantitative flow cytometric method, the percentage of apoptotic LTR6 cells was assessed after different incubation periods at the permissive temperature (Fig. 4.4). Although there was some degree of variation in the percentage of apoptotic cells at each timepoint in different experiments, it was clear that an incubation of 14–16 h at the permissive temperature was required to induce a level of apoptosis markedly higher than that seen in control cells (22 h at 37.5°C).

The increased incidence of apoptosis in LTR6 cells induced by a shift to the permissive temperature was also quantitated using a second flow cytometric

technique, based on the analysis of the DNA content within the cells (Darzynkiewicz, *et al.* 1992). The ordered cleavage of DNA is a well documented feature of apoptosis in many cell systems (Bicknell, *et al.* 1994; Jarvis, *et al.* 1994; Cain, *et al.* 1994; Sun, *et al.* 1994; Fearnhead, *et al.* 1995c; Zhu, *et al.* 1995). Permeabilised apoptotic cells have the ability to lose some of their fragmented DNA and consequently have a lower DNA content than their normal counterparts. A cellular DNA content of $< 2N$ (ie. that of a normal diploid nucleus) appears as a sub-G1 peak or hypo-diploid peak, and has been shown previously to correlate with apoptosis in other cell lines (Darzynkiewicz, *et al.* 1992).

The conformational change in p53 from mutant to wild-type induced a sub-G1 peak in LTR6 cells after approximately 16 h at the permissive temperature (Fig. 4.7), in the absence of an arrest in the cell cycle (Yonish-Rouach, *et al.* 1993; Table 4.1). The results obtained with the different quantitative methods of apoptosis correlated well, although, the DNA analysis method consistently gave a lower estimation of the percentage of apoptotic cells than the Hoechst 33342/PI method of assessment. This observation could be explained in two ways. Firstly, the apoptotic cells could be dying from all phases of the cell cycle. The DNA analysis method is based on the ability of permeabilised cells to lose their fragmented DNA, consequently cells dying from S phase would not necessarily be apparent in a sub-G1 population. Secondly, some of the cells exhibiting an increased Hoechst 33342 fluorescence may be at a stage prior to DNA fragmentation, which is generally regarded as a late stage in the apoptotic process (Brown, *et al.* 1993), and therefore would not appear in the sub-G1 population. The absence of a cell cycle arrest may be a feature of the over-expression system, ie. such an increase in the levels of intracellular p53^{WT} could fool the cell into believing that a large amount of DNA damage has been sustained, and have the effect of overriding an arrest at G0/G1 phase of the cell cycle, and inducing apoptosis in preference.

Previous studies have shown that the conformation change from mutant to wild-type p53 is complete within 2 h of the shift in temperature (Michalovitz, *et al.* 1990). The use of an antibody to p53, which only recognises an epitope on the mutant form of the protein under native conditions (Stephen and Lane, 1992), in conjunction with a secondary antibody conjugated to FITC, facilitated the quantitation of the conformation change (Fig. 4.5). Temperature-shifting LTR6 cells

for 22 h to the permissive temperature caused a marked decrease in green fluorescence (Fig. 4.5) consistent with a conformation change in p53 from mutant to wild-type. A slight decrease was detectable as early as 2 h after the temperature-shift. Thus, despite the rapid induction of p53^{WT} after the shift in temperature, apoptotic markers were not detectable until after 14–16 h. An obvious explanation for the time lag between the induction of p53^{WT} and the appearance of apoptotic characteristics would be the requirement for synthesis of new proteins for the mediation of p53^{WT}-induced apoptosis in LTR6 cells. However, it has been previously reported that only a partial inhibition of the p53^{WT}-induced response is achieved in these cells with protein synthesis inhibitors such as cycloheximide (Yonish-Rouach, *et al.* 1991). This would suggest that in this system, as has been reported for others, the basis of at least part of the apoptotic machinery pre-exists in the cells (Jacobson, *et al.* 1996; Fearnhead, *et al.* 1995b).

In addition, p53^{WT} has been shown to induce the expression of the Fas/APO-1/CD95 receptor at the cell membrane in the presence of cycloheximide (Owen-Schaub, *et al.* 1995). Crosslinkage of this receptor with its physiological ligand or an agonistic antibody induces apoptosis in cell types in which it is expressed (section 1.4.2.6). Therefore it is possible that p53^{WT} influences the apoptotic pathway both by the initiation of internal mechanisms and by making apoptosis-inducing receptors available for cross-linkage. In addition to Fas/APO-1/CD95, p53^{WT} has also recently been shown to upregulate *DR5/KILLER*, a new member of the TNFR1 death receptor family (Wu, *et al.* 1997), crosslinkage of which could lead to the demise of the cell via the activation of intracellular executionary mechanisms in a similar way to Fas.

Despite evidence supporting the pre-existence of the apoptotic machinery within cells, the partial attenuation of the apoptotic response by cycloheximide is consistent with at least some new protein synthesis being required for the execution of the apoptotic pathway. Indeed, the p53 protein is well documented as a transcription factor and has been shown to influence the transcription and subsequent protein synthesis of some players in the apoptotic response. Following the induction of p53^{WT} by temperature-shift in LTR6 cells, *transactivation* and *transrepression* from the *bax* and *bcl2* promoters, respectively, has been documented within 4 h of the temperature-shift, translating into corresponding

changes in protein levels within 20 h (Ginsberg, *et al.* 1991; Miyashita, *et al.* 1994; Miyashita and Reed, 1995). The levels of Bax and Bcl2 proteins were examined here also by Western blot analyses using antibodies to the Bcl2 and Bax proteins, however, consistent changes could not be identified (data not shown).

An increase in the Bax:Bcl2 ratio would be expected to favour apoptosis (Oltvai, *et al.* 1993), however, given that the protein changes are only identifiable after approximately 20 h, a significant role in the apoptotic process in this system is questionable. Indeed, the involvement of the bcl2 family members in several models of apoptotic cell death is controversial, and apoptosis has been shown to proceed effectively in the absence of the bax protein (Knudson, *et al.* 1995). The role of bcl2 in this system is itself contradictory. p53^{WT}-induced apoptosis is inhibitable by both interleukin-6 (IL-6) (Yonish-Rouach, *et al.* 1991) and bcl2 (Chiou, *et al.* 1994). However, IL-6 also decreases bcl2 levels within the cell (Lotem and Sachs, 1994), an event which would be expected to promote apoptosis.

4.4. SUMMARY

In this chapter I have described the characterisation of the related murine cell lines LTR6, LTRphe132 and M1, and have shown both qualitatively and quantitatively that a conversion in p53 status from mutant to wild-type leads to the morphological and biochemical changes that are indicative of apoptosis. Apoptosis induced in LTR6 cells by p53^{WT} was detectable after 14–16 h at the permissive temperature, and was characterised by condensation of chromatin, internucleosomal cleavage of DNA, the appearance of a sub-G1 population of cells with < 2N DNA content, and increased fluorescence of the DNA-binding dye Hoechst 33342. It remains to be determined what molecular and biochemical changes occur between temperature-shift and 14–16 h afterwards, when changes characteristic of apoptosis are detectable.

**CHAPTER 5 – ACTIVATION OF CASPASES IN P53^{WT}-INDUCED
APOPTOSIS**

5.1. INTRODUCTION

Recently the importance of a novel family of cysteine proteases has become evident in apoptosis. Studies of the nematode worm *Caenorhabditis elegans* identified two genes, *ced3* and *ced4* which are absolutely required for cell death (Hengartner and Horvitz, 1994). *Ced3* has significant structural and functional homology with interleukin-1 β -converting enzyme (ICE) (Yuan, *et al.* 1993), the founder member of an emerging family of mammalian cysteine proteases which now has at least 10 members, including caspase-3/ CPP32/apopain (Fernandes-Alnemri, *et al.* 1994; Nicholson, *et al.* 1995), caspase-6/Mch2 (Fernandes-Alnemri, *et al.* 1995), caspase-7/Mch3/ICE-LAP3 (Fernandes-Alnemri, *et al.* 1995; Duan, *et al.* 1996) and caspase-8/MACH/FLICE/Mch5 (Boldin, *et al.* 1996; Muzio, *et al.* 1996; Fernandes-Alnemri, *et al.* 1996).

The caspases exist primarily as inactive zymogens in normal cells and require processing at critical aspartate residues for activation (reviewed in Thornberry and Molineaux, 1995). Several cellular proteins have been identified as substrates of the caspases, including poly (ADP-ribose) polymerase (PARP) and nuclear lamins. Poly (ADP-ribose) polymerase is an enzyme required for DNA repair and maintenance of genome integrity which is cleaved primarily by caspase-3 and caspase-7 (Nicholson, *et al.* 1995; Fernandes-Alnemri, *et al.* 1995; Lazebnik, *et al.* 1994), whereas nuclear lamins are cleaved by caspase-6 (Orth, *et al.* 1996; Takahashi, *et al.* 1996) to contribute to the collapse of the nuclear structure and the apoptotic morphology.

Many different classes of apoptotic stimuli apparently execute apoptosis via the concerted activation of the caspases. As was demonstrated in the previous chapter, p53^{WT} leads to the induction of apoptosis in LTR6 cells following incubation for several hours at the permissive temperature (Yonish-Rouach, *et al.* 1991). However, despite the activation of caspase-3 following treatment with DNA-damaging agents (Datta, *et al.* 1996), there has been no direct evidence to link p53^{WT} induction to the activation of the caspases. Thus the experiments described in this chapter were aimed at determining which caspases, if any, are activated by p53^{WT} and the sequence in which their activation occurs.

5.2. RESULTS

5.2.1. z-VAD.fmk inhibits p53^{WT}-induced internucleosomal cleavage

As an initial assessment of the involvement of caspases in p53^{WT}-induced apoptosis in LTR6 cells, the effect of the tripeptide caspase inhibitor benzyloxycarbonyl-val-ala-aspartic acid-fluoromethylketone (z-VAD.fmk) on the internucleosomal cleavage of DNA induced by a temperature-shift to 32.5°C was assessed. LTR6 cells were incubated for 24 h at 37.5°C or 32.5°C, either alone, or in the presence of 50 µM z-VAD.fmk. After the appropriate incubation, apoptosis was assessed by CAGE as described in section 2.2.3.1. A 24 h incubation at 32.5°C induced a marked increase in internucleosomal cleavage compared with a 24 h incubation at 37.5°C (Fig. 5.1, compare lanes 5 and 6 with lanes 3 and 4). Incubation of the cells at the permissive temperature following a 1 h pretreatment with 50 µM z-VAD.fmk resulted in the inhibition of internucleosomal cleavage to levels below those observed in control samples (Fig. 5.1, lanes 7 and 8). A 50 µM treatment of z-VAD.fmk was still effective if added as late as 10 h after shifting the cells to the permissive temperature (Fig. 5.1, lanes 9 and 10).

Clearly, assessment of the inhibitory effects of z-VAD.fmk on p53^{WT}-induced apoptosis by measuring its effect on the incidence of internucleosomal cleavage is flawed on two accounts. Firstly, internucleosomal cleavage is a comparatively late event in the apoptotic pathway (Brown, *et al.* 1993) and secondly, CAGE is not a quantitative method of assessing apoptosis. Despite these reservations, the results suggested that, as z-VAD.fmk is a caspase inhibitor, caspases do have a role to play in p53^{WT}-induced apoptosis in LTR6 cells.

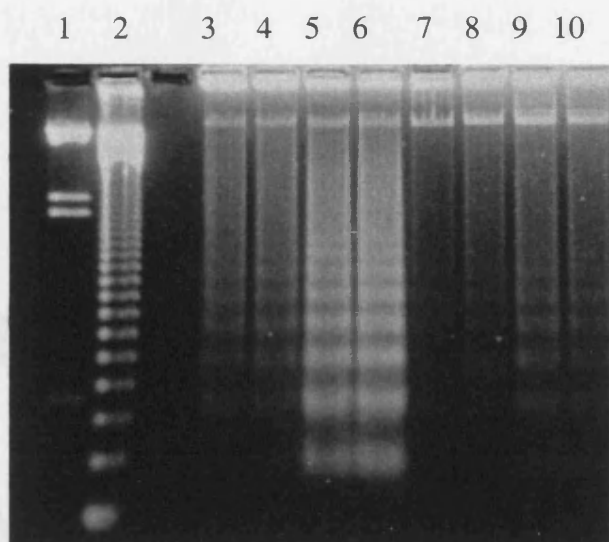


Fig. 5.1. z-VAD.fmk inhibits p53^{WT}-induced internucleosomal cleavage of DNA

LTR6 cells were retained at 37.5°C or shifted to 32.5°C for 22 h in the presence or absence of 50 μ M z-VAD.fmk and prepared for CAGE as described in section 2.2.3.1. Control cells (24 h 37.5°C), lanes 3 and 4; shifted cells (24 h 32.5°C), lanes 5 and 6; shifted cells preincubated for 1 h in the presence of 50 μ M z-VAD.fmk, lanes 7 and 8; shifted cells with 50 μ M z-VAD.fmk added 10 h post-temperature shift, lanes 9 and 10. 0.75×10^6 cells are loaded per lane. The standards used in lanes 1 and 2 are λ DNA digested with Hind III and 123 bp ladder, respectively.

5.2.2. z-VAD.fmk only partially inhibits apoptosis assessed by flow cytometry

As described in the previous chapter, p53^{WT} induced an apoptotic population of cells with enhanced Hoechst 33342 fluorescence, which was quantified by flow cytometric analysis (Fig. 4.2). To assess the effect of the tripeptide inhibitor z-VAD.fmk on the incidence of apoptosis assessed by this method, LTR6 cells were treated with different concentrations of z-VAD.fmk concomitant with a 22 h temperature shift to 32.5°C (Fig. 5.2A).

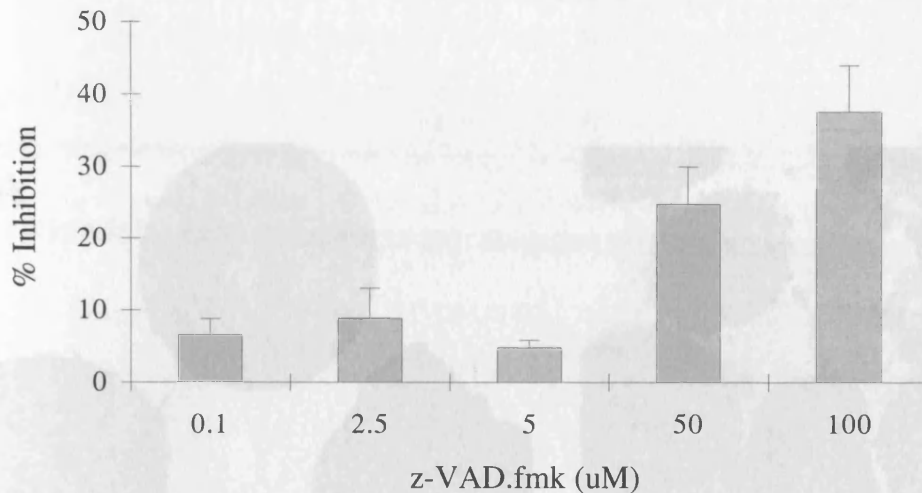


Fig. 5.2A. z-VAD.fmk only partially inhibits apoptosis induced by p53^{WT}

LTR6 cells were retained at 37.5°C for 22 h or shifted to 32.5°C for 22 h in the presence or absence of a concomitant addition of various concentrations (0.1–100 μ M) of z-VAD.fmk. The results are presented as the mean \pm S.E.M. of three separate experiments. In each case the results are normalised against the control value of apoptosis. (ie. the % of apoptosis after 22 h at 37.5°C is taken as 100% inhibition).

The results showed that even at concentrations of z-VAD.fmk as high as 100 μ M apoptosis was only inhibited by up to 45%. Interestingly, at lower concentrations of z-VAD.fmk (0.1 μ M) which apparently had no inhibitory effect on apoptosis as assessed by flow cytometry (Fig. 5.2A), examination under the electron microscope showed a marked inhibition of the condensation of the nuclear chromatin (Fig. 5.2B, compare panels B and C). Notably, incubation in the presence of 100 μ M z-VAD.fmk, while inhibiting the condensation of the nuclear material also caused the cells to ‘stick’ to one another. At present it is not clear whether this is a real effect, or whether it is a fixation artefact (Fig. 5.2B, panel D).

Fig. 5.2B. Low concentrations of z-VAD.fmk inhibit nuclear condensation
 LTR6 cells were either retained at 37.5°C for 22 h (control, panel A) or shifted to 32.5°C for 22 h in the absence (panel B) or presence of 0.1 μ M or 100 μ M z-VAD.fmk, panels C and D, respectively. Cells were prepared for electron microscopy as described in section 2.2.14. For each panel magnification is $\times 7000$.

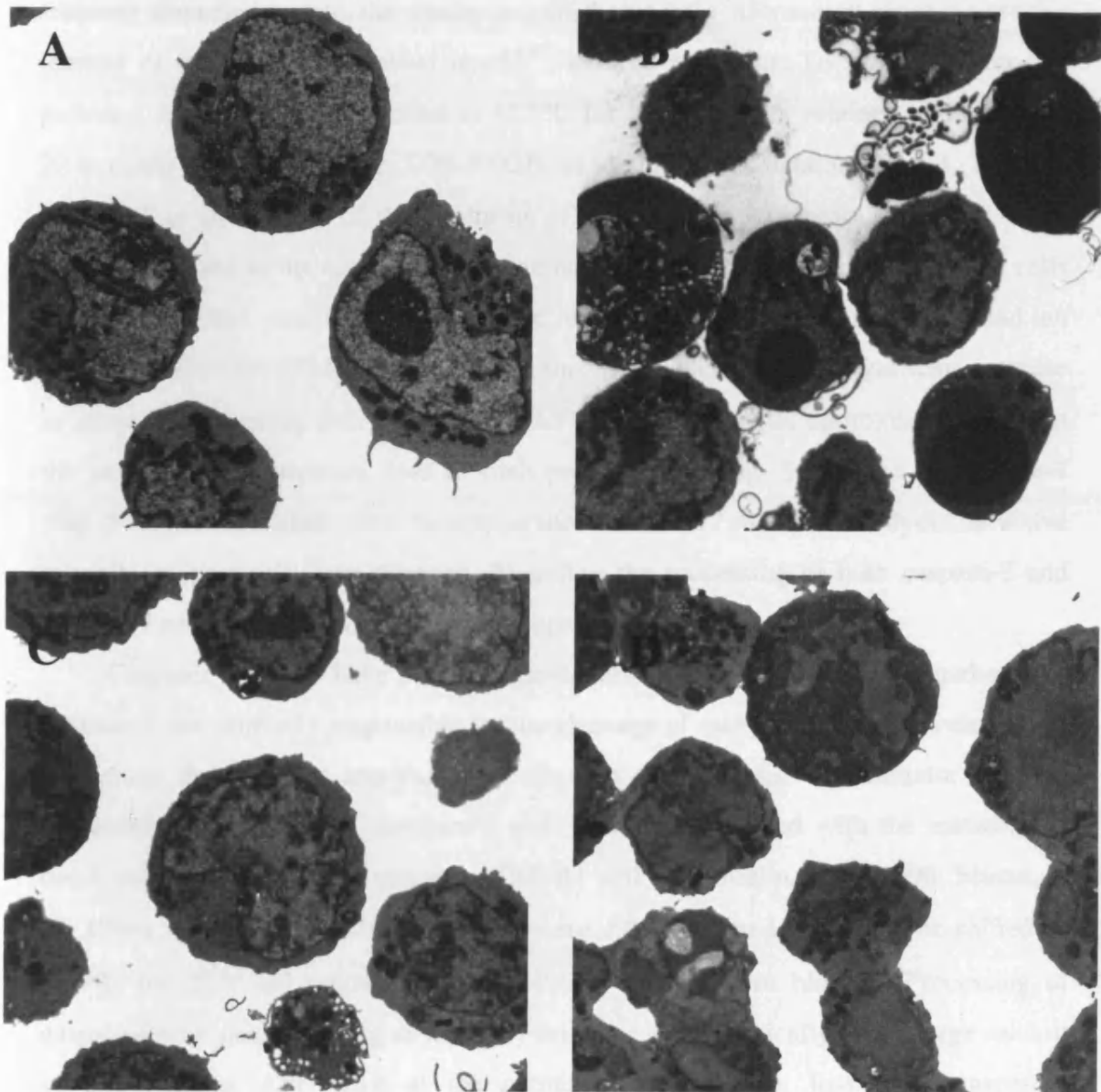


Fig. 5.2B. Low concentrations of z-VAD.fmk inhibit nuclear condensation

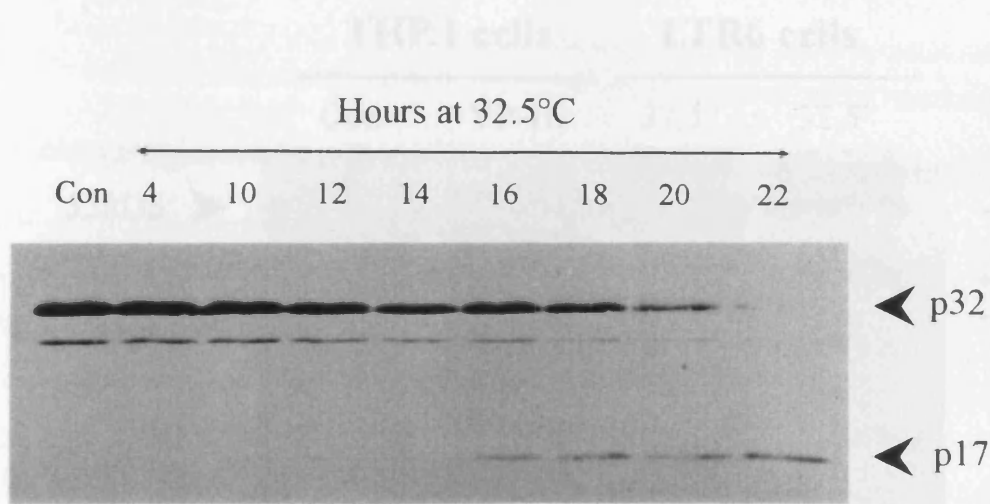
LTR6 cells were either retained at 37.5°C for 22 h (control; panel A) or shifted to 32.5°C for 22 h in the absence (panel B) or presence of 0.1 μ M or 100 μ M z-VAD.fmk, panels C and D, respectively. Cells were prepared for electron microscopy as described in section 2.2.16. For each panel magnification is $\times 3000$.

5.2.3. Processing of caspases in p53^{WT}-induced apoptosis

The results described in the previous section suggest that caspases are involved in p53^{WT}-induced apoptosis. However, given that z-VAD.fmk is an inhibitor of most caspases identified to date, the results described give little information about the precise identity of the caspases involved in p53^{WT}-induced apoptosis. To further dissect this pathway, LTR6 cells were shifted to 32.5°C for up to 22 h, or retained at 37.5°C for 22 h (control), prepared for SDS-PAGE as described in section 2.2.3.3, and the incidence of processing of the proforms of caspase-3 and caspase-7 assessed using antibodies raised to the catalytically active large subunits of both caspases. LTR6 cells incubated at the permissive temperature displayed apoptotic morphology and an increase in Hoechst 33342 fluorescence as shown previously, with a significant increase in apoptosis occurring after 14–16 h at 32.5°C (Fig. 4.4). After approximately 14 h at the permissive temperature, loss of both procaspase-3 (Fig. 5.3A) and procaspase-7 (Fig. 5.3B), concomitant with the appearance of the p17 and p19 catalytically active subunits, respectively, was detected. Therefore the processing of both caspase-3 and caspase-7 accompanied p53^{WT}-induced apoptosis.

Caspases-3 and -7 have been designated effector caspases as they, together with caspase-6, are primarily responsible for the cleavage of many of the proteins cleaved to precipitate the dramatic morphological changes of apoptosis. The initiator caspase, caspase-8, which activates caspases-3 and -7 and is associated with the intracellular death domains of the death receptors TNF-R1 and Fas (Boldin, *et al.* 1996; Muzio, *et al.* 1996) was also studied. LTR6 cells were either retained at 37.5°C or shifted to 32.5°C for 22 h and prepared for SDS-PAGE and Western blotting. Processing of caspase-8 was assessed using an antibody raised to the catalytically active large subunit of this caspase. After 22 h at the permissive temperature, loss of procaspase-8 (~55 kDa) and the appearance two fragments (~45 kDa and ~20 kDa), was detectable (Fig. 5.4, lane 4). This is the first time that the processing of caspase-8 had been shown after p53^{WT}-induced apoptosis. The processing of caspase-8 was also assessed in the human monocytic tumour cell line THP.1, treated for 4 h with 25 µM VP16. It was apparent that apoptosis in these cells was also accompanied by the loss of the proform of caspase-8, but was associated with the appearance of a doublet of approximately 43 kDa in size, consistent with the presence of two isoforms of caspase-8, caspase-8a

A Caspase-3



B Caspase-7

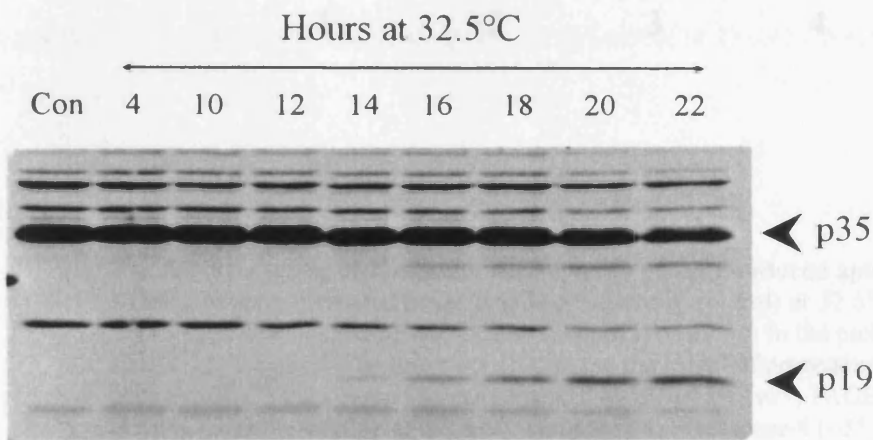


Fig. 5.3. Processing of Caspases-3 and -7 accompanies p53WT-induced apoptosis

LTR6 cells were incubated for up to 22 h at 32.5°C (lanes 2 - 9) or retained at 37.5°C for 22 h (lane 1; control). Lanes are numbered from the left. The samples were taken from a typical experiment (Fig. 4.4), and the extent of processing of A) Caspase-3 and B) Caspase-7 determined. Cellular proteins were separated by SDS/13% (w/v) PAGE, and Western blotting carried out using antibodies to the two caspases. The sizes of the proforms (upper arrowheads) and the catalytically active large subunits (lower arrowheads) are indicated.

Caspase-8

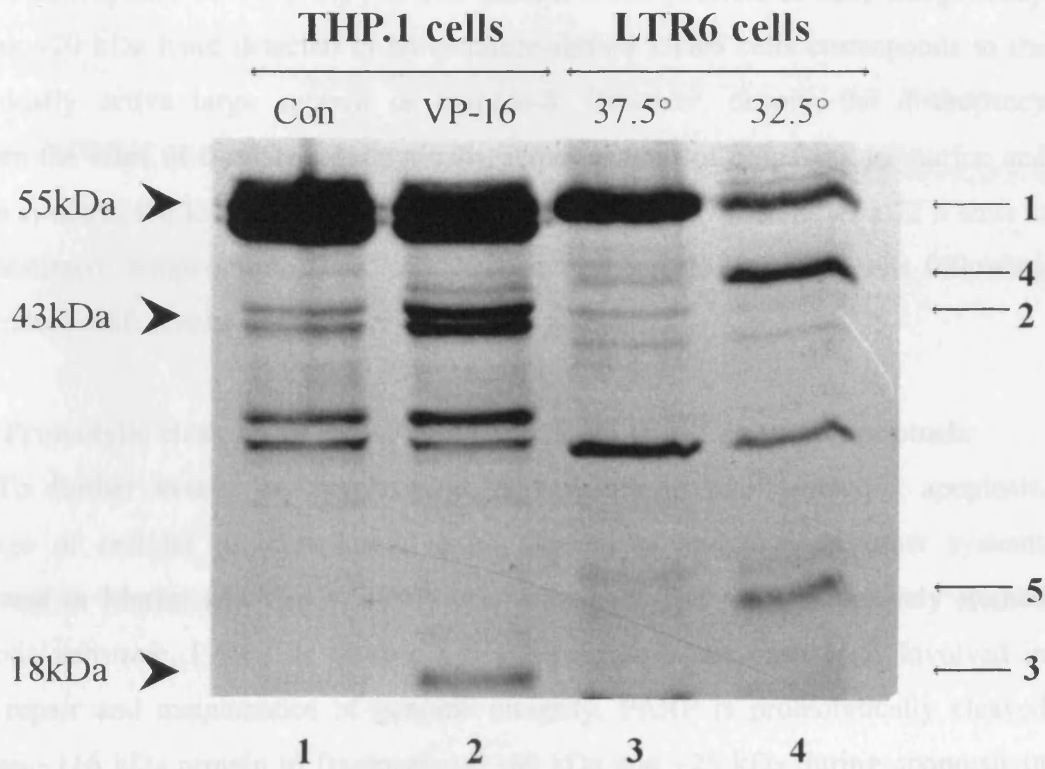


Fig. 5.4. Processing of Caspase-8 accompanies p53WT-induced apoptosis

LTR6 cells were incubated for 22 h at 37.5°C (lane 3; control) or 32.5°C (lane 4).

THP.1 cells were incubated alone (lane 1; control) or for 4 h in the presence of 25 μ M VP16 (lane 2). Samples were taken and the extent of processing of caspase-8 determined. Cellular proteins were separated by SDS/15% (w/v) PAGE, and Western blotting carried out using an antibody to caspase-8. Procaspase-8 (~55 kDa), the doublet (~43 kDa) in VP16-treated THP.1 cells (lane 2), the ~18 kDa large subunit in VP16-treated THP.1 cells and the ~45 kDa and ~20 kDa bands induced by p53WT in LTR6 cells (lane 4) are indicated by arrows 1–5, respectively.

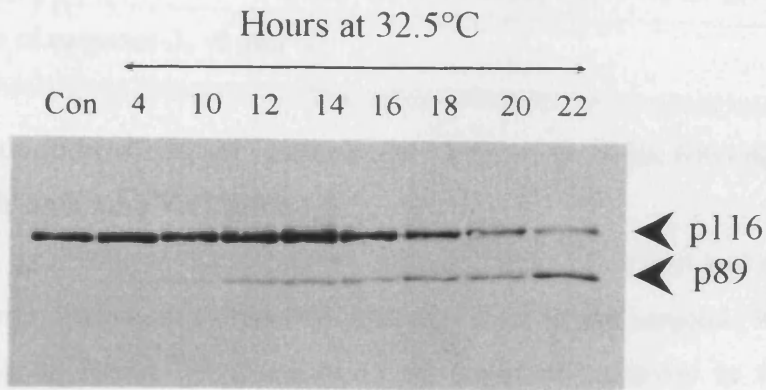
and b (Scaffidi, *et al.* 1997), and a further band with an apparent molecular weight of 18 kDa, consistent with the catalytically active large subunit of caspase-8. Because of the size discrepancy between the two cell lines, it is not possible to state categorically that the ~20 kDa band detected in temperature-shifted LTR6 cells corresponds to the catalytically active large subunit of caspase-8. However, despite the discrepancy between the sizes of the large, catalytically active subunit of caspase-8 in murine and human systems, the loss of the p55 proform of caspase-8 is evident after a 22 h shift to the permissive temperature. Thus, p53^{WT}-induced apoptosis in LTR6 cells following temperature-shift results in the processing of caspase-8.

5.2.4. Proteolytic cleavage of PARP and lamin B₁ in p53^{WT}-induced apoptosis

To further assess the involvement of caspases in p53^{WT}-induced apoptosis, cleavage of cellular proteins known to be cleaved in apoptosis in other systems (reviewed in Martin and Green, 1995) was examined. The most extensively studied apoptotic substrate, PARP, is cleaved by both caspase-3 and caspase-7. Involved in DNA repair and maintenance of genome integrity, PARP is proteolytically cleaved from an ~116 kDa protein to fragments of ~89 kDa and ~25 kDa during apoptosis in many systems (Nicholson, *et al.* 1995; Fernandes-Alnemri, *et al.* 1995; Lazebnik, *et al.* 1994). Following the induction of p53^{WT} by incubation of LTR6 cells at the permissive temperature of 32.5°C, PARP was cleaved to its signature apoptotic fragments after 10–12 h, providing further evidence of a proteolytic activity compatible with the activation of caspase-3 and/or caspase-7 (Fig. 5.5A). It is important to note that the occurrence of PARP proteolysis after 10–12 h at the permissive temperature, apparently precedes the processing of both caspase-3 and caspase-7.

The cleavage of nuclear lamins by caspase-6 during apoptosis may facilitate the collapse of the nuclear structure, a characteristic feature of the apoptotic process (Lazebnik, *et al.* 1995). In addition to PARP proteolysis, p53^{WT} induced the cleavage of lamin B₁, although this was not evident until after 16 h at the permissive temperature (Fig. 5.5B). These results were in agreement with other studies which showed that the cleavage of lamin B₁ is a later event than the cleavage of PARP (Lazebnik, *et al.* 1995; Greidinger, *et al.* 1996). The cleavage of lamin B₁ in LTR6 cells provided indirect evidence for the activation of caspase-6, as this caspase is the only caspase identified that is able to efficiently cleave nuclear lamins (Orth, *et al.* 1996; Takahashi, *et al.*

A PARP



B Lamin B₁

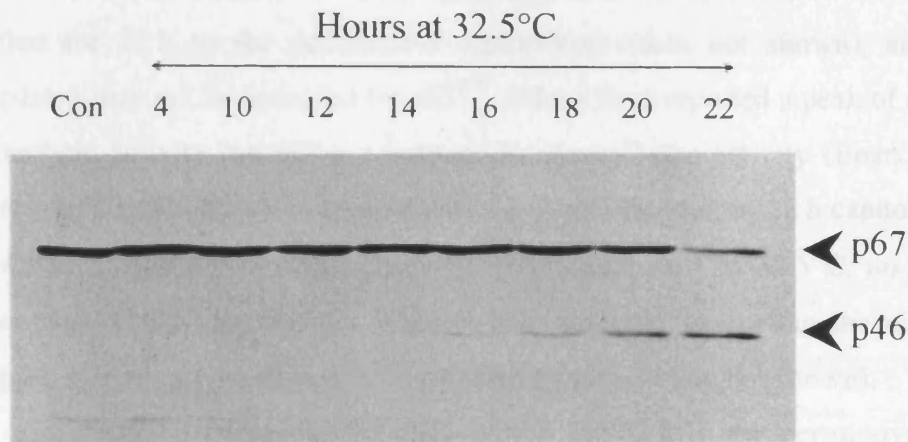


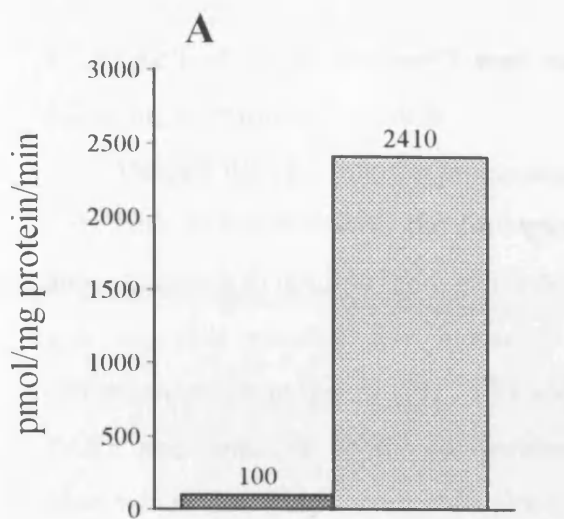
Fig. 5.5. Proteolytic cleavage of PARP and Lamin B₁ accompanies p53^{WT}-induced apoptosis
LTR6 cells were incubated for up to 22 h at 32.5°C (lanes 2 - 9) or retained at 37.5°C for 22 h (lane 1; control). Lanes are numbered from the left. The samples were taken from a typical experiment (Fig. 4.4) and the extent of processing of A) PARP and B) Lamin B₁ determined. Cellular proteins were separated by SDS/7% (w/v) PAGE (PARP) or SDS/10% (w/v) PAGE (Lamin B₁), and Western blotting carried out. The sizes of the intact substrates (upper arrowheads) and their cleavage fragments (lower arrowheads) are indicated.

1996). However, in the absence of an antibody capable of detecting murine caspase-6, the possibility of another homologue being responsible for the cleavage of nuclear lamins cannot be ruled out. Thus, p53^{WT}-induced apoptosis in LTR6 cells following temperature-shift was accompanied by the cleavage of cellular proteins known to be substrates of caspases-3, -6 and -7.

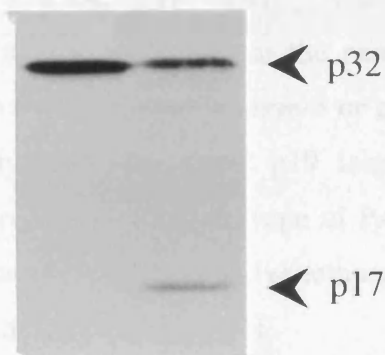
5.2.5. Activation of caspases as assessed by cleavage of the fluorogenic substrates z-DEVD.afc and Ac-YVAD.amc

The assembly of the tetrameric complex from two large and two small subunits derived from the inactive precursor, constitutes the active caspase (Walker, *et al.* 1994; Wilson, *et al.* 1994). To characterise the proteolytic activity in temperature-shifted LTR6 cells, lysates were prepared as described in section 2.2.5. Ac-YVAD.amc, which mimics the cleavage site in the natural caspase-1 substrate proIL-1 β , and is therefore a model substrate for caspase-1 activity, was used to determine whether any activation of caspase-1 had occurred following p53^{WT} activation in LTR6 cells. No hydrolysis of Ac-YVAD.amc was detected in lysates prepared from either control LTR6 cells or cells shifted for 22 h to the permissive temperature (data not shown), suggesting that caspase-1 may not be activated by p53^{WT}. Others have reported a peak of caspase-1-like proteolytic activity preceding a caspase-3/caspase-7-like activity (Enari, *et al.* 1996), therefore, a small, transient peak of caspase-1 activity prior to 22 h cannot be excluded. However, in the LTR6 cells following temperature-shift to 32.5°C, no processing of procaspase-1 was detected by Western blot analysis, supporting the conclusion that caspase-1 is not activated in p53^{WT}-induced apoptosis (data not shown).

In marked contrast, LTR6 cells shifted for 22 h to the permissive temperature exhibited at least a 24-fold increase in z-DEVD.afc (a substrate which mimics the caspase-3/-7 cleavage site within PARP) cleavage activity (DEVDase) above that seen in lysates prepared from control LTR6 cells (Fig. 5.6A). In agreement with these data, lysates from 22 h temperature-shifted LTR6 cells, but not from cells incubated for 22 h at the restrictive temperature, showed processing of both caspase-3 (Fig. 5.6B) and caspase-7 (Fig. 5.6C), together with the appearance of their catalytically active large subunits, p17 and p19, respectively. Thus, p53^{WT}-induced apoptosis in LTR6 cells was accompanied by the processing of caspase-3 and caspase-7 together with the induction of a cleavage activity consistent with their mutual ability to cleave PARP.



B Caspase-3



C Caspase-7

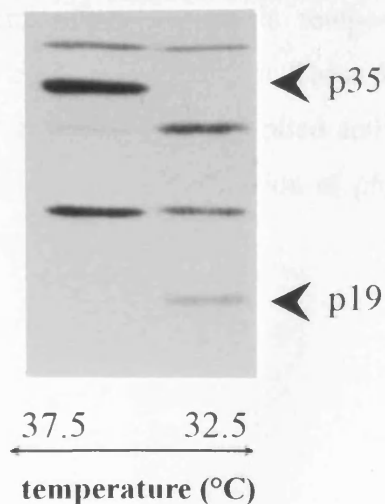


Fig. 5.6. p53WT-induced z-DEVD.afc cleavage activity in LTR6 cell lysates
 LTR6 cells were shifted to 32.5°C or retained at 37.5°C for 22 h. Lysates were prepared as described in section 2.2.5. and were A) assayed for z-DEVD.afc cleavage activity, B) analysed for the processing of caspase-3 and C) analysed for the processing of caspase-7. Cellular proteins (40 ug) were separated by SDS/13% (w/v) PAGE and Western blotting carried out as described in the legend to figure 5.3. Results shown are from a typical experiment.

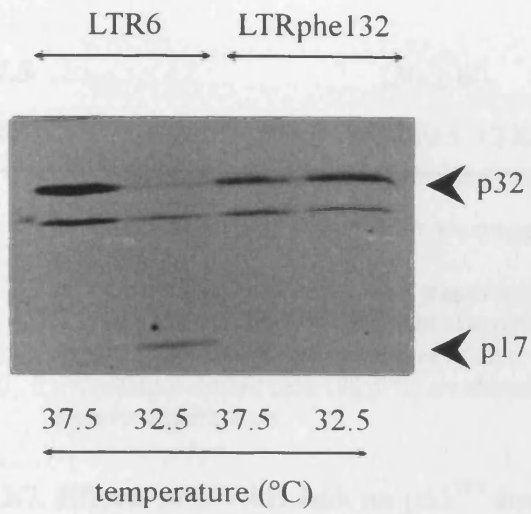
5.2.6. Activation of caspase-3 and caspase-7 is not induced in LTRphe132 cells following a temperature-shift

Despite the fact that the processing and activation of caspase-3 and caspase-7 has only been associated with the biological process of apoptosis, not enough is known about caspases to confine them solely to a role in mediation of the apoptotic pathway. It was therefore possible that a change in temperature had induced processing and activation of the caspases (Fig. 5.3) and the subsequent proteolysis of their substrates, PARP and lamin B₁ in the temperature-sensitive LTR6 cells (Fig. 5.5), despite the observation that temperature-shift alone does not induce apoptosis (Fig. 4.3).

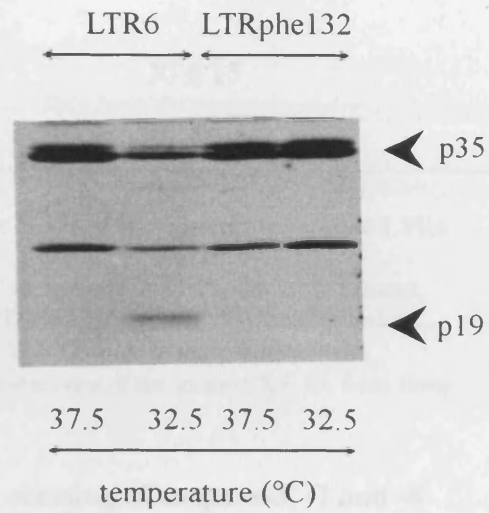
To exclude this possibility, the control cell line, LTRphe132 (containing a non-temperature-sensitive mutant p53) was shifted to the permissive temperature for 22 h and the incidence of caspase-3 and caspase-7 processing, proteolysis of PARP and lamin B₁, and DEVDase activity were assessed. Western blotting demonstrated that following a 22 h incubation at the permissive temperature, the LTRphe132 cell line showed no processing of caspase-3 or caspase-7, or the respective appearance of their catalytically active p17 and p19 large subunits (Fig. 5.7A and B, respectively). Furthermore, proteolytic cleavage of PARP and lamin B₁ was only detected in LTR6 cells incubated at the permissive temperature for 22 h and not in the LTRphe132 cells (Fig. 5.7C and D, respectively).

In agreement with the lack of caspase-3 and caspase-7 processing and proteolytic cleavage of PARP, lysates prepared from the temperature-shifted LTRphe132 cells after 22 h showed no significant increase in DEVDase activity (Table 5.1). In addition the lack of lamin B₁ cleavage in temperature-shifted LTRphe132 cells supported an absence of caspase-6 activation. These data demonstrate that the observed activation of caspases-3 and -7, and the implied activation of caspase-6, in LTR6 cells (Figs. 5.3–5.6) was caused by the induction of p53^{WT} and was not due merely to the change in temperature.

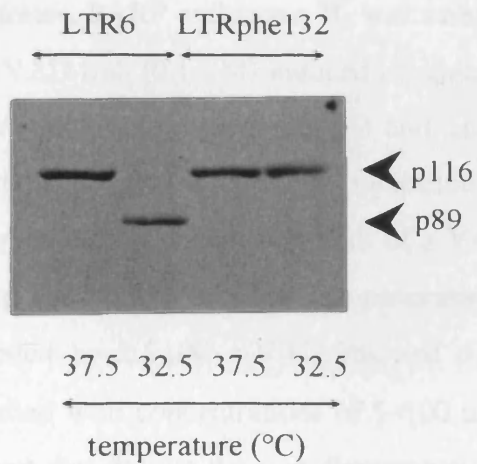
A Caspase-3



B Caspase-7



C PARP



D Lamin B1

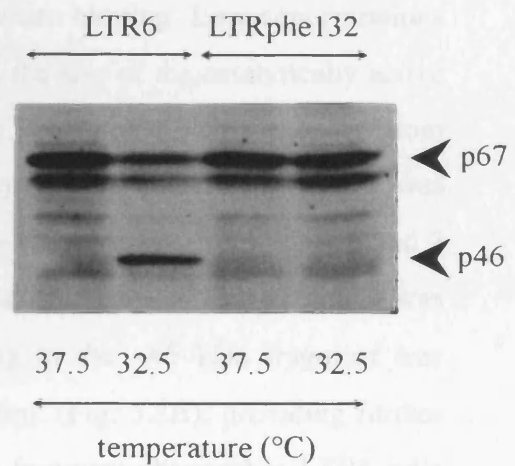


Fig. 5.7. Temperature-shift alone does not induce processing of caspases-3 and -7 or proteolytic cleavage of PARP and Lamin B1
LTR6 and LTRphe132 cells were retained at 37.5°C or shifted to 32.5°C for 22 h and assessed for the processing of A) caspase-3 and B) caspase-7 and the proteolytic cleavage of C) PARP and D) Lamin B1, as described in the legends to Figs. 5.3. and 5.5, respectively.

Temperature (°C)	Specific activity pmol/mg/min	
	LTR6	LTRphe132
37.5	130 ± 60	30 ± 15
32.5	3580 ± 1220	90 ± 10

Table 5.1. Increased z-DEVD.afc cleavage activity is confined to temperature-shifted LTR6 cells

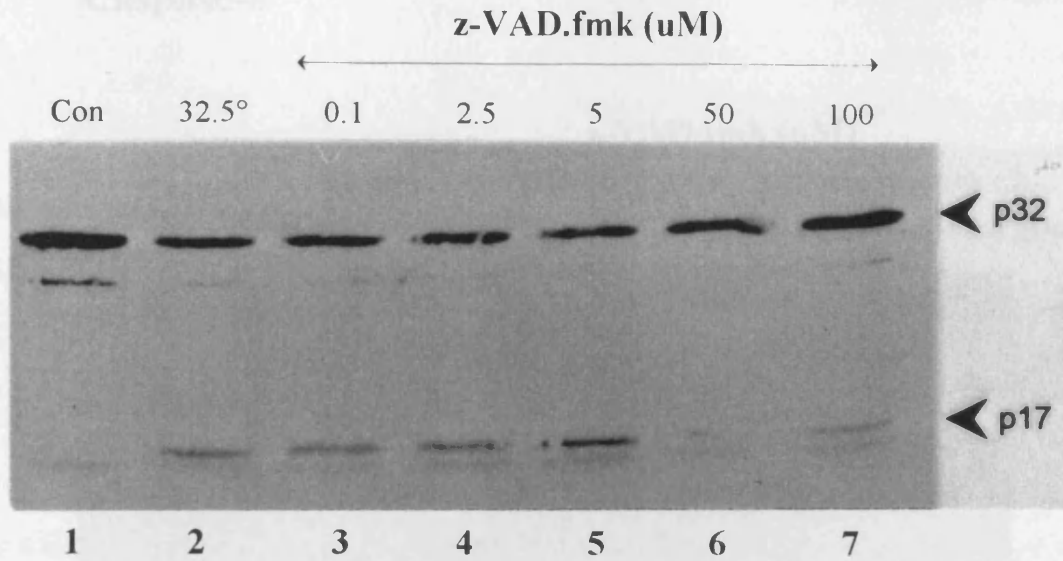
LTR6 and LTRphe132 cells were transferred to 32.5°C or retained at 37.5°C for 22 h. Lysates prepared from these cells were then assayed for z-DEVD.afc cleavage activity as described in section 2.2.5. The specific activities of control lysates (37.5°C) and lysates prepared from temperature-shifted cells (32.5°C) are shown. The values represent the mean ± S.E.M. from three separate experiments.

5.2.7. Effects of z-VAD.fmk on p53^{WT}-induced processing of caspase-3, -7 and -8

The results reported in sections 5.2.1–5.2.2 have demonstrated that the tripeptide caspase inhibitor z-VAD.fmk has only a partial inhibitory effect on apoptosis induced by a 22 h incubation of LTR6 cells at the permissive temperature (Fig. 5.2A). To investigate these observations further, the effect of the same treatments of z-VAD.fmk on the processing of caspases-3, -7 and -8, and on the cleavage of the apoptotic substrates, PARP and lamin B₁ was assessed by Western blotting. Low concentrations of z-VAD.fmk (0.1 μM) induced an apparent shift in the size of the catalytically active large subunits of both caspase-3 and caspase-7 (Fig. 5.8A, lane 3 of top and bottom panels), and almost complete inhibition of the formation of the large subunits was observed at higher concentrations of z-VAD.fmk (50–100 μM; Fig. 5.8B, lanes 6 and 7 of top and bottom panels). The processing of caspase-8 to the ~20 kDa fragment was inhibited by 2.5 μM z-VAD.fmk and the processing to the ~45 kDa fragment was inhibited with concentrations of 5–100 μM z-VAD.fmk (Fig. 5.8B), providing further support that despite the size discrepancy, the 20 kDa fragment observed in LTR6 cells following p53^{WT} induction is a cleavage product of the 55 kDa proform of caspase-8. Therefore, while z-VAD.fmk did not completely inhibit apoptosis assessed by Hoechst 33342/PI flow cytometry, it was able to almost completely abolish processing and therefore presumably activation of caspases-3, -7 and -8.

In addition, incubation with z-VAD.fmk almost completely inhibited the p53^{WT}-induced proteolytic cleavage of the caspase substrates, PARP and lamin B₁ (Fig. 5.9A and B, respectively). Therefore the ability of z-VAD.fmk to partially inhibit apoptosis

Caspase-3



Caspase-7

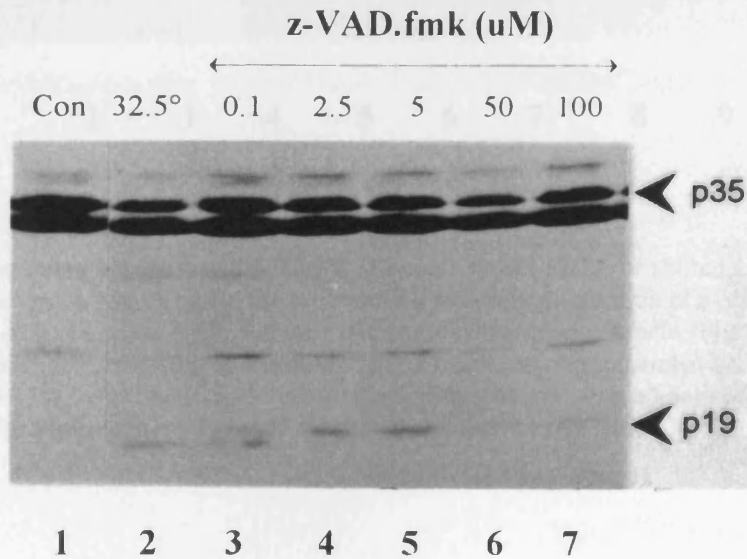


Fig. 5.8A. Effect of z-VAD.fmk on processing of caspases-3 and -7

LTR6 cells were incubated at 37.5°C (Con; lane 1) or shifted to 32.5°C for 22 h alone (lane 2) or in the presence of a concomitant addition of z-VAD.fmk (0.1 - 100 uM; lanes 3-7). Samples taken from a typical experiment (Fig. 5.2) were assessed for processing of caspase-3 (top panel) and caspase-7 (bottom panel). Cellular proteins were separated by SDS/13% (w/v) PAGE and Western blotting carried out using antibodies to the caspases. The sizes of the proforms (upper arrowheads) and the catalytically active large subunits (lower arrowheads) are indicated in each case.

Caspase-8

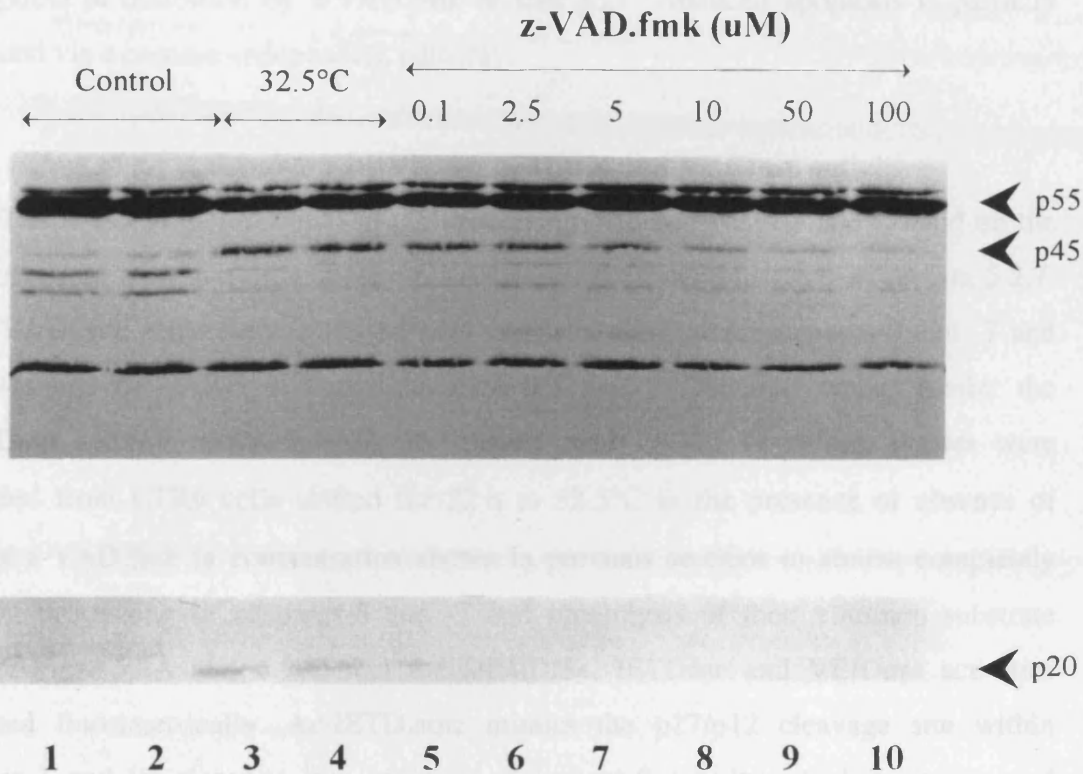


Fig. 5.8B Effect of z-VAD.fmk on processing of caspase-8

LTR6 cells were incubated at 37.5°C (Control; lanes 1 and 2) or shifted to 32.5°C for 22 h alone (lanes 3 and 4) or in the presence of a concomitant addition of z-VAD.fmk (0.1-100 uM; lanes 5-10). Samples taken from a typical experiment (Fig. 5.2) were assessed for processing of caspase-8. Cellular proteins were separated by SDS/15% (w/v) PAGE, and Western blotting carried out using an antibody to caspase-8. The proform (p55) and the p45 and p20 fragments are indicated.

as assessed by flow cytometry and to almost completely inhibit processing of procaspases-3, -7 and -8 and the proteolytic cleavage of PARP and lamin B₁, suggests that p53^{WT}-induced apoptosis is either not exclusively mediated by caspases which are susceptible to inhibition by z-VAD.fmk or that p53^{WT}-induced apoptosis is partially mediated via a caspase-independent pathway.

5.2.8. Effect of z-VAD.fmk on DEVDase, IETDase and VEIDase activities

The effect of z-VAD.fmk on the processing of procaspases-3 and -7, and on the proteolysis of their common substrate PARP, has been demonstrated in section 5.2.7. As z-VAD.fmk effectively inhibited both the processing of procaspases-3 and -7 and the cleavage of PARP, it would be expected that z-VAD.fmk would inhibit the DEVDase activity responsible for the cleavage of PARP. Therefore, lysates were prepared from LTR6 cells shifted for 22 h to 32.5°C in the presence or absence of 50 µM z-VAD.fmk (a concentration shown in previous sections to almost completely prevent processing of caspases-3 and -7 and proteolysis of their common substrate PARP; Figs. 5.8A and 5.9A) and the DEVDase, IETDase and VEIDase activities assessed fluorimetrically. Ac-IETD.amc mimics the p17/p12 cleavage site within caspase-3 and its cleavage is a measure of caspase-8 activity which processes and activates caspase-3 by cleavage at this site. Z-VEID.amc mimics the caspase-6 cleavage site within lamin A, and is thus a measure for activation of caspase-6.

A 22 h shift to the permissive temperature induced DEVDase, IETDase and VEIDase activities within lysates prepared from LTR6 cells. These activities were absent in lysates prepared from cells incubated for 22 h in the presence of 50 µM z-VAD.fmk (Fig. 5.10). This result was entirely consistent with the ability of z-VAD.fmk to prevent the proteolytic cleavage of PARP by caspase-3 and/or caspase-7 and the cleavage of lamin B₁, presumably by caspase-6.

However, it was possible that some residual z-VAD.fmk was present in the cell lysates preventing cleavage of the fluorogenic substrates during the fluorimetric assay. To rule out this possibility, the different LTR6 cell lysate preparations were combined and their DEVDase activities assessed again. The combination of equal volumes of lysate (total protein the same) prepared from shifted LTR6 cells and LTR6 cells shifted in the presence of z-VAD.fmk did not reduce the DEVDase activity measured in the shifted lysate alone. Therefore, any residual z-VAD.fmk was not having a direct

inhibitory effect on DEVDase activity, and the observed effect of z-VAD.fmk was exerted prior to the preparation of the cell lysates (Fig. 5.11). This confirms that on the basis of DEVDase, IETDase and VEIDase activity, this concentration of z-VAD.fmk was effectively inhibiting effector caspase activity in LTR6 cells.

Specific activity (pmol/mg/min)
(log₁₀ scale)

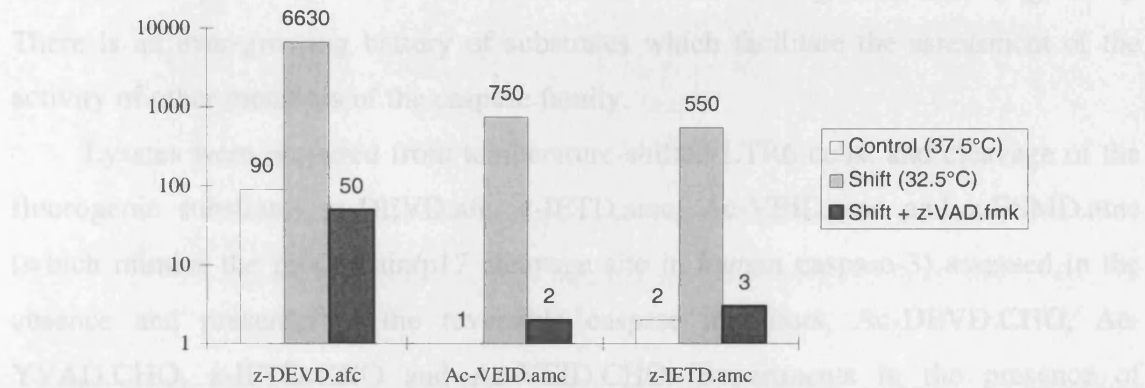


Fig. 5.10. Effect of z-VAD.fmk on LTR6 cell lysate cleavage activities

Lysates were prepared from LTR6 cells incubated for 22 h at 37.5°C (control) or for 22 h at 32.5°C in the absence (shift) or presence of 50 μ M z-VAD.fmk (shift + z-VAD.fmk). Lysates were then assayed for the presence of z-DEVD.afc, Ac-IETD.amc and z-VEID.amc cleavage activities as described in section 2.2.5. The data shown are from a typical experiment.

Specific activity (pmol/mg/min)

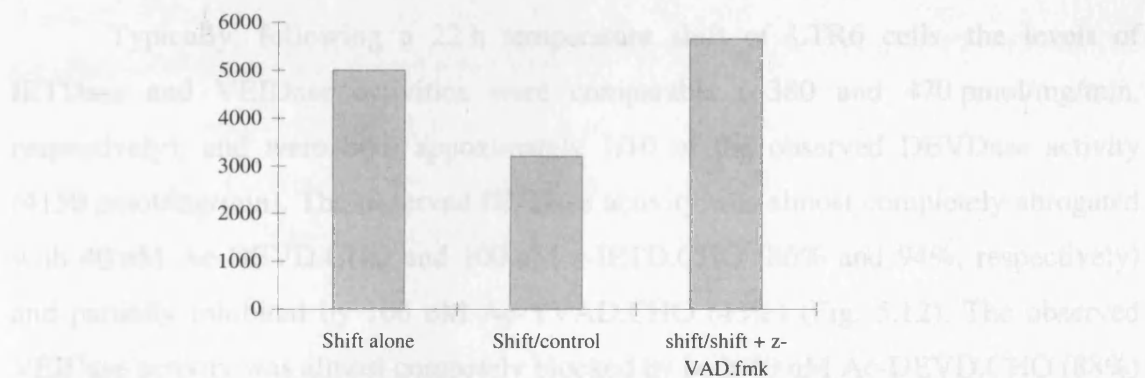


Fig. 5.11. Activities of combined LTR6 cell lysates

Lysates were prepared from LTR6 cells incubated for 22 h at 37.5°C (control) or 22 h at 32.5°C in the absence or presence of 50 μ M z-VAD.fmk and assayed alone (shift alone) or in equal volume combinations (shift/control and shift/shift + z-VAD.fmk) for the presence of DEVDase activity, as described in section 2.2.5. The data shown are from a typical experiment.

5.2.9. Characterisation of LTR6 cell lysates using fluorogenic tetrapeptide caspase substrates and inhibitors

To date, lysates prepared from LTR6 cells shifted for 22 h to 32.5°C have been shown to exhibit no induction of Ac-YVAD.amc cleavage activity but a significant induction of DEVDase activity, characteristic of active caspase-3 and caspase-7 and consistent with their ability to cleave PARP. In addition the previous section demonstrated p53^{WT}-induced VEIDase and IETDase cleavage activities (Fig. 5.10). There is an ever-growing battery of substrates which facilitate the assessment of the activity of other members of the caspase family.

Lysates were prepared from temperature-shifted LTR6 cells, and cleavage of the fluorogenic substrates, z-DEVD.afc, z-IETD.amc, Ac-VEID.amc and z-ESMD.amc (which mimics the prodomain/p17 cleavage site in *human* caspase-3) assessed in the absence and presence of the reversible caspase inhibitors, Ac-DEVD.CHO, Ac-YVAD.CHO, z-IETD.CHO and Ac-VEID.CHO. Experiments in the presence of caspase inhibitors were carried out as described in section 2.2.5.

No cleavage of z-ESMD.amc was detected. As has been previously demonstrated, p53^{WT} induced a massive increase in DEVDase activity (4150 pmol/mg/min) compared with that seen in lysates from control cells (100 pmol/mg/min). This p53^{WT}-induced proteolytic cleavage activity was almost completely inhibited with 40 nM Ac-DEVD.CHO and 1 µM z-IETD.CHO (99% and 93% inhibition, respectively), inhibited by 84% with 80 nM Ac-VEID.CHO, but only inhibited by ~50% with 100 nM z-IETD.CHO and by only < 3% with 100 nM Ac-YVAD.CHO (Fig. 5.12).

Typically, following a 22 h temperature shift of LTR6 cells, the levels of IETDase and VEIDase activities were comparable (~380 and 470 pmol/mg/min, respectively), and were both approximately 1/10 of the observed DEVDase activity (4150 pmol/mg/min). The observed IETDase activity was almost completely abrogated with 40 nM Ac-DEVD.CHO and 100 nM z-IETD.CHO (86% and 94%, respectively) and partially inhibited by 100 nM Ac-YVAD.CHO (43%) (Fig. 5.12). The observed VEIDase activity was almost completely blocked by both 40 nM Ac-DEVD.CHO (88%) and 80 nM Ac-VEID.CHO (93%), but was unaffected by incubation with 100 nM Ac-YVAD.CHO (6%) (Fig. 5.12).

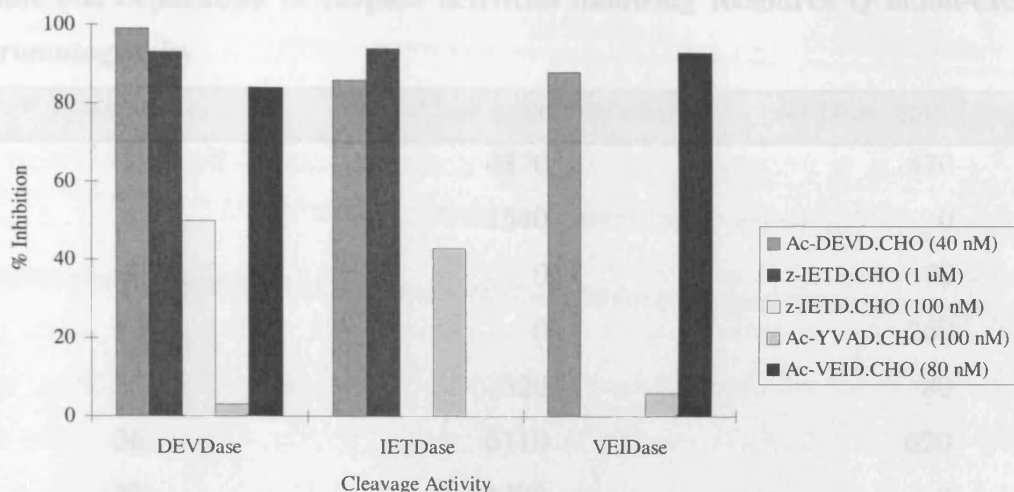


Fig. 5.12. Inhibition of z-DEVD.afc, z-IETD.amc and Ac-VEID.amc cleavage activities by caspase inhibitors

LTR6 cells were shifted to 32.5°C for 22 h and assessed for z-DEVD.afc, z-IETD.amc and Ac-VEID.amc cleavage activities (DEVDase, IETDase and VEIDase, respectively), as described in section 2.2.5. The effects of the caspase inhibitors Ac-DEVD.CHO, z-IETD.CHO, Ac-YVAD.CHO and Ac-VEID.CHO on the measured activities were assessed. The results shown are from a typical experiment.

5.2.10. Separation of z-DEVD.afc and Ac-VEID.amc cleavage activities in LTR6 cell lysates using anion-exchange chromatography

The previous sections have identified activities in LTR6 lysates consistent with the possible activation of four caspase homologues, namely caspase-3 (DEVDase activity), caspase-7 (DEVDase activity), caspase-6 (VEIDase activity) and caspase-8 (IETDase activity). However, a particular activity cannot be assigned to a specific caspase. Therefore an attempt was made to separate some of these caspase-like cleavage activities and to identify the caspase(s) responsible.

A cell lysate prepared from $\sim 500 \times 10^6$ LTR6 cells incubated for 22 h at the permissive temperature was run on a resource Q anion exchange column as described in section 2.2.6. Fractions were collected at 1 min intervals and analysed for the incidence of z-DEVD.afc and Ac-VEID.amc cleavage activity, to assess the activity of caspase-3 and/or caspase-7 and caspase-6, respectively (Table 5.2).

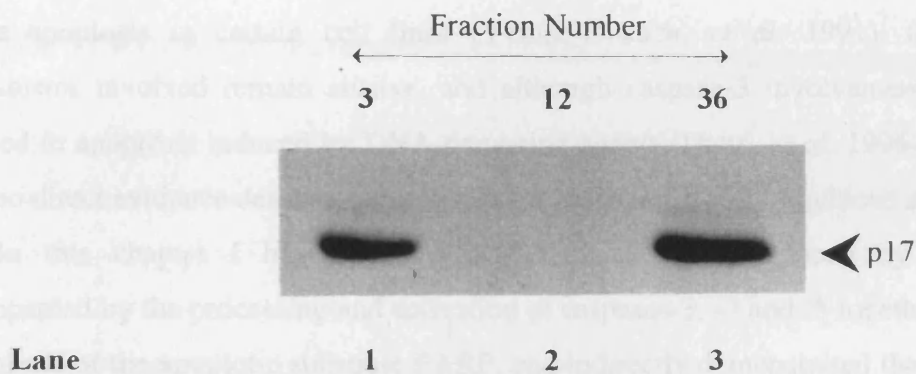
Table 5.2. Separation of caspase activities following Resource Q anion-exchange chromatography

Fraction No.	DEVDase (pmol/mg/min)	VEIDase (pmol/mg/min)
3	4870	470
4	1540	0
8	0	70
12	0	260
35	320	80
36	6110	620
37	1390	0

Analysis of the DEVDase activity identified two peaks of activity in fractions 3 and 36, whereas analysis of the VEIDase activity identified peaks of activity in fractions 3, 12 and 36. The presence of DEVDase activity in fractions 3 and 36 is accompanied by some VEIDase activity as both caspase-3 and caspase-7 are capable of cleaving Ac-VEID.amc to a certain degree. Therefore the presence of some VEIDase activity associated with the same fractions as high levels of DEVDase activity would agree with the activation of caspases-3, and -7 in these fractions. However, the presence of VEIDase activity in a fraction that lacks any detectable DEVDase activity would point to the activation of another homologue. Just such a situation is apparent in fractions 8 and 12, where a considerable degree of VEIDase activity is not associated with any detectable DEVDase activity. In particular, fraction 12 contains ~13% of the total VEIDase activity eluted from the column (data not shown). This is consistent with the activation of a third caspase homologue, most probably caspase-6, which preferentially cleaves a VEID motif and is the caspase primarily responsible for the cleavage of nuclear lamins (Orth, *et al.* 1996; Takahashi, *et al.* 1996). Thus, lysates prepared from temperature-shifted LTR6 cells contain DEVDase and VEIDase cleavage activities attributable to at least two separate caspases which could not be identified by fluorimetric assays on the crude lysates. Of course it is still possible that the DEVDase activity is caused by both caspase-3 and caspase-7 or indeed another homologue, and while the most likely candidate responsible for the VEIDase activity is caspase-6, a contribution from another homologue cannot be ruled out.

In an attempt to identify specific caspases responsible for the observed activities in the column fractions, fractions 3, 12 and 36 were examined by Western blotting for the incidence of processing of caspase-3 and caspase-7. Western blotting demonstrated the presence of the catalytically active p17 large subunit of caspase-3 in fractions 3 and 36 (Fig. 5.13A, lanes 1 and 3) as well as the catalytically active p19 large subunit of caspase-7 in the same fractions (Fig. 5.13B, lanes 1 and 3), although more was detectable in fraction 36. Interestingly, another band in addition to the p19 fragment was observed with the antibody to caspase-7, consistent with the further processing of the large subunit at Asp¹⁵, to yield a fragment with an apparent molecular weight of 17 kDa. In agreement with the proteolytic data, neither active caspase-3 or caspase-7 was detected in fraction 12. The unavailability of an antibody to caspase-6 meant that it was not possible to categorically identify the homologue responsible for, or contributing to, the observed VEIDase activity in the fraction devoid of DEVDase activity and processing of either caspase-3 or caspase-7.

A Caspase-3



B Caspase-7

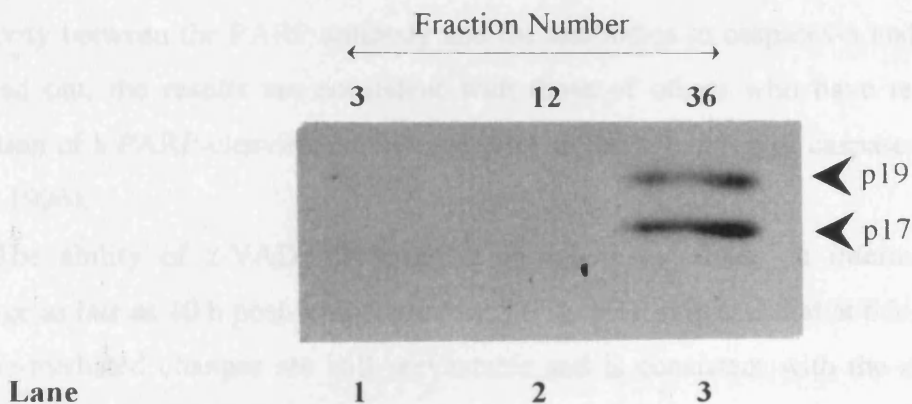


Fig. 5.13. Caspase-3 and caspase-7 in column fractions

Following anion-exchange chromatography (section 2.2.6) of a cell lysate prepared for LTR6 cells shifted for 22 h to 32.5°C, fractions 3, 12 and 36 were examined for the presence of processing of caspase-3 and caspase-7. Proteins were separated by SDS/12% (w/v) PAGE and Western blotting carried out. The sizes of the catalytically active large subunits are indicated.

5.3. DISCUSSION

DNA-damaging agents are well documented as inducers of apoptosis (reviewed in Donehower, 1994), primarily achieving their effects via a p53-dependent pathway (Clarke, *et al.* 1993; Lowe, *et al.* 1993b). Apoptosis was induced and assessed in LTR6 cells as described in the previous chapter. Despite the knowledge that p53^{WT} is able to induce apoptosis in certain cell lines (Yonish-Rouach, *et al.* 1991), the precise mechanisms involved remain elusive, and although caspase-3 involvement has been reported in apoptosis induced by DNA-damaging agents (Datta, *et al.* 1996), there has been no direct evidence demonstrating a role for caspases in p53^{WT}-induced apoptosis.

In this chapter I have demonstrated that apoptosis induced by p53^{WT} is accompanied by the processing and activation of caspases-3, -7 and -8 together with the proteolysis of the apoptotic substrate PARP, and indirectly demonstrated the activation of caspase-6 by showing the cleavage of lamin B₁ (Figs. 5.3–5.5). The results suggest that the proteolytic cleavage of PARP is a relatively early event, occurring between 10 and 12 h after temperature-shift and preceding both the onset of apoptosis assessed by flow cytometry and the processing of caspase-3 and caspase-7. Although a difference in sensitivity between the PARP antibody and the antibodies to caspases-3 and -7 cannot be ruled out, the results are consistent with those of others who have reported the activation of a PARP-cleaving homologue prior to the activation of caspase-3 (An and Knox, 1996).

The ability of z-VAD.fmk to exert an inhibitory effect on internucleosomal cleavage as late as 10 h post-temperature shift (Fig. 5.1), suggests that at this time point caspase-mediated changes are still preventable and is consistent with the observation that PARP proteolysis and processing of caspases-3 and -7 occur around this time, although Western blots suggest that PARP proteolysis precedes the processing of caspases-3 and -7 (Figs. 5.3 and 5.5).

Lysates prepared from temperature-shifted LTR6 cells showed a 24-fold increase in DEVDase activity compared with lysates prepared from control cells (Fig. 5.6A). Therefore, p53^{WT}-induced apoptosis in LTR6 cells was associated with the generation of a DEVDase activity which is attributable to members of the caspase-3 subfamily of cysteine proteases, namely caspase-3 and caspase-7. The processing of both caspase-3 and caspase-7 detected exclusively in lysates prepared from temperature-shifted LTR6 cells was consistent with this observation (Fig.5.6A and B, respectively). However, the

possibility of another z-DEVD.afc cleaving homologue contributing to, or accounting for, the observed DEVDase activity and the cleavage of PARP cannot be excluded at present.

In addition to the proteolytic cleavage of PARP, cleavage of lamin B₁ was also observed in LTR6 cells temperature-shifted for 14–16 h. This result provided indirect evidence for the activation of caspase-6, which, to date, is the only homologue identified as being able to cleave nuclear lamins efficiently (Orth, *et al.* 1996; Takahashi, *et al.* 1996). However, the described proteolytic cleavage of lamin B₁ may also be mediated by a Ca²⁺-regulated serine protease associated with the nuclear scaffold (Clawson, *et al.* 1992).

Activation of caspase-6 was further supported by the cleavage of z-VEID.amc, a substrate which mimics the cleavage site in nuclear lamins, in temperature-shifted LTR6 cell lysates. The cleavage of lamin B₁ after that of PARP is consistent with observations of others, that cleavage of lamin B₁ is a relatively late event in the apoptotic pathway (Lazebnik, *et al.* 1995; Greidinger, *et al.* 1996).

The change in temperature *per se* was not responsible for the processing of caspases-3 and -7, the proteolytic cleavage of PARP and lamin B₁ or the increase in z-DEVD.afc cleavage activity, as none of these changes were observed in LTRphe132 cells (non-temperature-sensitive p53) after a 22 h shift to the permissive temperature (Fig. 5.7 and Table 5.1).

Caspases have been implicated in the execution phase of apoptosis induced by a wide variety of stimuli (reviewed in Martin and Green, 1995). Studies of Fas receptor-mediated apoptosis recently provided the first direct link between a receptor-linked signalling pathway and the effector mechanisms of apoptosis (Boldin, *et al.* 1996; Muzio, *et al.* 1996). Ligation of the Fas receptor at the cell membrane by its natural ligand FasL or by an agonistic antibody recruits and activates caspase-8 which, in turn activates downstream effector caspases such as caspases- 3, -6 and -7.

Similarly, work recently carried out demonstrated that p53^{WT} induction by the DNA-damaging effect of doxorubicin lead to the transcription of a novel member of the apoptosis inducing receptor family TNFR, termed *KILLER/DR5* (Wu, *et al.* 1997), although upregulation of this death receptor has also been demonstrated with the non-genotoxic compound TNF α , regardless of the p53 status (Sheikh, *et al.* 1998). These data suggest that p53^{WT} may induce its apoptotic events, in part, via upregulation of a

receptor that ultimately leads to the demise of the cell, presumably by the initial recruitment and activation of ‘initiator’ caspases, such as caspase-8, and the subsequent activation of the ‘effector’ caspases-3, -6 and -7, and cleavage of their substrates PARP and nuclear lamins. The demonstration of p53^{WT}-induced processing of caspase-8 in LTR6 cells has not been shown previously and is consistent with this scenario. Accordingly, the processing of caspase-8 would be expected to precede that of both caspases-3 and -7, however, this has not been directly demonstrated here.

Interestingly, a size discrepancy was detected between the large catalytically active subunits of caspase-8 in human THP.1 cells and the LTR6 cells (Fig. 5.4). However, there are identified differences between other human and murine caspases. For example, the ESMD²⁸S amino acid sequence at the prodomain/p17 junction in human caspase-3 is not conserved in mouse (Juan, *et al.* 1996; Van de Craen, *et al.* 1997). Therefore it is feasible that the size difference detected with the antibody to caspase-8 is due to unconserved sequences at critical cleavage points. To date, however, the amino acid sequence of murine caspase-8 has not been published.

The emerging tenet from all of these studies is that widely diverse stimuli initiate apoptosis through specific mechanisms (private pathways), but that the execution phase involves the sequential activation of an amplifying cascade of caspases (common pathway). In agreement with these observations, the p53^{WT}-induced apoptosis described in this chapter provides a further example of an apoptotic stimulus which feeds into the common apoptotic pathway involving the sequential activation of caspases, demonstrated by the cleavage of PARP prior to that of lamin B₁ (Fig. 5.5).

Wild-type p53-induced apoptosis is accompanied by the processing and activation of caspases-3, -7 and -8, and a lamin protease, together with cleavage of their substrates PARP and lamin B₁. The data support a functional role for the sequential activation of caspases in the execution phase of p53^{WT}-induced apoptosis.

Although caspases clearly have an important role to play in p53^{WT}-induced apoptosis, they may not be exclusively responsible for mediating the p53^{WT}-induced apoptotic response. Indeed, there is a growing amount of evidence supporting the existence of caspase-independent pathways of p53^{WT}-induced apoptosis. The involvement of several pathways in p53^{WT}-induced apoptosis is consistent with the results presented in this chapter. While incubation of LTR6 cells for 22 h at the

permissive temperature in the presence of z-VAD.fmk only inhibited apoptosis assessed by Hoechst33342/PI flow cytometry by a maximum of 45% (Fig. 5.2), z-VAD.fmk almost completely prevented the processing of caspases-3 and -7 and -8 and the proteolytic cleavage of the apoptotic substrates PARP and lamin B₁ (Figs. 5.8 and 5.9). In addition, z-VAD.fmk completely abolished the p53^{WT}-induced DEVDase activity (Fig. 5.12). Taken together, these results suggest that p53^{WT}-induced apoptosis is either not exclusively mediated by caspases which are susceptible to z-VAD.fmk or is partially mediated by a caspase-independent pathway. Others have also shown that other classes of inhibitor, including cathepsin inhibitors are able to partially inhibit p53^{WT}-induced apoptosis in these cells (Lotem and Sachs, 1996).

It is, of course, also possible that z-VAD.fmk is not present at a sufficiently high concentration at critical times to be able to completely prevent apoptosis, however, it is also possible that p53^{WT}-induced apoptosis is mediated by caspases which are not inhibited by z-VAD.fmk. Alternatively, in the overexpression system under study here, p53^{WT} induction may simply present too severe an onslaught to be counteracted by inhibitors of apoptosis such as z-VAD.fmk.

The massive DEVDase activity induced following a 22 h shift to the permissive temperature was almost completely inhibited by 40 nM Ac-DEVD.CHO (Fig. 5.10), consistent with the inhibition of caspase-3 and/or caspase-7. Ac-DEVD.CHO inhibits caspase-3 and caspase-7 with K_i values of 0.5 and 35 nM, respectively (Margolin, *et al.* 1997). Therefore, the almost total abrogation of DEVDase activity by 40 nM Ac-DEVD.CHO would suggest that caspase-3 is the major contributor to the observed DEVDase activity in cell lysates prepared from LTR6 cells shifted for 22 h to 32.5°C. The DEVDase activity was also inhibited by z-IETD.CHO, and this can be rationalised because the tetrapeptide at the p17/p12 junction in caspase-3 is IETD. Thus z-IETD.CHO would be expected to prevent this processing and thus the subsequent ability of active caspase-3 to cleave z-DEVD.afc. The considerable inhibition of DEVDase activity by Ac-VEID.CHO would correlate with the ability of recombinant caspase-6 to cleave PARP *in vitro*. Although, given that caspase-6 is approximately 150 times less efficient at cleaving Ac-DEVD.afc than caspase-3, a higher degree of inhibition than expected is achieved here. The lack of inhibition of DEVDase activity with 100 nM Ac-YVAD.CHO supports the observation that the K_i value of Ac-YVAD.CHO towards both caspase-3 and caspase-7 is > 50 μM. Therefore, 100 nM

would be expected to achieve negligible inhibition. Although the lack of Ac-YVAD.amc cleavage activity is consistent with an absence of caspase-1 activity in p53^{WT}-induced apoptosis, it must be remembered that the lysate at 22 h represents a 'snap shot' of the apoptotic process and that the transient peak of ICE-like activity observed by others (Enari, *et al.* 1996), may have already occurred.

It was entirely predictive that no z-ESMD.amc cleavage activity would be observed, as the corresponding site is not conserved in the murine caspase-3, instead the amino acid sequence at the junction between the prodomain and the small subunit of caspase-3 has been identified as KSVD²⁸S in the mouse homologue (Van de Craen, *et al.* 1996). The almost complete abolition of the Ac-IETD.amc cleavage activity with 40 nM Ac-DEVD.CHO supports the observation that the autoprocessing of caspase-3 occurs at the p17/p12 junction.

Interestingly, Ac-YVAD.CHO partially (43%) inhibited z-IETD.amc cleavage activity despite the apparent absence of caspase-1 activation. Thus, this suggested that another caspase may be contributing to the z-IETD.amc cleavage activity as well as caspase-3 itself. A possible candidate would be caspase-8 which has been shown in previous sections to be processed, and therefore presumably activated, following p53^{WT} induction in LTR6 cells. Combinatorial studies into the preferred tetrapeptide cleavage sequence of the caspase family members designated LETD as the optimal cleavage site for caspase-8 (Thornberry, *et al.* 1997). However, the subgroup (III) of caspases to which caspase-8 belongs was found to tolerate many amino acids in the P₄ position, but with a preference for those amino acids with large, aliphatic side chains; eg. isoleucine. Thus the IETD tetrapeptide at the p17/p12 junction within the caspase-3 proform presents a favourable cleavage site for caspase-8.

The results described to date have shown that following the induction of p53^{WT} in LTR6 cells, caspases are activated and the apoptotic process executed, ultimately leading to the cleavage of various cellular proteins and the precipitation of the dramatic morphological events that characterise apoptosis. Despite the direct identification of processing of caspases-3, -7 and -8, and the indirect evidence implicating the involvement of caspase-6, no specific events that occur during apoptosis in LTR6 cells can be attributed to specific caspases. For example, PARP cleavage has been identified, but both caspase-3 and caspase-7 have been shown to effectively cleave PARP *in vitro*,

so it is difficult to ascertain whether one enzyme is responsible *in vivo*, or whether both (and perhaps others) contribute to its proteolysis.

In the last section of this chapter, an attempt was made to separate some cleavage activities and identify the caspase homologues responsible for those activities. Ac-VEID.amc and z-DEVD.afc cleavage activities were separated by anion-exchange chromatography (Table 5.2). Western blotting confirmed that the catalytically active large subunits of both caspase-3 and caspase-7 were present in the fractions which contained the peaks of DEVDase activity, but were absent from the fraction containing a peak of VEIDase activity (Fig. 5.13). Although both homologues were detectable in both fractions, the levels of caspase-7 suggested that caspase-7 was contributing to more DEVDase activity in fraction 36 than in fraction 3, although activity cannot be directly correlated with the level of the catalytically active large subunits. The presence of caspase-6 could not be directly demonstrated, although the recent availability of a caspase-6 antibody may make this question answerable in the near future.

Other events not dealt with here may have a role in p53^{WT}-induced apoptosis in LTR6 cells. It has been shown previously that p53^{WT} directly *transactivates* and *transrepresses* transcription from the *bax* and *bcl2* promoters, respectively. The resulting increase in the *bax*:*bcl2* protein ratio would be expected to facilitate apoptosis (Oltvai, *et al.* 1993). However, some cells are apoptosis-proficient in the absence of *bax* (Knudson, *et al.* 1995). In addition the role of *bcl2* in p53^{WT}-induced apoptosis in LTR6 cells is contradictory. Interleukin-6 was found to inhibit p53^{WT}-induced apoptosis in LTR6 cells while at the same time leading to a reduction in the level of *bcl2* protein, an event which would be expected to have an apoptosis-promoting effect. Thus, while *bcl2* has been shown to inhibit p53-induced apoptosis in other systems (Chiou, *et al.* 1994), its role in p53^{WT}-induced apoptosis in LTR6 cells is unclear.

5.4. SUMMARY

Caspases have been shown to play an important role in apoptosis induced by diverse stimuli. In this chapter I have demonstrated directly the p53^{WT}-induced activation of caspase-3 and caspase-7, supported by the proteolysis of their mutual substrate PARP and the induction of z-DEVD.afc cleavage activity. The activation of caspase-8, the initiator caspase was also demonstrated for the first time and was supported by the observed cleavage of z-IETD.amc. The proteolysis of lamin B₁ after that of PARP, together with the observed induction of Ac-VEID.amc cleavage activity, was consistent with the activation of caspase-6 and supported a role for the sequential activation of caspases in p53^{WT}-induced apoptosis. The prevention of processing of caspases-3, -7 and -8 and the abrogation of PARP and lamin B₁ proteolysis and DEVDase activity in the presence of incomplete inhibition of apoptosis assessed by flow cytometry suggested that other pathways may contribute to p53^{WT}-induced apoptosis.

Part of this chapter has been published in:

- Chandler, J.M., Alnemri, E.S., Cohen, G.M. and MacFarlane, M. (1997) Activation of CPP32 and Mch3 α in wild-type p53-induced apoptosis. *Biochem. J.* **322**, 19–23. (Appendix 1)

CHAPTER 6 – SUBCELLULAR LOCALISATION OF CASPASE-3 AND CASPASE-7 DURING P53^{WT}-INDUCED APOPTOSIS

6.1. INTRODUCTION

The results described in the previous chapters have demonstrated that apoptosis induced in LTR6 cells following the induction of p53^{WT} is accompanied by the activation of several members of the caspase family of cysteine proteases. The use of antibodies on Western blots demonstrated directly that the processing and activation of caspases-3, -7 and -8 occurred during apoptosis, which concurred with the observation that the cleavage of PARP, the mutual substrate of caspase-3 and caspase-7 (Lazebnik, *et al.* 1994; Nicholson, *et al.* 1995; Fernandes-Alnemri, *et al.* 1995), also accompanied p53^{WT}-induced apoptosis. The proteolytic cleavage of lamin B₁ provided indirect evidence that caspase-6 was also activated following the induction of p53^{WT} in LTR6 cells (Orth, *et al.* 1996; Takahashi, *et al.* 1996). Results from the Western blots were supported by the presence of z-DEVD.afc and Ac-VEID.amc cleavage activity in lysates prepared from temperature-shifted LTR6 cells. All these data were therefore consistent with the activation of caspases and the subsequent cleavage of their cellular substrates during p53^{WT}-induced apoptosis in LTR6 cells.

However, the fact remains that, to date, the majority of the proteins that have been identified as being substrates for the effector caspases, caspases-3, -6 and -7, are localised in the nucleus, including the 70 kDa protein component of the U1 small nuclear riboprotein (Casciola-Rosen, *et al.* 1994), DNA-dependent protein kinase (DNA-PK; Casciola-Rosen, *et al.* 1995; Song, *et al.* 1996), lamins A and C (Lazebnik, *et al.* 1995), PARP (Kaufmann, *et al.* 1993) and lamin B₁ (Kaufmann, *et al.* 1989; Oberhammer, *et al.* 1994). Therefore, the obvious question is how do caspases which have been assigned a cytosolic location (Ayala, *et al.* 1994; Nicholson, *et al.* 1995), cleave substrates that are largely nuclear?

It is possible that the effector caspases may have access to enough of their target substrates from the outside of the nucleus to facilitate cleavage, or alternatively it is possible that caspases, either prior to or following their activation, translocate into the nucleus to achieve cleavage of their substrates.

In order to address this question, the aims of the experiments in this chapter were to determine the subcellular localisation of caspases-3 and -7 during p53^{WT}-induced apoptosis in LTR6 cells.

6.2. RESULTS

6.2.1. Following p53^{WT}-induced apoptosis, caspase activity is not confined to LTR6 cell lysates

LTR6 cells were either retained at 37.5°C for 22 h or shifted to 32.5°C for 6 or 22 h. Following the appropriate incubation time, apoptosis was assessed by flow cytometry, and cells were either prepared directly for Western blot analysis or used to prepare cell lysates. In standard cell lysate preparations (section 2.2.5), the P20 pellet, which would be expected to contain nuclei and mitochondria, was discarded. However, for the purpose of the following experiments it was retained, washed twice in lysate buffer and re-pelleted (Fig. 6.1).

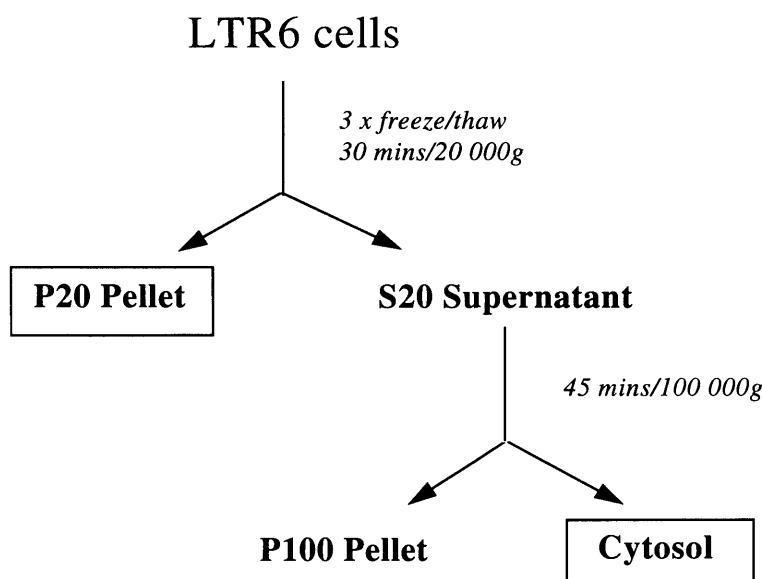


Fig 6.1. Preparation of cytosol (cell lysate) and P20 pellets

Cytosol (cell lysate) was prepared as described in section 2.2.5. In addition to the cytosol the P20 pellet (pellet after 30 min/20 000 g centrifugal spin) was retained.

The lysate and P20 pellets prepared from LTR6 cells shifted for 6 or 22 h to 32.5°C and those from cells retained at 37.5°C for 22 h (control) were assayed for the presence of DEVDase activity. In agreement with results in the previous chapters, lysates prepared from LTR6 cells shifted for 22 h to 32.5°C showed a marked increase in DEVDase activity (2890 pmol/mg/min) compared with those prepared from LTR6 cells retained for 22 h at 37.5°C (< 20 pmol/mg/min) (Fig. 6.2). The retained P20 pellets were also assessed for DEVDase activity

(section 2.2.5b). Interestingly, the pellets prepared from the 22 h temperature-shifted LTR6 cells likewise showed a substantial increase in activity (2220 pmol/mg/min) compared with P20 pellets from control LTR6 cells (80 pmol/mg/min). In both fractions preincubation for 15 min with 40 nM Ac-DEVD.CHO completely inhibited the DEVDase activity, consistent with a role for caspase-3 and/or caspase-7 in p53^{WT}-induced apoptosis. In neither the cytosolic nor the P20 pellet fraction from the LTR6 cells shifted for 6 h to 32.5°C was the DEVDase activity significantly higher than that in the corresponding samples from control LTR6 cells (Fig. 6.2). However, the DEVDase activity was considerably higher in the P20 pellets from control LTR6 cells and LTR6 cells shifted for 6 h to 32.5°C compared with the activity in the corresponding lysates (cytosol). Thus the data suggest that a caspase homologue with DEVDase activity (most likely caspase-3 and/or caspase-7) is localised in a subcellular compartment other than the cytosol. As the P20 pellet is likely to contain predominantly nuclei and mitochondria, this suggests that active caspase-3 and/or caspase-7 could be localised in one of these subcellular compartments.

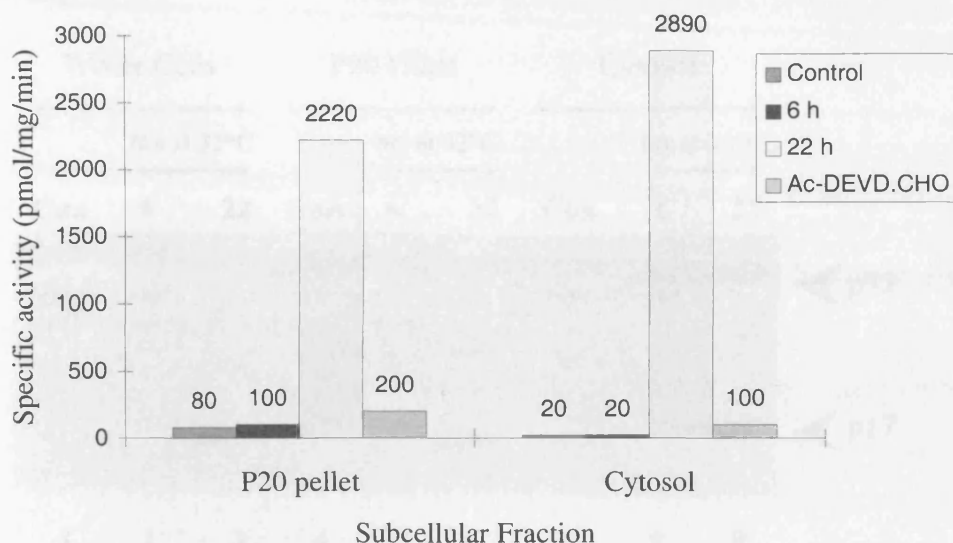


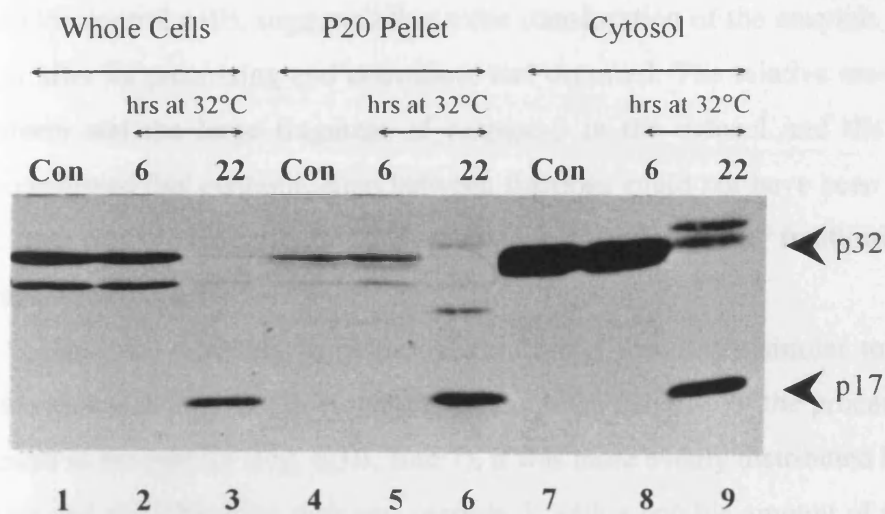
Fig. 6.2. DEVDase activity in fractions from LTR6 cells

LTR6 cells were retained at 37.5°C for 22 h (control) or shifted to 32.5°C for 6 or 22 h, and cytosol (cell lysate) and P20 pellet fractions prepared as indicated in Fig. 6.1. The extent of DEVDase activity was then assayed in each fraction and in addition the effect of a 15 min incubation with 40 nM Ac-DEVD.CHO was assessed on the activity measured in the cytosol and P20 pellet fractions obtained from the cells shifted for 22 h to 32.5°C. Results shown are from a typical experiment.

6.2.2. Active caspase-3 and active caspase-7 translocate from the cytosol following p53^{WT}-induced apoptosis

The processing and activation of caspase-3 and caspase-7 was examined by Western blotting in whole cells, and in the lysate and P20 pellet fractions, from control cells and cells shifted for 6 or 22 h to the permissive temperature (Fig. 6.3). The results using antibodies to both caspase-3 (Fig. 6.3A) and caspase-7 (Fig. 6.3B) showed essentially the same pattern of processing. In whole cells, clear processing of the proforms of both caspase-3 and caspase-7, together with the appearance of their large catalytically active subunits, was detected in temperature-shifted cells after 22 h compared with the corresponding control cells (Fig. 6.3, compare lanes 1 and 3). Using the antibody to caspase-3 it was clear that the majority of the proform of caspase-3 was located in the cytosol (Fig. 6.3A, lane 7), although some was detectable in the P20 pellet fraction (Fig. 6.3A, lane 4). Following a 22 h shift to 32.5°C, there were comparable levels of the catalytically active large subunit (p17) of caspase-3 in both the P20 pellet fraction and the cytosol (Fig. 6.3A, lanes 6 and

A Caspase-3



B Caspase-7

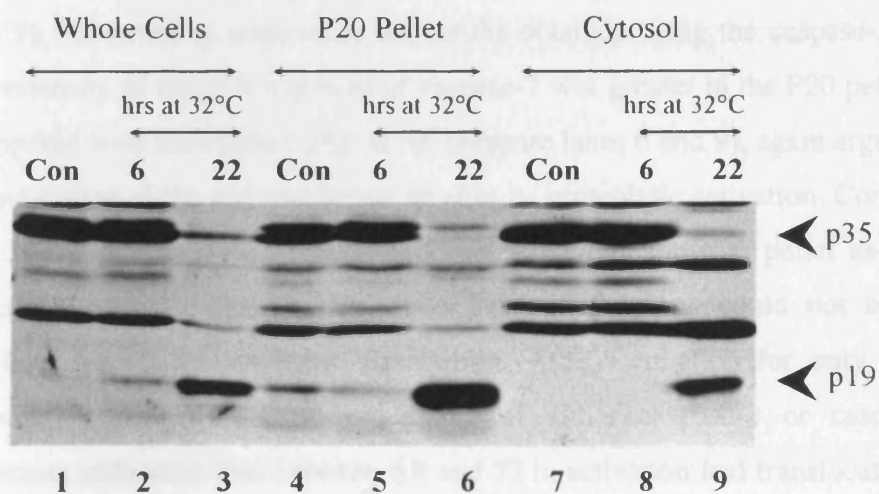


Fig. 6.3. Translocation of Caspases-3 and -7 from the cytosol

LTR6 cells were retained at 37.5°C for 22 h (Con) or shifted to 32.5°C for 6 or 22 h, and cytosol and P20 pellets prepared as indicated in Fig. 6.1. Samples were taken and the extent of processing of A) Caspase-3 and B) Caspase-7 determined. Cellular proteins were separated by SDS/13% (w/v) PAGE, and Western blotting was carried out using antibodies to the two caspases. The sizes of the proforms (upper arrowheads) and the catalytically active large subunits (lower arrowheads) are indicated.

9). The observation that the intensity of the p17 fragment in the P20 pellet from the 22 h shifted cells was greater than the intensity of procaspase-3 in the same fraction from the control cells, suggested that some translocation of the enzyme, either prior to or after its processing and activation, had occurred. The relative amounts of the proform and the large fragment of caspase-3 in the cytosol and the P20 pellet demonstrated that contamination between fractions could not have been responsible for the observed distribution of caspase-3 between these fractions following temperature-shift.

Using the antibody to caspase-7 the results were very similar to those seen with caspase-3 (Fig. 6.3B). However, although the majority of the procaspase-7 was located in the cytosol (Fig. 6.3B, lane 7), it was more evenly distributed between the lysate and the P20 pellet than was caspase-3, with a notable amount of the proform being detectable in the P20 pellet fraction from control cells (Fig. 6.3B, lane 4). Following a 22 h shift to 32.5°C, the catalytically active large (p19) subunit of caspase-7 was observed in both the P20 pellet and the cytosol (Fig. 6.3B, lanes 6 and 9). However, in contrast to the results obtained using the caspase-3 antibody, the intensity of the p19 fragment of caspase-7 was greater in the P20 pellet fraction compared with the cytosol (Fig. 6.3B, compare lanes 6 and 9), again arguing for the translocation of the enzyme before or after its proteolytic activation. Comparison of the levels of procaspase-7 and the large subunit in the P20 pellet and cytosolic fractions revealed that contamination between fractions could not be the only explanation for the observed distribution. After incubation for only 6 h at the permissive temperature, no processing of either caspase-3 or caspase-7 was detected, indicating that between 6 h and 22 h, activation and translocation of both caspase-3 and caspase-7 had occurred. This lack of caspase activation at 6 h agrees with the timecourse to apoptosis observed in the previous chapters (Fig. 5.3).

The P20 pellets prepared from each treatment were also assessed for the incidence of nuclear PARP cleavage. Interestingly, cleavage of PARP was detected in the P20 pellets prepared from cells maintained for 22 h at the restrictive temperature (Fig. 6.4, lane 4) and its incidence was increased following just 6 h at the permissive temperature (Fig. 6.4, lane 5), when neither caspase-3 nor caspase-7 were processed in the P20 pellets (Fig. 6.3, lanes 5). However, these data do agree with the previous observation that in LTR6 cells incubated for 22 h at the restrictive

PARP

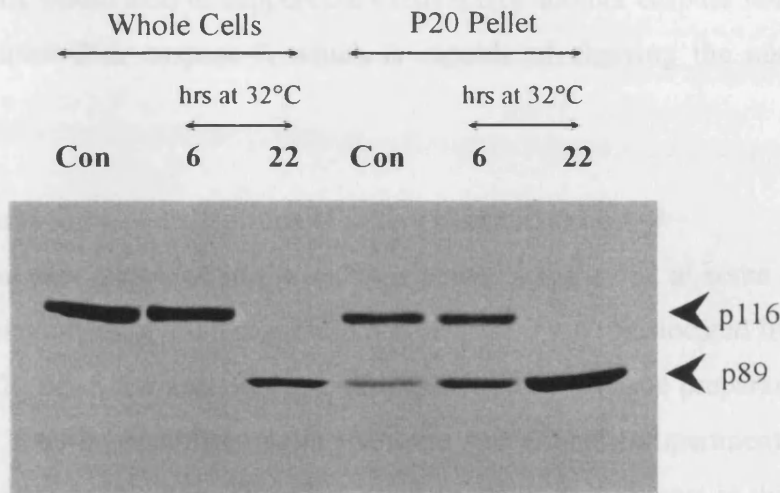


Fig. 6.4. Cleavage of PARP in the absence of processing of caspases-3 and -7
 LTR6 cells were retained at 37.5°C for 22 h or shifted to 32.5°C for 6 or 22 h, and P20 pellets prepared as indicated in Fig. 6.1. Lanes are numbered from the left. Samples were taken and the extent of processing of PARP determined. Cellular proteins were separated by SDS/7% (w/v) PAGE, and Western blotting carried out. The sizes of intact PARP (upper arrowhead) and the cleavage fragment (lower arrowhead) are indicated.

temperature (control) and for 6 h at the permissive temperature, the incidence of DEVDase activity is higher in the P20 pellet than in the cytosol (Fig. 6.2). Of course, the lack of processing of caspases-3 and -7 in the P20 pellets prepared from these cells would tend to support the existence of another caspase homologue, other than caspase-3 or caspase-7, which is capable of cleaving the nuclear substrate PARP.

6.2.3. Subcellular localisations of active caspases-3 and -7

The data presented in the sections above suggest that at some time before or after their activation, both caspase-3 and caspase-7 are translocated from the cytosol to the P20 pellet fraction. Because of the nature of the lysate preparation procedure, the P20 fraction comprises more than one subcellular compartment, and includes nuclei and mitochondria. Therefore, the remaining experiments in this section were aimed at identifying the precise subcellular localisation of active caspase-3 and caspase-7 following p53^{WT}-induced apoptosis.

Given that most caspase substrates identified to date, including PARP, are nuclear, it was logical to examine nuclei obtained from control and temperature-shifted LTR6 cells for evidence of caspase activation or the presence of catalytically active subunits. The method of lysate preparation, outlined in Fig. 6.1, involves the rather harsh process of freeze/thawing which whilst rupturing the plasma membrane is also likely to break up other membranes including those of the nuclei and mitochondria. Therefore, a gentler method of nuclei preparation was used utilising citric acid (section 2.2.13).

Nuclei isolated as described from LTR6 and LTRphe132 cells incubated for 22 h at 37.5°C (control) or 32.5°C (p53^{WT}) were analysed by Western blotting for the incidence of PARP proteolysis, and the processing and activation of caspases-3 and -7. As expected, PARP cleavage was clearly detectable in nuclei obtained from temperature-shifted LTR6 cells as well as in temperature-shifted whole cells, but not from control LTR6 cells or from the non-temperature-sensitive LTRphe132 cells incubated at 37.5°C or 32.5°C for 22 h (Fig. 6.5).

The antibodies to caspase-3 (Fig. 6.6A) and caspase-7 (Fig. 6.6B) detected some processing in whole, temperature-shifted LTR6 cells, but little or no

catalytically active subunit of either caspase-3 or caspase-7 was detectable in the corresponding nuclei (Fig. 6.6, lane 6, upper and lower panels).

To argue for translocation the levels of the catalytically active large subunits would have to be considerably greater than the levels of proform detected in the nuclei. Nevertheless, the incidence of PARP cleavage in isolated temperature-shifted LTR6 cell nuclei, suggested that an enzyme capable of its cleavage must have been activated in the nuclear compartment, and it was possible that the large catalytically active subunits of caspase-3 and caspase-7 had leached out of the nuclei due to the detergent or highly acidic conditions used in the citric acid method of nuclei extraction.

PARP

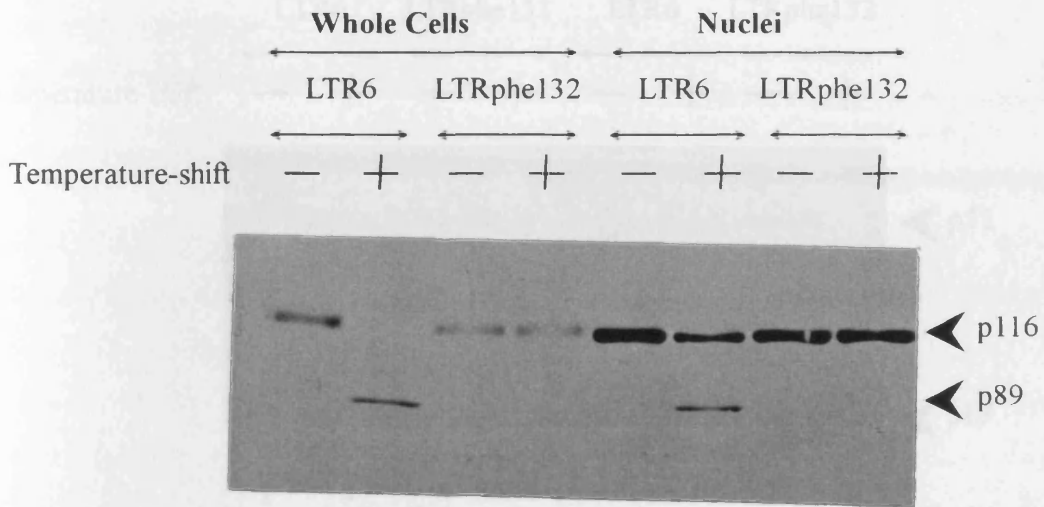
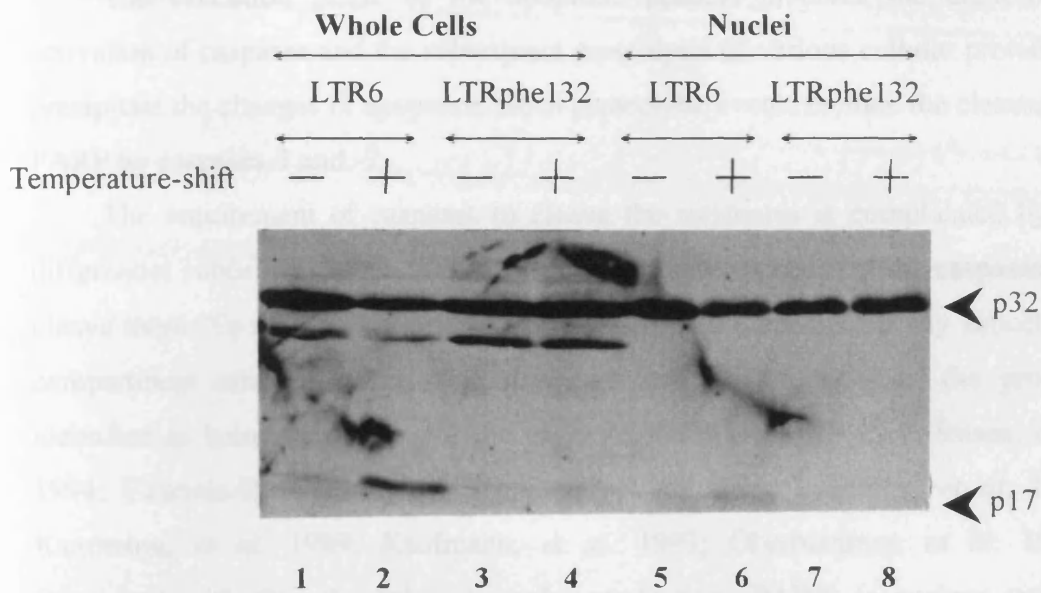


Fig. 6.5. Processing of PARP in isolated nuclei

Nuclei were isolated from LTR6 and LTRphe132 cells shifted to 32.5°C or retained at 37.5°C for 22 h as described in section 2.2.13. Lanes are numbered from the left. Samples were taken and the extent of processing of PARP determined. Cellular proteins were separated by SDS/7% (w/v) PAGE, and Western blotting carried out. The sizes of intact PARP (upper arrowheads) and the cleavage fragment (lower arrowheads) are indicated. Temperature shift to 32.5°C is designated by +, while - designates retention at 37.5°C.

A Caspase-3



B Caspase-7

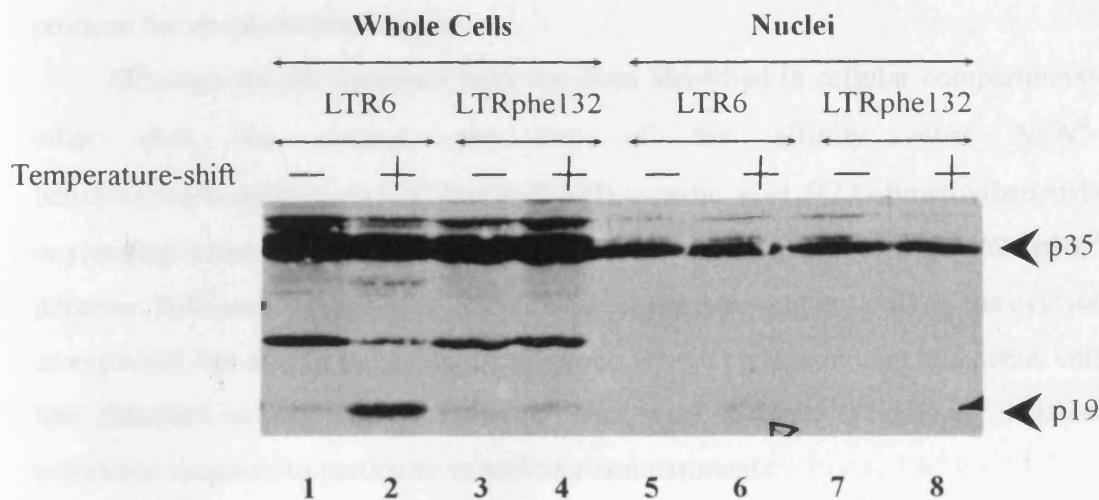


Fig. 6.6. Processing of caspase-3 and caspase-7 in isolated nuclei

Nuclei were isolated from LTR6 and LTRphe132 cells shifted to 32.5°C or retained at 37.5°C for 22 h as described in section 2.2.13. Samples were taken and the extent of processing of A) Caspase-3 and B) Caspase-7, determined. Cellular proteins were separated by SDS/13% (w/v) PAGE, and Western blotting carried out. The sizes of the procaspases (upper arrowheads) and the catalytically active large subunits (lower arrowheads) are indicated. Temperature shift to 32.5°C is designated by +, while - designates retention at 37.5°C.

6.3. DISCUSSION

The execution phase of the apoptotic process involves the orchestrated activation of caspases and the subsequent proteolysis of various cellular proteins to precipitate the changes of apoptosis. Such proteolytic events include the cleavage of PARP by caspases-3 and -7.

The requirement of caspases to cleave the substrates is complicated by the differential subcellular locations of the majority of substrates and the caspases that cleave them. To date no specific caspases have been identified in any subcellular compartment other than the cytosol. In contrast, the majority of the proteins identified as being substrates for the caspases are nuclear (Casciola-Rosen, *et al.* 1994; Casciola-Rosen, *et al.* 1995; Song, *et al.* 1996; Lazebnik, *et al.* 1995; Kaufmann, *et al.* 1989; Kaufmann, *et al.* 1993; Oberhammer, *et al.* 1994). Consistent with this, the substrate under study here, PARP, is nuclear and the caspases which have been shown to cleave it, namely caspase-3 and caspase-7, have been assigned a cytoplasmic subcellular localisation. Therefore, the question remains as to how cytosolic enzymes cleave predominantly nuclear proteins to produce the apoptotic phenotype.

Although specific caspases have not been identified in cellular compartments other than the cytosol, the use of the affinity label *N*-(*N*^α-benzyloxycarbonylglutamyl-*N*^ε-biotinyllysyl)-aspartic acid [(2,6-dimethylbenzoyl)oxy]methyl ketone, which binds to the active site of the active caspase (p20/p10)² tetramer, indicated that multiple active caspases were present not only in the cytosol as expected, but also in the nuclei of apoptotic HL-60 cells, a human leukaemic cell line (Martins, *et al.* 1997b). However, this work did not specifically localise individual caspases to particular subcellular compartments.

Lysates prepared from LTR6 cells shifted for 22 h showed a marked increase in DEVDase activity compared with lysates prepared from control cells (Fig. 6.2). In addition, considerable activity was detected in the P20 pellet fraction, which was abrogated by incubation with the tetrapeptide inhibitor Ac-DEVD.CHO, an inhibitor of caspase-3 and caspase-7. Thus, these data suggested that as well as a caspase-3/7-like activity being present in the cytosol of apoptotic LTR6 cells, a similar activity is present in the P20 pellet fraction. LTR6 cells shifted for 6 h to the permissive temperature showed no cleavage activity in either the cytosol or in the

P20 pellet fraction, in agreement with previous chapters which showed no apoptotic morphology or other features of apoptosis at this time (Fig. 4.4). Consistent with the presence of DEVDase activity in the cytosol and P20 pellet fraction, the major subunits of both caspase-3 and caspase-7 were observed in the lysate and also in the P20 pellet fractions prepared from LTR6 cells shifted for 22 h to 32.5°C (Fig. 6.3A and B, lanes 6 and 9), suggesting that both homologues may not be confined to a single subcellular compartment.

Interestingly, the intensity of the p17 catalytically active large subunit of caspase-3 in the P20 pellet fraction from cells incubated for 22 h at the permissive temperature was far in excess of the proform detected in the control P20 pellets, strongly suggesting that caspase-3 is translocated from the cytosol to a cellular compartment(s) present in the P20 pellet fraction. Although it cannot be determined whether or not translocation is likely to have occurred before or after activation, the Western blot data support the scenario where following proteolytic activation, perhaps by caspase-8, which is capable of cleaving all other known caspases (Fernandes-Alnemri, *et al.* 1996; Srinivasula, *et al.* 1996), some of the active caspase-3 is retained in the cytosol to cleave cytosolic proteins such as APC (Browne, *et al.* 1998) and PKC- δ (Emoto, *et al.* 1995) whereas some is translocated to other fractions to cleave other substrates. The P20 pellet fraction is likely to consist of mitochondria and nuclei. Therefore, given that no substrates to date have been designated as mitochondrial, it is reasonable to suggest that an active caspase is translocated to the nuclei to cleave nuclear substrates, such as PARP (Kaufmann, *et al.* 1993).

A similar picture was observed with caspase-7, with the catalytically active p19 large subunit being clearly detectable in both the P20 pellet fraction and the lysate prepared from LTR6 cells shifted to the permissive temperature for 22 h. No large subunit was detectable in controls or in cells shifted for only 6 h. Although the overall picture was similar for both caspase-3 and caspase-7, it is harder to argue for translocation of the active caspase-7 from the cytosol to the nucleus as the proform is also clearly detectable in the P20 pellet fraction prior to temperature-shift. However, comparison of the levels of the p19 catalytically active large subunit in the P20 pellet fraction and the lysate supports translocation. Once more, however,

it cannot be determined whether activation precedes or occurs after the translocation event.

The incidence of PARP cleavage was assessed in whole cells and in the P20 pellet fraction isolated from control LTR6 cells and LTR6 cells shifted to the permissive temperature for 6 or 22 h. In support of the higher DEVDase activity observed in pellets from control and LTR6 cells shifted for just 6 h to the permissive temperature compared with the cell lysates, a degree of PARP proteolysis was detected in control P20 pellets (Fig. 6.4), and this PARP cleavage was more pronounced in the P20 pellet fractions from LTR6 cells shifted for both 6 and 22 h to the permissive temperature, consistent with activation of caspase-3 and/or caspase-7 in this fraction. Since PARP is an exclusively nuclear protein, its cleavage in the P20 pellet fraction strongly implies the nuclear activation of either caspase-3 and/or caspase-7 or indeed another homologue capable of cleaving PARP.

The possible presence of active caspase-3 and caspase-7 in apoptotic nuclei was examined by gently preparing nuclei from control and 22 h temperature-shifted LTR6 cells. As expected proteolysis of PARP was clearly detectable in the nuclei isolated from LTR6 cells shifted to 32.5°C for 22 h, and was absent in controls, consistent with the activation of a caspase-3/7-like proteolytic activity (Fig. 6.5). In addition, the lack of cleavage in the control nuclei compared with that seen in the control P20 pellet fraction (Fig. 6.4, lane 4), suggests the latter may result from the isolation procedure, and supports the use of a gentler method of preparation of nuclei. To correspond the PARP cleavage to the activity of a particular caspase, the isolated nuclei were also assessed for the presence of processed caspase-3 and caspase-7 (Fig. 6.6). However, little evidence was obtained for activation of either caspase-3 or caspase-7 in the isolated nuclei. This notwithstanding, the PARP cleavage observed in nuclei from cells shifted for 22 h to 32.5°C demonstrates that a caspase-3/7-like activity had been present. Although this does not preclude the cleavage of PARP being achieved from outside the nucleus, it is also possible that the catalytically active large subunits of caspases-3 and -7 had leached out, as they are obviously considerably smaller than PARP, which is, in addition, likely to be more closely associated with the nuclear scaffold.

As described, the results could not rule out translocation of caspases-3 and -7 to the nucleus during p53^{WT}-induced apoptosis, but neither did they provide conclusive evidence for its occurrence. Given the impure nature of the P20 pellet fraction, another candidate organelle for the translocation of caspases-3 and -7 present in the P20 pellet fraction is the mitochondrion. However, given that a monocyte contains, on average, only approx. 50 mitochondria (D. Dinsdale, pers. comm.) it proved extremely difficult to prepare enough mitochondria to assess whether or not translocation of caspase-3 and/or caspase-7 from the cytosol to the mitochondria had occurred during p53^{WT}-induced apoptosis in LTR6 cells. Therefore to further analyse the subcellular localisation of various caspases during apoptosis we turned to the classic model of Fas-induced apoptosis in mouse liver.

The use of this system has several distinct advantages. Firstly, Fas-induced apoptosis in this system is relatively well characterised. Secondly, apoptosis can be studied *in vivo*. Thirdly, Fas-induced apoptosis via activation of the caspase executionary pathway is an example where a cascade of caspase activation has been identified. Finally, the subcellular fractionation of mouse liver is well documented, and the isolation of well-separated, uncontaminated fractions, the purity of which can be verified with established cell markers, is relatively simple. Therefore the aims of the next chapter were to study the subcellular distribution of caspases following Fas-induced apoptosis, in particular caspase-3 and caspase-7, which have indistinguishable substrate specificities (Thornberry, *et al.* 1997), and are both capable of cleaving the classic apoptotic substrate PARP.

6.4 SUMMARY

The results presented in this chapter have pointed to the activation of caspases in a subcellular compartment(s) other than the cytosol. Through Western blot analyses it was shown that the P20 pellet fraction contains processed and activated caspase-3 and caspase-7, supporting the translocation of one or both of these homologues from the cytosol to the nuclei or mitochondria during p53^{WT}-induced apoptosis. Although this scenario was not conclusively demonstrated, it warrants further examination since PARP, a common substrate of both caspase-3 and caspase-7 is confined to the nucleus.

**CHAPTER 7 – SUBCELLULAR LOCALISATION OF ACTIVE
CASPASE-3 AND ACTIVE CASPASE-7 IN FAS-INDUCED
APOPTOSIS *IN VIVO***

7.1. INTRODUCTION

The results in the previous chapter suggested that apoptosis induced by p53^{WT} in LTR6 cells may involve the translocation of active caspases to different subcellular compartments, thus leading to the cleavage of specific substrates and precipitation of the apoptotic phenotype.

A well studied *in vivo* model has been the induction of hepatocyte apoptosis in mice by an agonistic antibody to the Fas receptor (Ogasawara, *et al.* 1993). Crosslinkage of the receptor with the physiological Fas ligand (FasL) or the agonistic antibody JO2, leads to its trimerisation and the initiation of the intracellular events of apoptosis (Trauth, *et al.* 1989; Yonehara, *et al.* 1989; Itoh, *et al.* 1991). Thus, mice injected intravenously with this antibody show rapid liver destruction, with hepatocytes displaying morphology consistent with apoptosis, and the animals are typically dead within a few hours of exposure (Ogasawara, *et al.* 1993). Fas-induced apoptosis in mouse liver is prevented by the peptide inhibitors Ac-YVAD.cmk and z-VAD.fmk, consistent with a role for the activation of caspases in this mode of apoptosis (Rodriguez, *et al.* 1996; Rouquet, *et al.* 1996).

In contrast to *Caenorhabditis elegans*, where *ced-3* remains the only 'aspartase' required for apoptosis (Yuan and Horvitz, 1990), mammals contain at least 10 caspase homologues (reviewed in Cohen, 1997). However, it is not known precisely which of these caspases are activated *in vivo* following Fas-induced apoptosis, and which are responsible for the cleavage of specific substrates. Several of the caspases have overlapping substrate specificities suggesting that there may be some degree of redundancy (Thornberry, *et al.* 1997). Two such caspases are the effector caspases-3 and -7 which, in *in vitro* combinatorial studies, have been assigned virtually indistinguishable specificities for the tetrapeptide DXXD, consistent with their mutual cleavage site within PARP (Thornberry, *et al.* 1997). As described in the previous chapter, caspases have generally been assigned a cytosolic location, based largely on data with caspase-1 and on the isolation and purification of caspase-3 (Ayala, *et al.* 1994; Nicholson, *et al.* 1995). In this chapter the subcellular localisation of caspase-3 and caspase-7 during Fas-induced apoptosis of hepatocytes *in vivo* was examined to ascertain whether differential subcellular localisation of caspases may go some way towards explaining the existence of two caspase homologues with almost identical substrate specificities.

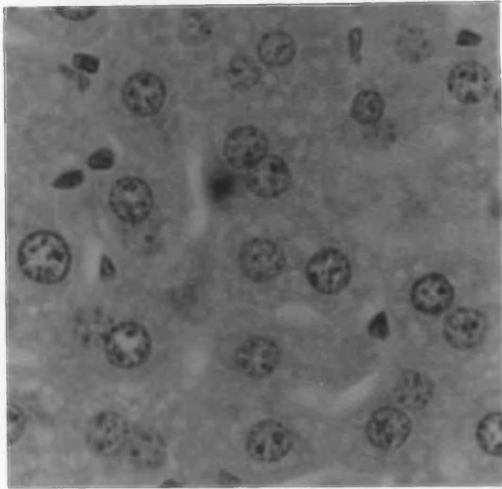
7.2. RESULTS

7.2.1. Fas-induced apoptosis, liver damage and caspase-3/7-like proteolytic activity are blocked by z-VAD.fmk

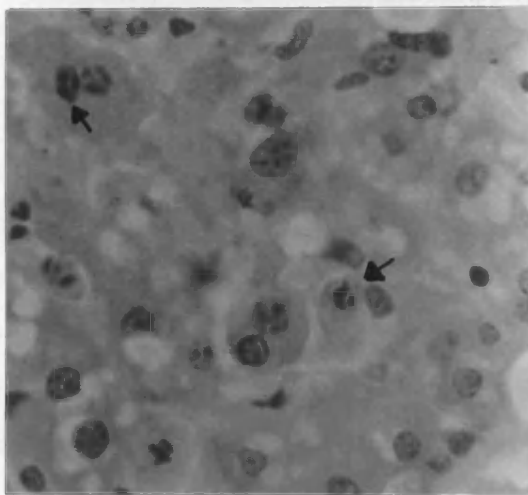
Intravenous injection of 10 µg of the agonistic Fas receptor antibody JO2 into 6–8 week old male Balb/c mice induced extensive liver damage and haemorrhage (typically, liver weight increased by ~90% due to engorgement with blood) with > 60% of hepatocytes showing apoptotic morphology after 4 h (Fig. 7.1B), consistent with previous studies (Ogasawara, *et al.* 1993). The caspase inhibitor, z-VAD.fmk (50 µmoles/kg) blocked Fas-induced liver damage and haemorrhage and dramatically reduced hepatocyte apoptosis to < 1% (Fig. 7.1C). Almost complete protection was still observed 24 h after exposure to the agonistic antibody (data not shown), and outwardly the animals appeared normal. The protection conferred by z-VAD.fmk was consistent with a critical role for the activation of caspases in Fas-induced apoptosis *in vivo*, as shown previously in studies using z-VAD.fmk or Ac-YVAD.cmk (Rodriguez, *et al.* 1996; Rouquet, *et al.* 1996).

To date, very few studies on Fas-induced apoptosis have been carried out *in vivo* (Ogasawara, *et al.* 1993; Rodriguez, *et al.* 1996; Rouquet, *et al.* 1996), most being *in vitro* (Nagata, 1997; Enari, *et al.* 1995; Schlegel, *et al.* 1996; Enari, *et al.* 1996; Kamada, *et al.* 1997). In order to confirm the involvement of caspases in Fas-induced apoptosis *in vivo*, their activation was assessed by measuring the cleavage of z-DEVD.afc in crude liver homogenates (*fraction A* in Fig. 2.2) from control and Fas-treated mice. The cleavage of z-DEVD.afc (DEVDase activity) is indicative primarily of caspase-3 and caspase-7 activities, although there may be a minor contribution from other caspases (Muzio, *et al.* 1996; Nicholson, *et al.* 1995; Tewari, *et al.* 1995; Fernandes-Alnemri, *et al.* 1995). Treatment with the JO2 antibody resulted in a marked increase in total liver DEVDase activity compared with that seen in controls after 4 h (Fig. 7.2). An intravenous injection of z-VAD.fmk (50 µmoles/kg) completely inhibited this Fas-induced DEVDase activity, even in animals sacrificed 24 h after injection of the JO2 antibody (Fig. 7.2). Although the total liver DEVDase activity following Fas administration is calculated for the weight of the liver following engorgement with blood, erythrocytes have not been shown to express the Fas receptor and it is unlikely that any of the observed activity in the crude homogenate is derived from the blood.

A Control 4 h



B Fas 4 h



C Fas + z-VAD.fmk 4 h

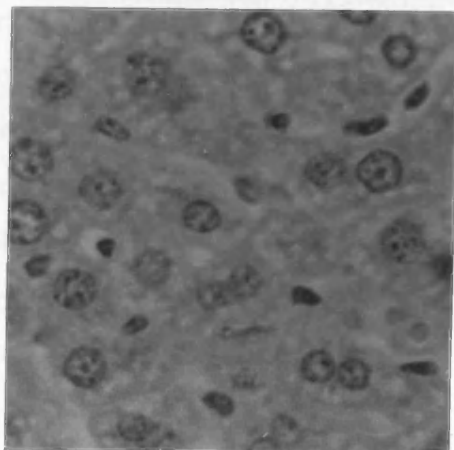


Fig. 7.1. Fas-induced hepatocyte apoptosis *in vivo* is inhibited by z-VAD.fmk.

Liver sections were prepared from control mice (A), mice 4 h after intravenous injection of the agonistic Fas receptor antibody JO2 (10 ug; B) and mice 4 h after intravenous injection of the antibody, followed 5 min later by intravenous injection of the caspase inhibitor z-VAD.fmk (C) as described in sections 2.2.7- 2.2.9. The arrows indicate examples of hepatocytes with typical apoptotic morphology.

Total liver DEVDase activity (nmol/min)

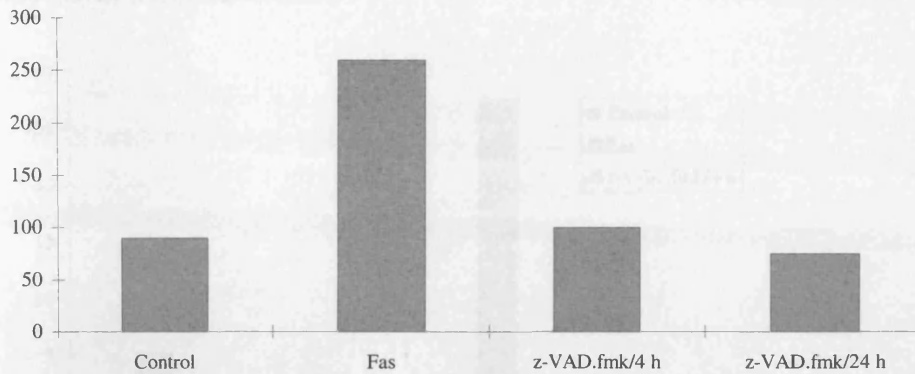


Fig. 7.2. Fas-induced mouse liver DEVDase activity is inhibited by z-VAD.fmk

Crude liver homogenates prepared from mice sacrificed 4 h after injection of 0.9% saline (control), 4 h after injection of 10 μ g JO2 antibody (Fas), 4 h after injection of 10 μ g JO2 antibody and 50 μ moles/kg z-VAD.fmk (z-VAD.fmk/4 h) and 24 h after injection of 10 μ g JO2 antibody and 50 μ moles/kg z-VAD.fmk (z-VAD.fmk/24 h) were assessed for cleavage of the fluorogenic substrate z-DEVD.afc (DEVDase activity) as described in section 2.2.5b. The data presented for control and Fas are the average of two experiments and the data from the z-VAD.fmk/4 h and z-VAD.fmk/24 h are from a typical experiment.

These results were consistent with the activation of caspase-3 and/or caspase-7 in Fas-induced apoptosis *in vivo*, and were in agreement with *in vitro* studies which have shown that the activation of these caspases follows treatment of cells with Fas or tumour necrosis factor (Schlegel, *et al.* 1996; Duan, *et al.* 1996a; Chinnaiyan, *et al.* 1996). In order to further dissect the role of caspases in Fas-induced apoptosis *in vivo*, the DEVDase activity in subcellular liver fractions prepared from control mice and from mice treated with either Fas antibody alone or Fas antibody in conjunction with z-VAD.fmk was examined, as indicated in Fig. 2.2.

DEVDase activity was assessed in the 'nuclear' pellet (*Fraction C*), the washed mitochondria (*Fraction F*), the cytosol (*Fraction H*) and the microsomal fraction (*Fraction I*). Treatment with the Fas antibody induced 45-, 23-, 11-, and 21-fold increases in total DEVDase activity in the 'nuclear', mitochondrial, cytosolic, and microsomal fractions, respectively (Fig. 7.3). In all cases, z-VAD.fmk almost completely inhibited the increases in DEVDase activity (Fig. 7.3). Thus z-VAD.fmk blocked apoptosis either by directly inhibiting the activity of caspases-3 and -7 or by inhibiting an upstream caspase, such as caspase-8. In addition to the measurement of DEVDase activity, the extent of processing of caspase-3 and caspase-7 was assessed in the different subcellular fractions.

DEVDase activity (nmol/fraction/min)

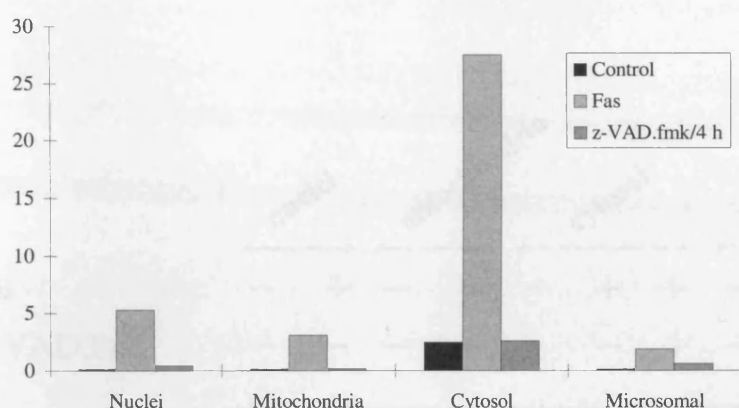


Fig. 7.3. DEVDase activity in subcellular liver fractions

Subcellular fractions were prepared from livers removed from mice sacrificed 4 h after injection of 0.9% saline (control), 4 h after injection of 10 μ g JO2 antibody (Fas) and 4 h after injection of JO2 antibody and 50 μ moles/kg z-VAD.fmk (z-VAD.fmk/4 h), and were assessed for cleavage of the fluorogenic substrate z-DEVD.afc (DEVDase activity) as described in section 2.2.5b.

7.2.2. Procaspace-3 and active caspase-3 are in the cytosol

Caspase-3 is generally present in control cells as an inactive p32 zymogen (Schlegel, *et al.* 1996; MacFarlane, *et al.* 1997a; Chinnaiyan, *et al.* 1996; section 1.4.2.3). On induction of apoptosis, this proform is initially processed at Asp¹⁷⁵ between the large and small subunits producing a p12 subunit and a p20 subunit, which is further processed at Asp⁹ and Asp²⁸ to yield p19 and p17 large subunits, respectively (Nicholson, *et al.* 1995; Fernandes-Alnemri, *et al.* 1996). In control mice, procaspase-3 was present in the cytosolic fraction (Fig. 7.4, lane 5) with none detectable in the 'nuclear', mitochondrial or microsomal fractions (Fig. 7.4, lanes 1, 3 and 8, respectively).

Following treatment with the Fas antibody, complete processing of procaspase-3 together with the appearance of its catalytically active p17 subunit was observed in the cytosolic fraction (Fig. 7.4, lane 6). In addition an immunologically reactive fragment of ~29 kDa (Fig. 7.4, lanes 5–9) was observed. Treatment with z-VAD.fmk resulted in complete inhibition of the processing of procaspase-3 and the formation of the p17 large subunit (Fig. 7.4, lane 7). Inhibition of caspase-3 processing was also accompanied by the appearance of a very small amount of a ~p19 fragment (Fig. 7.4, lane 7). The p17 subunit was detected

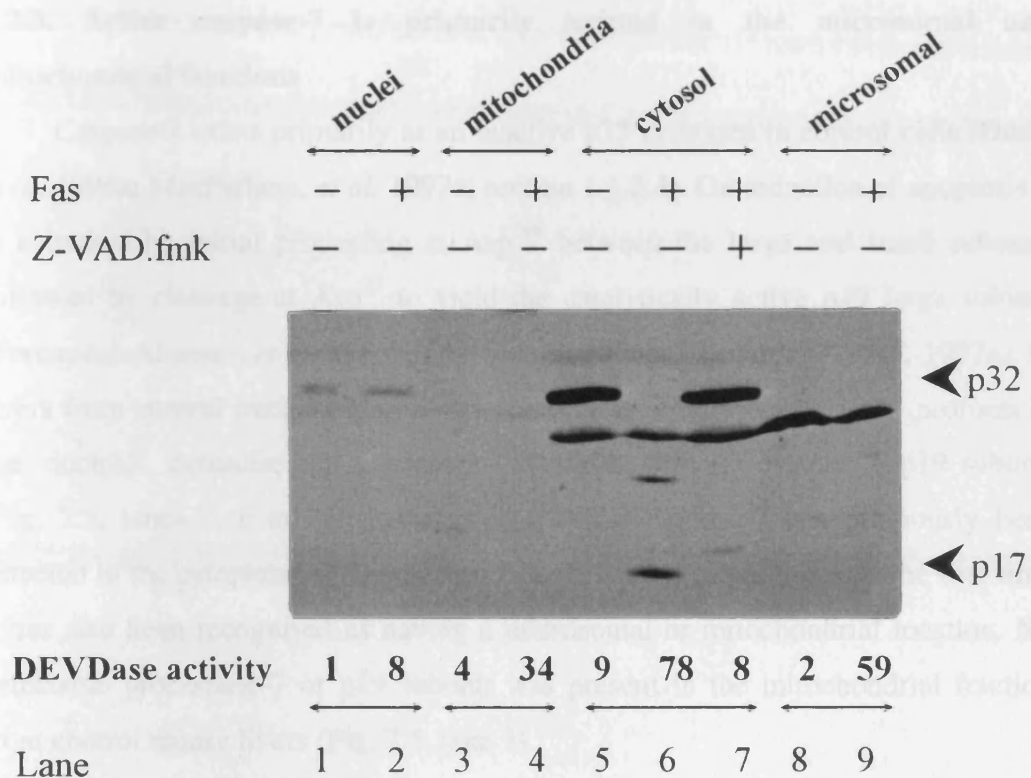


Fig. 7.4. Active caspase-3 is localised in liver cytosol following Fas-induced apoptosis
 Subcellular fractions were prepared from the livers of untreated mice or mice treated 4 h earlier with Fas antibody either alone or in the presence of z-VAD.fmk as indicated in Fig. 2.2. Proteins (100 µg) from nuclear, mitochondrial, cytosolic and microsomal fractions were separated by SDS/13% (w/v) PAGE and Western blot analysis carried out using an antibody to caspase-3. The DEVDase activity represents the amount of z-DEVD.afc cleavage activity loaded expressed as pmol/min/lane. The upper and lower arrows indicate the proform and the catalytically active large subunit of caspase-3, respectively.

exclusively in the cytosolic fraction of livers from Fas-treated mice (Fig. 7.4, lane 6), demonstrating that following induction of apoptosis by the agonistic Fas receptor antibody, active caspase-3 is located primarily in the cytosol.

7.2.3. Active caspase-7 is primarily located in the microsomal and mitochondrial fractions

Caspase-7 exists primarily as an inactive p35 zymogen in control cells (Duan, *et al.* 1996a; MacFarlane, *et al.* 1997a; section 1.1.2.4). On induction of apoptosis it is activated by initial processing at Asp¹⁹⁸ between the large and small subunits followed by cleavage at Asp²³ to yield the catalytically active p19 large subunit (Fernandes-Alnemri, *et al.* 1995b; Duan, *et al.* 1996a; MacFarlane, *et al.* 1997a). In livers from control mice, caspase-7 was present as an unprocessed p35 proform in the ‘nuclear’, cytosolic and microsomal fractions with no detectable p19 subunit (Fig. 7.5, lanes 1, 6 and 9, respectively). While caspase-7 has previously been detected in the cytoplasm of Jurkat cells (Duan, *et al.* 1996a), this was the first time it has also been recognised as having a microsomal or mitochondrial location. No detectable procaspase-7 or p19 subunit was present in the mitochondrial fraction from control mouse livers (Fig. 7.5, lane 3).

Following treatment with the Fas antibody, complete processing of procaspase-7 was observed in ‘nuclear’, cytosolic and microsomal fractions (Fig. 7.5, lanes 2, 7 and 10). This is the first demonstration of the activation of caspase-7 in mouse liver *in vivo* following Fas-induction of apoptosis. Although complete processing of caspase-7 was observed in the ‘nuclear’ and cytosolic fractions, little if any p19 subunit was detected in these fractions (Fig. 7.5, lanes 2 and 7). However, the p19 catalytically active large subunit of caspase-7 was clearly detected in both the mitochondrial and microsomal fractions (Fig. 7.5, lanes 4 and 10, respectively). In addition to the p19 subunit, an uncharacterized ~p32 fragment was also observed in the microsomal fraction (Fig. 7.5, lane 10), which was also observed in temperature-shifted LTR6 cells (Figs. 5.3B; 5.6C and 5.7B). These results suggested that caspase-7 was translocated from the cytosol to the microsomal fraction either prior to, or following, its catalytic activation by an ‘initiator’ caspase. The data clearly demonstrate that following Fas-induced apoptosis in mouse liver, caspase-7 is completely processed to its catalytically

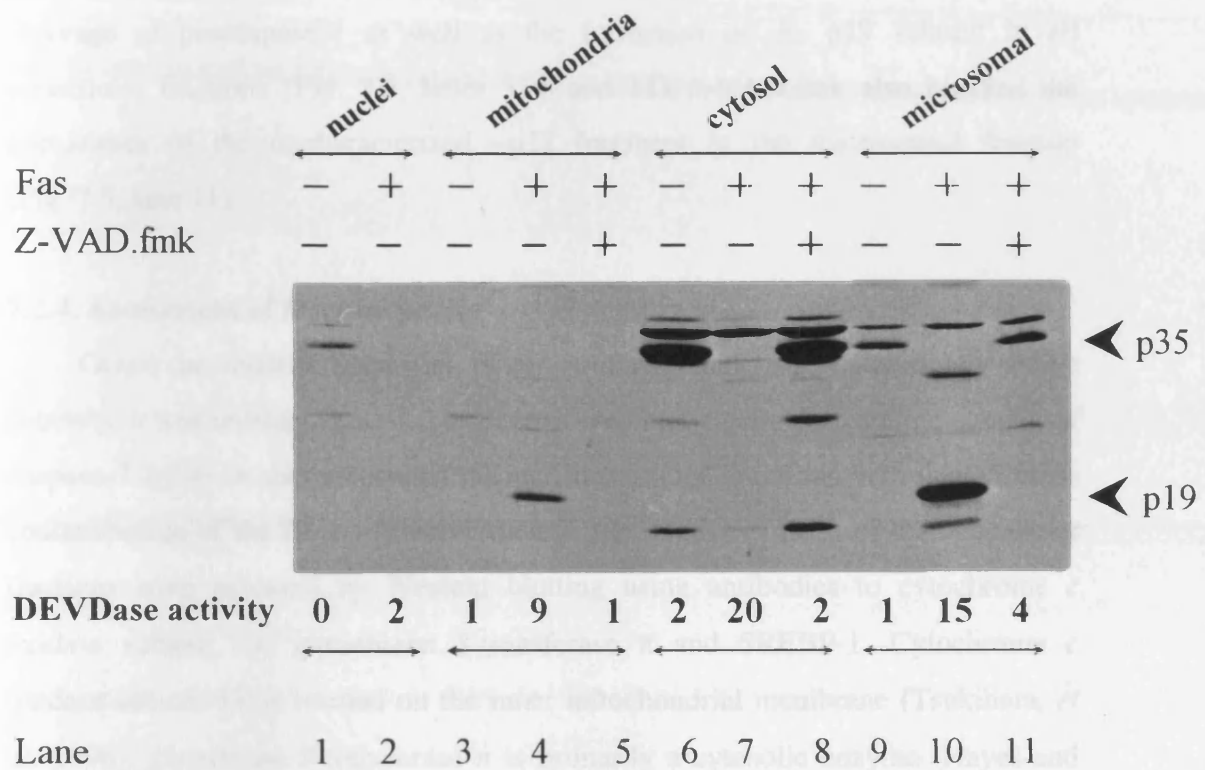


Fig. 7.5. Active caspase-7 is localised primarily in liver mitochondrial and microsomal fractions following Fas-induced apoptosis.

Subcellular fractions were prepared from the livers of untreated mice, or mice treated 4 h earlier with Fas antibody either alone or in the presence of z-VAD.fmk (50 μ moles/kg) as indicated and described in section 2.7. Proteins (25 μ g) from nuclear, mitochondrial, cytosolic and microsomal fractions were separated by SDS/13% (w/v) PAGE and Western blot analysis carried out using an antibody to caspase-7. The DEVDase activity represents the amount of z-DEVD.afc cleaving activity loaded expressed as pmol/min/lane. The upper and lower arrows indicate the proform and the catalytically active large subunit of caspase-7, respectively.

active p19 subunit, which is found primarily in the mitochondrial and microsomal fractions with little if any remaining in the cytosol (Fig. 7.5, lane 7).

These results were in marked contrast to the findings with caspase-3, where the catalytically active p17 subunit remained in the cytosol following processing of the inactive zymogen (Fig. 7.4). z-VAD.fmk completely inhibited the Fas-induced cleavage of procaspase-7 as well as the formation of the p19 subunit in all subcellular fractions (Fig. 7.5, lanes 5, 8 and 11). z-VAD.fmk also blocked the appearance of the uncharacterized ~p32 fragment in the microsomal fraction (Fig. 7.5, lane 11).

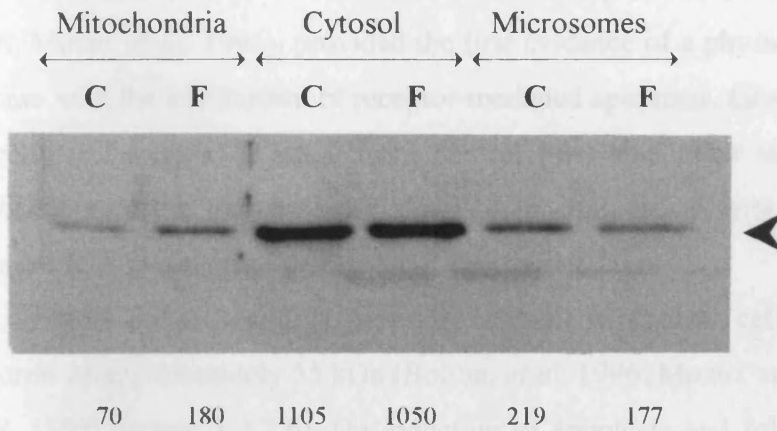
7.2.4. Assessment of fraction purity

Given the relative intensities of the proforms and large catalytically active subunits, it was unlikely that the presence of the catalytically active large subunit of caspase-7 (p19) in the mitochondrial and microsomal fractions was due to cross contamination of the fractions. Nevertheless, the relative purities of the subcellular fractions were assessed by Western blotting using antibodies to cytochrome *c* oxidase subunit IV, glutathione *S*-transferase π and SREBP-1. Cytochrome *c* oxidase subunit IV is located on the inner mitochondrial membrane (Tsukihara, *et al.* 1996), glutathione *S*-transferase π is primarily a cytosolic enzyme (Hayes and Pulford, 1995) and SREBP-1 is located in the endoplasmic reticulum (Wang, *et al.* 1994b). Densitometric analysis revealed that 77, 9 and 14% of total glutathione *S*-transferase and 5, 93 and 2% of total cytochrome *c* oxidase subunit IV were detected in the cytosolic, mitochondrial and microsomal fractions, respectively (Fig. 7.6). SREBP-1 was found almost exclusively in the endoplasmic reticulum (Fig. 7.8).

7.2.5. Processing and activation of caspase-8 in Fas-induced apoptosis *in vivo*

The results described above have demonstrated that the effector caspases, caspase-3 and caspase-7, are both processed during Fas-induced apoptosis *in vivo*, but that their subsequent subcellular localisation is markedly different, with active caspase-3 being confined to the cytosol (Fig. 7.4) and active caspase-7 being translocated to the mitochondrial and microsomal fractions (Fig. 7.5). These two effector caspases, together with all other known caspases, have been shown to be

A Glutathione *S*-transferase



B Cytochrome *c* oxidase IV

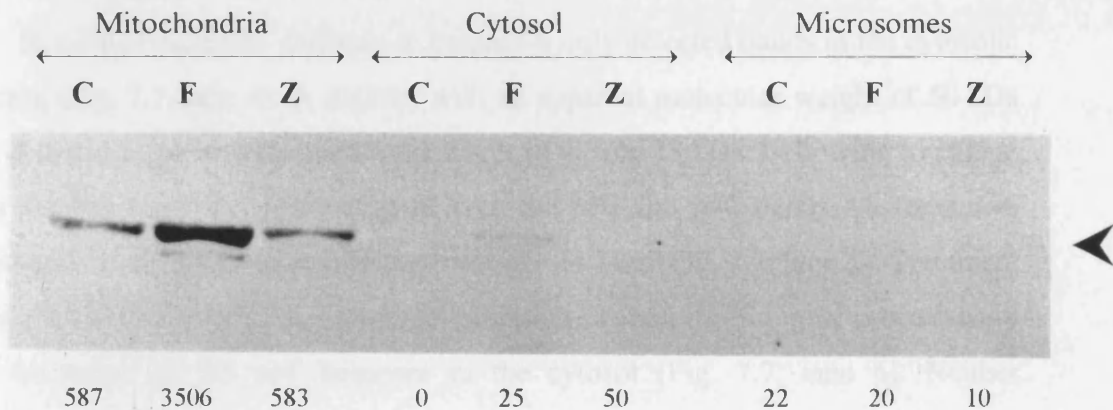


Fig. 7.6 Subcellular distribution of Glutathione *S*-transferase (Pi) and Cytochrome *c* oxidase subunit IV

Subcellular fractions were prepared from the livers of untreated mice (C), or mice treated 4 h earlier with Fas antibody either alone (F) or in the presence of z-VAD.fmk (Z) (50 umoles/kg) as indicated and described in section 2.2.7 and 2.2.9. A) Proteins (25 ug) from mitochondrial, cytosolic and microsomal fractions were separated by SDS/13% (w/v) PAGE and Western blot analysis carried out using an antibody to glutathione *S*-transferase Pi. B) Proteins (25 ug) from mitochondrial, cytosolic and microsomal fractions were separated by SDS/7% (w/v) PAGE and Western blot analysis carried out using an antibody to Cytochrome *c* oxidase subunit IV. Densitometry was carried out for each blot as described in section 2.2.14. and the intensity volumes are shown under each lane. The arrowheads indicate A) Glutathione *S*-transferase Pi and B) Cytochrome *c* oxidase subunit IV.

processed and activated *in vitro* by the upstream activator caspase, caspase-8 (reviewed in Cohen, 1997). The identification of the association of procaspase-8 with the intracellular death domain of the Fas-receptor and TNF-R1 (Boldin, *et al.* 1996; Muzio, *et al.* 1996), provided the first evidence of a physical association of a caspase with the mechanism of receptor-mediated apoptosis. Given this association, subcellular fractions obtained from control mice and mice sacrificed 4 h after treatment with the Fas antibody alone or in conjunction with z-VAD.fmk were assessed for the incidence of caspase-8 processing.

Human procaspase-8 is generally present in control cells as two inactive isoforms of approximately 55 kDa (Boldin, *et al.* 1996; Muzio, *et al.* 1997; Scaffidi, *et al.* 1997; section 1.4.2.6). On induction of apoptosis and following association with the receptor-associated DISC complex, both isoforms are initially processed at Asp³⁷⁴ and Asp³⁸⁴ between the large and small subunits producing a p11 fragment and a p43 fragment, which is further processed at Asp²¹⁶ to remove the large FADD-like prodomain to yield the catalytically active p18 large subunit (Boldin, *et al.* 1996; Muzio, *et al.* 1996; Scaffidi, *et al.* 1997).

In control mice, the antibody to caspase-8 only detected bands in the cytosolic fraction (Fig. 7.7, lane 4). A doublet with an apparent molecular weight of 50 kDa was detected together with two further bands of 40 and 18 kDa. Following treatment with the Fas antibody, processing of both the p50 and p40 bands was detected, together with the appearance of a fragment of ~14 kDa (Fig. 7.7, lane 5). Treatment with z-VAD.fmk resulted in complete inhibition of the processing of procaspase-8 and formation of the p14 fragment in the cytosol (Fig. 7.7, lane 6). Neither procaspase-8 nor the immunologically reactive p14 fragment were detected in the mitochondrial or microsomal fractions from control or Fas-treated mouse livers. In addition no fragment of a size consistent with the catalytically active large subunit of human caspase-8 (p18) was detected following treatment with the agonistic Fas antibody.

7.7. Fate of microsome SRBP-1 in Fas-induced apoptosis in quiescent

Previous studies have highlighted overlapping substrate specificities for caspase-8 and -9. For example, in rat hepatoma cells, caspase-8 and -9 were found to cleave the same substrate, SRBP-1, in response to Fas-induced apoptosis (Wang et al., 1998).

Caspase-8

Thrombin (Wang et al., 1993; Wang et al., 1995; Pambianco-Albertini et al., 1995) and

activated caspase-8 (Wang et al., 1998) were found to cleave SRBP-1 in the cytosol

of rat hepatoma cells. In contrast, caspase-9 was found to cleave SRBP-1 in the

mitochondria of these cells (Wang et al., 1998). The cleavage of SRBP-1 by

activated caspase-8 and -9 was blocked by the caspase inhibitor z-VAD.fmk (Wang

et al., 1998). The cleavage of SRBP-1 by activated caspase-8 and -9 was also

blocked by the caspase inhibitor z-DEVD.fmk (Wang et al., 1998). The cleavage

of SRBP-1 by activated caspase-8 and -9 was also blocked by the caspase

inhibitor z-LEHD.fmk (Wang et al., 1998). The cleavage of SRBP-1 by

activated caspase-8 and -9 was also blocked by the caspase inhibitor z-DEVD.fmk

(Wang et al., 1998). The cleavage of SRBP-1 by activated caspase-8 and -9

was also blocked by the caspase inhibitor z-LEHD.fmk (Wang et al., 1998).

The cleavage of SRBP-1 by activated caspase-8 and -9 was also blocked by

the caspase inhibitor z-DEVD.fmk (Wang et al., 1998). The cleavage of

SRBP-1 by activated caspase-8 and -9 was also blocked by the caspase

inhibitor z-LEHD.fmk (Wang et al., 1998). The cleavage of SRBP-1 by

activated caspase-8 and -9 was also blocked by the caspase inhibitor z-DEVD.fmk

(Wang et al., 1998). The cleavage of SRBP-1 by activated caspase-8 and -9

was also blocked by the caspase inhibitor z-LEHD.fmk (Wang et al., 1998).

The cleavage of SRBP-1 by activated caspase-8 and -9 was also blocked by

the caspase inhibitor z-DEVD.fmk (Wang et al., 1998). The cleavage of

SRBP-1 by activated caspase-8 and -9 was also blocked by the caspase

inhibitor z-LEHD.fmk (Wang et al., 1998). The cleavage of SRBP-1 by

activated caspase-8 and -9 was also blocked by the caspase inhibitor z-DEVD.fmk

(Wang et al., 1998). The cleavage of SRBP-1 by activated caspase-8 and -9

was also blocked by the caspase inhibitor z-LEHD.fmk (Wang et al., 1998).

The cleavage of SRBP-1 by activated caspase-8 and -9 was also blocked by

the caspase inhibitor z-DEVD.fmk (Wang et al., 1998). The cleavage of

SRBP-1 by activated caspase-8 and -9 was also blocked by the caspase

inhibitor z-LEHD.fmk (Wang et al., 1998). The cleavage of SRBP-1 by

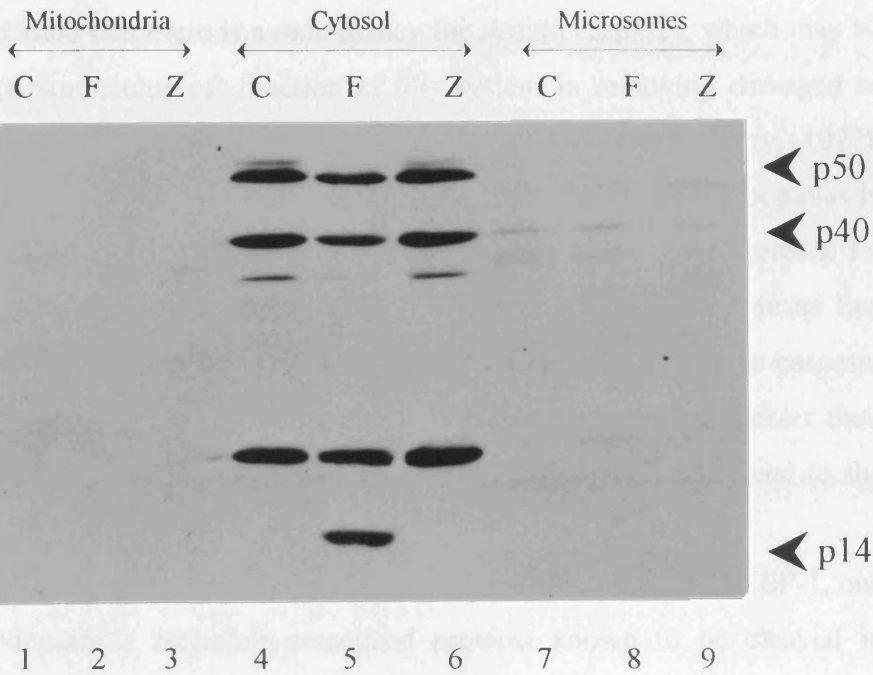


Fig. 7.7. Processing of caspase-8 following Fas-induced apoptosis.

Subcellular fractions were prepared from the livers of untreated mice (C), or mice treated 4 h earlier with Fas antibody either alone (F) or in the presence of z-VAD.fmk (Z) (50 umoles/kg) as indicated and described in section 2.2.7. Proteins (25 ug) from mitochondrial, cytosolic and microsomal fractions were separated by SDS/15% (w/v) PAGE and Western blot analysis carried out using an antibody to caspase-8. The upper and lower arrows indicate the proform and the p14 fragment, respectively.

7.2.6. Fate of microsomal SREBP-1 in Fas-induced apoptosis in mouse liver

Previous studies have highlighted overlapping substrate specificities for caspases-3 and -7. For example, *in vitro* combinatorial studies using tetrapeptide substrates assigned virtually indistinguishable substrate specificities to caspases-3 and -7 (Thornberry, *et al.* 1997) consistent with their mutual ability to cleave PARP (Nicholson, *et al.* 1995; Tewari, *et al.* 1995; Fernandes-Alnemri, *et al.* 1995). It has often been suggested that there is a redundancy for certain caspases, which may be due to the important biological function of this system in removing damaged or unwanted cells (reviewed in Cohen, 1997; Nicholson and Thornberry, 1997). However, results with caspase-3 knockout mice, which exhibit normal apoptosis in most tissues except neuronal cells (Kuida, *et al.* 1996), and the requirement for DCP-1 caspase in *Drosophila* oogenesis (McCall and Steller, 1998), indicate that some caspases may function in a tissue selective manner. Alternatively caspases with overlapping substrate specificities may, at least in some tissues, exert their functions in different cellular compartments, to cleave substrates confined to the subcellular compartment in question.

To explore this possibility in the model studied here, the fate of SREBP-1, one of the few endoplasmic reticulum-associated proteins known to be cleaved in apoptosis was examined (Wang, *et al.* 1994b; Wang, *et al.* 1996a; Pai, *et al.* 1996). SREBPs belong to the basic-helix-loop-helix-leucine zipper family of transcription factors and are involved in the regulation of sterol metabolism (Wang, *et al.* 1994b). These ~125 kDa proteins are proteolytically cleaved at different, but nearby, sites following sterol depletion or the induction of apoptosis. On the induction of apoptosis both SREBP-1 and SREBP-2 are cleaved by the hamster homologues of caspases-3 and -7 resulting in translocation of the transcriptionally active N-terminal domains to the nucleus (Wang, *et al.* 1996a; Pai, *et al.* 1996).

In livers from control mice, SREBP-1 was exclusively associated with the microsomal fraction with none being detectable in the cytosolic, nuclear or mitochondrial fractions (Fig. 7.8, compare lanes 1 and 2; and data not shown). Complete loss of the ~125 kDa SREBP-1 was observed in the microsomal fraction prepared from liver obtained from mice treated 4 h earlier with the agonistic Fas antibody (Fig. 7.8, lane 3). The antibody to SREBP-1 detected the intact but not the cleaved molecule. The Fas-induced cleavage of SREBP-1 was largely prevented by

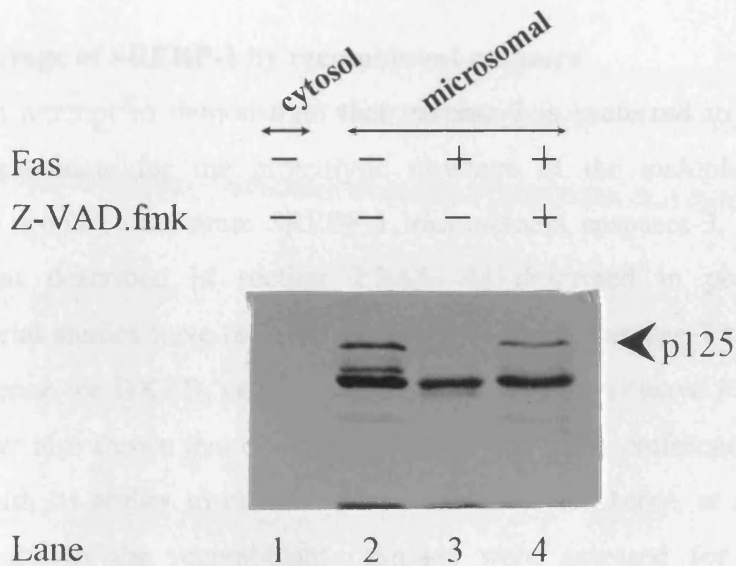


Fig. 7.8. Cleavage of the endoplasmic reticular-specific substrate SREBP-1

Subcellular fractions were prepared from the livers of untreated mice, or mice treated 4 h earlier with Fas antibody either alone or in the presence of Z-VAD.fmk as indicated in the legend to Fig. 7.7. Proteins (25 ug) from cytosolic or microsomal fractions were separated by SDS/8% (w/v) PAGE, and Western blotting carried out using an antibody to SREBP-1. The arrow indicates the intact form of SREBP-1, which was only found in the microsomal fraction.

z-VAD.fmk (Fig. 7.8, lane 4). As active caspase-7 and SREBP-1 share the same subcellular localisation, it was possible that caspase-7 is responsible for the Fas-induced cleavage of SREBP-1 *in vivo*.

7.2.7. Cleavage of SREBP-1 by recombinant caspases

In an attempt to demonstrate that caspase-7 is preferred to caspase-3 as a potential candidate for the proteolytic cleavage of the endoplasmic reticular-associated apoptotic substrate SREBP-1, recombinant caspases-3, -6 and -7 were prepared as described in section 2.2.15. As described in previous sections combinatorial studies have revealed that caspase-3 and caspase-7 share a cleavage site preference for DXXD, consistent with their ability to cleave PARP. The same studies have also shown that caspase-6 has a cleavage site preference for VEHD, in keeping with its ability to cleave nuclear lamins (Thornberry, *et al.* 1997). After their preparation the recombinant caspases were assessed for their cleavage activities towards the two fluorogenic substrates z-DEVD.afc and z-VEID.amc which mimic the cleavage sites within PARP and lamin A, respectively. As expected recombinant caspase-3 and caspase-7 displayed a considerable preference for the substrate z-DEVD.afc whereas recombinant caspase-6 showed a preference for the substrate z-VEID.amc (Fig. 7.9).

Specific activity (nmol/mg/min)

Log₁₀ scale

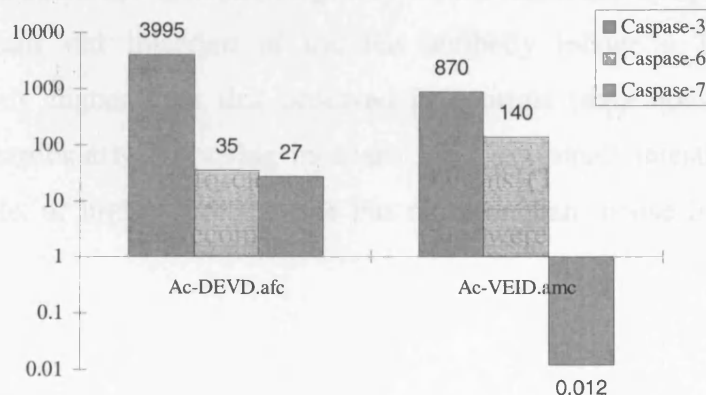


Fig. 7.9. Cleavage activities of recombinant caspases-3, -6 and -7

Recombinant caspases were prepared as described in section 2.2.15, and their abilities to cleave the fluorogenic substrates Ac-DEVD.afc and Ac-VEID.amc assessed fluorimetrically as described in section 2.2.5.

To assess the ability of each recombinant caspase to cleave SREBP-1, 50 µg protein from a control microsomal fraction was incubated for 1 h at 37°C in HEPES buffer (20 mM, pH 8.0; 0.1% CHAPS) alone or in the presence of 50 or 100 pmol z-DEVD.afc cleavage activity derived from recombinant caspase-3, caspase-6 or caspase-7. After the appropriate incubation, samples were analysed by SDS-PAGE and Western blotting for the incidence of SREBP-1 processing (Fig. 7.10).

Surprisingly, recombinant caspase-6 was the only one of the three homologues tested to be effective at cleaving SREBP-1 (Fig. 7.10, lanes 4 and 5). Incubation with recombinant caspase-6 lead to cleavage of the protein and the production of a fragment of approximately 110 kDa. However, the cleavage of SREBP-1 by recombinant caspase-6 may be non-specific, as *in vivo* cleavage of the substrate during both sterol metabolism and apoptosis occurs almost in the middle of the protein to yield two fragments of a similar size (Wang, *et al.* 1996a). Neither caspase-3 nor caspase-7 were capable of cleaving SREBP-1 in this system even after incubation for 1 h at 37°C in the presence of 2 nmol of DEVDase activity (data not shown).

7.2.8. Fas-induced apoptosis in other organs

In addition to livers removed from control mice and mice sacrificed 4 h after injection of the agonistic Fas receptor antibody alone or in the presence of 50 µmoles/kg z-VAD.fmk, samples from the heart, kidney, lung, small intestine and testis were examined histopathologically for the incidence of apoptosis. In none of these organs did injection of the Fas antibody induce a level of apoptosis significantly higher than that observed in controls (data not shown). This was perhaps particularly surprising in heart, lung and small intestine which express comparable, or higher levels of the Fas receptor than mouse liver (French, *et al.* 1996).

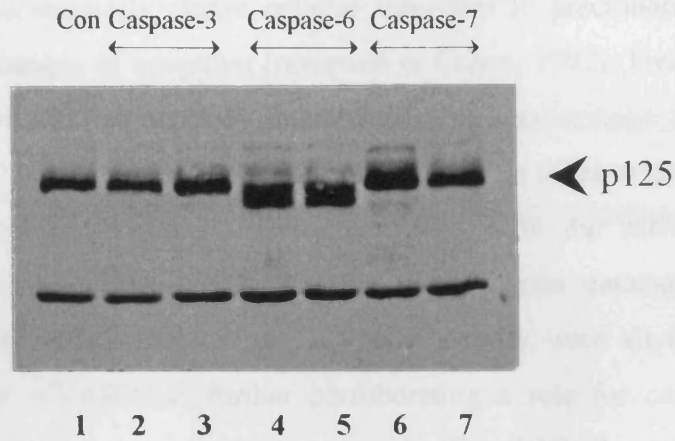


Fig. 7.10. Cleavage of SREBP-1 by recombinant caspases

The microsomal fraction from control mice was incubated either alone in Hepes (20 mM, pH 8.0; 0.1% CHAPS; lane 1) or in the presence of 50 pmols (lanes 2, 4 and 6) or 100 pmols (lanes 3, 5 and 7) of z-DEVD.afc cleavage activity derived from recombinant caspase-3, caspase-6 or caspase-7, respectively. Proteins (25 ug) from each treatment were separated by SDS/8% (w/v) PAGE and Western blot analysis carried out using an antibody to SREBP-1. The arrow indicates the intact protein.

7.3. DISCUSSION

Caspases play a key role in the execution phase of apoptosis. ‘Initiator’ caspases, such as caspase-8, activate the ‘effector’ caspases, including caspase-3 and -7, which subsequently cleave cellular substrates to precipitate the dramatic morphological changes of apoptosis (reviewed in Cohen, 1997). Treatment of mice with an agonistic anti-Fas antibody induced massive haemorrhage and hepatocyte apoptosis (Fig. 7.1B), in agreement with previous studies (Ogasawara, *et al.* 1993), as well as inducing DEVDase activity consistent with the activation of both caspase-3 and caspase-7 (Fig. 7.2). The Fas-induced liver damage, induction of hepatocyte apoptosis and increase in DEVDase activity were all blocked by the caspase inhibitor z-VAD.fmk, further corroborating a role for caspases in Fas-induced apoptosis *in vivo*, as reported previously (Fig. 7.1C; Rouquet, *et al.* 1996; Rodriguez, *et al.* 1996). Treatment of mice with the agonistic Fas receptor antibody results in the rapid death of the animal (Ogasawara, *et al.* 1993). There is, however, some discrepancy as to whether this fulminant liver damage is the primary cause of death in these animals. Some workers have reported that the liver-specific expression of a *bcl2* transgene prevented the observed liver damage as well as the lethal effects of the antibody (Lacronique, *et al.* 1996). However, others have shown that whilst *bcl2* expression in liver protected from fulminant liver destruction, it was not capable of preventing the animals from dying (Rodriguez, *et al.* 1996).

The role of caspases in Fas-induced apoptosis *in vivo* was analysed further by examination of subcellular fractions prepared from control mice, and mice sacrificed after injection of 10 µg JO2 antibody alone or together with 50 µmoles/kg z-VAD.fmk for the processing of caspase-3, caspase-7 and caspase-8. In control mice, procaspase-3 was present solely in the cytosolic fraction (Fig. 7.4, lane 5), with none being detectable in the ‘nuclear’, mitochondrial or microsomal fractions (Fig. 7.4, lanes 1, 3 and 8, respectively). On induction of apoptosis with the agonistic Fas antibody, the inactive procaspase-3 was processed completely to yield the catalytically active large (p17) subunit which remained confined to the cytosol (Fig. 7.4, compare lanes 5 and 6). The ~p29 fragment detected by the caspase-3 antibody was observed in all the cytosolic and microsomal fractions (Fig. 7.4, lanes 5–9). While the identity of this fragment is not known, it has been proposed to be due to processing of caspase-3 following cleavage at Asp²⁸, which yields a zymogen

which is not further processed to active caspase-3 (Boulakia, *et al.* 1996). This hypothesis is compatible with the data presented here, since similar levels of p29 were detected in subcellular fractions from both control and Fas-treated livers (Fig. 7.4, lanes 5–9). Treatment with z-VAD.fmk inhibited the processing of procaspase-3 and the formation of the p17 catalytically active large subunit (Fig. 7.4, lane 7), and was accompanied by the appearance of a very small amount of an uncharacterised ~p19 fragment (Fig. 7.4, lane 7). The appearance of this fragment may be attributed to the partial blocking of the processing of the large subunit at Asp⁹ (MacFarlane, *et al.* 1997a; Polverino and Patterson, 1997). In contrast to the data presented here, others have recently demonstrated that procaspase-3, as well as being localised in the cytosol can be detected in the intermembrane space of mitochondria (Mancini, *et al.* 1998). In this case, various apoptotic stimuli resulted in the loss of procaspase-3 from the mitochondria and the induction of caspase-3-like proteolytic activity.

In contrast to the subcellular localisation of caspase-3, procaspase-7 was located in the 'nuclear', cytosolic and microsomal fractions (Fig. 7.5, lanes 1, 6 and 9, respectively). Following the induction of apoptosis with the Fas antibody, inactive procaspase-7 was processed completely in all three fractions (Fig. 7.5, lanes 2, 7 and 10, respectively). However, despite complete processing, the catalytically active p19 large subunit was almost undetectable in both the 'nuclear' and cytosolic fractions (Fig. 7.5, lanes 2 and 6, respectively). In stark contrast, the p19 catalytically active large fragment was clearly detectable in the mitochondrial and microsomal fractions (Fig. 7.5, lanes 4 and 10, respectively). It was very unlikely that the p19 fragment in the mitochondrial fraction was due to microsomal contamination, because the uncharacterized p29 band detected using the caspase-3 antibody in the microsomal fraction from control or Fas-treated livers (Fig. 7.4, lanes 8 and 9) was not present in the mitochondrial fraction (Fig. 7.4, lanes 3 and 4). In addition to this, the endoplasmic reticular-specific SREBP-1 was confined solely to the microsomal fraction with none being detectable in the mitochondria (data not shown). The amount of the large p19 subunit of caspase-7 in the microsomal fraction following Fas-induced apoptosis was greater than the amount of procaspase-7 in control liver microsomes (Fig. 7.5, compare lanes 9 and 10). These results suggested that caspase-7 was translocated from the cytosol to the

microsomal fraction either prior to or following its catalytic activation by an 'initiator' caspase, although the detection of a small amount of p19 in the cytosol from Fas-treated mice may suggest that activation of caspase-7 occurs prior to its translocation to the mitochondrial and microsomal fractions. The tetrapeptide caspase inhibitor z-VAD.fmk completely inhibited the Fas-induced cleavage of procaspase-7 as well as the formation of the p19 large subunit in all subcellular fractions. The data clearly demonstrate that following Fas-induced apoptosis in mouse liver, caspase-7 is completely processed to its catalytically active p19 subunit, which is found primarily in the mitochondrial and microsomal fractions with little remaining in the cytosol. Taken together with the caspase-3 results, the data suggest that z-VAD.fmk blocks the processing of both caspase-3 and caspase-7 and may preclude the translocation of active caspase-7 to the mitochondria and the microsomes.

The data clearly demonstrate that active caspase-3 is located in the cytosol whereas active caspase-7 is associated with the mitochondrial and microsomal fractions during Fas-induced apoptosis *in vivo*. Further support for the hypothesis that different effector caspases are responsible for the enzymic activity in different subcellular compartments was provided by comparing the Western blot data with the DEVDase activity. DEVDase activity in cells undergoing apoptosis is believed to be due primarily to activation of caspase-3 and caspase-7 (Thornberry, *et al.* 1997; Nicholson, *et al.* 1995; Tewari, *et al.* 1995; Fernandes-Alnemri, *et al.* 1995). Although the total DEVDase activity loaded onto the polyacrylamide gel from the cytosolic fraction (20 pmol/min) (Fig. 7.5, lane 7) was greater than that from either the mitochondrial or microsomal fractions (9 and 15 pmol/min, respectively) (Fig. 7.5, lanes 4 and 10, respectively), the antibody to caspase-7 only detected the p19 large subunit in the mitochondrial and microsomal fractions (Fig. 7.5, lanes 4 and 10, respectively). This suggested that a caspase other than caspase-7 was primarily responsible for DEVDase activity in the cytosolic fraction. This was likely to be caspase-3, based on the data demonstrating that the p17 catalytically active large subunit of caspase-3 was primarily located in the cytosol (Fig. 7.4, lane 6). Thus, while a contribution from other caspases cannot be ruled out, the data strongly suggest that the major DEVDase activity in the microsomal and mitochondrial fractions is attributable to caspase-7 whilst in the cytosolic fraction it is due

primarily to caspase-3 (Fig. 7.3). Although a direct comparison between the amount of an enzyme and the degree of enzymic activity cannot be made, the extent of the DEVDase activity in the cytosol in the absence of active caspase-7 and in the presence of relatively low amounts of active caspase-3, could be consistent with activation of another DEVD-cleaving caspase. Taken together, the results suggest that following its activation, caspase-7 is translocated to the microsomal and mitochondrial fractions, while active caspase-3 remains in the cytosol. A recent study using an affinity label also noted differences in the pattern of active caspases in the nuclei and cytosol between two cell lines (Martins, *et al.* 1997b). Their results in conjunction with the data presented in this chapter raise the question about how different active caspases may be targeted to different subcellular localisations.

Presumably the localisation of caspases to distinct subcellular compartments would, at least in part, be expected to govern their specificities towards the cleavage of cellular substrates. Therefore the cleavage of the exclusively endoplasmic reticular-associated substrate SREBP-1 was studied. This protein has been shown to be cleaved, *in vitro*, by the hamster homologues of both caspase-3 and caspase-7 (Wang, *et al.* 1995; Pai, *et al.* 1996). The intact form of this substrate was indeed confined to the microsomal fraction of control mouse livers (Fig. 7.8, lane 2), and was cleaved following Fas induction of apoptosis (Fig. 7.8, lane 3). Its cleavage was largely prevented by incubation with z-VAD.fmk, consistent with a caspase being responsible (Fig. 7.8, lane 4). It was interesting to note that the cleavage of SREBP-1 in the microsomal fraction was not completely prevented by z-VAD.fmk, evidenced by the relative intensities of the bands representing the intact protein in the microsomal fractions prepared from the livers of control mice and mice treated with Fas antibody and z-VAD.fmk. This incomplete inhibition correlated with the partial inhibition of DEVDase activity (60%) observed in this fraction, and was in contrast with the almost complete inhibition achieved in the 'nuclear', mitochondrial and cytosolic fractions with z-VAD.fmk (Fig. 7.3).

Given that active caspase-7 was also associated with the microsomal fraction it was possible that this caspase was responsible for the cleavage of SREBP-1 *in vivo*. To test this hypothesis, the microsomal fraction from control mice was incubated in the presence of the recombinant caspases-3, -6 and -7. Interestingly, only recombinant caspase-6 was capable of cleaving SREBP-1 (Fig. 7.9, lanes 4 and

5), although the fragment was of a different size compared with that produced *in vivo*, and was likely to be due to a non-specific cleavage event. Thus the use of recombinant caspases *in vitro* was not able to support the cleavage of SREBP-1 by caspase-7 *in vivo*, although, given their colocalisation, caspase-7 remains a likely candidate. The SREBP-1 has been proposed to have a hairpin structure, with the N- and C-termini of the protein protruding into the cytosol, and leaving a 'loop' in the endoplasmic reticular lumen (Hua, *et al.* 1995). This loop appears to be in approximately the same location in the amino acid sequence as the caspase cleavage site within the protein (Wang, *et al.* 1995). Therefore it is tempting to speculate that the sequence is presented to caspase-7 in the intact cell, but that its orientation is disrupted in an *in vitro* system, precluding its cleavage by caspase-7. However, while the colocalisation of caspase-7 and SREBP-1 in the endoplasmic reticulum make it likely that caspase-7 contributes to the cleavage of this substrate *in vivo*, given the contiguous nature of the endoplasmic reticulum and the cytosol (and therefore active caspase-3), a contribution by caspase-3 to the cleavage of SREBP-1 *in vivo* cannot be ruled out. More definitive proof would be provided by an inhibitor which differentiated between caspase-3 and caspase-7. The tetrapeptide inhibitor Ac-DMQD.CHO, which mimics the caspase-3 cleavage site in PKC δ may be useful in answering these questions (Hirata, *et al.* 1998).

As well as caspase-7 and the apoptotic substrate SREBP-1, other molecules known to be involved in the apoptotic process have been shown to be associated with the endoplasmic reticulum. The 28 kDa protein, Bap31 is an integral protein of the endoplasmic reticulum and has been shown to interact with the anti-apoptotic proteins bcl2 and bcl-X_L (Ng, *et al.* 1997), an interaction which is prevented by the pro-apoptotic protein bax. In addition, Bap31 also associates with procaspase-8, contributed to by the interaction of a death effector homology domain which interacts with ced4, and presumably its mammalian homologue, Apaf-1 (Ng and Shore, 1998). In low bcl2 conditions *in vitro*, Bap31 is cleaved at two sites, AAVD↓G¹⁶⁵ and AAVD↓G²³⁹ by purified caspase-8 and caspase-1, but not by caspase-3 to release an N-terminal p20 fragment which is capable of inducing apoptosis when ectopically expressed in cells. It is tempting to speculate that this fragment somehow activates the endoplasmic reticular-associated caspase-7.

In addition to translocation to the microsomal fraction, the data presented here demonstrate, for the first time, that active caspase-7 is translocated to the mitochondrial fraction following Fas-induced apoptosis (Fig. 7.5, lane 4). This would support the localisation of a caspase-7 substrate in the mitochondria. Although no such substrates have been reported so far, mitochondrial DNA is known to sustain more extensive damage compared with nuclear DNA following oxidative stress (Yakes and Van Houten, 1997), and it is possible that mitochondria contain a form of PARP which could be cleaved during apoptosis. An alternative possibility would be bcl2, which is located on several intracellular membranes, including mitochondria, and has been shown recently to be cleaved by caspase-3 *in vitro* to alter its status from apoptosis-protective to apoptosis-promoting, and making it functionally similar to its apoptosis-inducing homologue bax (Cheng, *et al.* 1997). It is conceivable that *in vivo*, the translocation of active caspase-7 into mitochondria following Fas-induced apoptosis could result in the same conversion of Bcl2 from an apoptosis-inhibitory molecule to one which promotes apoptosis. Recently the movement of Bax from the cytosol to the mitochondria was observed in cells undergoing apoptosis and this movement preceded nuclear condensation and cell shrinkage (Wolter, *et al.* 1997). The relationship, if any, of the movement of Bax to that of caspase-7 remains to be determined.

Although it is not known precisely which caspase activates caspase-3 and caspase-7 during Fas-induced apoptosis *in vivo*, caspase-8, which has been considered the most upstream caspase in Fas-induced apoptosis has been considered the most likely candidate (Boldin, *et al.* 1996; Muzio, *et al.* 1996; Srinivasula, *et al.* 1996), and has been shown, *in vitro*, to cleave and activate all other known caspases (reviewed in Cohen, 1997). Some support for this was provided by the observations that z-VAD.fmk also blocked the activation of caspase-8 in livers from Fas-induced animals (Fig. 7.7A, compare lanes 5 and 6). However, crosslinkage of the Fas receptor, while resulting in the loss of the proform of caspase-8 in the cytosol (Fig. 7.7, lane 5) also resulted in the appearance of a ~14 kDa fragment, the formation of which was prevented with z-VAD.fmk. This fragment is smaller than that observed in the murine LTR6 cells or in human monocytic THP.1 cells (Fig. 5.5). Nevertheless, given that its formation is prevented with z-VAD.fmk, it is possible that it is either a further degradation product of the catalytically active large subunit

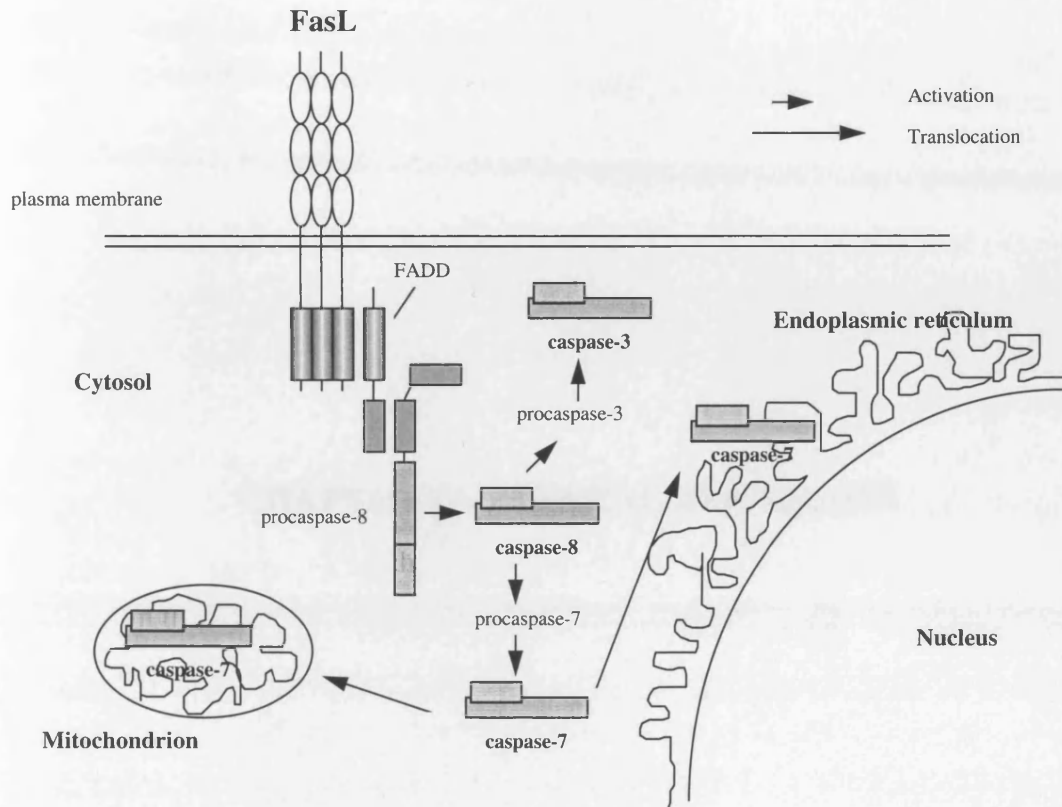
or that there are several variants of the active caspase in murine system as has been shown by 3D gel electrophoresis in other systems (Martins, *et al.* 1997b). The lack of a published sequence for murine caspase-8 again precludes a search for a cleavage motif which could account for the formation of the 14 kDa ‘subunit’.

The inhibition of processing of caspases-3, -7 and -8 by z-VAD.fmk following Fas-induced apoptosis in mouse liver does not distinguish between the possibilities that caspase-8 directly activates caspase-3 and/or caspase-7 or that there are one or more intermediate caspases. Recent studies have demonstrated that procaspase-9 binds to Apaf-1 (apoptotic protease activating factor 1) in a cytochrome c- and dATP-dependent manner (Zou, *et al.* 1997; Li, *et al.* 1997). This complex results in the activation of caspase-9, which in turn cleaves and activates caspase-3 (Li, *et al.* 1997). The mechanism of activation of procaspase-7 is not known and may be due to activation by caspase-8 (Srinivasula, *et al.* 1996) or to a mechanism involving Apaf-1 and procaspase-9 (Li, *et al.* 1997) but it does not appear to be due to a direct activation by caspase-3 (Hirata, *et al.* 1998). Although activation of caspase-8 is clearly a very early event following Fas-induced apoptosis, it is not yet clear how this is related to the activation of caspases following mitochondrial damage with the subsequent release of cytochrome c and the activation of procaspase-9. However, Z-VAD.fmk may exert its action by blocking the caspase cascade initiated by both caspase-8 and caspase-9.

7.4. SUMMARY

A pivotal role for caspases during Fas-induced apoptosis in mouse liver is undisputed. The data presented in this chapter demonstrate a differential subcellular localisation of members of the caspase family following Fas-induced apoptosis *in vivo*. While active caspase-3 was confined to the cytosol, active caspase-7 was translocated to the mitochondrial and the microsomal fractions. Thus these data represent the first example of the differential subcellular distribution of specific caspases in an *in vivo* model of apoptosis. In addition the data elude to a possible control mechanism for caspase activity. The colocalisation of caspases with their specific substrates, including caspase-7 and SREBP-1 in the microsomal fraction, may go some way to explain the existence of different mammalian homologues, some of which have indistinguishable substrate specificities.

The data described in this chapter are consistent with the apoptotic pathway presented in the scheme below;



Part of this chapter has been published in:

- Chandler, J.M., Cohen, G.M. and MacFarlane, M. (1998) Different subcellular distribution of caspase-3 and caspase-7 following Fas-induced apoptosis in mouse liver. *J. Biol. Chem.* **273**, 10815–10818. (Appendix 2)

CHAPTER 8 – GENERAL DISCUSSION

8. GENERAL DISCUSSION

Many studies in several systems have demonstrated the central, common role of caspases in the execution phase of apoptosis induced by a wide variety of stimuli. However, despite previous studies demonstrating processing and activation of caspase-3 following treatment with DNA-damaging agents (Datta, *et al.* 1996), this is the first demonstration of p53^{WT}-induced activation of the caspases.

Using a temperature-sensitive system (LTR6 cells), p53^{WT} was shown to induce morphological and biochemical changes characteristic of apoptosis, as previously described (Yonish-Rouach, *et al.* 1991; Fig. 4.1–4.3). Apoptosis induced in this manner was accompanied by the processing and activation of the effector caspases, caspase-3 and caspase-7 (Fig. 5.3A and B, respectively) and the proteolytic cleavage of their common substrate, PARP (Fig. 5.5A). In support of their activation, lysates prepared from LTR6 cells shifted for 22 h to the permissive temperature showed a massive induction of z-DEVD.afc cleavage activity (Fig. 5.6A). The processing of caspase-3 and caspase-7 was demonstrated directly using antibodies to their catalytically active large subunits. In contrast, indirect evidence of the activation of caspase-6 was gained by the observation that a 22 h shift to the permissive temperature resulted in cleavage of lamin B₁ (Fig. 5.5B), a substrate which has only been shown to be cleaved efficiently by caspase-6 (Takahashi, *et al.* 1996; Orth, *et al.* 1996). p53^{WT}-induced activation of caspase-6 was also supported by the increased Ac-VEID.amc cleavage activity in lysates prepared from temperature-shifted LTR6 cells.

In agreement with other studies, the cleavage of lamin B₁ was observed after that of PARP, suggesting that lamin cleavage is a relatively late event in the apoptotic pathway (Lazebnik, *et al.* 1995; Greidinger, *et al.* 1996), and supporting the sequential activation of caspases in p53^{WT}-induced apoptosis. Confirmation that all the observed effects in LTR6 cells were due to the change in p53 status from mutant to wild-type was supported by the absence of these changes in the control cell line containing a non-temperature sensitive p53 protein after 22 h at 32.5°C (Fig. 5.7).

The initiator caspase, caspase-8, is regarded as being at the apex of the hypothetical cascade which is the basis of the executionary mechanism of apoptosis, and has been shown to cleave all other caspases, including caspase-3 and caspase-7, *in vitro* (reviewed in Cohen, 1997). The processing of caspase-8 was also demonstrated here for the first time following p53^{WT} induction (Fig. 5.4, lane 4). However, although

it can be predicted that the activation of caspase-8 occurs prior to that of caspase-3, caspase-6 and caspase-7, the sequence of activation of these caspases following Fas-induced apoptosis was not directly addressed here. Despite this, the cleavage of the caspases following induction of p53^{WT} would be consistent with activation of the initiator caspase, caspase-8, and its subsequent processing and activation of the effector caspases-3, -6 and -7.

The initial identification and characterisation of caspase-8 provided the elusive, extracellular to intracellular link in receptor-mediated apoptosis (Muzio, *et al.* 1996; Boldin, *et al.* 1996). p53^{WT}-mediated activation of caspase-8 may be consistent with this scenario, as p53^{WT} has been shown to lead to the upregulation of two members of the TNFR death receptor family; Fas (Owen-Schaub, *et al.* 1995) and DR5/KILLER (Wu, *et al.* 1998; Sheikh, *et al.* 1998), and to subsequently induce apoptosis. Thus it is conceivable that after upregulation of receptors at the cell surface, p53^{WT} may result in recruitment and activation of caspase-8 and the subsequent activation of the effector caspases-3, -6 and -7 and proteolytic cleavage of particular proteins, including PARP and lamin B₁.

The data accrued from the *in vitro* studies in LTR6 cells were consistent with the activation of at least four caspase homologues following p53^{WT}-induced apoptosis, as has been shown during apoptosis in other systems (MacFarlane, *et al.* 1997a). Caspase-3 and caspase-7 activation were supported by increased z-DEVD.afc cleavage and the cleavage of PARP, caspase-8 activity was supported by the cleavage of z-IETD.amc activity and caspase-6 activation was supported by the cleavage of Ac-VEID.amc cleavage and the cleavage of lamin B₁. However, only the processing of caspase-3, caspase-7 and caspase-8 have been directly demonstrated.

Despite these data, which clearly support a role for caspases in p53^{WT}-induced apoptosis, results are also presented which suggest that p53^{WT}-induced apoptosis may not be mediated exclusively by caspases. Coincubation of the LTR6 cells with the tripeptide caspase inhibitor z-VAD.fmk, even at concentrations as high as 100 µM, while preventing processing of the caspases (Fig. 5.8), proteolysis of their substrates PARP and lamin B₁ (Fig. 5.9A and B, respectively) and cleavage of z-DEVD.afc (Figs. 5.10–5.11), failed to completely inhibit apoptosis assessed by flow cytometry (Fig. 5.2A). These observations suggest that p53^{WT}-induced apoptosis is either partially

mediated by caspases which are insensitive to z-VAD.fmk, or that apoptosis induced by p53^{WT} proceeds, at least to some degree, via a caspase-independent mechanism.

The existing literature supports the existence of more than one p53^{WT}-induced pathway to apoptosis. Previous studies have shown that other classes of inhibitor, such as cathepsin inhibitors, have a more profound apoptotic-inhibitory effect compared with caspase inhibitors such as z-VAD.fmk (Lotem and Sachs, 1996). In addition, previous studies on p53^{WT}-induced apoptosis in temperature-sensitive M1 cells have demonstrated that, whereas p53^{WT}-induced apoptosis can proceed in the absence of synthesis of new proteins, compounds such as cycloheximide do at least partially block p53^{WT}-induced apoptosis (Yonish-Rouach, *et al.* 1991). Indeed, p53^{WT}-induced apoptosis has been shown to have specific components which involve synthesis of new proteins, such as the upregulation of bax (Miyashita, *et al.* 1994) and some which can proceed in the presence of protein synthesis inhibitors, including the upregulation of the Fas receptor at the cell membrane (Owen-Schaub, *et al.* 1995). These observations further support a role for parallel pathways to apoptosis following p53^{WT} induction.

In contrast to p53^{WT}-induced apoptosis, Fas-induced apoptosis in mouse liver *in vivo* was completely blocked by the caspase inhibitor z-VAD.fmk which entirely abrogated the production of the apoptotic morphology (Fig. 7.1), prevented caspase processing (Fig. 7.4–7.5 and 7.7), and inhibited the cleavage of z-DEVD.afc (Fig. 7.2–7.3), as well as preventing death of the animals. These data would be consistent with the exclusive mediation of the Fas-induced apoptotic pathway by caspases. However, longer studies using the Fas antibody in conjunction with z-VAD.fmk would have to be performed to determine whether Fas-induced apoptosis involves a caspase-independent or z-VAD.fmk insensitive pathway which manifests itself at a later timepoint.

Despite the diverse nature of the two stimuli, both p53^{WT} and the agonistic Fas antibody induce a common apoptotic phenotype, characterised morphologically by the condensation of nuclear chromatin, and biochemically by the processing and activation of caspases and the induction of z-DEVD.afc cleavage. Thus, p53^{WT} and Fas apparently support previous observations whereby diverse stimuli feed into a common executionary mechanism involving the sequential activation of different caspases (reviewed in Martin and Green, 1995).

The common apoptotic morphology is contributed to, at least in part, by the proteolysis of certain cellular proteins, the majority of which are nuclear in nature. The primary location of the caspases responsible for the cleavage of these proteins during apoptosis is the cytosol (Ayala, *et al.* 1994; Nicholson, *et al.* 1995), which consequently poses accessibility problems.

Following Fas-induced apoptosis in mouse liver *in vivo*, a differential subcellular distribution of the two active effector caspases, caspase-3 and caspase-7, was observed. In control mice, procaspase-3 was located exclusively in the cytosol, and following Fas-induced apoptosis, active caspase-3 remained confined to the cytosol (Fig. 7.4, lane 6), in support of previous findings (Nicholson, *et al.* 1995). However, these results differ from recent results of others who, in addition to its localisation in the cytosol, have recently demonstrated the colocalisation of some procaspase-3 with mitochondrial markers in mitochondria isolated from human liver and several human cell lines (Mancini, *et al.* 1998). However, in HeLa cells, the mitochondrial procaspase-3 represented only ~10% of the procaspase-3 observed in the cytosol. In cells displaying apoptotic morphology induced by staurosporine, ceramide and UVB irradiation, the overall staining for procaspase-3 was diminished and colocalisation of this caspase with the mitochondria was no longer observed. In these studies, however, the inability of the antibody to recognise the active subunit precluded investigation into the destination of active caspase-3 during apoptosis, although induction of a caspase-3-like proteolytic activity was detected in the cytosol (Mancini, *et al.* 1998).

Others have also demonstrated the localisation of procaspase-3 in both the cytosol and the mitochondria recently, and have shown that the relative procaspase-3 content of the mitochondria and cytosol pools is tissue-dependent (Samali, *et al.* 1998). Interestingly, a larger proportion of the cellular procaspase-3 is associated with the mitochondria in tissues such as the thymus where spontaneous apoptosis plays an important role.

In contrast to the localisation of active caspase-3 following Fas-induced apoptosis, active caspase-7 was translocated from the cytosol to both the endoplasmic reticulum and the mitochondria (Fig. 7.5, lanes 4 and 10, respectively). Examination of the mitochondrial marker (cytochrome *c* oxidase subunit IV), the cytosolic marker (Glutathione *S* transferase π) and the endoplasmic reticulum marker (SREBP-1),

confirmed that the observed levels of protein following translocation could not merely be explained by cross-contamination of the subcellular fractions (Figs. 7.6 and 7.8). The slight indication of the catalytically active large subunit of caspase-7 in the cytosol was consistent with activation of the caspase prior to translocation, although this was not directly demonstrated.

Most proteins reported to be cleaved during apoptosis have been localised to the nucleus. However, SREBPs are found exclusively in the endoplasmic reticulum (Wang, *et al.* 1993; Fig. 7.8). The colocalisation of caspase-7 and the substrate SREBP-1 to the endoplasmic reticulum is consistent with the cleavage of SREBP-1 by caspase-7 *in vivo*, and is in agreement with previous *in vitro* studies which demonstrated the cleavage of SREBP-1 by the hamster homologues of both caspase-3 and caspase-7 (Wang, *et al.* 1996; Pai, *et al.* 1996). However, *in vitro* studies using recombinant caspases failed to demonstrate recombinant caspase-7-mediated cleavage of SREBP-1 protein from the microsomal fraction prepared from control mice (Fig. 7.10). This, however, could be due to the disruption of a critical *in vivo* environment during the fractionation procedure.

Although the demonstrated colocalisation of active caspase-7 with SREBP-1 would make caspase-7 cleavage of this protein feasible, the contiguous nature of the endoplasmic reticulum and the cytosol, and therefore with active caspase-3, means that a contribution by caspase-3 to the cleavage of SREBP-1 cannot be ruled out. However, despite these reservations, the possibility that caspase-7 is responsible for SREBP-1 cleavage *in vivo* offers a level of control of apoptosis whereby the cleavage of a substrate by a particular caspase is governed by their colocalisation to a specific subcellular compartment. This in turn may go some way to rationalise the existence of so many caspase homologues, in particular those which, through combinatorial studies, have been shown to exhibit virtually indistinguishable substrate specificities (Thornberry, *et al.* 1997), and are capable of cleaving the same substrates *in vitro*.

Following the reasoning above, the mitochondrial localisation of caspase-7 would be consistent with the existence of a mitochondrial substrate. Although no substrates have been colocalised to the mitochondria to date, the existence of a mitochondrial molecule homologous to PARP is not inconceivable given that this organelle has its own genome and that its DNA suffers more damage than the nuclear genetic material due to oxidative stress (Yakes and Van Houten, 1997). Recently, the

cleavage of bcl2, an apoptosis-inhibitory protein localised to the contact points of the inner and outer mitochondrial membranes, as well as other internal membranes, by caspase-3 has been shown *in vitro* (Cheng, *et al.* 1997). The result of this cleavage event is to convert bcl2 to an apoptosis-promoting molecule, comparable to its homologue bax. Again, given the virtually identical substrate specificities of caspase-3 and caspase-7 *in vitro*, it is possible that *in vivo*, caspase-7 is capable of the proteolytic cleavage of bcl2 in the mitochondria, and a consequent alteration in its apoptotic status.

In addition to the translocation of caspase-7 from the cytosol to the mitochondria and microsomal fractions reported here, other caspases have been localised to the nuclei recently, the location of many of the proteins known to be cleaved during apoptosis. Translocation of procaspase-1 to the nucleus during TNF-induced apoptosis in HeLa cells (Mao, *et al.* 1998) as well as nuclear translocation of GFP-tagged procaspase-2 in NIH-3T3 cells (Colussi, *et al.* 1998) has been demonstrated. In both cases translocation of procaspase-1 and procaspase-2 is apparently dependent on a nuclear localisation sequence within the prodomain. In the case of procaspase-1, translocation occurs prior to its activation within the nucleus (Mao, *et al.* 1998). The observed translocation-mediation properties of the long prodomains of class I caspases is not a feature of all subfamily members. Fusion of the prodomain of caspase-9 to GFP does not result in translocation of the protein to the nucleus. However, fusion of the prodomain of caspase-2 to caspase-3 did result in nuclear translocation (Colussi, *et al.* 1998). Thus in addition to a role in recruitment to the DISC, the prodomain of some class I caspases apparently has a role to play in nuclear translocation and presumably the subsequent cleavage of nuclear proteins.

In the present studies, active caspases were not directly demonstrated in the nuclei. However, the existence of an enzyme capable of cleaving PARP was demonstrated in nuclei isolated from temperature-shifted LTR6 cells, but not from their non-temperature sensitive counterparts (Fig. 6.5). In agreement with this, others have demonstrated the nuclear localisation of multiple active caspases in HL60 cells (Martins, *et al.* 1997b). Z-DEVD.afc and Ac-VEID.amc cleavage activities were both detected in the nuclei of apoptotic HL60 cells, consistent with the activation of caspase-3 and/or caspase-7 and caspase-6, respectively. In addition the substrate *N*-(*N*^α-benzyloxycarbonyl-glutamyl-*N*^ε-biotinyllysyl)-aspartic acid [(2,6-dimethylbenzoyl)

oxy] methylketone, which binds to the active site of caspases, detected two different caspase homologues, which although not conclusively identified comigrated with the cloned human caspases, caspase-3 and caspase-6. In contrast to the above, a caspase comigrating with cloned caspase-1 was not detected in nuclei from apoptotic HL60 cells. Thus, although there is evidence to support the existence of active caspases in the nucleus, and some suggestions as to their identities, the specific identity of the caspase(s) responsible for the cleavage of the plethora of nuclear proteins during apoptosis remains unknown. Of course it is still possible that substrates such as nuclear lamins can be accessed sufficiently from outside the nucleus to facilitate their cleavage and make translocation unnecessary. An interesting possibility is that caspase-7 having been localised in the endoplasmic reticulum, may proceed further and gain access to the nucleus via a nuclear pore. This, however, is purely speculative.

The data pointing to the translocation of caspases were supported in the *in vitro* model of p53^{WT}-induced apoptosis. Although procaspase-3 and procaspase-7 as well as their catalytically active large subunits were both detected in the cytosol, their relative levels in the different fractions from control and temperature-shifted cells were consistent with translocation of both caspases from the cytosol to another compartment in the P20 pellet fraction following p53^{WT} induction. In addition, z-DEVD.afc cleavage activity was detected in the P20 pellet fraction as well as in the cytosol (Figs. 6.2–6.3). However, in contrast to the *in vivo* data, active caspase-7 was clearly detectable in the cytosol (Fig. 6.3B, lane 9) and active caspase-3 was detectable in the P20 pellet fraction (Fig. 6.3A, lane 6). Thus, the different subcellular localisation could depend on the precise nature of the apoptotic stimulus, as well as on the cell line or system under study.

Recently, work into Fas-induced apoptosis in two cell lines has identified two Fas-induced pathways to apoptosis; one dependent on the involvement of mitochondria and one independent of their involvement (Scaffidi, *et al.* 1998). Thus two pathways could exist which would govern translocation of caspases, especially as p53^{WT} has been shown to be associated with a receptor component via its upregulation of the DR5/KILLER receptor and the subsequent induction of apoptosis (Wu, *et al.* 1998). Equally the detection of active caspase-7 in the cytosol and not confined to the P20 pellet in the LTR6 cells could be due to some rupturing of the endoplasmic reticular and

mitochondrial membranes during the harsh method of freeze thawing used in these cells.

The presence of active caspase-3 in the pellet is more difficult to correlate with the *in vivo* data, but could perhaps represent translocation to the nucleus. In nuclei isolated from LTR6 cells shifted for 22 h to the permissive temperature, cleavage of PARP was readily demonstrated although no caspase-3 or caspase-7 processing was detected. Therefore, although the data indirectly suggest either caspase-3 and/or caspase-7 activity within the nuclei, this was not directly demonstrated in nuclei from temperature-shifted LTR6 cell nuclei and could not be addressed in Fas-induced apoptosis in liver as no attempt was made to isolate and purify the nuclei.

8.2. SUMMARY

p53^{WT}-induced activation of caspases was demonstrated here for the first time. p53^{WT}-induced apoptosis was accompanied by the processing and activation of caspase-3 and caspase-7, together with the cleavage of their mutual substrate, PARP, and the cleavage of the fluorogenic substrate z-DEVD.afc. p53^{WT}-induced activation of caspase-8 was also demonstrated directly, and supported by the cleavage of z-IETD.amc. Indirect evidence for the activation of a fourth caspase, caspase-6, was gained through the cleavage of lamin B₁ and supported by cleavage of the fluorogenic substrate Ac-VEID.amc. The complete inhibition of these parameters, in the absence of total abrogation of apoptosis assessed by flow cytometry, was consistent with additional pathways, either insensitive to z-VAD.fmk, or independent of caspase activation being operational in p53^{WT}-induced apoptosis.

Fas-induced apoptosis in mouse liver *in vivo* was similarly associated with the processing and activation of caspase-3 and caspase-7, together with the cleavage of z-DEVD.afc. Apoptotic morphology, caspase processing and activation and z-DEVD.afc cleavage, were all prevented by z-VAD.fmk. The reason for the existence of so many caspase homologues may have been partly elucidated by the observation that active caspase-3 and caspase-7 are located in different subcellular compartments following Fas-induced apoptosis. Active caspase-3 is located primarily in the cytosol, whereas active caspase-7 is translocated to the endoplasmic reticulum and mitochondria. The colocalisation of caspase-7 and SREBP-1 in the endoplasmic reticulum is consistent

with the cleavage of SREBP-1 by caspase-7 *in vivo*, and may go some way to explain the existence of two caspases with almost identical substrate specificities.

8.3. FUTURE DIRECTIONS

Future studies should be focused on more rigorously defining the apoptotic process *in vivo*. *In vitro* studies, while useful, provide no definitive answers as to which caspase is responsible for the cleavage of which substrate and the production of which aspect of apoptotic morphology. The *in vivo* results presented suggest that SREBP-1 could be cleaved by caspase-7, and that caspase-3 may cleave those substrates which are cytosolic. The colocalisation of caspase-7 with SREBP-1 would make it a more likely candidate for the *in vivo* cleavage of this substrate, although this issue could be further addressed by assessing whether caspase-7 and/or caspase-3 are capable of cleaving SREBP-1 translated *in vitro* rather than SREBP-1 derived from the microsomal fraction.

Most intriguing is the possibility of following the translocation of active caspases within the cells prior to, and during, apoptosis. The laboratory currently has access to green fluorescent protein (GFP)-tagged caspases which when used in conjunction with confocal microscopy will allow the further monitoring and dissection of the apoptotic pathway.

Questions still remain regarding the aspects of the p53^{WT}-induced pathway which are apparently not mediated by caspases or are mediated by caspases which are insensitive to z-VAD.fmk. One possible caspase-independent pathway may exist involving mitochondria. The disruption of mitochondria and the subsequent release of cytochrome c, while being capable of activating caspases, may also result in the demise of the cell in a caspase-independent manner as cell survival in the absence of an energy source is not possible. This type of cell death is unlikely to appear classically apoptotic, due to the absence of caspase activity to bring about cleavage of nuclear lamins and other structural proteins. However, caspase-independent cell death has been reported (McCarthy, *et al.* 1997; Déas, *et al.* 1998).

Fas administration lead to the processing of caspase-8, the caspase thought to be at the apex of the cascade. Caspase-3 and caspase-7 were also processed and activated presumably by caspase-8. Caspase-8 has been shown recently to cleave bid, a proapoptotic member of the bcl2 family (Li, *et al.* 1998) and to result in the translocation

of its C-terminus to the mitochondria (Luo, *et al.* 1998). This translocation event is prevented by both bcl2 and bcl_{xL}, and is followed by interaction of Apaf-1 with caspase-9. Thus, these studies provide a link between receptor ligation, mitochondrial damage and caspase activation.

p53^{WT} also resulted in the processing and activation of caspase-8. Thus, it would be interesting to investigate whether p53^{WT} similarly results in the cleavage of bid, and the subsequent events leading to apoptosis.

CHAPTER 9 – REFERENCES

9. REFERENCES

- Addison, C., Jenkins, J.R. and Stürzbecher, H.W. (1990) The p53 localisation signal is structurally linked to a p34(cdc2) kinase motif. *Oncogene* **5**, 423–426.
- Ahmad, M., Srinivasula, S.M., Wang, L., Talanian, R.V., Litwack, G., Fernandes-Alnemri, T. and Alnemri, E.S. (1997) CRADD, a novel human apoptotic adaptor molecule for caspase-2, and FasL/Tumor Necrosis Factor Receptor-interacting protein RIP. *Cancer Res.* **57**, 615–619.
- Alnemri, E.S., Livingston, D.J., Nicholson, D.W., Salvesen, G., Thornberry, N.A., Wong, W.W. and Yuan, J. (1996) Human ICE/CED3 nomenclature. *Cell* **87**, 171.
- Ameisen, J.C., Estaquier, J., Idziorek, T. and De Beis, F. (1995) The relevance of apoptosis to AIDS pathogenesis. *Trends in Cell Biol.* **5**, 27–31.
- An, S. and Knox, K.A. (1996) Ligation of CD40 rescues Ramos-Burkitt lymphoma B cells from calcium ionophore- and antigen receptor-triggered apoptosis by inhibiting activation of the cysteine protease CPP32/Yama and cleavage of its substrate PARP. *FEBS Lett.* **386**, 115–122.
- Anand, R. and Southern, E.M. (1990) Pulsed Field Gel Electrophoresis. In: Gel Electrophoresis of Nucleic Acids: A Practical Approach 2nd Ed. Edited by D. Rickwood and B.D. Hames. IRL Press, Oxford. pp. 101–123.
- Arends, M.J., Morris, R.G. and Wyllie, A.H. (1990) Apoptosis: the role of the endonuclease. *Am. J. Pathol.* **136**, 593–608.
- Arends, M.J., and Wyllie, A.H. (1991) Apoptosis: mechanisms and roles in pathology. *Int. Rev. Exp. Path.* **32**, 223–254.
- Armstrong, R.C., Aja, T., Xiang, J., Gaur, S., Krebs, J.F., Hoang, K., *et al.* (1996) Fas-induced activation of the cell death-related protease CPP32 is inhibited by bcl-2 and by ICE family protease inhibitors. *J. Biol. Chem.* **271**, 16850–16855.
- Ayala, J.M., Yamin, T.-T., Egger, L.A., Chin, J., Kostura, M.J., and Miller, D.K. (1994) Interleukin -1beta converting enzyme is present in monocytic cells as an inactive 45 kDa precursor. *J. Immunol.* **153**, 2592–2599.
- Barde, Y.A. (1989) Trophic factors and neuronal survival. *Neuron* **2**, 1525–1534.
- Bertrand, R., Solary, E., O'Connor, P., Kohn, K.W. and Pommier, Y. (1994) Induction of a common

- pathway of apoptosis by staurosporine. *Exp. Cell Res.* **211**, 314–321.
- Bicknell, G.R., Snowden, R.T. and Cohen, G.M. (1994) Formation of high molecular mass DNA fragments is a marker of apoptosis in the human leukaemic cell line, U937. *J. Cell Sci.* **107**, 2483–2489.
- Bischoff, J.R., Friedman, P.N., Marshck, D.R., Prives, C. and Beach, D. (1990) Human p53 is phosphorylated by p60-cdc2 and cyclin B-cdc2. *Proc. Natl. Acad. Sci. USA* **87**, 4766–4770.
- Black, R.A., Kronheim, S.R. and Sleath, P.R. (1989) Activation of interleukin-1 β by a co-induced protease. *FEBS Lett.* **247**, 386–390.
- Boise, L.H., González-García, M., Postema, C.E., Ding, L., Lindsten, T., Turka, L.A., *et al.* (1993) Bcl-x, a bcl-2-related gene that functions as a dominant regulator of apoptotic cell death. *Cell* **74**, 597–608.
- Boldin, M.P., Goncharov, T.M., Goltsev, Y.V. and Wallach, D. (1996) Involvement of MACH, a novel MORT1/FADD-interacting protease, in Fas/APO-1- and TNF receptor-induced cell death. *Cell* **85**, 803–815.
- Bottger, A., Bottger, V., Garcia-Echeverria, C., Cheng, P., Hochkeppel, H.-K., Sampson, W., *et al.* (1997) Molecular characterisation of the mdm2-p53 interaction. *J. Mol. Biol.* **269**, 744–756.
- Boulakia, C.A., Chen, G., Ng, F.W.H., Teodoro, J.G., Branton, P.E., Nicholson, D.W., *et al.* (1996) Bcl2 and adenovirus E1B 19 kDa protein prevent E1A-induced processing of CPP32 and cleavage of poly(ADP ribose)polymerase. *Oncogene* **12**, 529–535.
- Boyd, J.M., Gallo, G.J., Elangoran, B., Houghton, A.B., Malstrom, S., Avery, B.J., *et al.* (1995) Bik, a novel death-inducing protein shares a distinct sequence motif with Bcl-2 family proteins and interacts with viral and cellular survival-promoting proteins. *Oncogene* **11**, 1921–1928.
- Bracey, T.S., Miller, J.C., Preece, A. and Paraskeva, C. (1995) Gamma-radiation-induced apoptosis in human colorectal adenoma and carcinoma cell lines can occur in the absence of wild-type p53. *Oncogene* **10**, 2391–2396.
- Briggs, M.R., Yokoyama, C., Wang, X., Brown, M.S. and Goldstein, J.L. (1993) Nuclear protein that binds sterol regulatory element of low density lipoprotein receptor promoter I. Identification of the protein and delimitation of its target nucleotide sequence. *J. Biol. Chem.* **268**, 14490–14496.
- Brown, D.G., Sun, X.-M. and Cohen, G.M. (1993) Dexamethasone-induced apoptosis involves cleavage of DNA to large fragments prior to internucleosomal fragmentation. *J. Biol. Chem.* **268**, 3037–3039.

- Browne, S.J., Williams, A.C., Hague, A., Butt, A.J. and Paraskeva, C. (1994) Loss of APC protein expressed by human colonic epithelial cells and the appearance of a specific low-molecular weight form is associated with apoptosis *in vitro*. *Int. J. Cancer* **59**, 56–64.
- Browne, S.J., MacFarlane, M., Cohen, G.M. and Paraskeva, C. (1998) The adenomatous polyposis coli protein and retinoblastoma protein are cleaved early in apoptosis and are potential substrates for caspases. *Cell Death Diff.* **5**, 206–213.
- Bruno, S., Ardelt, B., Skierski, J.S., Traganos, F. and Darzynkiewicz, Z. (1992) Different effects of staurosporine, an inhibitor of protein kinases, on the cell cycle and chromatin structure of normal and leukaemic lymphocytes. *Cancer Res.* **52**, 470–473.
- Buttke, T.M. and Sandstrom, P.A. (1994) Oxidative stress as a mediator of apoptosis. *Immunol. Today* **15**, 7–10.
- Caelles, C., Helmberg, A. and Karin, M. (1994) p53-dependent apoptosis in the absence of transcriptional activation of p53-target genes. *Nature (Lond.)* **370**, 220–223.
- Cain, K., Inayat-Hussain, S.H., Kokileva, L. and Cohen, G.M. (1994) DNA cleavage in rat liver nuclei activated by Mg^{2+} or $Ca^{2+} + Mg^{2+}$ is inhibited by a variety of structurally unrelated inhibitors. *Biochem. Cell Biol.* **72**, 631–638.
- Casciola-Rosen, L.A., Miller, D.K., Anhalt, G.J. and Rosen, A. (1994) Specific cleavage of the 70-kDa protein component of the U1 small nuclear ribonucleoprotein is a characteristic biochemical feature of apoptotic cell death. *J. Biol. Chem.* **269**, 30757–30760.
- Casciola-Rosen, L.A., Anhalt, G.J. and Rosen, A. (1995) DNA-dependent protein kinase is one of a subset of autoantigens specifically cleaved early during apoptosis. *J. Exp. Med.* **182**, 1625–1634.
- Chandler, J.M., Alnemri, E.S., Cohen, G.M., and MacFarlane, M. (1997) Activation of CPP32 and Mch3 α in wild-type p53 induced apoptosis. *Biochem. J.* **322**, 19–23.
- Chandler, J.M., Cohen, G.M. and MacFarlane, M. (1998) Different subcellular distribution of caspase-3 and caspase-7 following Fas-induced apoptosis in mouse liver. *J. Biol. Chem.* **273**, 10815–10818.
- Cheng, E. H.-Y., Kirsch, D.G., Clem, R.J., Ravi, R., Kastan, M.B., Bedi, A., *et al.* (1997) Conversion of Bcl-2 to a Bax-like Death Effector by Caspases. *Science* **278**, 1966–1968.

Chinnaiyan, A.M., Tepper, C.G., Seldin, M.F., O'Rourke, K., Kischkel, F.C., Hellbardt, S., *et al.* (1996a) FADD/MORT1 is a common mediator of CD95(Fas/APO-1) and tumour necrosis factor receptor-induced apoptosis. *J. Biol. Chem.* **271**, 4961–4965.

Chinnaiyan, A.M., Orth, K., O'Rourke, K., Duan, H., Poirier, G.G., and Dixit, V.M. (1996) Molecular ordering of the cell death pathway. Bcl2 and BclX_L function upstream of the Ced-3-like proteases. *J. Biol. Chem.* **271**, 4573–4576.

Chiou, S.-K., Rao, L. and White, E. (1994) Bcl-2 blocks p53-dependent apoptosis. *Mol. Cell. Biol.* **14**, 2556–2563.

Chow, S.C., Weis, M., Kass, G.E.N., Holmström, T.H., Eriksson, J.E. and Orrenius, S. (1995) Involvement of multiple proteases during Fas-mediated apoptosis in T lymphocytes. *FEBS Letts.* **364**, 134–138.

Chowdary, D.R., Dermody, J.J., Jha, K.K. and Ozer, H.L. (1994) Accumulation of p53 in mutant cell lines defective in the ubiquitin pathway. *Mol. Cell. Biol.* **14**, 1997–2003.

Clarke, P. and Clarke, S. (1996) Nineteenth century research on naturally occurring cell death and related phenomena. *Anatomy & Embryology* **193**, 81–89.

Clarke, A.R., Purdie, C.A., Harrison, D.J., Morris, R.G., Bird, C.C., Hooper, M.L. and Wyllie, A.H. (1993) Thymocyte apoptosis induced by p53-dependent and independent pathways. *Nature (Lond.)* **362**, 849–852.

Clawson, G.A., Norbeck, L.L., Hatem, C.L., Rhodes, C., Amiri, P., McKerrow, J.H., *et al.* (1992) Ca²⁺-regulated serine protease associated with the nuclear scaffold. *Cell Growth Differ.* **3**, 827–838.

Cohen, G.M. (1997) Caspases: the executioners of apoptosis. *Biochem. J.* **326**, 1–16.

Colussi, P.A., Harvey, N.L. and Kumar, S. (1998) Prodomain-dependent nuclear localization of the caspase-2 (Nedd2) precursor. *J Biol. Chem.* **273**, 24535–24542.

Cotter, T.G., Glynn, J.M., Echeverri, F. and Green, D.R. (1992) The induction of apoptosis by chemotherapeutic agents occurs in all phases of the cell cycle. *Anticancer Res.* **12**, 773–779.

Coucouvanis, E. and Martin, G.R. (1995) Signals for death and survival: a two-step mechanism for cavitation in the vertebrate embryo. *Cell* **83**, 279–287.

Crook, T. and Vousden, K.H. (1992) Properties of p53 mutations detected in primary and secondary cervical cancers suggests mechanisms of metastasis and involvement of environmental carcinogenesis. *EMBO J.* **11**, 3935–3940.

Darzynkiewicz, Z., Bruno, S., Del Bino, G., Gorczyca, W., Hotz, M.A., Lassota, P. and Traganos, F. (1992) Features of apoptotic cells measured by flow cytometry. *Cytometry* **13**, 795–808.

Datta, R., Banach, D., Kojima, H., Talanian, R.V., Alnemri, E.S., Wong, W.W. and Kufe, D.W. (1996) Activation of the CPP32 protease in apoptosis induced by 1- β -D-arabinofuranosylcytosine and other DNA-damaging agents. *Blood* **88**, 1936–1943.

Déas, O., Dumont, C., MacFarlane, M., Hebib, C., Rouleau, M., Harper, F., *et al.* (1998) Caspase-independent apoptosis induced by anti-CD2 or staurosporine in activated human peripheral T lymphocytes. *Accepted J. Immunol.*

Donehower, L.A., Harvey, M., Slagle, B.L., McArthur, M.J., Montgomery, Jr., C.A., Butel, J.S. and Bradley, A. (1992) Mice deficient for p53 are developmentally normal but susceptible to spontaneous tumours. *Nature (Lond.)* **356**, 215–221.

Donehower, L.A. (1994) Tumor suppressor gene p53 and apoptosis. *Cancer Bull.* **46**, 161–166.

Duan, H., Chinnaiyan, A.M., Hudson, P.L., Wing, J.P., He, W.-W. and Dixit, V.M. (1996a) ICE-LAP3, a novel mammalian homologue of the *Caenorhabditis elegans* cell death protein ced-3 is activated during Fas- and tumour necrosis factor-induced apoptosis. *J. Biol. Chem.* **271**, 1621–1625.

Duan, H., Orth, K., Chinnaiyan, A.M., Poirier, G.G., Froelich, C.J., He, W.-W. and Dixit, V.M. (1996b) ICE-LAP6, a novel member of the ICE/Ced3 gene family, is activated by the cytotoxic T cell protease Granzyme B. *J. Biol. Chem.* **271**, 16720–16724.

Duan, H. and Dixit, V.M. (1997) RAIDD is a new ‘death’ adaptor molecule. *Nature (Lond.)* **385**, 86–89.

Duke, R.C. and Cohen, J.J. (1986) IL-2 addiction: withdrawal of growth factor activates a suicide program in dependent T cells. *Lymphokine Res.* **5**, 289–299.

Duvall, E., Wyllie, A.H. and Morris, R.G. (1985) Macrophage recognition of cells undergoing programmed cell death. *Immunology* **56**, 351–358.

Earnshaw, W.C. (1995) Apoptosis: lessons from *in vitro* systems. *Tr. Cell Biol.* **5**, 217–220.

- El-Deiry, W.S., Tokino, T., Velculescu, V.E., Levy, D.B., Parsons, R., Trent, J.M. *et al.* (1993) Waf1, a potential mediator of p53 tumour suppression. *Cell* **75**, 817–825.
- Ellis, H.M. and Horvitz, H.R. (1986) Genetic control of programmed cell death in the nematode *C. elegans*. *Cell* **44**, 817–829.
- Ellis, R.E., Yuan, Y.Y. and Horvitz, H.R. (1991) Mechanisms and functions of cell death. *Annu. Rev. Cell Biol.* **7**, 663–698.
- Emoto, Y., Manome, Y., Meinhardt, G., Kisaki, H., Kharbanda, S., Robertson, M., Ghayur, T., Wong, W.W., Kamen, R., Weichselbaum, R. and Kufe D. (1995) Proteolytic activation of protein kinase C delta by an ICE-like protease in apoptotic cells. *EMBO J.* **24**, 6148–6156.
- Enari, M., Sakahira, H., Yokoyama, H., Okawa, K., Iwamatsu, A. and Nagata, S. (1998) A caspase-activated DNase that degrades DNA during apoptosis, and its inhibitor ICAD. *Nature (Lond.)* **391**, 43–50.
- Enari, M., Hug, H., and Nagata S. (1995) Involvement of ICE-like proteases in Fas-mediated apoptosis. *Nature* **375**, 78–81.
- Enari, M., Talanian, R.V., Wong, W.W., and Nagata, S. (1996) Sequential activation of ICE-like and CPP32-like proteases during Fas-mediated apoptosis *Nature* **380**, 723–726.
- Faucheu, C., Diu, A., Chan, A.W.E., Blanchet, A.M., Miossec, C., Herve, F., *et al.* (1995) A novel human protease similar to Interleukin-1beta converting enzyme induces apoptosis in infected cells. *EMBO J.* **14**, 1914–1922.
- Fearnhead, H.O., Dinsdale, D. and Cohen, G.M. (1995a) An interleukin-1 β -converting enzyme-like protease is a common mediator of apoptosis in thymocytes. *FEBS Letts.* **375**, 283–288.
- Fearnhead, H.O., Rivett, A.J., Dinsdale, D. and Cohen, G.M. (1995b) A pre-existing protease is a common effector of thymocyte apoptosis mediated by diverse stimuli. *FEBS Letts.* **357**, 242–246.
- Fearnhead, H.O., MacFarlane, M., Dinsdale, D. and Cohen, G.M. (1995c) DNA degradation and proteolysis in thymocyte apoptosis. *Tox.Letts.* **82/83**, 135–141.
- Fernandes-Alnemri, T., Litwack, G. and Alnemri, E.S. (1994) CPP32, a novel human apoptotic protein with homology to *Caenorhabditis elegans* cell death protein ced-3 and mammalian interleukin-1 β -converting enzyme. *J. Biol. Chem.* **269**, 30761–30764.

Fernandes-Alnemri, T., Litwack, G. and Alnemri, E.S. (1995a) *Mch2*, a new member of the apoptotic *ced-3/Ice* cysteine protease gene family *Cancer Res.* **55**, 2737–2742.

Fernandes-Alnemri, T., Takahashi, A., Armstrong, R., Krebs, J., Fritz, L., Tomaselli, K.J., *et al.* (1995b) *Mch3*, a novel human apoptotic cysteine protease highly related to CPP32 *Cancer Res.* **55**, 6045–6052.

Fernandes-Alnemri, T., Armstrong, R.C., Krebs, J., Srinivasula, S.M., Wang, L., Bullrich, F., *et al.* (1996) *In vitro* activation of CPP32 and *Mch3* by *Mch4*, a novel human apoptotic cysteine protease containing two FADD-like domains. *Proc. Natl. Acad. Sci. USA* **93**, 7464–7469.

Fraser, A. and Evan G. (1996) A license to kill. *Cell* **85**, 781–784.

French, L.E., Hahne, M., Viard, I., Radlgruber, G., Zanone, R., Becker, K., *et al.* (1996) Fas and Fas ligand in embryos and adult mice: ligand expression in several immune-privileged tissues and coexpression in adult tissues characterized by apoptotic cell turnover. *J. Cell Biol.* **133**, 335–343.

Friend, C., Scher, W., Holland, J.G. and Sato, T. (1971) Haemoglobin synthesis in murine virus-induced leukaemic cells in vitro: stimulation of erythroid differentiation by dimethyl sulphoxide. *Proc. Natl. Acad. Sci. USA* **68**, 378–382.

Fuchs, E.J., McKenna, K.A. and Bedi, A. (1997) p53-dependent DNA damage-induced apoptosis requires Fas/APO-1-independent activation of CPP32 β . *Cancer Res.* **57**, 2550–2554.

Gibson, L., Holmgren, S.P., Huang, D.C.S., Bernard, O., Copeland, N.G., Jenkins, N.A., *et al.* (1996) *Bcl-w*, a novel member of the *Bcl-2* family, promotes cell survival. *Oncogene* **13**, 665–675.

Ginsberg, D., Mechta, F., Yaniv, M. and Oren, M. (1991) Wild-type p53 can down-modulate the activity of various promoters. *Proc. Natl. Acad. Sci. USA* **88**, 9979–9983.

Granville, D.J., Jiang, H., An, M.T., Levy, J.G., McManus, B.M. and Hunt, D.W.C. (1998) Overexpression of *BclxL* prevents caspases-3-mediated activation of DNA fragmentation factor (DFF) produced by treatment with the photochemotherapeutic agent BPD-MA. *FEBS LETTS.* **422**, 151–154.

Greidinger, E.L., Miller, D.K., Yamin, T.-T., Casciola-Rosen, L. and Rosen, A. (1996) Sequential activation of three distinct ICE-like activities in Fas-ligated Jurkat cells. *FEBS Lett.* **390**, 299–303.

Guru, T. (1997) How TRAIL kills cancer cells, but not normal cells. *Science* **277**, 768.

- Halenbeck, R., MacDonald, H., Roulston, A., Chen, T.T., Conroy, L. and Williams, L.T. (1998) CPAN, a human nuclease regulated by the caspase-sensitive inhibitor DFF45. *Curr. Biol.* **8**, 537–540.
- Han, Z., Malik, N., Carter, T., Reeves, W.H., Wyche, J.H. and Hendrickson, E.A. (1996) DNA-dependent protein kinase is a target for a CPP32-like apoptotic protease. *J. Biol. Chem.* **271**, 25035–25040.
- Hara, H., Friedlander, R.M., Gagliardini, V., Ayata, C., Fink, K., Huang, Z., *et al.* (1997) Inhibition of interleukin-1 β converting enzyme family proteases reduces ischemic and excitotoxic neuronal damage. *Proc. Natl. Acad. Sci. USA* **94**, 2007–2012.
- Harris, C.C. (1993) p53: at the crossroads of molecular carcinogenesis and risk assessment. *Science* **262**, 1980–1981.
- Haupt, Y., Maya, R., Kazaz, A. and Oren, M. (1997) Mdm2 promotes the rapid degradation of p53. *Nature (Lond.)* **387**, 296–299.
- Hayes, J.D. and Pulford, D.J. (1995) The glutathione S-transferase supergene family. Regulation of GST and the contribution of the isoenzymes to cancer chemoprotection and drug resistance. *Crit. Rev. Biochem. Mol. Biol.* **30**, 445–600.
- Hengartner, M.O. and Horvitz, H.R. (1994) Programmed cell death in *C. elegans*. *Curr. Opin. Genet. Dev.* **4**, 581–586.
- Hirata, H., Takahashi, A., Kobayashi, S., Yonehara, S., Sawai, H., Okazaki, T., *et al.* (1998) Caspases are activated in a branched protease cascade and control distinct downstream processes in Fas-induced apoptosis. *J. Exp. Med.* **187**, 587–600.
- Hollstein, M., Sidransky, D., Vogelstein, B. and Harris, C.C. (1991) p53 mutations in human cancers. *Science* **253**, 49–52.
- Hsu, H., Xiong, J. and Goeddel, D.V. (1995) The tumour necrosis factor receptor 1-associated protein TRADD signals cell death and NF κ B activation. *Cell* **81**, 495–504.
- Hsu, H., Huang, J., Shu, H.-B., Baichwal, V. and Goeddel, D.V. (1996) TNF-dependent recruitment of the protein kinase RIP to the TNF receptor-1 signaling complex. *Immunity* **4**, 387–396.
- Hu, Y., Benedict, M.A., Wu, D., Inohara, N. and Núñez. (1998) Bcl-x_L interacts with Apaf-1 and inhibits Apaf-1-dependent caspase-9 action. *Proc. Natl. Acad. Sci. USA* **95**, 4386–4391.

Hua, X., Sakai, J., Ho, Y.K., Goldstein, J.L. and Brown, M.S. (1995) Hairpin orientation of sterol regulatory element-binding protein-2 in cell membranes as determined by protease protection. *J. Biol. Chem.* **270**, 29422–29427.

Ishizaki, Y., Cheng, L., Mudge, A.W. and Raff, M.C. (1995) Programmed cell death by default in embryonic cells, fibroblasts and cancer cells. *Mol. Cell Biol.* **6**, 1443–1458.

Itoh, N., Yonehara, S., Ishii, A., Yonehara, M., Mizushima S.-I., Sameshima, M., *et al.* (1991) The polypeptide encoded by the dDNA for human cell surface antigen Fas can mediate apoptosis. *Cell* **66**, 233–243.

Itoh, N. and Nagata, S. (1993) A novel protein domain required for apoptosis. Mutational analysis of human Fas antigen. *J. Biol. Chem.* **268**, 10932–10937.

Jacobson, M.D., Weil, M. and Raff, M.C. (1996) Role of ced-3/ICE family proteases in staurosporine-induced programmed cell death. *J. Cell Biol.* **133**, 1041–1051.

Janicke, R.U., Walker, P.A., Yu Lin, X. and Porter, A.G. (1996) Specific cleavage of the retinoblastoma protein by an ICE-like protease in apoptosis. *EMBO J.* **15**, 6969–6978.

Jarvis, W.D., Turner, A.J., Povirk, L.F., Traylor, S. and Grant, S. (1994) Induction of apoptotic DNA fragmentation and cell death in HL-60 human promyelocytic leukemia cells by pharmacological inhibitors of protein kinase C. *Cancer Res.* **54**, 1707–1714.

Jiang, S., Chow, S.C., Nicotera, P. and Orrenius, S. (1994) Ca²⁺ signals activate apoptosis in thymocytes: studies using the Ca²⁺ATPase inhibitor thapsigargin. *Exp. Cell Res.* **212**, 84–92.

Johnson, E.M., Deckwerth, T.L. and Deshmukh, M. (1996) Neuronal death in developmental models: possible implications in neuropathology. *Brain Pathol.* **6**, 397–409.

Jost, C.A., Marin, M.C. and Kaelin, Jnr., W.G. (1997) p73 is a human p53-related protein that can induce apoptosis. *Nature (Lond.)* **389**, 191–194.

Juan, T.S.-C., McNiece, I.K., Jenkins, N.A., Gilbert, D.J., Copeland, N.G. and Fletcher, F.A. (1996) Molecular characterization of mouse and rat CPP32 β gene encoding a cysteine protease resembling interleukin-1 β converting enzyme and CED-3. *Oncogene* **13**, 749–755.

Kamada, S., Washida, M., Hasegawa, J.-I. Kusano, H., Funahashi, Y., and Tsujimoto, Y. (1997)

- Involvement of caspase-4-like protease in Fas-mediated apoptotic pathways. *Oncogene* **15**, 285–290.
- Kamens, J., Paskind, M., Hugunin, M., Talanian, R.V., Allen, H., Banach, D., *et al.* (1995) Identification and characterisation of Ich2, a novel member of the ICE family of cysteine proteases. *J. Biol. Chem.* **270**, 15250–15256.
- Kastan, M.B., Onyekwere, O., Sidransky, D., Vogelstein, B. and Craig, R.W. (1991) Participation of p53 protein in the cellular response to DNA damage. *Cancer Res.* **51**, 6304–6311.
- Kaufmann, S.H. (1989) Induction of endonucleolytic DNA cleavage in human acute myelogenous leukemia cells by etoposide, camptothecin and other cytotoxic anticancer drugs: a cautionary note. *Cancer Res.* **49**, 5870–5878.
- Kaufmann, S.H., Desnoyers, S., Ottaviano, Y., Davidson, N.E. and Poirier, G.G. (1993) Specific proteolytic cleavage of poly(ADP-ribose)polymerase: an early marker of chemotherapy-induced apoptosis. *Cancer Res.* **53**, 3976–3985.
- Kerr, J.F.R., Wyllie, A.H. and Currie, A.R. (1972) Apoptosis, a basic biological phenomenon with wider implications in tissue kinetics. *Br. J. Cancer* **26**, 239–245.
- Kischkel, F.C., Hellbardt, S., Behrmann, I., Germer, M., Pawlita, M., Krammer, P.H. and Peter, M.E. (1995) Cytotoxicity-dependent APO-1 (Fas/CD95)-associated proteins form a death-inducing signalling complex (DISC) with the receptor. *EMBO J.* **14**, 5579–5588.
- Kiyoto, I., Yamamoto, S., Aizu, E. and Kato, R. (1987) *Biochem. Biophys. Res. Commun.* **148**, 740–746.
- Kluck, R.M., Bossy-Wetzell, E., Green, D.R. and Newmeyer, D.D. (1997) The release of cytochrome c from mitochondria: a primary site for bcl-2 regulation of apoptosis. *Science* **275**, 1132–1136.
- Knudson, C.M., Tung, K.S.K., Tourtellotte, W.G., Brown, G.A.J. and Korsmeyer, S.J. (1995) Bax-deficient mice with lymphoid hyperplasia and male germ cell death. *Science* **270**, 96–99.
- Kostura, M.J., Tocci, M.J., Limjuco, G., Chin, J., Cameron, P., Hillman, A.G., *et al.* (1989) Identification of a monocyte specific pre-interleukin-1 β convertase activity. *Proc. Natl. Acad. Sci. USA.* **86**, 5227–5231.
- Kozopas, K.M., Yang, T., Buchan, H.L., Shou, P. and Craig, R.W. (1993) Mcl-1, a gene expressed in programmed myeloid cell differentiation, has sequence similarity to Bcl-2. *Proc. Natl. Acad. Sci. USA.* **90**, 3516–3520.

- Kubbutat, M.H.G., Jones, S.N. and Vousden, K.H. (1997) Regulation of p53 stability by Mdm2. *Nature (Lond.)* **387**, 299–303.
- Kuida, K., Lippke, J.A., Ku, G., Harding, M.W., Livingston, D.J., Su, M.S.-S. and Flavell, R.A. (1995) Altered cytokine export and apoptosis in mice deficient in ICE. *Science* **267**, 2000–2003.
- Kuida, K., Zheng, T.S., Na, S., Kuan, C-Y., Yang, D., Karasuyama, H., Rakic, P., and Flavell, R.A. (1996) Decreased apoptosis in the brain and premature lethality in CPP32-deficient mice. *Nature (Lond.)* **384**, 368–372.
- Kumar, S., Kinoshita, M., Noda, M., Copeland, N.G. and Jenkins, N.A. (1994) Induction of apoptosis by the mouse Nedd2 gene, which encodes a protein similar to the product of the *C. elegans* cell death gene *ced3* and the mammalian interleukin-1 β converting enzyme. *Genes Dev.* **8**, 1613–1626.
- Künstle, G., Leist, M., Uhlig, S., Revesz, L., Feifel, R., MacKenzie, A. and Wendel, A. (1997) ICE-protease inhibitors block murine liver injury and apoptosis caused by CD95 or by TNF- α . *Immunol. Letts.* **55**, 5–10.
- Kussie, P.H., Gorina, S., Marechal, V., Elenbaas, B., Moreau, J., Levine, A.J. and Pavletich, N.P. (1996) Structure of the mdm2 oncoprotein bound to the p53 tumour suppressor transcription domain. *Science* **274**, 948–953.
- Lacronique, V., Mignon, A., Fabre, M., Viollet, B., Rouquet, N., Molina, T., *et al.* (1996) Bcl2 protects from lethal hepatic apoptosis induced by an anti-Fas antibody in mice. *Nat. Med.* **2**, 80–86.
- Lane, D.P. and Crawford, L.V. (1979) T antigen is bound to a host protein in SV40-transformed cells. *Nature (Lond.)* **278**, 261–263.
- Lane, D.P. (1992) Cancer: p53, Guardian of the Genome. *Nature* **358**, 15–16.
- Lazebnik, Y.A., Kaufmann, S.H., Desnoyers, S., Poirier, G.G. and Earnshaw, W.C. (1994) Cleavage of poly(ADP-ribose)polymerase by a proteinase with properties like ICE. *Nature (Lond.)* **371**, 346–347.
- Lazebnik, Y.A., Takahashi, A., Moir, R.D., Goldman, R.D., Poirier, G.G., Kaufmann, S.H. and Earnshaw, W.C. (1995) Studies of the lamin proteinase reveal multiple parallel biochemical pathways during apoptotic execution. *Proc. Natl. Acad. Sci. USA* **92**, 9042–9046.
- Li, H., Zhu, H., Xu, C. and Yuan, J. (1998) Cleavage of BID by caspase-8 mediates the mitochondrial

damage in the Fas pathway of apoptosis. *Cell* **94**, 491–501.

Li, P., Allen, H., Banerjee, S., Franklin, S., Herzog, L., Johnston, C., *et al.* (1995) Mice deficient in ICE are defective in production of mature IL1 β and resistant to endotoxic shock. *Cell* **80**, 401–411.

Li, P., Nijhawan, D., Budihardjo, I., Srinivasula, S.M., Ahmad, M., Alnemri, E.S., and Wang, X. (1997) Cytochrome c and dATP-dependent formation of Apaf-1/caspase-9 complex initiates an apoptotic protease cascade. *Cell* **91**, 479–489.

Liebermann, D.A., Hoffman, B. and Steinman, R.A. (1995) Molecular controls of growth arrest and apoptosis: p53-dependent and independent pathways. *Oncogene* **11**, 199–210

Lin, E.Y., Orlofsky, A., Berger, M.S. and Prystowsky, M.B. (1993) Characterisation of A1, a novel hemopoietic-specific early-response gene with sequence simialrity to bcl-2. *J. Immunol.* **151**, 1797–1988.

Lin, Y. and Benchimol, S. (1995) Cytokines inhibit p53-mediated apoptosis by not p53-mediated G1 arrest. *Mol. Cell Biol.* **15**, 6045–6054.

Liu, Y.J., Joshua, D.E., Williams, G.T., Smith C.A., Gordon, J. and McClennan, I.C.M. (1989) The mechanisms of antigen-driven selection in germinal centres. *Nature (Lond.)* **342**, 929–931.

Liu, X., Zou, H., Slaughter, C. and Wang, X. (1997) DFF, a heterodimeric protein that functions downstream of capsase-3 to trigger DNA fragmentation during apoptosis. *Cell* **89**, 175–184.

Lotem, J. and Sachs, L. (1994) Control of sensitivity to induction of apoptosis in myeloid leukemic cells by differentiation and bcl-2 dependent and independent pathways. *Cell Growth and Diff.* **5**, 321–327.

Lotem, J. and Sachs, L. (1996) Differential suppression by protease inhibitors and cytokines of apoptosis induced by wild-type p53 and cytotoxic agents. *Proc. Natl. Acad. Sci. USA.* **93**, 12507–12512.

Lowe, S.W., Schmitt, E.M., Smith, S.W., Osborne, B.A. and Jacks, T. (1993b) p53 is required for radiation-induced apoptosis in mouse thymocytes. *Nature (Lond.)* **362**, 847–849.

Luo, X., Budihardjo, I., Zou, H., Slaughter, C. and Wang, X. (1998) Bid, a Bcl2 interactin protein, mediates cytochrome c release from mitochondria in response to activation of cell surface death receptors. *Cell* **94**, 481–490

Luo, Y., Horwitz, J. and Massague, J. (1995) Cell cycle inhibition by independent CDK and PCNA binding domains in p21(Cip1). *Nature (Lond.)* **375**, 159–161.

- MacFarlane, M., Jones, N.A., Dive, C. and Cohen, G.M. (1996) DNA damaging agents induce both p53-dependent and p53-independent apoptosis in immature thymocytes. *Mol. Pharmacol.* **50**, 900–911.
- MacFarlane, M., Cain, K., Sun, X.-M., Alnemri, E.S., and Cohen, G.M. (1997a) Processing/activation of at least for ICE-like proteases occurs during the execution phase of apoptosis in human monocytic tumour cells. *J. Cell Biol.* **137**, 469–479.
- MacFarlane, M., Ahmad, M., Srinivasula, S.M., Fernandes-Alnemri, T., Cohen, G.M. and Alnemri, E.S. (1997b) Identification and molecular cloning of two novel receptors for the cytotoxic ligand TRAIL. *J. Biol. Chem.* **272**, 25417–25420.
- Mancini, M., Nicholson, D.W., Roy, S., Thornberry, N.A., Peterson, E.P., Casciola-Rosen, L.A. and Rosen, A. (1998) The caspase-3 precursor has a cytosolic and mitochondrial distribution: implications for apoptotic signaling. *J. Cell Biol.* **140**, 1485–1495.
- Mao, P.-L., Jiang, Y., Wee, B.Y. and Porter, A.G. (1998) Activation of caspase-1 in the nucleus requires nuclear translocation of procaspase-1 mediated by its prodomain. *J. Biol. Chem.* **273**, 23621–23624.
- Margolin, N., Raybuck, S.A., Wilson, K.P., Chen, W., Fox, T. and Livingston, D.J. (1997) Substrate and inhibitor specificities of ICE and related caspases. *J. Biol. Chem.* **272**, 7223–7228.
- Marsters, S.A., Pitti, R.M., Donahue, C.J., Ruppert, S., Bauer, K.D. and Ashkenazi, A. (1996) Activation of apoptosis by Apo-2 ligand is independent of FADD but blocked by crmA. *Curr. Biology* **6**, 750–752.
- Martin, D.P., Schmidt, R.E., DiStefano, P.S., Lowry, O.H., Carter, J.G. and Johnson, E.M. (1988) Inhibitors of protein synthesis and RNA synthesis prevent neuronal death caused by nerve growth factor deprivation. *J. Cell Biol.* **106**, 829–844.
- Martin, S.J. and Green, D.R. (1995) Protease activation during apoptosis: Death by a thousand cuts? *Cell* **82**, 349–352.
- Martin, S.J., Newmeyer, D.D., Mathias, S., Farschon, D.M., Wang, H.G., Reed, J.C., *et al.* (1995) Cell-free reconstitution of Fas-, UV radiation- and ceramide-induced apoptosis. *EMBO J.* **14**, 5191–5200.
- Martins, L.M., Mesner, P.W., Kottke, T.J., Basi, G.S., Sinha, S., Tung, J.S., *et al.* (1997a) Comparison of caspase activation and subcellular localisation in HL60 cells undergoing etoposide-induced apoptosis. *Blood* **90**, 4283–4296.

- Martins, L.M., Kottke, T., Mesner, P.W., Basi, G.S., Sinha, S., Figon, Jnr., N., *et al.* (1997b) Activation of multiple interleukin-1 β converting enzyme homologues in cytosol and nuclei of HL-60 cells during etoposide-induced apoptosis. *J. Biol. Chem.* **272**, 7421–7430.
- McCall, K. and Steller, H. (1998) Requirement for DCP-1 Caspase during *Drosophila* oogenesis. *Science* **279**, 230–234.
- McCarthy, N., Whyte, M.K.B., Gilbert, C.S. and Evan, G.I. (1997) Inhibition of Ced3/ICE-related proteases does not prevent cell death induced by oncogenes, DNA damage or the Bcl2 homologue Bak. *J. Cell Biol.* **136**, 215–227.
- McMahon, G., Alsina, J.L. and Levy, S.B. (1984) Induction of a Ca²⁺/Mg²⁺-dependent endonuclease activity during the early stages of murine erythroleukaemic cell differentiation. *Proc. Natl. Acad. Sci. USA.* **81**, 7461–7465.
- Michalovitz, D., Halevy, O. And Oren, M. (1990) Conditional inhibition of transformation and of cell proliferation by a temperature-sensitive mutant of p53. *Cell* **62**, 671–680.
- Milligan, S.J., Prevette, D., Yaginuma, H., Homma, S., Cardwell, C., Fritz, L.C., *et al.* (1995) Peptide inhibitors of the ICE protease family arrest programmed cell death of motoneurons *in vivo* and *in vitro*. *Neuron* **15**, 385–393.
- Milner, J. and Medcalf, E.A. (1990) Temperature-dependent switching between ‘wild-type’ and ‘mutant’ forms of p53-val135. *J. Mol. Biol.* **216**, 481–484.
- Miura, M., Zhu, H., Rotello, R., Hartweg, E.A. and Yuan, J. (1993) Induction of apoptosis in fibroblasts by ICE, a mammalian homologue of *C elegans* cell death gene ced3. *Cell* **75**, 653–660.
- Miyashita, T. and Reed, J.C. (1995) Tumor suppressor p53 is a direct transcriptional activator of the human bax gene. *Cell* **80**, 293–299.
- Miyashita, T., Krajewski, S., Krajewska, M., Wang, H.G., Lin, H.K., Liebermann, D.A., *et al.* (1994) Tumor suppressor p53 is a regulator of *bcl-2* and *bax* gene expression *in vitro* and *in vivo*. *Oncogene* **9**, 1799–1805.
- Mizushima, N., Koike, R., Kohsaka, H., Kushi, Y., Handa, S., Yagita, H. and Miyasaka, N. (1996) Ceramide induces apoptosis via CPP32 activation. *FEBS Letts.* **395**, 267–271.
- Munroe, D.G., Peacock, J.W. and Benchimol, S. (1990) Inactivation of the cellular p53 gene is a

common feature of Friend Virus-induced erythroleukaemia: relationship of inactivation to dominant transforming alleles. *Mol. Cell. Biol.* **10**, 3307–3313.

Muzio, M., Chinnaiyan, A.M., Kischkel, F.C., O'Rourke, K., Shevchenko, A., Ni, J., *et al.* (1996) FLICE, A novel FADD-homologous ICE/CED-3-like protease, is recruited to the CD95 (Fas/APO-1) death-inducing signaling complex. *Cell* **85**, 817–827.

Nagata, S. (1997) Apoptosis by death factor. *Cell* **88**, 355–365.

Nagata, S. and Goldstein, P. (1995) The Fas death factor. *Science* **267**, 1449–1456.

Nakano, H., Tamaoki, T., Kobayashi, E., Takahashi, I., Kuzuu, Y. and Iba, H. (1987) Staurosporine inhibits tyrosine-specific protein kinase activity of Rous sarcoma virus transforming protein p60. *J. Antibiot. (Tokyo)* **40**, 706–708.

Neamati, N., Fernandez, A., Wright, S., Kiefer, J. and McConkey, D.J. (1995) Degradation of lamin B1 precedes oligonucleotide DNA fragmentation in apoptotic thymocytes and isolated thymocyte nuclei. *J. Immunol.* **154**, 3788–3795.

Neer, E.J., Schmidt, C.J. Nambudripad, R. and Smith, T.F. (1994) The ancient regulatory-protein family of WD-repeat proteins. *Nature (Lond.)* **371**, 297–300.

Ng, F.W.H., Nguyen, M., Kwan, T., Branton, P.E., Nicholson, D.W., Cromlish, J.A. and Shore, G.C. (1997) p28 Bap31, a Bcl2/BclX_L- and procaspase-8-associated protein in the endoplasmic reticulum. *J. Cell Biol.* **139**, 327–338.

Ng, F.W.H. and Shore, G.C. (1998) BclX_L cooperatively associates with the Bap31 complex in the endoplasmic reticulum, dependent on procaspase-8 and ced-4 adaptor. *J. Biol. Chem.* **273**, 3140–3143.

Nicholson, D.W. (1996) ICE/CED3-like proteases as therapeutic targets for the control of inappropriate apoptosis. *Nature Biotech.* **14**, 297–301.

Nicholson, D.W., Ali, A., Thornberry, N.A., Vaillancourt, J.P., Ding, C.K., Gallant, M., *et al.* (1995) Identification and inhibition of the ICE/CED-3 protease necessary for mammalian apoptosis. *Nature* **376**, 37–43.

Nicholson, D.W., and Thornberry, N.A. (1997) Caspases: killer proteases. *Trends Biochem. Sci.* **22**, 299–306.

- Norimura, T., Nomoto, S., Katsuki, M., Gondo, Y. and Kondo, S. (1996) p53-dependent apoptosis suppresses radiation-induced teratogenesis. *Nat. Med.* **2**, 577–580.
- Oberhammer, F.A., Hochegger, K., Fröschl, G., Tiefenbacher, R. and Pavelka, M. (1994) Chromatin condensation during apoptosis is accompanied by degradation of lamin A+B, without enhanced activation of cdc2 kinase. *J. Cell Biol.* **126**, 827–837.
- Oehm, A., Behrmann, I., Falk, W., Pawlita, M., Maier, G., Klas, C., *et al.* (1992) Purification and molecular cloning of the APO1 cell surface antigen, a member of the TNF/NGF receptor superfamily. Sequence identity with the Fas antigen. *J. Biol. Chem.* **267**, 10709–10715.
- Ogasawara, J., Watanabe-Fukunaga, R., Adachi, M., Matsuzawa, A., Kasugai, T., Kitamura, Y., *et al.* (1993) Lethal effect of the anti-Fas antibody in mice. *Nature* **364**, 806–809.
- Oltvai, Z.N., Milliman, C.L. and Korsmeyer, S.J. (1993) Bcl-2 heterodimerises in vivo with a conserved homolog, Bax, that accelerates programmed cell death. *Cell* **74**, 609–619.
- Omura, S., Iwai, Y., Hirano, A., Nagakawa, A., Awaya, J., Tsuchiya, H., Takahashi, Y. and Masuma, R. (1977) *J. Antibiot. (Tokyo)* **30**, 275–281.
- Onishi, Y., Azuma, Y., Sato, Y., Mizuno, Y., Tadakuma, T. and Kizaki, H. (1993) Topoisomerase inhibitors induce apoptosis in thymocytes. *Biochimica Biophysica Acta.* **1175**, 147–154.
- Oppenheim, R.W., Prevette, M., Tytell and Homma, S. (1990) Naturally occurring and induced neuronal death in the chick embryo *in vivo* requires protein and RNA synthesis: evidence for the role of cell death genes. *Dev. Biol.* **138**, 104–113.
- Oppenheim, R.W. (1991) Cell death during development of the nervous system. *Annu. Rev. Neurosci.* **14**, 453–501.
- Ormerod, M.G., Sun, X.-M., Snowden, R.T., Davies, R., Fearnhead, H.O. and Cohen, G.M. (1993) Increased membrane permeability of apoptotic thymocytes: a flow cytometric study. *Cytometry* **14**, 595–602.
- Orth, K., Chinnaiyan, A.M., Garg, M., Froelich, C.J. and Dixit, V.M. (1996) The CED-3/ICE-like protease Mch2 is activated during apoptosis and cleaves the death substrate lamin A. *J. Biol. Chem.* **271**, 16443–16446.
- Otto, F. (1990) DAPI staining of fixed cells for high resolution flow cytometry of nuclear DNA. *Methods*

Cell Biol. **33**, 105–111.

Owen-Schaub, L.B., Zhang, W., Cusack, J.C., Angelo, L.S., Santee, S.M., Fujiwara, T., Rothe, J.A., Deisseroth, A.B., Zhang, W.-W., Kruzel, E. and Radinsky, R. (1995) Wild-type human p53 and a temperature-sensitive mutant induce Fas/APO-1 expression. *Mol. Cell Biol.* **15**, 3032–3040.

Pai, J.-T., Brown, M.S., and Goldstein, J.L. (1996) Purification and cDNA cloning of a second apoptosis-related cysteine protease that cleaves and activates sterol regulatory element binding proteins. *Proc. Natl. Acad. Sci.* **93**, 5437–5442.

Pan, G., O'Rourke, K., Chinnaiyan, A.M., Gentz, R., Ebner, R., Ni, J. and Dixit, V.M. (1997a) The receptor for the cytotoxic ligand TRAIL. *Science* **276**, 111–113.

Pan, G., Ni, J., Wei, Y.-F., Yu, G., Gentz, R. and Dixit, V.M. (1997b) An antagonist decoy receptor and a death domain-containing receptor for TRAIL. *Science* **277**, 815–818.

Pan, G., O'Rourke, K. and Dixit, V.M. (1998) Caspase-9, Bcl_{xL}, and Apaf-1 form a ternary complex. *J. Biol. Chem.* **273**, 5841–5845.

Pavletich, N.P., Chambers, K.A. and Pabo, C.O. (1993) The DNA-binding domain of p53 contains four conserved regions and the major mutation hot spots. *Genes Dev.* **7**, 2556–2564.

Peled, A., Zipori, D. and Rotter, V. (1996) Cooperation between p53-dependent and p53-independent apoptotic pathways in myeloid cells. *Cancer Res.* **56**, 2148–2156.

Pitti, R.M., Marsters, S.A., Ruppert, S., Donahue, C.J., Moore, A. and Ashkenazi, A. (1996) Induction of apoptosis by Apo-2 ligand, a new member of the TNF cytokine family. *J. Biol. Chem.* **271**, 12687–12690.

Polverino, A.J. and Patterson, S.D. (1997) Selective activation of caspases during apoptotic induction in HL-60 cells. Effects of a tetrapeptide inhibitor. *J. Biol. Chem.* **272**, 7013–7021.

Raffray, M. and Cohen, G.M. (1997) Apoptosis and necrosis in toxicology: A continuum or distinct modes of cell death? *Pharm. Ther.* **75**, 153–177.

Rao, L., Perez, D. and White, E. (1996) Lamin proteolysis facilitates nuclear events during apoptosis. *J. Cell Biol.* **135**, 1441–1455.

Reed, M., Woelker, B., Wang, P., Wang, Y., Anderson, M.E. and Tegtmeyer, P. (1995) The C-terminal

domain of p53 recognizes DNA damaged by ionising radiation. *Proc. Natl. Acad. Sci. USA*. **92**, 9455–9459.

Rodriguez, I., Matsuura, K., Ody, C., Nagata, S. and Vassalli, P. (1996a) Systemic injection of a tripeptide inhibits the intracellular activation of CPP32-like proteases *in vivo* and fully protects mice against Fas-mediated fulminant liver destruction and death. *J. Exp. Med.* **184**, 2067–2072.

Rodriguez, I., Matsuura, K., Khatib, K., Reed, J.C., Nagata, S. and Vassalli, P. (1996b) A bcl2 transgene expressed in hepatocytes protects mice from fulminant liver destruction but not from rapid death induced by anti-Fas antibody injection. *J. Exp. Med.* **183**, 1031–1036.

Rouquet, N., Pagès, J-C, Molina, T., Briand, P. and Joulin, V. (1996) ICE inhibitor YVAD.cmk is a potent therapeutic agent against *in vivo* liver apoptosis. *Curr. Biol.* **6**, 1192–1195.

Ryan, J.J., Danish, R., Gottlieb, C.A. and Clarke, M.F. (1993) Cell cycle analysis of p53-induced cell death in murine erythroleukaemia cells. *Mol. Cell. Biol.* **13**, 711–719.

Samali, A., Zhivotovsky, B., Jones, D.P. and Orrenius, S. (1998) Detection of pro-caspase-3 in cytosol and mitochondria of various tissues. *FEBS Letts.* **431**, 167–169.

Savill, J.S., Dransfield, I., Hogg, N. and Haslett, C. (1990) Vitronectin receptor-mediated phagocytosis of cells undergoing apoptosis. *Nature (Lond.)* **343**, 170–173.

Scaffidi, C., Medema, J.P., Krammer, P.H. and Peter, M.E. (1997) FLICE is predominantly expressed as two functionally active isoforms, caspase-8/a and caspase-8/b. *J. Biol. Chem.* **272**, 26953–26958.

Scaffidi, C., Fulda, S., Srinivasan, A., Friesen, C., Li, F., Tomaselli, K.J., *et al.* (1998) Two CD95 (APO-1/Fas) signalling pathways. *EMBO J.* **17**, 1675–1687.

Schlegel, J., Peters, I. and Orrenius, S. (1995) Isolation and partial characterization of a protease involved in Fas-induced apoptosis. *FEBS Lett.* **364**, 139–142.

Schlegel, J., Peters, I., Orrenius, S., Miller, D.K., Thornberry, N.A., Yamin, T.-T. and Nicholson, D.W. (1996) CPP32/Apopain is a key interleukin 1 β -converting enzyme-like protease involved in Fas-mediated apoptosis. *J. Biol. Chem.* **271**, 1841–1844.

Screaton, G.R., Mongkolsapaya, J., Xu, X.-N., Cowper, A.E., McMichael, A.J. and Bell, J.I. (1997) TRICK2, a new alternatively spliced receptor that transduces the cytotoxic signal from TRAIL. *Curr. Biol.* **7**, 693–696.

Shaulsky, G., Goldfinger, N., Ben-Ze'ev, A. and Rotter, V. (1990) Nuclear accumulation of p53 is mediated by several nuclear localisation sequences and plays a role in tumourigenesis. *Mol. Cell. Biol.* **10**, 6565–6577.

Sheikh, M.S., Burns, T.T., Huang, Y., Wu, G.S., Amundson, S., Brooks, K.S., *et al.* (1998) p53-dependent and independent regulation of the death receptor *KILLER/DR5* gene expression in response to genotoxic stress and TNF. *Cancer Res.* **58**, 1593–1598.

Sheridan, J.P., Marsters, S.A., Pitti, R.M., Gurney, A., Skubatch, M., Baldwin, D., *et al.* (1997) Control of TRAIL-induced apoptosis by a family of signaling and decoy receptors. *Science* **277**, 818–821.

Shi, Y., Sahai, B.M and Green, D.R. (1989) Cyclosporin A inhibits activation-induced cell death in T-cell hybridomas and thymocytes. *Nature (Lond.)* **339**, 625–626.

Skowronski, E.W., Kolesnik, R.N. and Green, D.R. (1996) Fas-mediated apoptosis and sphingomyelinase signal transduction: the role of ceramide as a second messenger for apoptosis. *Cell Death Diff.* **3**, 171–176.

Slee, E.A., Zhu, H., Chow, S.C., MacFarlane, M., Nicholson, D.W. and Cohen, G.M. (1996) Benzylloxycarbonyl-Val-Ala-Asp (OMe) fluoromethylketone (Z-VAD.FMK) inhibits apoptosis by blocking the processing of CPP32. *Biochem. J.* **315**, 21–24.

Song, Q., Lees-Miller, S.P., Kumar, S., Zhang, N., Smith, G.C.M., Jackson, S.P., *et al.* (1996) DNA-dependent protein kinase catalytic subunit: a target for the ICE-like protease CPP32 in apoptosis. *EMBO J.* **15**, 3238–3246.

Sorenson, C.M., Barry, M.A. and Eastman, A. (1990) Analysis of events associated with cell cycle at G0 phase and cell death induced by cisplatin. *J. Natl. Cancer Inst.* **82**, 749–755.

Soussi, T., Caron de Fromentel, C., Breugnot, C. and May, P. (1990) Structural aspects of the p53 protein in relation to gene evolution. *Oncogene* **5**, 945–952.

Spencer, C.A. and Groudine, M. (1991) Regulation in normal and neoplastic cells. *Adv. Cancer Res.* **56**, 1–48.

Srinivasula, S.M., Ahmad, M., Fernandes-Alnemri, T., Litwack, G., and Alnemri, E.S. (1996) Molecular ordering of the Fas apoptotic pathway: the Fas/Apo1 protease Mch5 is a CrmA-inhibitable protease that activates multiple ced3/ICE-like cysteine proteases. *Proc. Natl. Acad. Sci. USA* **93**, 14486–14491.

Stanger, B.Z., Leder, P., Lee, T.-H., Kim, E. and Seed, B. (1995) RIP: a novel protein containing a death domain that interacts with Fas/APO1 (CD95) in yeast and causes cell death. *Cell* **81**, 513–523.

Stephen, C.W. and Lane, D.P. (1992) Mutant conformation of p53. Precise epitope mapping using a filamentous phage epitope library. *J. Mol. Biol.* **225**, 577–583.

Stewart, N., Hicks, G.G., Paraskevas, F. and Mowat, M. (1995) Evidence for a second cell cycle block at G2/M by p53. *Oncogene* **10**, 109–115.

Strasser, A., Harris, A.W., Jacks, T. and Cory, S. (1994) DNA damage can induce apoptosis in proliferating lymphoid cells via p53-independent mechanisms inhibitable by Bcl2. *Cell* **79**, 329–339.

Stürzbecher, H.W., Brain, R., Addison, C., Rudge, K., Remm, M., Grimaldi, M., *et al.* (1992) A C-terminal alpha-helix plus basic region motif is the major structural determinant of p53 tetramerisation. *Oncogene* **7**, 1513–1523.

Sun, X.-M., Snowden, R. T., Skilleter, D.N., Dinsdale, D., Ormerod, M.G. and Cohen, G.M. (1992) A flow cytometric method for the separation and quantitation of normal and apoptotic thymocytes. *Anal. Biochem.* **204**, 351–356.

Sun, X.-M. and Cohen, G.M. (1994) Mg²⁺-dependent cleavage of DNA into kilobase pair fragments is responsible for the initial degradation of DNA in apoptosis. *J. Biol. Chem.* **269**, 14857–14860.

Takahashi, A., Alnemri, E.S., Lazebnik, Y.A., Fernandes-Alnemri, T., Litwack, G., Moir, R.D., *et al.* (1996) Cleavage of lamin A by Mch2 α but not CPP32: multiple interleukin 1 β -converting enzyme-related proteases with distinct substrate recognition properties are active in apoptosis. *Proc. Natl. Acad. Sci. USA* **96**, 8395–8400.

Takayama, S., Sato, T., Krajewski, S., Kochel, S.I., Millan, J.A. and Reed, J.C. (1995) Cloning and Functional analysis of BAG-1: a novel Bcl-2-binding protein with Anti-cell death activity. *Cell* **80**, 279–284.

Tam, S.W. and Schlegel, R. (1992) Staurosporine overrides checkpoints for mitotic onset in BHK cells. *Cell Growth Diff.* **3**, 811–817.

Tamaoki, T., Nomoto, H., Takahashi, I., Kato, Y., Morimoto, M. and Tomita, F. (1986) Staurosporine, a potent inhibitor of phospholipid/ Ca²⁺-dependent protein kinase. *Biochem. Biophys. Res. Commun.* **135**, 397–402.

Tartaglia, L.A., Goeddel, D.V., Reynolds, C., Figari, I.S., Weber, R.F., Fendly, B.M. and Palladino Jr., M.A. (1993) Stimulation of human T-cell proliferation by specific activation of the 75 kDa tumour necrosis factor receptor. *J. Immunol.* **151**, 4637–4641.

Tewari, M., Quan, L.T., O'Rourke, K., Desnoyers, S., Zeng, Z., Beidler, D.R., Poirier, G.G., Salvesen, G.S., and Dixit, V.M. (1995) Yama/ CPP32 β , a mammalian homologue of Ced3, is a CrmA-inhibitable protease that cleaves the death substrate poly(ADP ribose)polymerase. *Cell* **81**, 801–809.

Thornberry, N.A., Bull, H.G., Calaycay, J.R., Chapman, K.T., Howard, A.D., Kostura, M.J., *et al.* (1992) A novel heterodimeric cysteine protease is required for interleukin-1 β processing in monocytes. *Nature (Lond.)* **356**, 768–774.

Thornberry, N.A. (1994) Interleukin-1 β converting enzyme. *Methods Enzymol.* **244**, 615–631.

Thornberry, N.A. and Molineaux, S.M. (1995) ICE: a novel cysteine protease required for IL1 β production and implicated in programmed cell death. *Protein Sci.* **4**, 3–12.

Thornberry N.A., Rano, T.A., Peterson, E.P., Rasper, D.M., Timkey, T., Garcia-Calvo, M., *et al.* (1997) A combinatorial approach defines specificities of members of the caspase family and granzyme B. *J. Biol. Chem.* **272**, 17907–17911.

Ting, A.T., Pimentel-Muños, F.X. and Seed, B. (1996) RIP mediates tumour necrosis factor receptor 1 activation of NF-KB but not Fas/APO-1-initiated apoptosis. *EMBO J.* **15**, 6189–6196.

Trauth, B.C., Klas, C., Peters, A.M.J., Matzku, S., Moller, P., Falk, W., *et al.* (1989) Monoclonal antibody-mediated tumour regression by induction of apoptosis. *Science* **245**, 301–305.

Tsujimoto, Y., Finger, L.R., Yunis, J., Nowell, P.C. and Croce, C.M. (1984) Cloning of the chromosome breakpoint of neoplastic B cells with the t(14;18) chromosomal translocation. *Science* **226**, 1097–1099.

Tsukihara, T., Aoyama, H., Yamashita, E., Tomizaki, T., Yamaguchi, H., Shinzawa-Itoh, K., *et al.* (1996) The whole structure of the 13-subunit oxidized cytochrome c oxidase at 2.8 Å. *Science* **272**, 1136–1144.

Unger, T., Nau, M.M., Segal, S. and Minna, J.D. (1992) p53: a transdomain regulator of transcription whose function is ablated by mutations occurring in human cancer. *EMBO J.* **11**, 1383–1390.

Unger, T., Mietz, J.A., Scheffner, M., Yee, C.L. and Howley, P. (1993) Functional domains of wild-type and mutant p53 proteins involved in transcriptional regulation, transdomain inhibition and transformation

repression. *Mol. Cell. Biol.* **13**, 5186–5194

Van de Craen, M., Vandenaabeele, P., Declerq, W., Van den Brande, I., Van Loo, G., Molemans, F., *et al.* (1997) Characterisation of seven murine caspase family members. *FEBS.Letts.* **403**, 61–69.

Villa, P., Kaufmann, S.H. and Earnshaw, W.C. (1997) Caspases and caspase inhibitors. *TIBS* **22**, 388–393.

Waldman, T., Zhang, Y., Dillehay, L., Yu, J., Kinzler, K., Vogelstein, B. and Williams, J. (1997) Cell-cycle arrest versus cell death in cancer therapy. *Nature Medicine*, **3**, 1034–1036.

Walker, N.P.C., Talanian, R.V., Brady, K.D., Dang, L.C., Bump, N.J., Ferenz, C.R., *et al.* (1994) Crystal structure of the cysteine protease interleukin-1 β converting enzyme: a (p20/p10)² homodimer. *Cell* **78**, 343–352.

Walker, P.R., Smith, C., Youdale, T., Leblanc, J., Whitfield, J.F. and Sikorska, M. (1991) Topoisomerase II-reactive chemotherapeutic drugs induce apoptosis in thymocytes. *Cancer Res.* **51**, 1078–1085.

Walker, P.R., Lach, B., Leblanc, J. and Sikorska, M. (1994) Endonuclease activities associated with high molecular weight and internucleosomal DNA fragmentation in apoptosis. *Exp. Cell Res.* **213**, 100–106.

Wang, X., Briggs, M.R., Hua, X., Yokoyama, C., Goldstein, J.L. and Brown, M.S. (1993) Nuclear protein that binds sterol regulatory element of low density lipoprotein receptor protein II: purification and characterisation. *J. Biol. Chem.* **268**, 14497–14504.

Wang, L., Miura, M., Bergeron, L., Zhu, H. and Yuan, J. (1994a) *Ich-1*, and *Ice/ced-3*-related gene, encodes both positive and negative regulators of programmed cell death. *Cell* **78**, 739–750.

Wang, X., Sato, R., Brown, M.S., Hua, X., and Goldstein, J.L. (1994b) SREBP1, a membrane bound transcription factor released by sterol regulated proteolysis. *Cell* **77**, 53–62.

Wang, X., Pai, J., Wiedenfeld, E.A., Medina, J.C., Slaughter, C.A., Goldstein, J.L. and Brown, M.S. (1995) Purification of an Interleukin-1 β Converting Enzyme-related cysteine protease that cleaves sterol regulatory element-binding proteins between the leucine zipper and transmembrane domains. *J. Biol. Chem.* **270**, 18044–18050.

Wang, X., Zelenski, N.G., Yang, J., Sakai, J., Brown, M.S. and Goldstein, J.L. (1996a) Cleavage of sterol regulatory element binding protein (SREBP) by CPP32 during apoptosis. *EMBO J.* **15**, 1012–1020.

- Wang, K., Yin, X.M., Chao, D.T., Milliman, C.L. and Korsmeyer, S.J. (1996b) Bid: a novel BH3 domain-only death agonist. *Genes Dev.* **10**, 2859–2869.
- Waring, P. (1990) DNA fragmentation induced in macrophages by gliotoxin does not require protein synthesis and is preceded by raised inositol triphosphate levels. *J. Biol. Chem.* **265**, 14476–14480.
- Weaver, V.M., Lach, B., Walker, P.R. and Sikorska, M. (1993) The role of proteolysis in apoptosis: involvement of serine proteases in internucleosomal DNA fragmentation in mature thymocytes. *Cell Biol.* **71**, 488–500.
- Weil, M., Jacobson, M.D., Coles, H.S.R., Davies, T.J., Gardner, R.L., Raff, K.D. and Raff, M.C. (1996) Constitutive expression of the machinery for programmed cell death. *J. Cell Biol.* **133**, 1053–1059.
- White, K., Grether, M.E., Abrams, J.M., Young, L., Farrell, K. and Steller, H. (1994) Genetic control of programmed cell death in *Drosophila*. *Science* **264**, 677–683.
- Wiley, S.R., Schooley, K., Smolak, P.J., Din, W.S., Huang, C.P., Nicholl, J.K., Sutherland, G.R., Davis, T.D., Smith, C., Rauch, C., Smith, C.A. *et al.* (1995) Identification and characterisation of a new member of the TNF family that induces apoptosis. *Immunity* **3**, 673–682.
- Wilson, K.P., Black, J.-A.F., Thomson, J.A., Kim, E.E., Griffith, J.P., Navia, M.A., Murcko, M.A., Chambers, S.P., Aldape, R.A., Raybuck, S.A. and Livingston, D.J. (1994) Structure and mechanism of interleukin-1 β converting enzyme. *Nature (Lond.)* **370**, 270–275.
- Wolter, K.G., Hsu, Y.-T., Smith, C.L., Nechushtan, A., Xi, X.-G., and Youle, R.J. (1997) Movement of Bax from the cytosol to mitochondria during apoptosis. *J. Cell Biol.* **139**, 1281–1292.
- Wu, X.W., Bayle, J.H., Olson, D. and Levine, A.J. (1993) The p53 mdm-2 autoregulatory feedback loop. *Genes Dev.* **7**, 1126–1132.
- Wu, G.S., Burns, T.F., McDonald III, E.R., Jiang, W., Meng, R., Krantz, I.D., *et al.* (1997a) *KILLER/DR5* is a DNA-damage-inducible p53-regulated death receptor gene. *Nature Genetics* **17**, 141–143.
- Wu, D., Wallen, H.D. and Nunez, G. (1997b) Interaction and regulation of subcellular localization of ced4 by ced9. *Science* **275**, 1126–1129.
- Wyllie, A.H. (1980) Glucocorticoid-induced thymocyte apoptosis is associated with endogenous

- endonuclease activation. *Nature (Lond.)* **284**, 555–556.
- Wyllie, A.H., Kerr, J.F.R. and Currie, A.R. (1980) Cell death: the significance of apoptosis. *Int. Rev. Cytology* **68**, 251–306.
- Xiong, Y., Hannon, G.J., Zhang, H., Casso, D., Kobayashi, R and Beach D. (1993) p21 is a universal inhibitor of cyclin kinases. *Nature (Lond.)* **366**, 701–704.
- Yakes, F.M. and Van Houten, B. (1997) Mitochondrial DNA damage is more extensive and persists longer than nuclear DNA damage in human cells following oxidative stress. *Proc. Natl. Acad. Sci. USA* **94**, 514–519.
- Yang, E., Zha, J., Jockel, J., Boise, L.H., Thompson, C.B. and Korsmeyer, S.J. (1995) Bad, a heterodimeric partner for Bcl-xL and Bcl-2, displaces bax and promotes cell death. *Cell* **80**, 285–291.
- Yang, J., Liu, X., Bhalla, K., Kim, C.N., Ibrado, A.M., Cai, J., *et al.* (1997) Prevention of apoptosis by bcl2; release of cytochrome c from mitochondria blocked. *Science* **275**, 1129–1132.
- Yokoyama, C., Wang, X., Briggs, M.R., Admon, A., Wu, J., Hua, X., *et al.* (1993) SREBP-1, a basic-helix-loop-helix-leucine zipper protein that controls transcription of the low density lipoprotein. *Cell* **75**, 187–197.
- Yonehara, S., Ishii, A. and Yonehara, M. (1989) A cell killing monoclonal antibody (anti-Fas) to a cell surface antigen co-downregulated with the receptor of TNF. *J. Exp. Med.* **169**, 1747–1756.
- Yonish-Rouach, E., Resnitzky, D., Lotem, J., Sachs, L., Kimchi, A. and Oren, M. (1991) Wild-type p53 induces apoptosis of myeloid leukaemic cells that is inhibited by interleukin-6. *Nature (Lond.)*. **352**, 345–347.
- Yonish-Rouach, E., Grunwald, D., Wilder, S., Kimchi, A., May, E., Lawrence, J.-J., *et al.* (1993) p53-mediated cell death: relationship to cell cycle control. *Mol. Cell. Biol.* **13**, 1415–1423.
- Yuan, J.-Y., Shaham, S., Ledoux, S., Ellis, H.M. and Horvitz, H.R. (1993) The *C elegans* cell death gene *ced3* encodes a protein similar to mammalian ICE. *Cell* **75**, 641–652.
- Yuan, J.-Y. and Horvitz, H.R. (1990) The *C elegans* genes *ced3* and *ced4* act cell autonomously to cause programmed cell death. *Develop. Biol.* **138**, 35–41.
- Zambetti, G.P. and Levine, A.J. (1993) A comparison of the biological activities of wild-type and mutant

p53. *FASEB J.* **7**, 855–865.

Zanzami, N., Susin, S.A., Marchetti, P., Gomez-Monterrey, I., Castedo, M., Hirsch, T. and Kroemer, G. (1996) Mitochondrial control of nuclear apoptosis. *J. Exp. Med.* **183**, 1533–1544.

Zha, H., Fisk, H.A., Yaffe, M.P., Mahagan, N., Herman, B. and Reed, J.C. (1996) Structure-function comparisons of the pro-apoptotic protein bax in yeast and mammalian cells. *Mol. Cell. Biol.* **16**, 6494–6508.

Zhang, J., Dawson, V.L., Dawson, T.M. and Snyder, S.H. (1994) Nitric oxide activation of poly(ADP ribose) synthetase in neurotoxicity. *Science* **263**, 687–689.

Zhu, H., Fearnhead, H.O. and Cohen, G.M. (1995) An ICE-like protease is a common mediator of apoptosis induced by diverse stimuli in human monocytic THP.1 cells. *FEBS Letts.* **374**, 303–308.

Zou, H., Henzel, W.J., Liu, X., Lutschg, A., and Wang, X. (1997) Apaf-1, a human protein homologous to *C. elegans* ced4, participates in cytochrome c-dependent activation of caspase-3. *Cell* **90**, 405–413.

APPENDIX 1

RESEARCH COMMUNICATION

Activation of CPP32 and Mch3 α in wild-type p53-induced apoptosis

Julia M. CHANDLER*, Emad S. ALNEMRI†, Gerald M. COHEN* and Marion MacFARLANE*‡

*Medical Research Council Toxicology Unit, Hodgkin Building, University of Leicester, P.O. Box 138, Lancaster Road, Leicester LE1 9HN, U.K., and †Center for Apoptosis Research and the Kimmel Cancer Institute, Jefferson Medical College, Philadelphia, PA 19107, U.S.A.

DNA-damaging agents induce apoptosis primarily by a p53-dependent pathway. LTR6 cells containing a temperature-sensitive p53 were used to dissect further the mechanisms of p53-induced apoptosis. Apoptosis was accompanied by the processing

and activation of CPP32 and Mch3 α , together with the cleavage of poly(ADP-ribose) polymerase and lamin B₁. These results demonstrate a critical role for the activation of interleukin-1 β -converting enzyme-like proteases in p53-induced apoptosis.

INTRODUCTION

Apoptosis is the morphological description of an active form of cell death, largely distinct from necrosis, that is widespread in multicellular-organism development and plays an important role in tissue homeostasis [1]. Induced by a variety of cellular stresses, apoptosis is highly conserved between species and is characterized, among other features, by profound chromatin condensation and internucleosomal cleavage of DNA [1]. Recently, the importance of a novel family of cysteine proteases has become evident in apoptosis. Studies of the nematode worm *Caenorhabditis elegans* have identified two genes, *Ced3* and *Ced4*, which are absolutely required for cell death [2]. *Ced3* has significant structural and functional homology with interleukin-1 β -converting enzyme (ICE) [3], the founder member of an emerging family of mammalian cysteine proteases which includes CPP32/apopain [4,5], Mch2 [6], NEDD2/Ich1 [7,8], Ich2/TX [9,10], Mch3/ICE-LAP3 [11,12], ICE-LAP6/Mch6 [13,14], MACH/FLICE/Mch5 [15–17] and Mch4 [17]. These cysteine proteases exist primarily as inactive proforms in normal cells and require processing at critical aspartate residues for activation (reviewed in [18]). Several cellular proteins have been identified as substrates of the ICE family of cysteine proteases (reviewed in [19]). These include poly(ADP-ribose) polymerase (PARP), an enzyme required for DNA repair and maintenance of genome integrity, which is cleaved primarily by CPP32 and Mch3 α [5,11,20], and nuclear lamins which are cleaved by Mch2 α [21,22].

Although there are exceptions [23,24], apoptosis induced by DNA-damaging agents such as etoposide and ionizing radiation, is primarily mediated by the nuclear phosphoprotein p53 [25,26]. Wild-type p53 is classified as a tumour suppressor gene because loss of this protein is a feature of more than half of all human tumours [27] and because mice that have no functional p53 gene rapidly develop multiple lesions [28]. DNA-damaging agents lead to the accumulation of wild-type p53 by post-translational stabilization [29] causing either cell cycle arrest at G₀/G₁, which facilitates DNA repair [30], or, in some systems, the induction of apoptosis [31].

One of the best models for studying mechanisms of p53 action

is the temperature-sensitive cell line, LTR6. LTR6 cells are a subclone of the murine myeloid leukaemic M1 cell line, stably transfected with a gene encoding a temperature-sensitive p53 protein. The transfected protein behaves as the mutant protein at 37.5 °C and as the wild-type protein at 32.5 °C. Cells shifted from 37.5 to 32.5 °C show no evidence of a cell cycle arrest [32] but instead rapidly lose viability and undergo apoptosis [31]. Although wild-type p53 leads to the induction of apoptosis in some systems, there has been no evidence to link wild-type p53 induction with the activation of ICE-like proteases. Using the LTR6 cell line we provide direct evidence for the activation of CPP32 and Mch3 α , and indirect evidence for the activation of Mch2 α . Our data support a mechanism of p53-induced apoptosis involving the sequential activation of members of the ICE family of cysteine proteases.

MATERIALS AND METHODS

Media and serum were purchased from Gibco (Paisley, Scotland, U.K.). Benzylloxycarbonyl-Asp-Glu-Val-Asp-7-amino-4-trifluoromethylcoumarin (Z-DEVD.AFC) was from Enzyme Systems Inc. (Dublin, CA, U.S.A.). Acetyl-Tyr-Val-Ala-Asp-7-amino-4-methylcoumarin (Ac-YVAD.AMC) and all other chemicals were from Sigma Chemical Co. (Poole, Dorset, U.K.).

Cell culture

The murine myeloid leukaemic cell lines M1 (parental; p53 null), LTRphe132 (non-temperature-sensitive mutant p53) and LTR6 (temperature-sensitive mutant p53) were generously given by Professor Moshe Oren (Weizmann Institute, Rehovot, Israel). All three cell lines were cultured in RPMI 1640 medium with L-glutamine, supplemented with 10% heat-inactivated foetal-calf serum in CO₂/air (1:19) and at 37.5 °C [31]. For the temperature shift, cells were transferred to a second incubator maintained at 32.5 °C.

Abbreviations used: Ac-YVAD.AMC, acetyl-Tyr-Val-Ala-Asp-7-amino-4-methylcoumarin; ICE, interleukin-1 β -converting enzyme; PARP, poly(ADP-ribose) polymerase; Z-DEVD.AFC, benzylloxycarbonyl-Asp-Glu-Val-Asp-7-amino-4-trifluoromethylcoumarin.

‡ To whom correspondence should be addressed.

Flow cytometry and fluorescence microscopy

Flow-cytometric analysis was used to quantify apoptosis as described previously, with minor modifications [33]. The cells were stained at 37 °C for 10 min in the presence of 1.8 μ M Hoechst 33342. Propidium iodide (7.5 μ M) in PBS was added and the cells were analysed by flow cytometry (Becton Dickinson FACS Vantage), or examined by fluorescence microscopy.

Conventional agarose-gel electrophoresis

After the appropriate treatment, 0.75×10^6 cells/lane were applied on to a 1.8% agarose gel and separated by electrophoresis. The gels were analysed for the presence of internucleosomal cleavage as described previously [33].

Western blot analysis

After the appropriate treatment, cells were subjected to SDS/PAGE and Western blotting as described previously [34]. The membranes were probed using a rabbit polyclonal antibody to the p17 subunit of CPP32 (kindly provided by Merck Frosst, Canada), a rabbit polyclonal antibody to PARP (318) (kindly provided by Dr. G. G. Poirier, Laval University, Quebec, Canada), a mouse monoclonal antibody to lamin B₁ (Serotec Ltd., Oxford, U.K.) and a rabbit polyclonal antibody raised to the p17 fragment of recombinant Mch3 α . Western-blot analysis verified that the antibody to Mch3 α recognized both intact Mch3 α (~ 36 kDa) and the p19 subunit, but did not recognize CPP32 (M. MacFarlane, K. Cain, X.-M. Sun, E. S. Alnemri and G. M. Cohen; unpublished work). Detection was achieved using the appropriate secondary antibody conjugated to horseradish peroxidase and enhanced chemiluminescence (Amersham Life Sciences, Little Chalfont, Bucks., U.K.).

Lysate preparation and fluorometric measurement of proteolytic activity

Lysates from LTR6 cells were prepared as described previously for other cell lines [34]. The proteolytic activity of LTR6 cell lysates was measured using a continuous fluorimetric assay modified from the method of Thornberry [35]. Cleavage of Z-DEVD.AFC, which mimics the CPP32/Mch3 α cleavage site within PARP, and Ac-YVAD.AMC, which mimics the ICE cleavage site within proIL1 β , releases the fluorescent moieties 7-amino-4-trifluoromethylcoumarin (AFC) and 7-amino-4-methylcoumarin (AMC) respectively. This allows the quantitative analysis of any CPP32/Mch3 α - and ICE-like proteolytic activity. Liberation of AFC and AMC was measured using excitation wavelengths of 400 and 380, and emission wavelengths of 505 nm and 460 nm respectively. Lysates in 1.25 ml of 100 mM Hepes/10% (w/v) sucrose/0.1% (w/v) CHAPS/10 mM dithiothreitol, pH 7.5, were assayed at 37 °C in a modified cuvette holder fitted with a thermostat (Perkin-Elmer LS50B luminescence fluorimeter). Routinely, assays contained 15 μ g of lysate protein and 20 μ M substrate.

RESULTS

Wild-type p53 induces apoptosis in murine LTR6 cells

The murine LTR6 cell line contains a temperature-sensitive p53 protein that shows mutant characteristics at 37.5 °C and is indistinguishable from the wild-type protein at 32.5 °C [31,36]. Cells transferred to 32.5 °C for 22 h showed apoptotic characteristics, such as chromatin condensation and increased internucleosomal cleavage, which accorded with previous studies (Figures 1A and 1B; [31]). To obtain a quantitative rather than

qualitative assessment of p53-induced apoptosis in these cells, a modified flow-cytometric technique was used [33]. When temperature-shifted LTR6 cells were examined by flow cytometry, two distinct populations were observed: an apoptotic population of cells with high Hoechst 33342 fluorescence and a normal population with low Hoechst 33342 fluorescence. In contrast, no apoptotic population was detected in cells retained at 37.5 °C for 22 h (Figure 1C). To confirm that the apoptotic effects reported here were induced by the change in p53 status, two related cell lines, LTRphe132 and M1, were studied. LTRphe132 cells contain a non-temperature-sensitive mutant p53 and the M1 cells are the p53 null cell line from which both mutant lines are derived [31]. When LTRphe132 and M1 cells were transferred to 32.5 °C for 22 h, the cells retained normal morphology and displayed no chromatin condensation, internucleosomal cleavage or increase in Hoechst 33342 fluorescence (results not shown). Therefore the apoptotic changes observed in the LTR6 cells were a consequence of wild-type p53 induction.

Activation of CPP32 and Mch3 α in wild-type-p53-induced apoptosis

Cysteine proteases showing extensive structural and functional similarity to *Ced3* have been shown to play a pivotal role in mammalian apoptosis induced by a wide variety of stimuli. To determine whether members of this family of cysteine proteases play a role in p53-induced apoptosis, LTR6 cells were incubated at 32.5 °C or retained at 37.5 °C for up to 22 h. Cells transferred to 32.5 °C and assessed by flow cytometry showed a time-dependent increase in apoptosis, which increased significantly after 14–16 h at the permissive temperature (Figure 2). Cells retained at 37.5 °C for 22 h showed a basal level of apoptosis of approx. 9% when assessed by this method (Figure 2). Using antibodies raised to the p17 subunits of CPP32 and Mch3 α , Western blots were used to look for evidence of processing of these two ICE homologues. After approx. 14 h at the permissive temperature, loss of the pro-forms of both CPP32 and Mch3 α was detected, concomitant with the appearance of the p17 and p19 cleavage fragments of CPP32 and Mch3 α respectively (Figure 2). Therefore the processing of both CPP32 and Mch3 α accompanied p53-induced apoptosis in LTR6 cells.

p53-induced apoptosis in LTR6 cells is accompanied by cleavage of identified substrates of ICE-like proteases

To assess further the involvement of ICE-like proteases in p53-induced apoptosis, cleavage of two cellular proteins, PARP and lamin B₁, known to be substrates for this family of cysteine proteases, was examined. The induction of wild-type p53 resulted in the cleavage of PARP into its signature apoptotic fragments after approx. 10–12 h, and provided further evidence for the presence of CPP32/Mch3 α -like proteolytic activity within these cells (Figure 3). Wild-type p53 induced the cleavage of lamin B₁ but this was not evident until after 16 h at the permissive temperature (Figure 3). This result is in agreement with previous observations that lamin cleavage is a relatively late event in the apoptotic pathway, occurring after the degradation of PARP [37,38]. The cleavage of lamin B₁ in LTR6 cells provided indirect evidence of Mch2 α activity induced by wild-type p53, as Mch2 α is the only ICE-like protease identified that is able to cleave lamins [21,22]. Thus p53-induced apoptosis in LTR6 cells is accompanied by the cleavage of cellular proteins known to be substrates of CPP32, Mch3 α and Mch2 α .

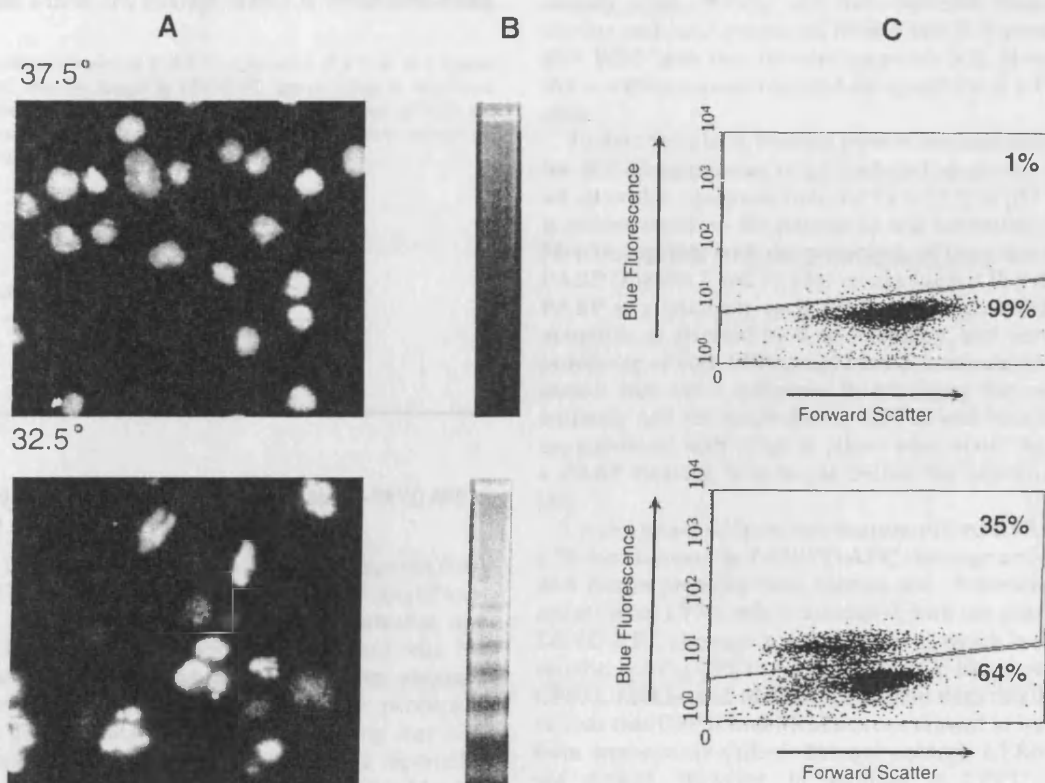


Figure 1 Wild-type-p53-induced apoptosis in LTR6 cells

LTR6 cells were transferred to 32.5 °C (lower panels) or retained at 37.5 °C (upper panels) for 22 h. (A) Cells were double-stained with Hoechst 33342 and propidium iodide and examined by fluorescence microscopy. (B) Cells were analysed for formation of internucleosomal DNA fragments by conventional agarose-gel electrophoresis. (C) Cells were double-stained as in (A) and analysed by flow cytometry. The numbers in each region of the cytogram represent the percentage of cells exhibiting basal and increased Hoechst 33342 fluorescence. The results shown are from a typical experiment and demonstrate that cells transferred to 32.5 °C for 22 h exhibit apoptotic morphology, increased internucleosomal cleavage of DNA and increased Hoechst 33342 fluorescence.

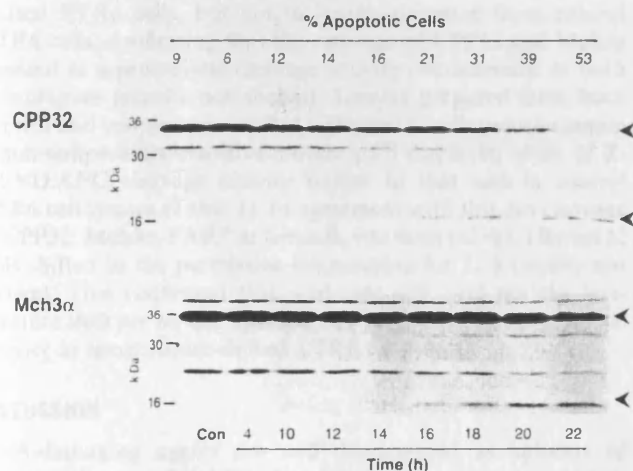


Figure 2 Wild-type-p53-induced processing of CPP32 and Mch3 α

LTR6 cells were incubated for up to 22 h at 32.5 °C (lanes 2–9) or retained at 37.5 °C (lane 1; control). Lanes are numbered from the left. The percentage of apoptotic cells at each time point (determined by flow cytometry) is indicated above the appropriate lane. Samples were taken from the same experiment to determine the extent of processing of both CPP32 and Mch3 α . Cellular proteins were separated by SDS 13% (w/v) PAGE, and Western blotting was carried out using antibodies to CPP32 (upper panel) and Mch3 α (lower panel). The proform (upper arrowheads) and major subunit (lower arrowheads) of each protease are indicated. Molecular-mass markers are indicated in kDa on the left.

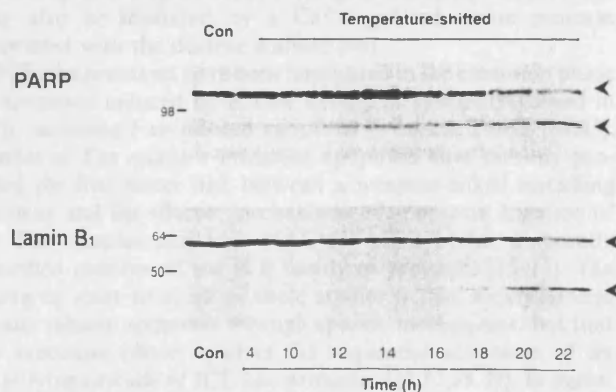


Figure 3 Wild-type p53 induces PARP and lamin B $_1$ cleavage

LTR6 cells were incubated for up to 22 h at 32.5 °C (lanes 2–9) or retained at 37.5 °C (lane 1; control). Lanes are numbered from the left. Cellular proteins were separated by SDS 7% (w/v) PAGE (PARP) or SDS/10% (w/v) PAGE (lamin B $_1$) and Western blotting was carried out to assess the incidence of PARP cleavage (upper panel) and lamin B $_1$ cleavage (lower panel). The intact substrates (upper arrowheads) and their cleavage fragments (lower arrowheads) are indicated. Molecular-mass markers are indicated in kDa on the left.

Table 1 Increased Z-DEVD.AFC cleavage activity in temperature-shifted LTR6 cell lysates

LTR6 and LTRphe132 cells were transferred to 32.5 °C or retained at 37.5 °C for 22 h. Lysates prepared from these cells were then assayed for Z-DEVD.AFC cleavage activity as described in the Materials and methods section. The specific activities of control lysates (37.5 °C) and lysates prepared from temperature-shifted cells (32.5 °C) are shown. The values represent the means \pm S.E.M. for three experiments.

Temperature °C	Specific activity (pmol/min per mg of protein)	
	LTR6	LTRphe132
37.5	130 \pm 60	30 \pm 15
32.5	3580 \pm 1220	90 \pm 10

Lysates prepared from apoptotic LTR6 cells exhibit Z-DEVD.AFC cleavage activity

To characterize the proteolytic activity in lysates prepared from temperature-shifted LTR6 cells, Ac-YVAD.AMC, a model substrate for ICE activity was used to determine whether any activation of ICE had occurred in temperature-shifted cells. No hydrolysis of Ac-YVAD.AMC was detected in lysates obtained from either control cells or cells shifted to the permissive temperature for 22 h (results not shown), suggesting that ICE may not be activated by wild-type p53. Others have reported a peak of ICE-like proteolytic activity preceding a CPP32/Mch3 α -like activity [39]; therefore, at this stage, we cannot exclude the possibility that there is a small but transient increase in ICE activity which may occur before 22 h. In marked contrast, using Z-DEVD.AFC, which mimics the CPP32/Mch3 α cleavage site within PARP, lysates from temperature-shifted LTR6 cells showed at least a 28-fold increase in Z-DEVD.AFC cleavage activity above that seen in lysates prepared from control LTR6 cells (Table 1). Processing of the pro-forms of both CPP32 and Mch3 α was detected in lysates prepared from temperature-shifted LTR6 cells, but not in lysates prepared from control LTR6 cells, confirming that the cleavage of CPP32 and Mch3 α resulted in a proteolytic cleavage activity characteristic of both homologues (results not shown). Lysates prepared from both control and temperature-shifted LTRphe132 cells (which contain a non-temperature-sensitive mutant p53) displayed levels of Z-DEVD.AFC cleavage activity similar to that seen in control LTR6 cell lysates (Table 1). In agreement with this, no cleavage of CPP32, Mch3 α , PARP or lamin B₁ was detected in LTRphe132 cells shifted to the permissive temperature for 22 h (results not shown). This confirmed that wild-type p53, and not the temperature shift *per se*, had induced CPP32/Mch3 α -like proteolytic activity in temperature-shifted LTR6 cell lysates.

DISCUSSION

DNA-damaging agents are well documented as inducers of apoptosis (reviewed in [40]). A number of these agents including etoposide, UV light and ionizing radiation induce apoptosis primarily via a p53-dependent mechanism [29]. DNA damage induced by these agents results in the accumulation of wild-type p53 by post-translational stabilization causing either cell-cycle arrest or apoptosis. Apoptosis was induced in LTR6 cells containing a temperature-sensitive mutant p53 transgene, by incubation at the permissive temperature for up to 22 h (Figure 1; [31]). Although the precise biochemical effects mediated by p53 in apoptosis have yet to be determined, wild-type p53

directly *trans*-activates and *trans*-represses transcription from the *bax* and *bcl-2* promoters respectively [41], resulting in a high Bax:Bcl-2 ratio that favours apoptosis [42]. However, whether this is a crucial event required for apoptosis in LTR6 cells is not clear.

To date there have been no reports demonstrating a direct role for ICE-like proteases in p53-induced apoptosis. In this report we show that apoptosis induced by wild-type p53 in LTR6 cells is accompanied by the processing and activation of CPP32 and Mch3 α , together with the proteolysis of their common substrate PARP (Figures 2 and 3). Our results suggest that the cleavage of PARP is a relatively early event, which precedes the onset of apoptosis as assessed by flow cytometry, and occurs before the processing of both CPP32 and Mch3 α is detectable. Although we cannot rule out a difference in sensitivity between the PARP antibody and the antibodies to CPP32 and Mch3 α , our results are consistent with those of others who report the activation of a PARP-cleaving homologue before the activation of CPP32 [43].

Lysates prepared from temperature-shifted LTR6 cells showed a 28-fold increase in Z-DEVD.AFC cleavage activity compared with lysates prepared from control cells. Therefore p53-induced apoptosis in LTR6 cells is associated with the generation of a Z-DEVD.AFC cleavage activity (Table 1) which is attributable to members of the CPP32 subfamily of ICE-like proteases, namely CPP32, Mch3 α and Mch2 α . Consistent with this are our observations that CPP32 and Mch3 α are processed in lysates prepared from temperature-shifted, but not control, LTR6 cells (results not shown). However, in addition to CPP32, Mch3 α and Mch2 α , we cannot exclude the possibility that the increase in Z-DEVD.AFC cleavage activity observed in temperature-shifted LTR6 cells may be due, in part, to another as yet unidentified CPP32 subfamily member(s) that also cleaves PARP.

Besides the activation of CPP32 and Mch3 α during wild-type p53-induced apoptosis, we also report the p53-induced cleavage of lamin B₁. Lamin cleavage occurs after the occurrence of PARP cleavage (Figure 3, bottom panel), in agreement with previous studies [37,38]. To date, Mch2 α is the only ICE homologue reported to be capable of cleaving nuclear lamins [21,22]. The cleavage of lamin B₁ in our system provides indirect evidence for the involvement of a third ICE homologue, Mch2 α , in p53-induced apoptosis. However, we cannot exclude the possibility that the proteolytic cleavage of lamin B₁ in LTR6 cells may also be mediated by a Ca²⁺-regulated serine protease associated with the nuclear scaffold [44].

ICE-like proteases have been implicated in the execution phase of apoptosis induced by a wide variety of stimuli (reviewed in [19]), including Fas-induced apoptosis in Jurkat T-cells [34,45]. Studies of Fas receptor-mediated apoptosis have recently provided the first direct link between a receptor-linked signalling pathway and the effector mechanisms of apoptosis. Ligation of the Fas receptor activates MACH/FLICE/Mch5, a recently identified member of the ICE family of proteases [15–17]. The emerging tenet from all of these studies is that widely diverse stimuli initiate apoptosis through specific mechanisms, but that the execution phase involves the sequential activation of an amplifying cascade of ICE-like proteases [13,17,38,39]. In agreement with these observations, the p53-induced apoptosis described here provides a further example of an apoptotic stimulus that feeds into the common apoptotic execution pathway involving the sequential activation of ICE-like proteases.

The results of the present study provide a direct link between p53-induced apoptosis and the activation of members of the ICE-family of proteases. We have shown that p53-induced apoptosis is accompanied by the processing and activation of

CPP32, Mch3 α and a lamin protease, together with the cleavage of their substrates, PARP and lamin B₁. In summary, our data support a functional role for the sequential activation of ICE-like proteases in the execution phase of p53-induced apoptosis.

We thank Professor M. Oren for the LTR6, LTRphe132 and M1 cell lines. We also thank Dr. D. W. Nicholson, Merck Frosst, for the CPP32 antibody and Dr. G. G. Poirier for the PARP antibody. We thank Dr. X.-M. Sun for generating the antibody to Mch3 α , Dr. K. Cain for help and advice with the fluorometric measurement of proteolytic cleavage activity and Mr. R. T. Snowden for help with the flow cytometry. J. M. C. is the recipient of a grant from the Medical Research Council.

REFERENCES

- Arends, M. J. and Wyllie, A. H. (1991) *Int. Rev. Exp. Pathol.* **32**, 223–254
- Hengartner, M. O. and Horvitz, H. R. (1994) *Curr. Opin. Genet. Dev.* **4**, 581–586
- Yuan, J.-Y., Shaham, S., Ledoux, S., Ellis, H. M. and Horvitz, H. R. (1993) *Cell* **75**, 641–652
- Fernandes-Alnemri, T., Litwack, G. and Alnemri, E. S. (1994) *J. Biol. Chem.* **269**, 30761–30764
- Nicholson, D. W., Ali, A., Thornberry, N. A., Vaillancourt, J. P., Ding, C. K., Gallant, M., Gareau, Y., Griffin, P. R., Labelle, M., Lazebnik, Y. A. et al. (1995) *Nature (London)* **376**, 37–43
- Fernandes-Alnemri, T., Litwack, G. and Alnemri, E. S. (1995) *Cancer Res.* **55**, 2737–2742
- Kumar, S., Kinoshita, M., Noda, M., Copeland, N. G. and Jenkins, N. A. (1994) *Genes Dev.* **8**, 1613–1626
- Wang, L., Miura, M., Bergeron, L., Zhu, H. and Yuan, J. (1994) *Cell* **78**, 739–750
- Faucheu, C., Diu, A., Chan, A. W. E., Blanchet, A. M., Miossec, C., Herve, F., Collard-Dutilleul, V., Gu, Y., Aldape, R. A., Lippke, J. A. et al. (1995) *EMBO J.* **14**, 1914–1922
- Kamens, J., Paskind, M., Hugunin, M., Talanian, R. V., Allen, H., Banach, D., Bump, N., Hackett, M., Johnston, C. G., Li, P. et al. (1995) *J. Biol. Chem.* **270**, 15250–15256
- Fernandes-Alnemri, T., Takahashi, A., Armstrong, R., Krebs, J., Fritz, L., Tomaselli, K. J., Wang, L., Yu, Z., Croce, C. M., Salveson, G. et al. (1995) *Cancer Res.* **55**, 6045–6052
- Duan, H., Chinnaiyan, A. M., Hudson, P. L., Wing, J. P., He, W.-W. and Dixit, V. M. (1996) *J. Biol. Chem.* **271**, 1621–1625
- Duan, H., Orth, K., Chinnaiyan, A. M., Poirier, G. G., Froelich, C. J., He, W.-W. and Dixit, V. M. (1996) *J. Biol. Chem.* **271**, 16720–16724
- Srinivasula, S. M., Fernandes-Alnemri, T., Zangrilli, J., Robertson, N., Armstrong, R. C., Wang, L., Trapani, J. A., Tomaselli, K. J., Litwack, G. and Alnemri, E. S. (1996) *J. Biol. Chem.* **271**, 27099–27106
- Boldin, M. P., Goncharov, T. M., Goltsev, Y. V. and Wallach, D. (1996) *Cell* **85**, 803–815
- Muzio, M., Chinnaiyan, A. M., Kischkel, F. C., O'Rourke, K., Shevchenko, A., Ni, J., Scaffidi, C., Bretz, J. D., Zhang, M., Gentz, R. et al. (1996) *Cell* **85**, 817–827
- Fernandes-Alnemri, T., Armstrong, R. C., Krebs, J., Srinivasula, S. M., Wang, L., Bullrich, F., Fritz, L. C., Trapani, J. A., Tomaselli, K. J., Litwack, G. and Alnemri, E. S. (1996) *Proc. Natl. Acad. Sci. U.S.A.* **93**, 7464–7469
- Thornberry, N. A. and Molineaux, S. M. (1995) *Protein Sci.* **4**, 3–12
- Martin, S. J. and Green, D. R. (1995) *Cell* **82**, 349–352
- Lazebnik, Y. A., Kaufmann, S. H., Desnoyers, S., Poirier, G. G. and Earnshaw, W. C. (1994) *Nature (London)* **371**, 346–347
- Orth, K., Chinnaiyan, A. M., Garg, M., Froelich, C. J. and Dixit, V. M. (1996) *J. Biol. Chem.* **271**, 16443–16446
- Takahashi, A., Alnemri, E. S., Lazebnik, Y. A., Fernandes-Alnemri, T., Litwack, G., Moir, R. D., Goldman, R. D., Poirier, G. G., Kaufmann, S. H. and Earnshaw, W. C. (1996) *Proc. Natl. Acad. Sci. U.S.A.* **96**, 8395–8400
- Strasser, A., Harris, A. W., Jacks, T. and Cory, S. (1994) *Cell* **79**, 329–339
- MacFarlane, M., Jones, N. A., Dive, C. and Cohen, G. M. (1996) *Mol. Pharmacol.* **50**, 900–911
- Clarke, A. R., Purdie, C. A., Harrison, D. J., Morris, R. G., Bird, C. C., Hooper, M. L. and Wyllie, A. H. (1993) *Nature (London)* **362**, 849–852
- Lowe, S. W., Schmitt, E. M., Smith, S. W., Osborne, B. A. and Jacks, T. (1993) *Nature (London)* **362**, 847–849
- Hollstein, M., Sidransky, D., Vogelstein, B. and Harris, C. C. (1991) *Science* **253**, 49–52
- Donehower, L. A., Harvey, M., Slagle, B. L., McArthur, M. J., Montgomery, Jr., C. A., Butel, J. S. and Bradley, A. (1992) *Nature (London)* **356**, 215–221
- Kastan, M. B., Onyekwere, O., Sidransky, D., Vogelstein, B. and Craig, R. W. (1991) *Cancer Res.* **51**, 6304–6311
- Ryan, J. J., Danish, R., Gottlieb, C. A. and Clarke, M. F. (1993) *Mol. Cell. Biol.* **13**, 711–719
- Yonish-Rouach, E., Resnitzky, D., Lotem, J., Sachs, L., Kimchi, A. and Oren, M. (1991) *Nature (London)* **352**, 345–347
- Yonish-Rouach, E., Grunwald, D., Wilder, S., Kimchi, A., May, E., Lawrence, J.-J., May, P. and Oren, M. (1993) *Mol. Cell. Biol.* **13**, 1415–1423
- Sun, X.-M., Snowden, R. T., Skilleter, D. N., Dinsdale, D., Ormerod, M. G. and Cohen, G. M. (1992) *Anal. Biochem.* **204**, 351–356
- Slee, E. A., Zhu, H., Chow, S. C., MacFarlane, M., Nicholson, D. W. and Cohen, G. M. (1996) *Biochem. J.* **315**, 21–24
- Thornberry, N. A. (1994) *Methods Enzymol.* **244**, 615–631
- Michalovitz, D., Halevy, O. and Oren, M. (1990) *Cell* **62**, 671–680
- Lazebnik, Y. A., Takahashi, A., Moir, R. D., Goldman, R. D., Poirier, G. G., Kaufmann, S. H. and Earnshaw, W. C. (1995) *Proc. Natl. Acad. Sci. U.S.A.* **92**, 9042–9046
- Greidinger, E. L., Miller, D. K., Yamin, T.-T., Casciola-Rosen, L. and Rosen, A. (1996) *FEBS Lett.* **390**, 299–303
- Enari, M., Talanian, R. V., Wong, W. W. and Nagata, S. (1996) *Nature (London)* **380**, 723–726
- Donehower, L. A. (1994) *Cancer Bull.* **46**, 161–166
- Miyashita, T., Krajewski, S., Krajewska, M., Wang, H. G., Lin, H. K., Liebermann, D. A., Hoffman, B. and Reed, J. C. (1994) *Oncogene* **9**, 1799–1805
- Oltvai, Z. N., Millman, C. L. and Korsmeyer, S. J. (1993) *Cell* **74**, 609–619
- An, S. and Knox, K. A. (1996) *FEBS Lett.* **386**, 115–122
- Clawson, G. A., Norbeck, L. L., Hatem, C. L., Rhodes, C., Amiri, P., McKerrow, J. H., Patierno, S. R. and Fiskum, G. (1992) *Cell Growth Differ.* **3**, 827–838
- Schlegel, J., Peters, I., Orrenius, S., Miller, D. K., Thornberry, N. A., Yamin, T.-T. and Nicholson, D. W. (1996) *J. Biol. Chem.* **271**, 1841–1844

APPENDIX 2

Different Subcellular Distribution of Caspase-3 and Caspase-7 following Fas-induced Apoptosis in Mouse Liver*

(Received for publication, December 29, 1997, and in revised form, February 16, 1998)

Julia M. Chandler, Gerald M. Cohen,
and Marion MacFarlane†

From the Medical Research Council Toxicology Unit, Hodgkin Building, University of Leicester, P. O. Box 138, Lancaster Road, Leicester LE1 9HN, United Kingdom

Caspases play a key role in the execution phase of apoptosis. "Initiator" caspases, such as caspase-8, activate "effector" caspases, such as caspase-3 and -7, which subsequently cleave cellular substrates thereby precipitating the dramatic morphological changes of apoptosis. Following treatment of mice with an agonistic anti-Fas antibody to induce massive hepatocyte apoptosis, we now demonstrate a distinct subcellular localization of the effector caspases-3 and -7. Active caspase-3 is confined primarily to the cytosol, whereas active caspase-7 is associated almost exclusively with the mitochondrial and microsomal fractions. These data suggest that caspases-3 and -7 exert their primary functions in different cellular compartments and offer a possible explanation of the presence of caspase homologs with overlapping substrate specificities. Translocation and activation of caspase-7 to the endoplasmic reticulum correlates with the proteolytic cleavage of the endoplasmic reticular-specific substrate, sterol regulatory element-binding protein 1. Liver damage, induction of apoptosis, activation and translocation of caspase-7, and proteolysis of sterol regulatory element-binding protein 1 are all blocked by the caspase inhibitor, benzyloxycarbonyl-Val-Ala-Asp fluoromethyl ketone (Z-VAD.fmk). Our data demonstrate for the first time the differential subcellular compartmentalization of specific effector caspases following the induction of apoptosis *in vivo*.

Apoptosis is a crucial mechanism by which multicellular organisms control cell numbers and ensure the removal of damaged or potentially harmful cells (1). Administration of an agonistic anti-Fas antibody results in ligation of the Fas (CD95, APO-1) receptor, extensive hepatocyte apoptosis, and liver damage (2). The intracellular death domain of the Fas receptor binds to FADD/MORT1, which in turn recruits and activates caspase-8 (MACH/FLICE/Mch5) through its N-terminal death effector domain (3–5). Recombinant caspase-8 cleaves and activates all other known caspases and has been proposed to be at the apex of a hypothetical caspase cascade (3–5). Caspases are

a family of aspartate-specific cysteine proteases, which pre-exist in the cytoplasm as single chain inactive zymogens (6, 7). They are proteolytically processed to active heterodimeric enzymes during the execution phase of apoptosis. Caspases may be divided into "initiator" caspases with long prodomains (caspases-8, -9, and -10), which activate "effector" caspases with short prodomains (caspases-3, -6, and -7), which in turn cleave intracellular substrates, resulting in the dramatic morphological and biochemical changes of apoptosis (6–8). Following Fas-induced apoptosis of cells *in vitro*, activation of a number of caspases, including caspases-3, -4, -6, -7, -8, and a caspase-1-like activity have all been reported (4, 9–13).

To date, a family of at least 10 caspases have been identified, but it is not known precisely which of these caspase(s) are activated *in vivo* and which are responsible for the cleavage of particular substrates. Many of the caspases have overlapping substrate specificities, suggesting that there may be redundancy (6, 7, 14). Many cellular proteins are cleaved during the execution phase of apoptosis at a DXXD motif by the effector caspases-3 and -7 (reviewed in Refs. 6 and 7). Relatively little is known about the subcellular distribution of the caspases. Caspase-1 is found predominantly in the cytosol (15) although some has been localized to the external cell surface membrane (16). Other caspases have been considered to be cytosolic, a conclusion based largely on data with caspase-1 and on the isolation and purification of caspase-3 (17). In this study, we demonstrate for the first time the differential subcellular distribution of specific caspases during the induction of apoptosis *in vivo*. Following Fas-induced apoptosis *in vivo*, active caspase-3 is found primarily in the cytosol, whereas active caspase-7 is associated almost exclusively with the mitochondrial and microsomal fractions. Both the activation of caspase-7 in the endoplasmic reticulum and the cleavage of the endoplasmic reticular-specific substrate, sterol regulatory element-binding protein 1 (SREBP-1),¹ are blocked by the caspase inhibitor benzyloxycarbonyl-Val-Ala-Asp fluoromethyl ketone (Z-VAD.fmk). These results support the hypothesis that during the execution phase of apoptosis, different caspase homologs cleave specific substrates in different cellular compartments.

EXPERIMENTAL PROCEDURES

Mice—In this study 6–8-week-old (20 g) Balb/c males were used. All mice were bred in the Biomedical Sciences Department of the University of Leicester.

Anti-Fas Antibody and Caspase Inhibitor Z-VAD.fmk—Mice were injected either with 10 µg of purified hamster monoclonal antibody to mouse Fas (JO2) (PharMingen, Los Angeles, CA) (2) in 160 µl of 0.9% (w/v) saline, 12.5% (v/v) Me₂SO, or 160 µl of 0.9% (w/v) saline, 12.5% (v/v) Me₂SO (controls). Where indicated, mice were injected with JO2 antibody (10 µg) in 80 µl of 0.9% (w/v) saline followed 5 min later by Z-VAD.fmk (500 µg) (Enzyme Systems Ltd., Dublin, CA) in 80 µl of 0.9% (w/v) saline, 25% (v/v) Me₂SO. Animals were sacrificed at the indicated times by cervical dislocation.

Tissue Preparation and Histopathological Examination—Livers were removed and fixed in 10% formaldehyde in buffered saline. Rep-

* The costs of publication of this article were defrayed in part by the payment of page charges. This article must therefore be hereby marked "advertisement" in accordance with 18 U.S.C. Section 1734 solely to indicate this fact.

† To whom correspondence should be addressed. Tel.: 44-116-2525553; Fax: 44-116-2525616; E-mail: mm21@le.ac.uk.

¹ The abbreviations used are: SREBP, sterol regulatory element-binding protein; Z-VAD.fmk, benzyloxycarbonyl-Val-Ala-Asp fluoromethyl ketone; Z-DEVD.afc, benzyloxycarbonyl-Asp-Glu-Val-Asp-7-amino-4-trifluoromethylcoumarin; DEVDase, proteolytic activity to cleave Z-DEVD.afc; MOPS, 4-morpholinepropanesulfonic acid; CHAPS, 3-[(3-cholamidopropyl)dimethylammonio]-1-propanesulfonate; PAGE, polyacrylamide gel electrophoresis.

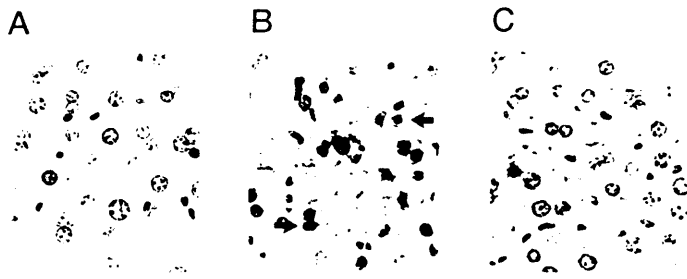


FIG. 1. Fas-induced hepatocyte apoptosis *in vivo* is inhibited by Z-VAD.fmk. Liver sections were prepared from control mice (A), mice 4 h after intravenous injection of the agonistic Fas receptor antibody JO2 (10 μ g) (B), and mice 4 h after intravenous injection of the antibody together with the caspase inhibitor Z-VAD.fmk (C) as described under "Experimental Procedures." The arrows indicate examples of hepatocytes with typical apoptotic morphology.

representative sections of the left lateral, median, and posterior lobes were stained with hematoxylin and eosin and examined for apoptosis.

Fractionation of Liver—Following removal of the livers, excess hair and blood were removed by washing several times in buffer A (0.3 M mannitol, 5 mM MOPS, 1 mM EGTA, 4 mM KH_2PO_4). The livers were then chopped up and homogenized using a dounce homogenizer in 5 ml of buffer A supplemented with protease inhibitors (20 μ g/ml leupeptin, 10 μ g/ml pepstatin A, 10 μ g/ml aprotinin, 2 mM phenylmethylsulfonyl fluoride). The crude homogenates were centrifuged at $650 \times g$ for 10 min at 4 $^\circ\text{C}$ and the resultant supernatant centrifuged at $10,000 \times g$ for 15 min at 4 $^\circ\text{C}$ to sediment the mitochondria. The mitochondria were washed in supplemented buffer A and pelleted. The microsomal and cytosolic fractions were obtained following centrifugation of the $10,000 \times g$ supernatant fraction at $100,000 \times g$ for 45 min at 4 $^\circ\text{C}$. Purity of the mitochondrial, cytosolic, and microsomal fractions was assessed by Western blotting using antibodies to cytochrome *c* oxidase subunit IV (Molecular Probes, Eugene, OR), glutathione *S*-transferase π (18) (kindly provided by Dr. M. Manson, Medical Research Council Toxicology Unit) and SREBP-1. Cytochrome *c* oxidase subunit IV is located on the inner mitochondrial membrane (19), glutathione *S*-transferase π is a cytosolic enzyme (20), and SREBP-1 is located in the endoplasmic reticulum (21). Densitometric analysis revealed that 77, 9, and 14% of total glutathione *S*-transferase and 5, 93, and 2% of total cytochrome *c* oxidase subunit IV were detected in the cytosolic, mitochondrial, and microsomal fractions, respectively. SREBP-1 was found almost exclusively in the endoplasmic reticulum (Fig. 4 and data not shown).

Western Blotting—SDS-PAGE and Western blotting were carried out on liver fractions as described previously (22). The membranes were probed using a rabbit polyclonal antibody to the p17 subunit of caspase-3 (kindly provided by Merck Frosst, Quebec, Canada) (11, 23), a rabbit polyclonal antibody to the p17 fragment of caspase-7 (22), and a rabbit polyclonal antibody to amino acids 470–479 of human SREBP-1 (Santa Cruz Biotechnology, Inc., Santa Cruz, CA).

Fluorometric Measurement of Proteolytic Activity—The proteolytic activity of the liver fractions was measured using a continuous fluorometric assay with benzoyloxycarbonyl-Asp-Glu-Val-Asp-7-amino-4-trifluoromethylcoumarin (Z-DEVD.afc) (Enzyme Systems Products, Dublin, CA) as substrate as described previously (22). Cleavage of Z-DEVD.afc releases the fluorescent moiety, 7-amino-4-trifluoromethylcoumarin, allowing the quantitative analysis of the proteolytic activities of caspases-3 and -7 (referred to as DEVDase).

RESULTS AND DISCUSSION

Fas-induced Apoptosis, Liver Damage, and Caspase 3/7-like Proteolytic Activity Are Blocked by Z-VAD.fmk—The agonistic Fas receptor antibody JO2 induced extensive liver damage and hemorrhage in Balb/c mice, with >60% of hepatocytes showing apoptotic morphology after 4 h (Fig. 1B) (2). The caspase inhibitor, Z-VAD.fmk (50 μ mol/kg) blocked Fas-induced liver damage and hemorrhage and dramatically reduced hepatocyte apoptosis to <1% (Fig. 1C). Almost complete protection was still observed 24 h after exposure to the agonistic antibody (data not shown). The protection conferred by Z-VAD.fmk suggested a critical role for the activation of caspases in Fas-induced apoptosis *in vivo*, consistent with previous studies (24, 25).

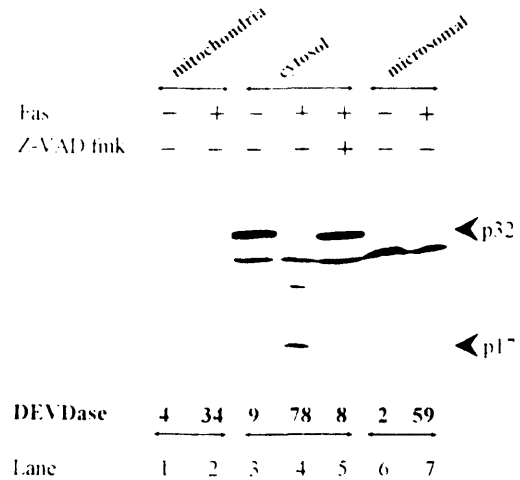


FIG. 2. Active caspase-3 is localized primarily in liver cytosol following Fas-induced apoptosis. Subcellular fractions were prepared from the livers of untreated mice or mice treated 4 h earlier with Fas antibody either alone or in the presence of Z-VAD.fmk as indicated and described under "Experimental Procedures." Proteins (100 μ g) from mitochondrial, cytosolic, and microsomal fractions were separated by SDS, 13% (w/v) PAGE, and Western blot analysis was carried out using an antibody to caspase-3. The DEVDase represents the amount of Z-DEVD.afc cleaving activity loaded expressed as picomoles/min/lane. The upper and lower arrows indicate the proform and the catalytically active large subunit of caspase-3, respectively.

To date, very few studies on Fas-induced apoptosis have been carried out *in vivo*, most being *in vitro* (9–13). In order to confirm the involvement of caspases in Fas-mediated apoptosis *in vivo*, their activation was assessed by measuring DEVDase in crude liver homogenates from control and treated mice. This activity is primarily a measure of caspase-3 and caspase-7 activities, although there may be a minor contribution from other caspases (14, 17, 26, 27). Treatment with the agonistic Fas antibody resulted in a marked increase in total liver DEVDase (270 nmol/min) after 4 h in comparison with that in controls (80 nmol/min). These results demonstrated the activation of the effector caspase-3 and/or caspase-7 in Fas-induced apoptosis *in vivo* in agreement with *in vitro* studies, which have shown the activation of these caspases following treatment of cells with Fas or tumor necrosis factor (11, 28, 29). In order to further dissect the role of caspases in Fas-induced apoptosis *in vivo*, we examined DEVDase and caspase processing in subcellular liver fractions prepared from control and Fas-treated mice. Fas treatment induced 11-, 21-, and 23-fold increases in total DEVDase in cytosolic, microsomal, and mitochondrial fractions, respectively. In all cases, Z-VAD.fmk markedly inhibited the increases in DEVDase. Thus Z-VAD.fmk blocked apoptosis either by directly inhibiting the activity of caspases-3 and -7 or by inhibiting an upstream caspase, such as caspase-8.

Procaspase-3 and Active Caspase-3 Are in the Cytosol—Caspase-3 is generally present in control cells as an inactive p32 zymogen (11, 22, 29). On induction of apoptosis, it is initially processed at Asp-175 between the large and small subunits, yielding a p20 subunit, which is further processed at Asp-9 and Asp-28 to yield p19 and p17 large subunits, respectively (17, 30). In control mice, procaspase-3 was present in the cytosolic fraction (Fig. 2, lane 3) with none detected in the mitochondrial or microsomal fractions (Fig. 2, lanes 1 and 6). Following treatment with the Fas antibody, complete processing of procaspase-3 together with the appearance of its catalytically active p17 subunit was observed in the cytosolic fraction (Fig. 2, lane 4). In addition, immunologically reactive fragments of ~29 kDa (Fig. 2, lanes 3–7) and ~25 kDa (Fig. 2, lane 4) were also observed. The ~29 fragment was observed in all the cytosolic and microsomal fractions (Fig. 2, lanes 3–7).

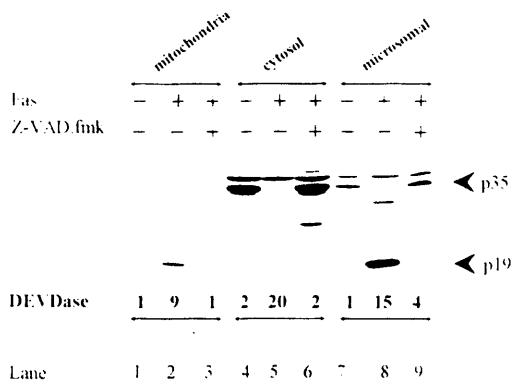


FIG. 3. Active caspase-7 is localized primarily in liver mitochondrial and microsomal fractions following Fas-induced apoptosis. Subcellular fractions were prepared from the livers of untreated mice or mice treated 4 h earlier with Fas antibody either alone or in the presence of Z-VAD.fmk as indicated in the legend to Fig. 2. Proteins (25 μ g) from different subcellular fractions were separated and analyzed using an antibody to caspase-7. The *upper* and *lower* arrows indicate the proform and the catalytically active large subunit of caspase-7, respectively. Other details are as described in the legend to Fig. 2.

While the identity of this fragment is not known, it has been proposed to be due to processing of caspase-3 following cleavage at Asp-28, yielding a zymogen, which is not further processed to active caspase-3 (23). Treatment with Z-VAD.fmk resulted in almost complete inhibition of the processing of procaspase-3, formation of the p17 large subunit, and the p25 fragment (Fig. 2, lane 5). Inhibition of caspase-3 processing was also accompanied by the appearance of a very small amount of an \sim p19 fragment (Fig. 2, lane 5), which may be attributed either to irreversible binding of Z-VAD.fmk to the p17 subunit or to partial blocking of the processing of the large subunit (22, 31). The p17 subunit was detected primarily in the cytosolic fraction of livers from Fas-treated mice (Fig. 2, lane 4) with little if any being present in any other fraction (Fig. 2). These data demonstrate that following Fas induction of apoptosis, active caspase-3 is located primarily in the cytosol.

Active Caspase-7 Is Primarily in the Microsomal and Mitochondrial Fractions—Caspase-7 exists as an inactive p35 zymogen in control cells (22, 28, 32). On induction of apoptosis it is activated by initial processing at Asp 198 between the large and small subunits followed by cleavage at Asp-23 to yield the catalytically active p19 large subunit (22, 27, 28). In livers from control mice, caspase-7 was present as an unprocessed p35 proform in both the cytosolic and microsomal fractions with no detectable p19 subunit (Fig. 3, lanes 4 and 7). While caspase-7 has previously been detected in the cytoplasm of Jurkat cells (28), this is the first time it has also been recognized to have a microsomal location. No detectable procaspase-7 or p19 subunit was present in the mitochondrial fraction from control mouse livers (Fig. 3, lane 1).

Following treatment with the Fas antibody, complete processing of procaspase-7 was observed in both the cytosolic and microsomal fractions (Fig. 3, lanes 5 and 8). Although complete processing of caspase-7 was observed in the cytosolic fraction, little if any p19 subunit was detected (Fig. 3, lane 5). However, the p19 catalytically active large subunit of caspase-7 was clearly detected in both the mitochondrial and microsomal fractions (Fig. 3, lanes 2 and 8). It was very unlikely that the p19 fragment in the mitochondrial fraction was due to microsomal contamination, because the endoplasmic reticular protein SREBP-1 was located exclusively in the microsomal fraction (Fig. 4 and data not shown). In addition, the uncharacterized p29 band, detected using the caspase-3 antibody, in the microsomal fraction from control or Fas-treated livers (Fig. 2, lanes 6 and 7) was not present in the mitochondrial fraction (Fig. 2,

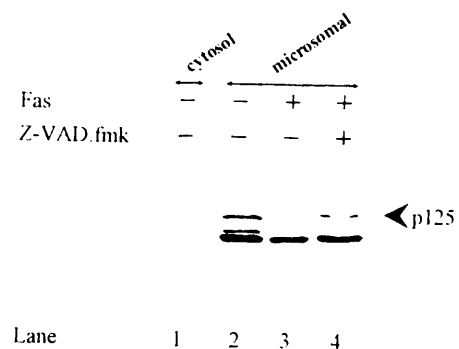


FIG. 4. Cleavage of the endoplasmic reticular-specific substrate SREBP-1. Subcellular fractions were prepared from the livers of untreated mice or mice treated 4 h earlier with Fas antibody either alone or in the presence of Z-VAD.fmk as indicated in the legend to Fig. 2. Proteins (25 μ g) from cytosolic or microsomal fractions were separated by SDS, 8% (w/v) PAGE, and Western blotting was carried out using an antibody to SREBP-1. The *arrow* indicates the intact form of SREBP-1, which was only found in the microsomal fraction.

lanes 1 and 2). The amount of the large p19 subunit of caspase-7 in the microsomal fraction following Fas-induced apoptosis was greater than the amount of procaspase-7 in control liver microsomes (Fig. 3, compare lanes 7 and 8). These results suggested that caspase-7 was translocated from the cytosol to the microsomes following its catalytic activation by an initiator caspase. The data clearly demonstrate that following Fas induction of apoptosis in mouse liver, caspase-7 is completely processed to its catalytically active p19 subunit, which is found primarily in the mitochondrial and microsomal fractions with little if any remaining in the cytosol.

Z-VAD.fmk completely inhibited the Fas-induced cleavage of procaspase-7 as well as the formation of the p19 subunit in all subcellular fractions (Fig. 3, lanes 3, 6, and 9). Z-VAD.fmk also blocked the appearance of an uncharacterized \sim p32 fragment in the microsomal fraction (Fig. 3, lane 9). Taken together with the caspase-3 results, our data suggest that Z-VAD.fmk blocks the processing of both caspase-3 and caspase-7. Although it is not known precisely which caspase activates caspase-3 and caspase-7 during Fas-induced apoptosis, caspase-8 has been considered the most likely candidate (3–5). Recent studies have demonstrated that procaspase-9 binds to Apaf-1 (apoptotic protease-activating factor 1) in a cytochrome *c*- and dATP-dependent manner (33, 34). This complex results in the activation of caspase-9, which in turn cleaves and activates caspase-3 (34). The mechanism of activation of procaspase-7 is not known, it may be due to activation by caspase-8 (5) or to a mechanism involving Apaf-1 and procaspase-9 (34), but it does not appear to be due to a direct activation by caspase-3 (35). Although activation of caspase-8 is clearly a very early event following Fas-induced apoptosis, it is not yet clear how this is related to the activation of caspases following mitochondrial damage with the subsequent release of cytochrome *c* and the activation of procaspase-9. Therefore, Z-VAD.fmk may exert its action by blocking the caspase cascade initiated by both caspase-8 and caspase-9.

Further support for the hypothesis that different effector caspases are responsible for the enzymic activity in different subcellular compartments was provided by comparing the Western blot data with DEVDase. DEVDase in cells undergoing apoptosis is believed to be primarily due to activation of caspase-3 and caspase-7 (14, 17, 26, 27). Although the total DEVDase loaded onto the polyacrylamide gel from the cytosolic fraction (20 pmol/min) (Fig. 3, lane 5) was greater than that from either the mitochondrial or microsomal fractions (9 and 15 pmol/min) (Fig. 3, lanes 2 and 8, respectively), the antibody to caspase-7 only detected the p19 large subunit in the mitochon-

drial and microsomal fractions (Fig. 3, lanes 2 and 8). This suggested that a caspase other than caspase-7 was primarily responsible for DEVDase in the cytosolic fraction. Most probably this was caspase-3, based on the data demonstrating that the p17 catalytically active large subunit of caspase-3 was primarily located in the cytosol (Fig. 2). Thus our results strongly suggest that the major DEVDase in the microsomal and mitochondrial fractions is due to caspase-7, while in the cytosolic fraction it is due to caspase-3. Taken together, our results suggest that following its activation, caspase-7 is translocated to the microsomal and mitochondrial fractions, where it is responsible for the cleavage of specific substrates in these distinct subcellular compartments. A recent study using an affinity label also noted differences in the pattern of active caspases in the nuclei and cytosol between two cell lines (36). Their results together with the present study raise the question about how different active caspases may be targeted to different subcellular localizations.

Fate of Microsomal SREBP-1 following Fas-induced Apoptosis in Mouse Liver—Many previous studies have highlighted overlapping substrate specificities of caspases-3 and -7. For example, combinatorial studies using tetrapeptide substrates assigned virtually indistinguishable substrate specificities to caspases-3 and -7 (14), and both enzymes effectively cleave poly(ADP-ribose) polymerase (17, 26, 27). It has often been suggested that there is a redundancy for certain caspases, which may be due to the important biological function of this system in removing damaged or unwanted cells (6, 7). However results with caspase-3 knockout mice, which exhibit normal apoptosis in most tissues except neuronal cells, indicate that some caspases may function in a tissue selective manner (37). Alternatively our data suggest that, at least in some tissues, caspases with overlapping substrate specificity may exert their functions in different cellular compartments, where they catalyze the cleavage of specific substrates. To explore this possibility, we examined the fate of SREBP-1, one of the few endoplasmic reticulum-associated proteins known to be cleaved in apoptosis (21, 38, 39). SREBPs belong to the basic-helix-loop-helix-leucine zipper family of transcription factors and are involved in the regulation of sterol metabolism (21). On the induction of apoptosis both SREBP-1 and SREBP-2 are cleaved by the hamster homologs of caspases-3 and -7 (38, 39).

In livers from control mice, SREBP-1 was exclusively associated with the microsomal fraction with none being detectable in the cytosolic or mitochondrial fractions (Fig. 4, compare lanes 1 and 2, and data not shown). Complete loss of the ~125-kDa SREBP-1 was observed in liver microsomes obtained from mice treated 4 h earlier with the agonistic Fas antibody (Fig. 4, lane 3). The antibody to SREBP-1 detected the intact but not the cleaved molecule. The Fas-induced cleavage of SREBP-1 was largely prevented by Z-VAD.fmk (Fig. 4, lane 4). As active caspase-7 and SREBP-1 share the same subcellular localization, it is possible that *in vivo* caspase-7 is responsible for the Fas-induced cleavage of SREBP-1. However based on our present data and the contiguous nature of the cytosol and endoplasmic reticulum, we cannot totally exclude the possibility that SREBP-1 may also be cleaved, at least in part, by caspase-3.

We have clearly shown that following Fas-induced apoptosis *in vivo*, active caspase-3 was located primarily in the cytosol, whereas active caspase-7 was associated with both the mitochondrial and microsomal fractions. Our data represent the first example of the differential subcellular distribution of specific caspases in an *in vivo* model of apoptosis.

Acknowledgments—We thank Drs. K. Cain, P. Carthew, and B. Nolan for their helpful advice.

REFERENCES

- Arends, M. J., and Wyllie, A. H. (1991) *Int. Rev. Exp. Pathol.* **32**, 223-254
- Ogasawara, J., Watanabe-Fukunaga, R., Adachi, M., Matsuzawa, A., Kasugai, T., Kitamura, Y., Itoh, N., Suda, T., and Nagata, S. (1993) *Nature* **364**, 806-809
- Boldin, M. P., Goncharov, T. M., Goltsev, V. V., and Wallach, D. (1996) *Cell* **85**, 803-815
- Muzio, M., Chinnaiyan, A. M., Kischkel, F. C., O'Rourke, K., Shevchenko, A., Ni, J., Scaffidi, C., Bretz, J. D., Zhang, M., Gentz, R., Mann, M., Kramer, P. H., Peter, M. E., and Dixit, V. M. (1996) *Cell* **85**, 817-827
- Srinivasula, S. M., Ahmad, M., Fernandes-Alnemri, T., Litwack, G., and Alnemri, E. S. (1996) *Proc. Natl. Acad. Sci. U. S. A.* **93**, 14486-14491
- Cohen, G. M. (1997) *Biochem. J.* **326**, 1-16
- Nicholson, D. W., and Thornberry, N. A. (1997) *Trends Biochem. Sci.* **22**, 299-306
- Fraser, A., and Evan, G. (1996) *Cell* **85**, 781-784
- Nagata, S. (1997) *Cell* **88**, 355-365
- Enari, M., Hug, H., and Nagata, S. (1995) *Nature* **375**, 78-81
- Schlegel, J., Peters, I., Orrenius, S., Miller, D. K., Thornberry, N. A., Yamin, T.-T., and Nicholson, D. W. (1996) *J. Biol. Chem.* **271**, 1841-1844
- Enari, M., Talianian, R. V., Wong, W. W., and Nagata, S. (1996) *Nature* **380**, 723-726
- Kanada, S., Washida, M., Hasegawa, J.-I., Kusano, H., Funahashi, Y., and Tsujimoto, Y. (1997) *Oncogene* **15**, 285-290
- Thornberry, N. A., Rano, T. A., Peterson, E. P., Rasper, D. M., Timkey, T., Garcia-Calvo, M., Houtzager, V. M., Nordstrom, P. A., Roy, S., Vaillancourt, J. P., Chapman, K. T., and Nicholson, D. W. (1997) *J. Biol. Chem.* **272**, 17907-17911
- Ayala, J. M., Yamin, T.-T., Egger, L. A., Chin, J., Kostura, M. J., and Miller, D. K. (1994) *J. Immunol.* **153**, 2592-2599
- Singer, I. I., Scott, S., Chin, J., Bayne, E. K., Limjuco, G., Weidner, J., Miller, D. K., Chapman, K., and Kostura, M. J. (1995) *J. Exp. Med.* **182**, 1447-1459
- Nicholson, D. W., Ali, A., Thornberry, N. A., Vaillancourt, J. P., Ding, C. K., Gallant, M., Gareau, Y., Griffin, P. R., Labelle, M., Lazebnik, Y. A., Munday, N. A., Raju, S. M., Smulson, M. E., Yamin, T.-T., Yu, V. L., and Miller, D. K. (1995) *Nature* **376**, 37-43
- Manson, M. M., Ball, H. W. L., Barrett, M. C., Clark, H. L., Judah, D. J., Williamson, G., and Neal, G. E. (1997) *Carcinogenesis* **18**, 1729-1738
- Tsukihara, T., Aoyama, H., Yamashita, E., Tomizaki, T., Yamaguchi, H., Shinzawa-Itoh, K., Nakashima, R., Yaono, R., and Yoshikawa, S. (1996) *Science* **272**, 1136-1144
- Hayes, J. D., and Pulford, D. J. (1995) *Crit. Rev. Biochem. Mol. Biol.* **30**, 445-600
- Wang, X., Sato, R., Brown, M. S., Hua, X., and Goldstein, J. L. (1994) *Cell* **77**, 53-62
- MacFarlane, M., Cain, K., Sun, X.-M., Alnemri, E. S., and Cohen, G. M. (1997) *J. Cell Biol.* **137**, 469-479
- Boulakia, C. A., Chen, G., Ng, F. W. H., Teodoro, J. G., Branton, P. E., Nicholson, D. W., Poirier, G. G., and Shore, G. C. (1996) *Oncogene* **12**, 529-535
- Rodriguez, I., Matsuura, K., Ody, C., Nagata, S., and Vassalli, P. (1996) *J. Exp. Med.* **184**, 2067-2072
- Rouquet, N., Pagès, J.-C., Molina, T., Briand, P., and Joulin, V. (1996) *Curr. Biol.* **6**, 1192-1195
- Tewari, M., Quan, L. T., O'Rourke, K., Desnoyers, S., Zeng, Z., Beidler, D. R., Poirier, G. G., Salvesen, G. S., and Dixit, V. M. (1995) *Cell* **81**, 801-809
- Fernandes-Alnemri, T., Takahashi, A., Armstrong, R., Krebs, J., Fritz, L., Tomaselli, K. J., Wang, L., Yu, Z., Croce, C. M., Salvesen, G., Earnshaw, W. C., Litwack, G., and Alnemri, E. S. (1995) *Cancer Res.* **55**, 6045-6052
- Duan, H., Chinnaiyan, A. M., Hudson, P. L., Wing, J. P., He, W.-W., and Dixit, V. M. (1996) *J. Biol. Chem.* **271**, 1621-1625
- Chinnaiyan, A. M., Orth, K., O'Rourke, K., Duan, H., Poirier, G. G., and Dixit, V. M. (1996) *J. Biol. Chem.* **271**, 4573-4576
- Fernandes-Alnemri, T., Armstrong, R. C., Krebs, J., Srinivasula, S. M., Wang, L., Bullrich, F., Fritz, L. C., Trapani, J. A., Tomaselli, K. J., Litwack, G., and Alnemri, E. S. (1996) *Proc. Natl. Acad. Sci. U. S. A.* **93**, 7464-7469
- Polverino, A. J., and Patterson, S. D. (1997) *J. Biol. Chem.* **272**, 7013-7021
- Chandler, J. M., Alnemri, E. S., Cohen, G. M., and MacFarlane, M. (1997) *Biochem. J.* **322**, 19-23
- Zou, H., Henzel, W. J., Liu, X., Lutschg, A., and Wang, X. (1997) *Cell* **90**, 405-413
- Li, P., Nijhawan, D., Budihardjo, I., Srinivasula, S. M., Ahmad, M., Alnemri, E. S., and Wang, X. (1997) *Cell* **91**, 479-489
- Hirata, H., Takahashi, A., Kobayashi, S., Yonehara, S., Sawai, H., Okazaki, T., Yamamoto, K., and Sasada, M. (1998) *J. Exp. Med.* **187**, 587-600
- Martins, L. M., Mesner, P. W., Kottke, T. J., Basi, G. S., Sinha, S., Tung, J. S., Svingen, P. A., Madden, B. J., Takahashi, A., McCormick, D. J., Earnshaw, W. C., and Kaufmann, S. H. (1997) *Blood* **90**, 4283-4296
- Kuida, K., Zheng, T. S., Na, S., Kuan, C.-Y., Yang, D., Karasuyama, H., Rakic, P., and Flavell, R. A. (1996) *Nature* **384**, 368-372
- Wang, X., Zelenski, N. G., Yang, J., Sakai, J., Brown, M. S., and Goldstein, J. L. (1996) *EMBO J.* **15**, 1012-1020
- Pai, J.-T., Brown, M. S., and Goldstein, J. L. (1996) *Proc. Natl. Acad. Sci. U. S. A.* **93**, 5437-5442